CRANFIELD UNIVERSITY

Maria Martinez Luengo

ADVANCED STRUCTURAL HEALTH MONITORING STRATEGIES FOR CONDITION-BASED MAINTENANCE PLANNING OF OFFSHORE WIND TURBINE SUPPORT STRUCTURES

SCHOOL OF WATER, ENERGY AND ENVIRONMENT
EngD in Renewable Energy Marine Structures

EngD
Academic Years: 2014 – 2019

Principal Supervisor: Dr Mahmood Shafiee
Associate Supervisor: Prof. Athanasios Kolios

April 2019

CRANFIELD UNIVERSITY

SCHOOL OF WATER, ENERGY AND ENVIRONMENT
EngD in Renewable Energy Marine Structures

EngD
Academic Years: 2014 – 2019

Maria Martinez Luengo

ADVANCED STRUCTURAL HEALTH MONITORING STRATEGIES FOR CONDITION-BASED MAINTENANCE PLANNING OF OFFSHORE WIND TURBINE SUPPORT STRUCTURES

Principal Supervisor: Dr Mahmood Shafiee
Associate Supervisor: Prof. Athanasios Kolios

April 2019

This thesis is submitted in partial fulfilment of the requirements for the degree of EngD

ABSTRACT

Condition-based maintenance strategies need to be adopted as distance-to-shore and water depth increase in the offshore wind industry. The aim of the research presented herein is to develop advance structural health monitoring strategies that enhance the condition-based maintenance of offshore wind turbine support structures. The focus is on the selection of technologies, the implementation process, the analysis of the asset's structural response under complex loading, the economic justification for structural health monitoring implementation and the effective structural health monitoring data analysis. Research activities consist of the provision of a comprehensive study for structural health monitoring technologies' utilisation in the offshore wind industry. This is followed by parametric structural modelling, simulation and validation of an operational offshore wind turbine tower, support structure and soil-structure interaction, using commercial software. The evaluation of the asset's response under complex loading subject to design changes and failure mechanisms is also undertaken. A combination of existing and newly developed methodologies is deployed for the effective data management of structural health monitoring systems and validated with industrial data for the case of strain monitoring. These include unsupervised learning algorithms (neural networks), deterministic and probabilistic methods for noise cleansing and missing data imputation. Guidelines for the structural health monitoring implementation from design stage of a wind farm are proposed and applied to a baseline scenario. This is utilised to assess the economic impact that structural health monitoring has in the lifecycle of the assets. The achieved results show that the implementation of structural health monitoring in offshore wind turbine following the Statistical Pattern Recognition paradigm and the proposed guidelines has the potential to reduce the Operational Expenditure. This reduction is much greater than the cost associated with the implementation of these systems. Monitoring from the commissioning of the assets is crucial for the system's calibration and establishing thresholds. The developed noise cleansing and missing data imputation methodologies can successfully be employed together to produce more complete low-disturbed datasets.

Keywords:

Parametric structural modelling, noise cleansing, missing data imputation, neural networks, guidelines for structural health monitoring implementation, cost-benefit analysis.

DECLARATION

I declare that no portion of the work referred to in the thesis has been submitted in support of an application for another degree or qualification of this or any other university or another institute of learning.

The four journal papers contained in this thesis were published by Elsevier and MDPI, which allow reusing and reproducing the entire published material in an unchanged form in the EngD Thesis.

Elsevier[i]

“Theses and dissertations which contain embedded PJAs [Published Journal Article] as part of the formal submission can be posted publicly by the awarding institution with DOI links back to the formal publications on ScienceDirect.”

[i]Elsevier (2019), Article sharing, Elsevier B.V., available online: www.elsevier.com/about/company-information/policies/sharing (last accessed: 27/02/2019)

MDPI[ii]

“All articles published by MDPI are made immediately available worldwide under an open access license. This means the published material can be used in this thesis as long as proper accreditation/citation of the original publication is given”

[ii]MDPI (2019), MDPI Open Access Information and Policy., available online: https://www.mdpi.com/about/openaccess (last accessed 27/02/2019)

“*Resilience is the process of adapting well in the face of adversity, trauma threats or significant sources of stress – such as family and relationship problems, serious health problems or workplace and financial stressors. It means “bouncing back” from difficult experiences”.*

American Psychological Association.

After these four and a half years of EngD project I am not certain I have become an exceptional researcher. However, one thing I am certain about is that I have become exceptionally resilient.

Unfortunately this was not by choice, but out of necessity. Nevertheless, it is a quality I will keep for the rest of my life.

ACKNOWLEDGEMENTS

I would like to express my sincere gratitude to my friends and colleagues who have supported me during good and bad times throughout these years.

I would also like to show immense appreciation María Erans who was by my side and shared the PhD experience with me through the majority of these years. My time in Cranfield would have been very different without you.

To my parents, Luis and Carmen, thank you for the education and opportunities you have given me growing up. Thank you for never limiting my potential, supporting me in my good decisions and in the not-so-good ones too, and pushing me to pursue new challenges. I love you both. I don’t think anyone could ask for better parents.

To my abuela Paquita and tia Tere who, even though they are from a different generation, have been the best role models a young woman could have wanted.

My most sincere gratitude to Dr Mahmood Shafiee, Dr Ali Mehmanparast and Sam Skears for helping me in a particular time of need.

To that individual that made me the resilient person I am today. You made me have the worst year of my life. However, I not only made it through, but I learned from it and became stronger.

Finally, to my rock: thank you for your unconditional support (moral and scientific) and most importantly for standing me and keeping me sane the past year and a half. I know it wasn’t easy at times. For this, I would always be grateful.

LIST OF PUBLICATIONS

Published:

Martinez-Luengo M, Kolios A, Wang L. Structural health monitoring of offshore wind turbines: A review through the Statistical Pattern Recognition Paradigm. Renew Sustain Energy Rev 2016;64:91–105. doi:10.1016/j.rser.2016.05.085.

Martinez-Luengo M, Kolios A, Wang L. Parametric FEA modelling of Offshore Wind Turbine Support Structures: towards scaling-up and CAPEX reduction. Int J Mar Energy 2017;19:16–31.

Martinez-Luengo M, Shafiee M, Kolios A. Data management for structural integrity assessment of offshore wind turbine support structures: data cleansing and missing data imputation. Ocean Engineering, 2019; 173:867-883.

Martinez-Luengo M, Shafiee M. Guidelines and cost-benefit analysis of the structural health monitoring implementation in offshore wind turbine support structures. Energies, 2019; 12, 1176.

TABLE OF CONTENTS

ABSTRACT i
DECLARATION iii
ACKNOWLEDGEMENTS i
LIST OF PUBLICATIONS iii
TABLE OF CONTENTS v
LIST OF FIGURES ix
LIST OF TABLES xi
LIST OF EQUATIONS xiii
LIST OF ABBREVIATIONS xv
1 INTRODUCTION 1
  1.1 Background and motivation 1
  1.2 Aim and Objectives 4
  1.3 Novelty and linkage of project outputs 5
  1.4 Outline of the Thesis 11
2 STRUCTURAL HEALTH MONITORING OF OFFSHORE WIND TURBINES: A REVIEW THROUGH THE STATISTICAL PATTERN RECOGNITION PARADIGM 15
  2.1 Introduction 19
  2.2 Structural Health Monitoring Systems for Offshore Wind Turbines 22
    2.2.1 History and Evolution 22
    2.2.2 SHM technologies 24
  2.3 Operational Evaluation 30
    2.3.1 Offshore wind turbines damage definition and detection 30
    2.3.2 Variation in environmental and operational conditions 31
  2.4 Data acquisition, normalisation and cleansing 32
    2.4.1 Sensor types 32
    2.4.2 Data collection and storage 36
    2.4.3 Data normalisation and cleansing 38
  2.5 Feature extraction and information condensation 39
  2.6 Statistical Model Development 41
    2.6.1 Supervised Learning 41
    2.6.2 Unsupervised Learning 44
  2.7 Discussion 46
  2.8 Conclusions 50
  2.9 Acknowledgements 50

3 PARAMETRIC FINITE ELEMENT ANALYSIS MODELLING OF OFFSHORE WIND TURBINE SUPPORT STRUCTURES: TOWARDS SCALING-UP AND CAPEX REDUCTION 51
3.1 Introduction 55
3.2 Design Provisions and parametric modelling of offshore wind turbine monopile structures 58
3.2.1 Key Design Parameters of OWT support structures 58
3.2.2 Geometry 60
3.2.3 Materials 61
3.2.4 Mesh Sensitivity Analysis 63
3.2.5 Validation 63
3.3 Load Calculations for Offshore Wind Turbine Support Structures 64
3.3.1 Wind 64
3.3.2 Wave 66
3.3.3 Tidal and current induced loads 68
3.3.4 Hydrostatic Pressure 69
3.3.5 Nacelle's and Rotor's weight 69
3.4 Limit States Formulation 70
3.4.1 ULS 70
3.4.2 FLS 71
3.4.3 Buckling 73
3.4.4 Natural Frequencies 73
3.5 Sensitivity Analysis and Results 74
3.5.1 Design Case A: TP's and GC's length 75
3.5.2 Design Case B: Effect of size and number of stoppers 77
3.5.3 Design Case C: scour development 80
3.6 Discussion 83
3.7 Conclusion 85
3.8 Acknowledgements 87
4 DATA MANAGEMENT FOR STRUCTURAL INTEGRITY ASSESSMENT OF OFFSHORE WIND TURBINE SUPPORT STRUCTURES: DATA CLEANSING AND MISSING DATA IMPUTATION 89
4.1 Introduction 93
4.2 Development of a framework for data management of offshore wind applications 98
4.2.1 Data Synchronisation 98
4.2.2 Data Cleansing 100
4.2.3 Missing Data Imputation 110
4.2.4 Fatigue Assessment 114
4.3 Results and Discussion 116
4.3.1 Data Cleansing 117
4.3.2 Missing Data Imputation 120

4.3.3 Fatigue Assessment 128
4.4 Conclusion 132
4.5 Acknowledgements 134
5 GUIDELINES AND COST-BENEFIT ANALYSIS OF STRUCTURAL HEALTH MONITORING IMPLEMENTATION IN OFFSHORE WIND TURBINE SUPPORT STRUCTURES 135
5.1 Introduction 139
5.2 Guidelines for structural integrity monitoring of offshore wind turbine support structures 141
5.2.1 Regulations and standards 143
5.2.2 SHM strategy 147
5.2.3 Inspection strategy 155
5.3 Cost-Benefit analysis 158
5.3.1 Scenarios 159
5.3.2 CAPEX increase due to SHM implementation 162
5.3.3 OPEX reduction due to SHM implementation 164
5.3.4 Sensitivity analysis 168
5.4 Results and discussion 169
5.5 Conclusions 175
5.6 Acknowledgements 176
6 GENERAL DISCUSSION AND LIMITATIONS 177
7 GENERAL CONCLUSION AND RECOMMENDATIONS 189
7.1 Summary 189
7.2 Contribution to knowledge 194
7.3 Recommendations for future work 198
7.3.1 Confidence in SHM and model updating 198
7.3.2 Optimisation of O&M through inspections and SHM 199
7.3.3 SHM data analysis 200
8 References 201
APPENDICES 241
Appendix A The effect of Marine growth dynamics in offshore wind turbine support structures 241
Appendix B The damage equivalent load calculation using rainflow counting 251

LIST OF FIGURES

Figure 1-1 Offshore wind farm projects and distance from port, 2001-2017 [5] .. 2

Figure 1-2 Interconnections of the project outputs 9

Figure 1-3 Thesis outline 13

Figure 2-1 Algorithms classification for Statistical Model Development 21

Figure 3-1 a) Assembly of OWT SS b) TP c) Stoppers within TP d) TP-GC-MP assembly 60

Figure 4-1 Framework for the effective data management of SHMS of OWT ... 97

Figure 4-2 Low level of noise: Sensors in perfect correlation 102

Figure 4-3 Unknown level of noise: Sensors not in correlation 102

Figure 4-4 Sensors 1 and 3 in full and not complete correlation (above and below respectively) 104

Figure 4-5 Sensor 2-6 noise thresholds 106

Figure 4-6 Noise Criteria 109

Figure 4-7 Missing Data Imputation Framework 111

Figure 4-8 a) Histogram of real input data b) statistical distributions fitted to real input data 113

Figure 4-9 Scenarios for fatigue assessment 114

Figure 4-10 Filtered dataset follows power curve 116

Figure 4-11 Noise Thresholds for 0-4 m/s. a) Sensors 1-2 b) Sensors 3-7 118

Figure 4-12 Sensors' percentage of cleansed data 119

Figure 4-13 ANN’s Error Histogram for Turbine 1 121

Figure 4-14 ANN's Regression plots for Turbine 1 122

Figure 4-15 ANN selection with (above) & without (below) data cleansing: turbine 1 123

Figure 4-16 ANN Selection with (above) & without (below) Data Cleansing: Turbine 2 124

Figure 4-17 ANN Selection with (above) & without (below) Data Cleansing: Turbine 3 125

Figure 4-18 Missing Data Imputation comparison for Turbines 1, 2 and 3 respectively 126

Figure 4-19 Comparison of Missing Data Imputation results between turbines 127

Figure 4-20 Fatigue scenarios: Turbine 1 129

Figure 4-21 Fatigue scenarios: Turbine 2 130

Figure 4-22 Fatigue scenarios: Turbine 3 131

Figure 5-1 Statistical Pattern Recognition stages 148

Figure 5-2 CAPEX increase due to SHM implementation in scenario 3, optimistic case of hardware costs 170

Figure 5-3 CAPEX increase due to SHM implementation in scenario 3, average case of hardware costs 171

Figure 5-4 CAPEX increase due to SHM implementation in scenario 3, pessimistic case of hardware costs 171

Figure 5-5 Graphical comparison of lifetime cost of structural inspections under different scenarios 172

Figure 5-6 Lifetime OPEX reduction from baseline case 173

Figure 5-7 Lifetime cost of inspection depending on the lifetime inspection frequency 174

LIST OF TABLES

Table 2-1 Technology assessment: capabilities and limitations 48

Table 3-1 Soil properties based on site measurements 62

Table 3-2 Validation of eigenfrequencies: System and Tower 64

Table 3-3 Normal and extreme wind parameters 65

Table 3-4 Summary of extreme metocean conditions 66

Table 3-5 Maximum utilization rate for MP and TP in the baseline case 71

Table 3-6 Case A: Percentage of variation of modal frequencies........................76

Table 3-7 Case A: ULS check: MURs (%) of the OWT SS 76

Table 3-8 Case A: buckling check..77

Table 3-9 Case A: FLS analysis 77

Table 3-10 Stopper's dimensions keeping a constant volume of steel 78

Table 3-11 Case B: sensitivity analysis of modal frequencies..............................79

Table 3-12 Case B: buckling analysis...79

Table 3-13 Case B: ULS check: MURs (%) of the OWT SS.................................80

Table 3-14 Case B: FLS analysis 80

Table 3-15 Case C: sensitivity analysis of modal frequencies 82

Table 3-16 Case C: ULS check: MURs (%) of the OWT SS.................................82

Table 3-17 Case C: buckling analysis 83

Table 3-18 Case C: FLS analysis...83

Table 4-1 Imputation Error within Noise Thresholds 128

Table 4-2 Number of samples for fatigue estimations according to different scenarios...132

Table 5-1 BSH regulations to be abided for the development and operation of OWF in Germany...144

Table 5-2 Technical standards for the design and operation of OWF 145

Table 5-3 Minimum requirements for the periodic inspection of SS according to the BSH [8] 146

Table 5-4 WF baseline scenario and EOCs 150

Table 5-5 Failure modes of offshore wind turbine support structures and their effects on structure integrity. 150
Table 5-6 SHM strategy: number, type and hardware location 154
Table 5-7 Scenarios of SHM implementation 161
Table 5-8 Hardware costs in Baseline scenario 162
Table 5-9 Mobilisation / demobilisation costs for the different scenarios 163
Table 5-10 Vessel costs 165
Table 5-11 Equipment costs 165
Table 5-12 Average transit times and cost 165
Table 5-13 Activities specifications: vessel type, personnel, working time and equipment 167
Table 5-14 Sensitivity analysis of hardware price 168
Table 5-15 Sensitivity analysis of inspection time 169
Table 5-16 SHMS cost and CAPEX % for hardware sensitivity analysis 170
Table 5-17 Lifetime inspection costs and inspection-time sensitivity analysis for Baseline case, Scenario 1, 2 and 3 172
Table 5-18 Lifetime OPEX reduction due to SHM implementation and inspection time 173
Table 5-19 CAPEX increase versus OPEX reduction due to SHMS implementation 175
Table 7-1 Summary of research novelty, scientific soundness and value 197

LIST OF EQUATIONS

3-1 65
3-2 65
3-3 66
3-4 67
3-5 67
3-6 67
3-7 68
3-8 68
3-9 68
3-10 68
3-11 68
3-12 68
3-13 69
3-14 69
3-15 71
3-16 72
4-1 99
4-2 99
4-3 105
4-4 107
4-5 108
4-6 108
4-7 115
5-1 162
5-2 163
5-3 163
5-4 163

LIST OF ABBREVIATIONS

AE	Acoustic Emission
BSH	Bundesamt für Seeschifffahrt und Hydrographie
CAE	Computer-Aided Engineering
CAPEX	Capital Expenditure
CM	Condition Monitoring
CTV	Crew Transfer Vessel
CVI	Close Visual Inspection
DAU	Data Acquisition Unit
DEL	Damage Equivalent Load
DVI	Detailed Visual Inspection
EEZ	Exclusive Economic Zone
EOC	Environmental and Operational Conditions
EU	European Union
FBG	Fiber Bragg Grating
FE	Finite Element
FEA	Finite Element Analysis
FLS	Fatigue Limit State
FW	Floating Wind
GC	Grouted Connection
GVI	General Visual Inspection
HAT	Highest Astronomical Tide
H&S	Health and Safety
ICCP	Impressed Current Corrosion Protection
KDP	Key Design Parameter
KPI	Key Performance Indicator
LAT	Lowest Astronomical Tide
LCoE	Levelised Cost of Electricity
LVDT	Linear Variable Differential Transformer
MCA	Maritime and Coastguard Agency
MDI	Missing Data Imputation
MEMS	Micro-electromechanical system
MG	Marine Growth

MP	Monopile
MSA	Maximum Stresses Allowed
MSE	Minimum Squared Error
MUR	Maximum Utilisation Rate
NDT	Non-Destructive Testing
NN	Neural Networks
OPEX	Operational Expenditure
OM	Operational Management
OMA	Operational Modal Analysis
OW	Offshore Wind
OWF	Offshore Wind Farm
OWT	Offshore Wind Turbines
O&M	Operation and Maintenance
R	Residuals
RoI	Return Of Investment
ROV	Remotely Operated Vehicle
SACP	Sacrificial Anodes Cathodic Protection
SCADA	Supervisory Control and Data Acquisition
SHM	Structural Health Monitoring
SHMS	Structural Health Monitoring Systems
SPR	Statistical Pattern Recognition
SS	Support Structure
SV	Service Vessel
TP	Transition Piece
UK	United Kingdom
ULS	Ultimate Limit State
WACC	Weighted Average Cost of Capital
WF	Wind Farm
WSN	Wireless Sensor Network
WT	Wind Turbines

1 INTRODUCTION

1.1 Background and motivation

For the past couple of decades the concept of global warming and climate change has progressively soaked into society. Climate change constitutes a global challenge and therefore needs to be battled globally and united, as emissions threaten the environment regardless of where they have been produced. In order to slow down climate change, 196 countries adopted the Paris Agreement at the COP21 in Paris on 12 December 2015 [1]. Before this took place, the European Union had already set renewable energy targets for all Member States back in 2006 [2]. These targets were recently reviewed in June 2018 and raised to 32% of the European Union's final energy consumption by 2030, up from the previous goal of 27% [3].

The Levelised Cost of Electricity (LCoE) represents the total lifecycle costs of producing a unit of power using a specific technology [4]. The LCoE of a Wind Farm (WF) is driven by its design, fabrication, installation and commissioning costs, wind resource at that location, type of Offshore Wind Turbine (OWT) concept used, Operation and Maintenance (O&M) costs and the expected service life of the project [5]. Other factors influencing LCoE are the capacity factor and the weighted average cost of capital (WACC), which is the cost of debt, the equity premium of the investors, and the share of debt and equity in a project [5]. Reducing the LCoE of offshore wind farms (OWF) will attract higher investments to the industry. An increase in investment for the construction of new OWF will contribute to the achievement of EU targets and accelerate the technology's development producing further LCoE reductions [6].

Recently, there has been a rapid growth in offshore wind (OW) projects with regards to turbine size, capacity, increased number of turbines within projects, etc [5]. Distance-to-shore and water depth are also progressively increasing as can be appreciated in Figure 1-1 [5], leading to higher complexity in access, O&M [7]. O&M is estimated to account for 25%–30% of total OWF project lifecycle costs [8]. The reduction of operational expenditure (OPEX) is crucial for the OW energy industry to make the produced electricity price-competitive with non-renewable sources and maintain the same growth-rate of the past few years. For this reason, strategies are being put in place to allow the deployment of larger WF further offshore and to focus in reducing the LCoE through the optimisation of the O&M activities. Distance-to-shore is an important factor in asset integrity management because, as distance increases, so do failures' cost implications and time to repair, which directly impacts loss of production.

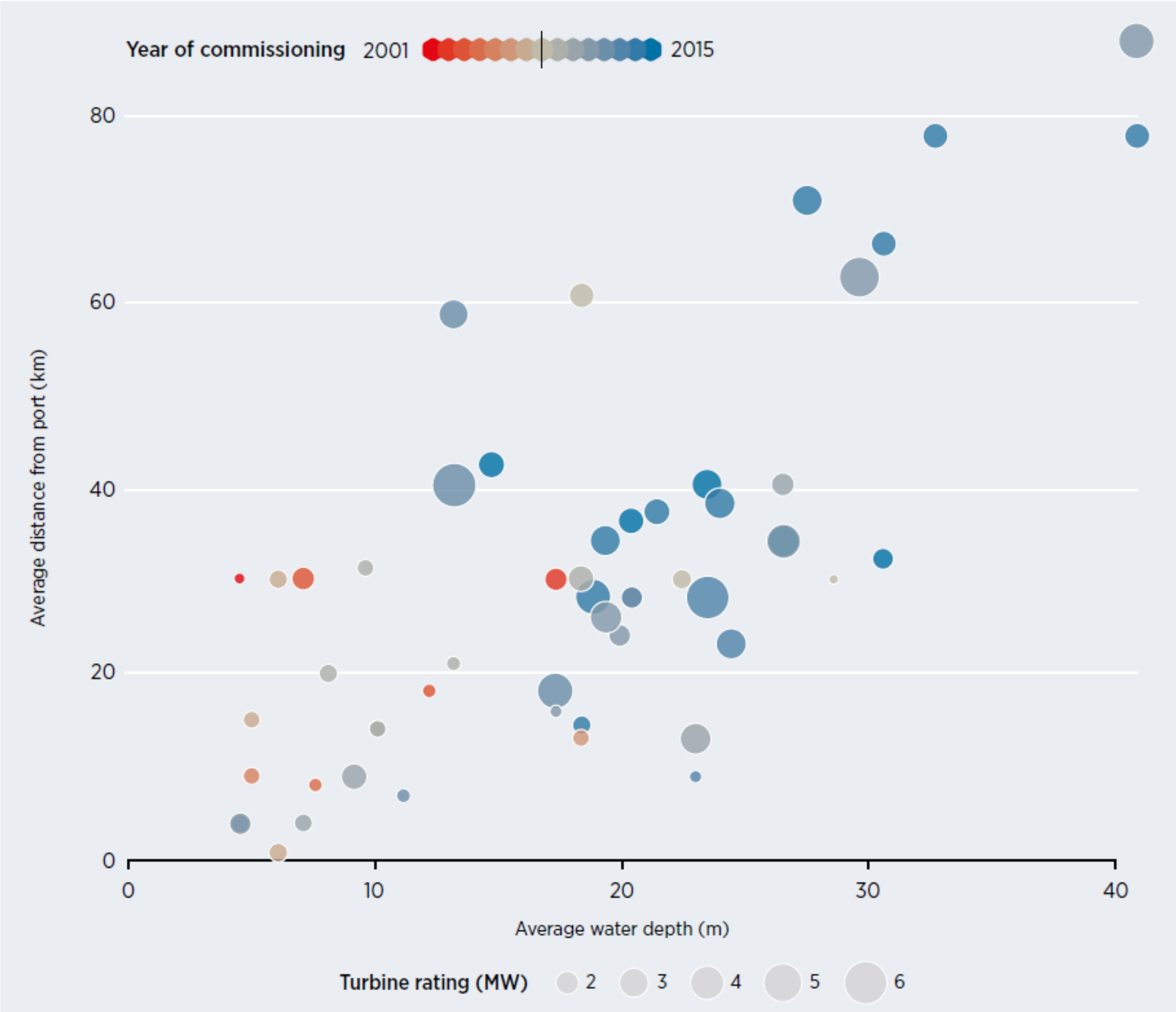

Figure 1-1 Offshore wind farm projects and distance from port, 2001-2017 [5]

Structural Health Monitoring/Condition Monitoring (SHM/CM) systems can be employed to mitigate the risks arising from the increment of distance-to-shore, hence the increase in attention towards them over the past few years. SHM are utilised to detect and alert of anomalous structural responses indicating changes in the condition of the structures. Early detection of these phenomena enables the shut-down of the affected asset for further root cause analysis of the developed failure mechanism. Furthermore, a repair/mitigation strategy can be put in place, reducing time to repair and production losses. Despite all the benefits, Structural Health Monitoring Systems (SHMS) have only started to be implemented holistically in the past few years. SHMS were originally used to monitor assets where damages were suspected or had already developed.

SHM/CM systems have already been widely used in other industries or even in some OWT's subsystems, such as generators and gearboxes. However, strategies for advance SHM of other OWT elements, like the support structure (SS), still need to be developed. This involves the creation and/or improvement of methodologies that aid the selection, implementation, collection, economic justification and data management of SHMS in OWT SS in order to draw conclusions of their condition. This constitutes the research gap identified and addressed throughout this project.

It should be noted that, within the context of this work, a differentiation between SHM and CM has been made, being SHM referred to the monitoring of structural components of a WT (ie. foundation, transition piece (TP), tower, etc.) and CM referred to the monitoring of mechanical and rotating components in the nacelle of the WT (ie. shafts, generator, transformer, etc.).

Furthermore, within the context of this work, the term "strategies" has been understood as: "the actions or procedures used to contribute towards the achievement of a goal".

1.2 Aim and Objectives

The aim of this research is to develop advance structural health monitoring strategies that enhance the condition-based inspection and maintenance of offshore wind turbine support structures. The focus is on the selection of technologies to be employed, the sequence of tasks to be carried out for the implementation of these technologies, the understanding of the structural response of the asset under complex loading, the economic justification for such implementation and how structural health monitoring data is managed and analysed effectively.

In order to achieve this aim there are six different objectives to accomplish:

Objective I: Conduct a detailed review of structural health monitoring technologies and their application in offshore wind turbines. Provision of a comprehensive study of the utilisation of structural health monitoring technologies in the offshore wind industry.

Objective II: Develop a parametric finite element model of an offshore wind turbine support structure and validate it with data from an operational wind farm.

Objective III: Evaluate an offshore wind turbine support structure's response under complex loading in order to understand how design changes and failure mechanisms affect the structure's condition.

Objective IV: Formulate a framework for the effective data management of structural health monitoring systems for offshore wind turbine support structures and validate it for a real case study utilising industrial data.

Objective V: Create guidelines for the implementation of structural health monitoring systems from the design stage of a wind farm.

Objective VI: Evaluate the economic impact that of the implementation of structural health monitoring systems in offshore wind farm support structures through the proposed guidelines.

1.3 Novelty and linkage of project outputs

In order to reach the objectives established for this research project, a number of contributions have been made to the scientific body of knowledge. These have been reported in four peer-reviewed journal publications.

The scope of this research project is very broad. Due to time and resources (data) limitations, not every aspect of the scope has been explored during this project. Figure 1-2 shows the linkage of project outputs and the scope limitations of this project. For further details about scope limitations refer to Section 6, where these have been discussed.

The implementation of SHMS in OWT can contribute to the development of condition-based inspection and maintenance strategies by the collection of data used to assess the integrity of the assets. The enhancement of these procedures may lead to reducing costs of WT inspection, avoiding unnecessary replacement/ repair of components, discovering design weaknesses before failure, improving the availability of the WF while preventing WTs overloading. All these aspects are linked to OPEX and LCoE reduction and maximisation of the WF's return of investment (RoI), therefore contributing towards achieving United Kingdom's 2030 and 2050 renewable energy targets. The implementation of SHM technologies is done effectively by the application of the four stages of the Statistical Pattern Recognition (SPR) paradigm, adapted to the OW industry. These four stages were investigated throughout this project (some in more detail than others) and case studies were developed, when appropriate, with industrial data combined with academically/public data.

A detailed literature review of the different SHM technologies applicable to OWT was carried out with the aim to understand how their data is collected and how it needs to be handled, pre-processed, analysed and interpreted. The Statistical Pattern Recognition Paradigm was chosen as the best approach for the implementation of damage detection strategies. However, this paradigm still had to be adapted to the OW industry. This adaptation was carried out and published in the form of Publication 1 in the journal of Renewable and Sustainable Energy Reviews [9], which fulfils Objective I.

In order to accomplish Objective IV, where a framework for data management is to be developed and validated, a better understanding of the asset's response under complex loading is required. To this purpose, a parametric FE model of an OWT SS was developed in Abaqus Computer-Aided Engineering (CAE) and validated with real static data from an offshore wind operator (Objective III). In the FE model, key design parameters (KDPs) can be directly modified in the code to assess their effect on the structure's behaviour. The model consists of: monopile (MP) foundation, TP, grouted connection (GC), tower and soil-structure interaction.

This model was published at the International Journal of Marine Energy and constitutes Publication 2 [10]. In it, the structure's response to complex loading was analysed (via static, buckling and modal analyses) in four case studies and the different KDPs that impact design, scaling-up and O&M activities of OWT SS were identified. The aim of two of the analyses is determining how different geometry variations will affect the structural integrity of the unit. Case A investigates how the TP's and GC's length influences the structural integrity. Case B evaluated the effect of size and number of stoppers in the TP, keeping a constant volume of steel. Another case study was developed to assess the structure's response to scour development, which is a common failure mechanism of OWT. The evaluation of the effect in the OWT's SS integrity of the design changes and failure mechanisms presented in these four case studies fulfilled Objective III. Finally, a fourth case study analysing the effect that marine growth has in the structural integrity of the units was also developed during this research project. This piece of work was presented in the International Conference of Marine Structures, celebrated in Lisbon in May

2017. As this case study was presented as a conference paper, it has not been included as a Chapter in this EngD thesis. Further details of this piece of work can be found in Section 6.

A good understanding of how geometrical modifications to the structure will affect its structural integrity and end of life is important to adapt these structures to harsher environments further from shore and to develop an appropriate SHM Strategy to keep the units in operation. Through the combination of FE models and SHM activities (such as smart loads management and smart scheduling of inspections) high-confidence integrity assessment of the offshore assets can be carried out with the aim of reducing CAPEX and OPEX as much as possible, while increasing power production. This is discussed in Publication 4, where an economic feasibility study of SHM implementation is performed and the importance of updating the Finite Element Analysis (FEA) models with data from SHMS is emphasised.

In order to fulfil Objective IV, a systematic methodology for data synchronisation, normalisation, cleansing and missing data imputation (MDI) was proposed for SHMS of OWT and implemented to the particular case of strain monitoring. This methodology is presented in a journal paper published in the Journal of Ocean Engineering [11], which constitutes Publication 3. Also in this piece of work, the aforementioned methodology is validated with industrial data from three different turbines. MDI was applied to cleansed and non-cleansed datasets for these three operating wind turbines in the Irish Sea, proving that data cleansing enhances the accuracy in the imputation of missing data. Fatigue was calculated for four different scenarios: without cleansing/without MDI, without cleansing/with MDI, with cleansing/without MDI and with cleansing/with MDI.

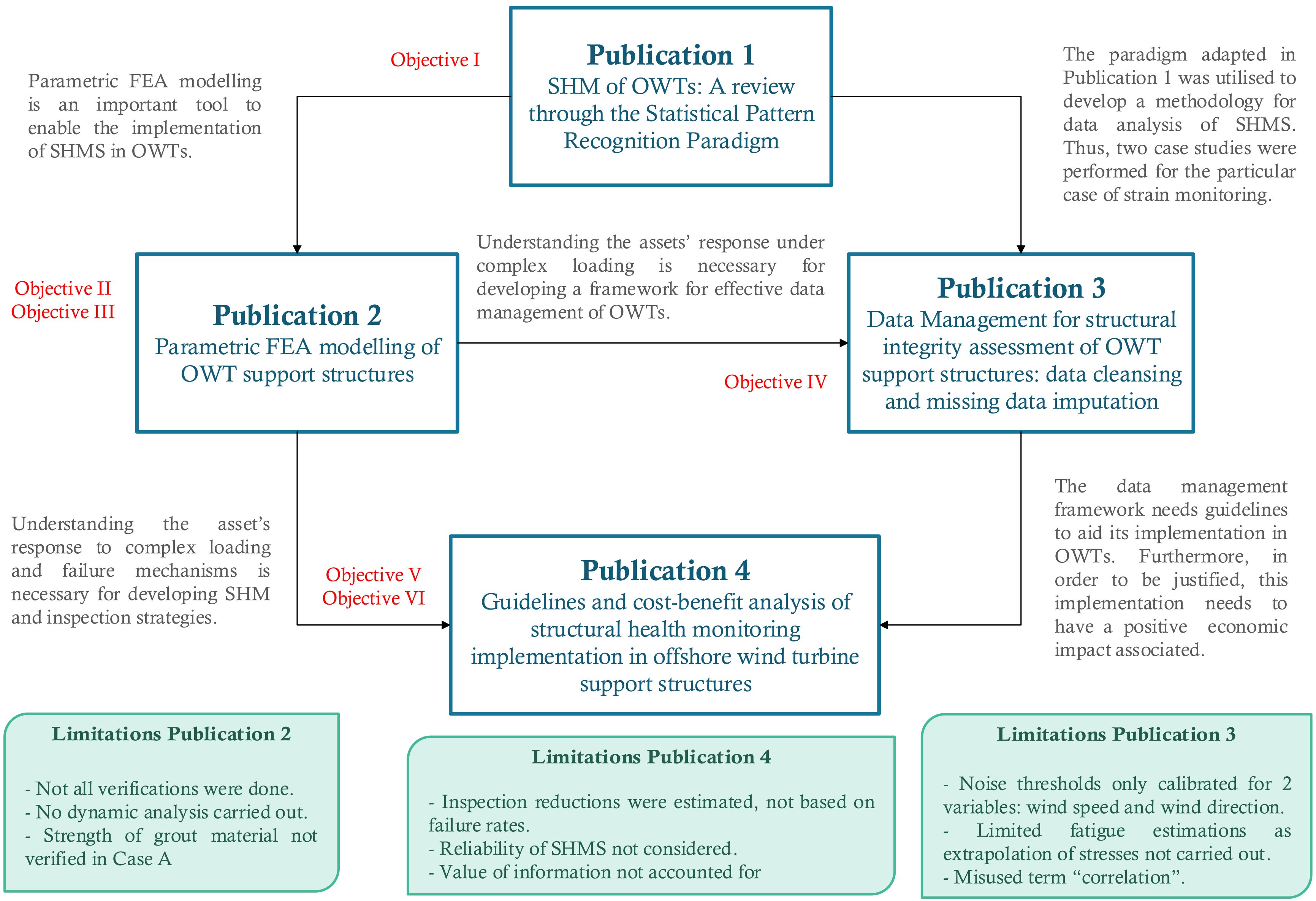

Figure 1-2 Interconnections of the project outputs

Publication 4 aims to unify the different contributions of previous publications, fulfilling Objectives V and VI [12]. This is achieved by developing guidelines for the holistic implementation of SHMS from the design stages of a WF and demonstrating that the implementation of SHMS following these guidelines is economically justified. As part of these guidelines, a SHM strategy and an Inspection strategy were prepared and their cost quantified. A cost-benefit analysis of the implementation of the SHM strategy and Inspection strategy for a baseline case (10% instrumented assets) and three other scenarios with 20%, 30% and 50% of instrumented assets is presented. The reduction in the number of inspections throughout the service life based on the SHM implementation percentage was estimated for the three scenarios, which constitutes the main limitation of this study. Furthermore, a sensitivity analysis is also conducted to evaluate the effects of SHM hardware cost and the time spent in completing the inspections on OPEX and CAPEX of the WF.

1.4 Outline of the Thesis

The structure of this doctoral thesis with a brief description of the content of each chapter is detailed below and follows the sequence of Figure 1-3:

- **Chapter 1** comprises the background and motivation of this research project, the aims and objectives and an overview of the contribution to science and how the publications are linked with these aims and objectives.
- **Chapter 2** offers a detailed literature review of the different types of SHMS for OWT. The purpose is to understand how these could enhance O&M activities, how their data is collected and how it needs to be handled, pre-processed, analysed and interpreted. The SPR paradigm is adapted to the OW industry.
- **Chapter 3** presents the parametric FE model developed for the structural analysis of OWT SS. This constitutes the first academic 3D tool, validated with industrial data. This tool enhances the understanding of the asset's response to complex loading and different failure mechanisms, which improves SHMS design. As discussed in Chapter 5, once SHM data is

recovered from offshore, it can be utilised to calibrate the structural model and assess the structural integrity status of the asset.

- **Chapter 4** presents the developed and validated framework for effective data management of SHMS of OWT applied to strain monitoring. Methodologies and results of the three last stages of the SPR paradigm are presented here utilising real strain data from an OWF.
- **Chapter 5** develops guidelines for the implementation of SHMS to OWT SS in an efficient manner. It also verifies the positive economic impact of SHM implementation in OPEX.
- **Chapter 6** presents a general discussion of all the work done through the course of this research linking all the chapters together.
- **Chapter 7** deals with concluding remarks, contributions to existing knowledge and recommendations for future work.

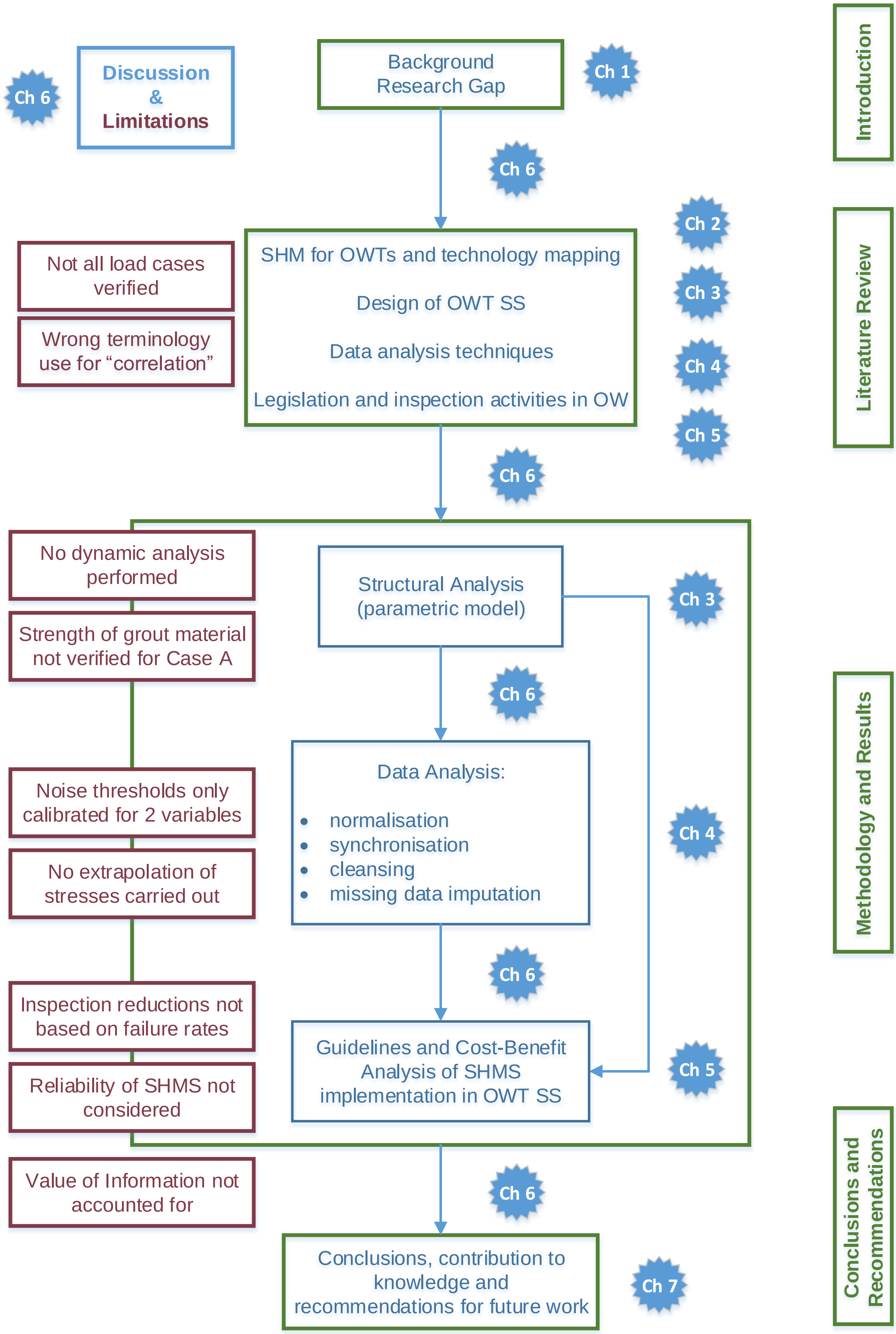

Figure 1-3 Thesis outline

2 STRUCTURAL HEALTH MONITORING OF OFFSHORE WIND TURBINES: A REVIEW THROUGH THE STATISTICAL PATTERN RECOGNITION PARADIGM

Maria Martinez-Luengo, Athanasios Kolios and Lin Wang

Centre for Offshore Renewable Energy Engineering, School of Water, Energy and Environment, Cranfield University, Bedford, Bedfordshire, United Kingdom

Submitted 6th February 2016, Accepted 23rd May 2016

Published in Renewable and Sustainable Energy Reviews, 2016, 64, 91-105

DOI: 10.1016/j.rser.2016.05.085

Statement of contributions of joint authorship

Maria Martinez-Luengo conducted the literature review on the subject, adapted the paradigm, planned and drafted and critically reviewed this manuscript. Also, María produced figures and tables in this paper. Athanasios Kolios and Lin Wang proof-read and critically commented the manuscript before its submission to Renewable and Sustainable Energy Reviews.

Abstract

Offshore Wind has recently become a profitable renewable energy source due to the remarkable development it has experienced in Europe over the last decade. In this paper, a review of Structural Health Monitoring Systems (SHMS) for Offshore Wind Turbines (OWT) has been carried out considering the topic as a Statistical Pattern Recognition (SPR) problem. Therefore, each one of the stages of this paradigm has been reviewed focusing on OWT application. These stages are: Operational Evaluation; Data Acquisition, Normalization and Cleansing; Feature Extraction and Information Condensation; and Statistical Model Development. It is expected that optimizing each stage, SHMS can contribute to the development of efficient Condition-Based Maintenance Strategies. Optimizing this strategy will help reduce labor costs of OWT's inspection, avoid unnecessary maintenance, identify design weaknesses before failure, improve the availability of power production while preventing wind turbines' overloading, therefore, maximizing the investments' return. In the forthcoming years, a growing interest in Structural Health Monitoring (SHM) technologies for OWT is expected, enhancing the potential of Offshore Wind Farm (OWF) deployments further offshore. Increasing efficiency in operational management (OM) will contribute towards achieving United Kingdom's 2020 and 2050 targets, through ultimately reducing Levelised Cost of Electricity (LCoE).

Keywords: Offshore wind turbines, Structural health monitoring, Statistical Pattern Recognition Paradigm, Sensors, Statistical model development

2.1 Introduction

Over the past 15 years, Wind Energy has experienced a remarkable growth in the Europe. While in 2000 wind energy contributed 2.4% of the European Union's electricity demand, by 2015 this percentage raised to 11.4%, or in absolute numbers, 12.9 GW of installed capacity became 141.6 GW [13]. This rapid development is not only due to the targets set by the European Union in 2006 for all Member States [13], but also due to the scalability of wind energy with units of larger capacity been deployed in larger farms, further offshore [14]. According to Renewable UK, OW has officially become the most profitable renewable energy source since it can produce more renewable energy than all of the other sources combined [15]. In Europe, including sites under construction, there are 84 OWF in 11 countries as of the end of 2015. Furthermore, 3,230 turbines are installed and operational, reaching a cumulative installed capacity of 11,027 MW. In 2015 only, a grid-connected capacity of 3,019 MW, was added, accounting for almost double of the capacity added in 2014 [16]. Moreover, due to the increased deployment of 4–6 MW turbines in 2015, the average OWT size became 4.2 MW, constituting a 13% increase over 2014.

Considering wind energy as a mature technology, allows developers and operators to gain confidence to include this energy technology within their mainstream portfolios. Increasing availability of farms and reliability of units, decreasing unscheduled maintenance and eliminating unexpected catastrophic failures are the targets that attract focus towards deploying the next generation of Wind Farms (WF). SHMS can contribute significantly towards enhancing OWT's profitability, reliability and sustainability through more systematic OM approaches. SHM represents the procedure of implementing a damage detection strategy for engineering infrastructures related to aerospace, civil and mechanical engineering [17], being damage referring to the variations in material and/or geometric properties of these systems [18]. Some of the most known structural damage roots causes are: moisture absorption, fatigue, wind gusts [19], thermal stress, corrosion [20], fire and lightning strikes [21]. Usually, there are two critical aspects that influence SHMS development: the sensing technology (and the associated signal analysis), and the interpretation algorithm [22] Damage identification is performed through five similar disciplines [23]: SHM, Condition Monitoring (CM) [24], Non-Destructive Evaluation [25], Statistical Process Control [26], and Damage Prognosis [27,28]. Apart from the CM of rotating machines, SHM for OWT remains a research topic which is slowly getting into the field deployment stage. This is due to the early stage of the technology's deployment, the additional challenge that offshore environments pose to these technologies, and associated costs to operators for hardware installation and data processing

Farrar and Sohn [29] were the first to introduce the SPR paradigm in the SHM field. This methodology follows four stages:

1) Operational evaluation: This stage aims to set the boundaries of the problem by replying to four questions concerning the implementation of the Damage Identification Facility. Questions are related to: the motivation and economic justification for implementing the SHMS, the different Systems' damage definitions, the Environmental and Operational Conditions (EOC) in which the SHMS are used, and the data acquisition limitations in the operational environment.

2) Data acquisition, normalization and cleansing: Data Acquisition refers to the selection of the excitation methods, type, quantity and location of sensors, and the data acquisition/storage/transmittal hardware [30]. Data Normalization is another crucial aspect for the Damage Identification Process, as there are numerous conditions in which measurements can be taken [31]. Therefore, this Normalization constitutes the procedure of separating variations in sensor readings produced by damage, from those produced by the variation in EOC. Data cleansing is the procedure of selecting data which is passing on to or rejecting from the Feature Selection procedure [32]. Two examples of Data Cleansing processes are filtering and resampling, which constitute Signal Processing Techniques [33].

3) Feature extraction and information condensation: This is the aspect of the SHMS that attracts most attention, as these features allow the distinction between damaged and non-damaged structures [34,35]. Data Condensation is essential when analogue feature sets acquired along the structure's lifetime are envisioned. Due to the extraction of data from a structure during long periods of time, robust data reduction techniques have to be developed to preserve feature sensitivity to the changes of interest.

4) Statistical model development: It is related with the implementation of the algorithms that work with the extracted features and calculate the extent of the damage to the structure. These algorithms can be divided into two categories that are shown in Figure 2-1. All of these algorithms assess statistical distributions of the measured or derived features, to enhance the damage identification process [36–38].

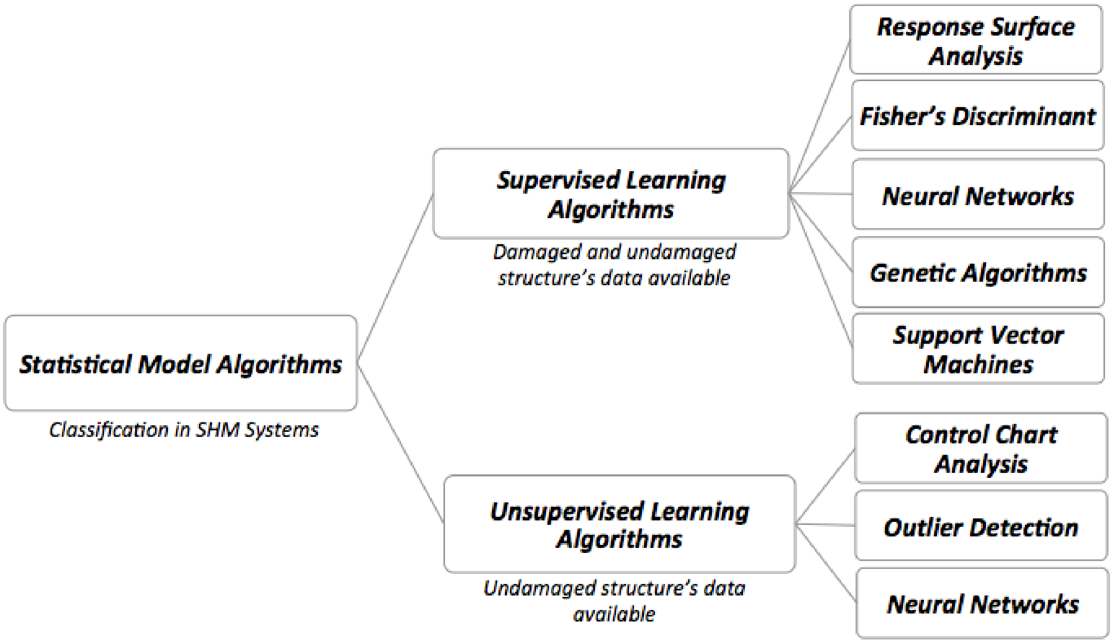

Figure 2-1 Algorithms classification for Statistical Model Development

This publication presents a comprehensive review of SHMS of OWT following the process of the SPR paradigm. The paper has been divided in eight sections. In Section 2.2, a comprehensive review of the SHMS for OWT is carried out, presenting the history and evolution of SHMS and the different technologies that can be employed to Offshore Wind (OW). Each one of the abovementioned framework's stages has been reviewed in greater detail focusing on OWT applications (Sections 2.3–2.6). Discussions of the capabilities and limitations of SHMS, the most used methods in the OW industry and current technology gaps are presented in Section 2.7, followed by conclusions in Section 2.8.

2.2 Structural Health Monitoring Systems for Offshore Wind Turbines

2.2.1 History and Evolution

The identification of changes in the dynamic response of systems has been carried out qualitatively, since practice has introduced tools by employing acoustic techniques [39,40]. Lately the emergence of SHM techniques has come together with the evolution, miniaturization and cost reduction of digital computing hardware [23]. Depending on the sector, this evolution took place sooner or later. For example, CM systems for rotating machines constituted one of the first developed systems, whilst SHMS for the OW industry are currently an emerging research topic. Nowadays, CM of rotating machines constitutes the most prosperous application of SHM Technology in terms of profitability, reliability and level of development. The failure identification process is based on pattern recognition related to displacement, velocity or acceleration time histories, commonly located at one point on the housing or shafts of the machinery during standard-operating conditions and start-up or shut-down transients [41]. Commercial software integrated with measurement hardware is marketed to help the user systematically apply this technology to the operating equipment [23]. These facts mentioned above, supposed the transition of SHMS in this field from a research topic to a common industry practice. A good example of this is the US Navy's Integrated Condition Assessment System [42].

The aerospace sector started studying the use of vibration-based Damage Identification during the late 70 s and early 80 s in conjunction with the development of the space shuttle programs [23]. That effort carried out on other applications that are being investigated for the National Aeronautics and Space Administration's Space Station [17]. Some of the most widely used technologies in this field are: fastener monitoring [43], blade tip clearance [44], and fatigue monitoring. The Civil Engineering community has researched on vibration-based Damage Identification of bridges and buildings since the 80s [45,46]. This research is currently being applied to offshore structures due to the similarities across industries.

During the 70 s and 80 s, the Oil and Gas industry carried out extensive research to develop vibration-based damage identification techniques for offshore platforms [47]. Related to this technique, one of the research objectives was the detection of near-failing drilling equipment and the prevention of expensive oil pumps from becoming inoperable [48]. Unfortunately, most efforts were not successful, as this problem is fundamentally different to that of the rotating machines due to the impossibility of predicting where damage will occur and the structure's inaccessibility for data acquisition purposes. Besides, numerous practical issues were found apart from measurement acquisition difficulties, occasioned by platform noise, instrumentation difficulties in hostile environments, changing mass caused by marine growth (MG), varying fluid storage levels, temporal variability of foundation conditions and the inability of wave motion to excite higher vibration modes [23]. However, different applications could finally overcome these issues and be implemented. For example, fatigue gauges are commonly employed for fatigue monitoring by measuring the crack-growth proportional to the cumulative fatigue damage for welded joints [49]. This approach was reviewed by [50] and [51]. Another example was presented in [52], where different techniques for corrosion monitoring were introduced and the application of flexible ultrasonic thin-film piezoelectric transducer arrays was described. Lastly, [53] suggests a methodology to enhance the reliability of SHM for flexible risers, which are widely used in offshore oil exploration facilities and are essentially composite structures consisting of several metal armours and polymeric layers.

Most of the WF are either at the beginning or in the middle of their service life and, currently, the trend is to build these WFs much further offshore. Therefore, special consideration due to extreme weather conditions and complex dynamics, such as sensor tolerance and endurance, data acquisition and transmission, among others, have to be accounted for [54–56]. As this sector grows, business economics currently demands management of Capital Expenditure and Operational Expenditure (CAPEX and OPEX) [57]. For example, considering a 750 kW turbine with an expected 20-year service life, the operations and maintenance (O&M) costs account for between 25% and 30% of the overall energy generation cost or 75–90% of the investment costs [58]. Some of the technologies employed in OW differ from those employed by the civil or the oil and gas industries in aspects of accessibility, severity of the environmental conditions and more complex loading due to excessive operational loads. Due to these differences, further development and research in these technologies has been prioritized in the past years aiming to adapt them to OW applications. In order to make wind power price-competitive with other sources of energy, some of the performance indicators, such as availability, reliability, efficiency and integrity of turbines, still have to be improved [57]. In the following section, a review of the current SHM techniques used in the OW industry is presented.

2.2.2 SHM technologies

SHMS of OWT are becoming very much in demand now that WTs are growing in size and OWF are being developed further from the coasts. In order to decrease the power generation costs and therefore, the LCoE, Wind Turbine (WT) mass of components need to be optimized without compromising the structure's integrity. This can be achieved through making the turbines more structurally flexible, which directly affects their modal parameters, i.e. the resonance frequency [59]. Another important aspect is that inspection and maintenance for OWT is considerably more expensive than for onshore ones. Therefore, SHMS which are able to predict structural changes are becoming crucial to diminish O&M costs and to assess the remaining lifetime of these structures. An example of a good application of SHMS to an onshore WT is presented in [60], where a life-cycle management framework for online monitoring and performance assessment is applied to WT.

SHM has become a useful method to enhance OM and optimize maintenance activities of modern infrastructure [47], as the information gathered can be employed in the development of a tailored, condition-based maintenance program [61]. This program aims to reduce the necessary downtime due to components inspection, prevent unnecessary failures, avoid unnecessary replacements, and improve availability. Furthermore, due to the capacity of monitoring the structure's integrity, design improvements can be implemented such as selection of lighter blades that will enhance performance with less conservative margins of safety [62] and which will adapt quicker to the wind's variability, generating more energy [63].

General reviews of SHM can be found in [64] and [65,66] where assessment of the different methodologies was carried out. SHM techniques for WT were reviewed by [67], however, the majority of the review was dedicated to bridges and civil infrastructures. A wide overview of how the EOC affects SHM techniques and the normalization of the data that needs to be carried out for compensating these variations is given in [37]. A discussion between SHM and CM costs can be found in [68].

Within this section, the different SHM techniques and especially those suitable for OWT blades, tower and foundation, are explained.

2.2.2.1 Acoustic emission monitoring

Failure mechanisms such as cracking, excessive deformation, debonding, delamination, impacts, crushing, among others, all provoke transient changes in stored elastic energy in particular points of a structure. This energy release can be effectively used to monitor WTs and, particularly, their blades. As Ciang mentioned in [17], Acoustic Emission (AE) is a very effective technique that detects damage mechanism up to the microscale. However, this technique is less effective when it comes to damage characterization and assessment in the case that an appropriate algorithm is not available. Complex damage mechanisms in WT blades have been better understood since AE monitoring was carried out in a blade during loading, enhancing the ability to assess damage during testing [69–71]. Also during a certification test, the damaged area due to cracking in the blade was located due to the sound of the cracking mechanism [70]. Fatigue tests can also be monitored, as [72] presents; such as the sound produced due to stress released waves or energy dissipation using piezoelectric sensors [73,74].

AE signals are defined by their amplitude and energy [75]. As [73] explains, AE events will occur around a particular point, at a structure under certain loading. That particular point will be the one at which the structure will fail at some point, being the feature extremely useful in locating the failure. Even though most of the relevant literature is related to tests in WT blades, a few cases explain how the technique could be applied to a WT blade during operation [76], by using a broadband radio to send the AE data from the rotating frame to the ground with no signal resolution loss. Even though the previously collected data had acceptable levels of noise in low to moderate wind speeds, verification of the fact that the noise does not increase with wind speeds and the feasibility of those signals to be filtered, has to be assessed.

2.2.2.2 Thermal imaging method

This method aims to detect defects or anomalies in the material beneath the surface and it is based on the subsurface's temperature gradients. Thermal imaging can be applied to a WT blade by installing infrared cameras [63]. Irregularity of or damage to material is detected due to a change in the thermal diffusivity. Moreover, this technique can be divided in two categories depending on the thermal excitation method used: active or passive. The passive thermal imaging method aims to investigate materials at different temperatures, other than the ambient, and therefore, it is not normally used in SHMS of OWT; the active approach has an external stimulus source (i.e. optical flash lamps, or heat lamps).

A particular type of active thermal imaging method is called the thermoelastic stress method and it is based on the thermoelastic effect, which consists of the change in temperature of an elastic solid produced by a change of stress [64]. As explained in [77], in the damaged or abnormal region, different heat conduction, higher acoustical damping, and stress concentration take place.

This technique has been proven to be useful in WT blades fatigue tests [75,78], as stress concentrations during the test can be observed before damage in the surface is appreciated. A promising variation of this methodology involves applying high power ultrasounds [79], or oscillating stresses with a mechanical shaker, to the surface that is being tested [80]. This technique is called vibro-thermographic and is able to locate and assess crack dimensions, as [81] states. Furthermore, it can be used for assessing voids and stress concentration in composites. Nevertheless, this method has the potential to become a promising SHM technique for WTs, and more research needs to be carried out in order to reduce the sensitivity to temperature variations [75].

2.2.2.3 Ultrasonic methods

Ultrasound is a method commonly used for assessing the inner structures of solid objects [82]. It has also turned out to be very useful with composite structures. The basic principle of this technique is that ultrasonic waves, emitted by a transmitter, pass through the tested material and are reflected and/or mode converted by a flaw or anomaly. This modified signal is picked up by a receiver once it has passed through the material (if not reflected). In the simplest arrangement, transmitter and receiver are placed on opposite surfaces of the material [83]. The aim of this technique is to reveal planar cracks that take place perpendicularly to the sound wave propagation direction [84]. An advantage of this method is that it can detect cracks of just a few millimeters in length.

2.2.2.4 Fatigue and modal properties monitoring

Fatigue and modal properties monitoring are among the most important SHM techniques for OWT structures, as the consequences of structural damage may be catastrophic. These methods are very simple to implement on structures of any size as they are based on another CM technique, which is the most mature and successful methodology for rotating machinery monitoring; the vibration-based inspection method [47,85].

Modal properties monitoring is based on the principle that modal parameters, such as resonance frequency, damping coefficient and modal curvatures, among others, experience certain variations due to a change in different physical properties (i.e. reduction in mass or stiffness) [86,87]. Due to these changes, the structure is considered to be damaged; that damage being identifiable by comparison between the structure's modal parameters before and after an event. In other words, due to the fact that modal properties changes are considered as damage indicators, this SHM technique is categorised as a pattern recognition problem [66].

Accelerometers are often installed on a wind turbine (WT) to analyze the structure's dynamic response by studying its mode shapes. Other analyses that can be carried out by accelerometers are curvature mode shapes and wavelet maps. These analyses are particularly relevant when they are carried out in service conditions [88]. However, performing these analyses accurately to a full scale OWT during operation is extremely difficult due to the high number of uncertainties which the offshore environment presents [59] and, therefore, special effort has been given to solve this issue in the past years [89]. One reason that makes this analysis difficult is the fact that wind and wave loading applied to the structure cannot be measured accurately in a continuous manner. This introduces the difficulty of having to employ Operational Modal Analysis (OMA) for calculating the modal parameters based on the assumption that the structure is subjected to unknown random loads [90–93]. OMA methods are based on the principle that in the analyzed time interval, the system is linear and does not vary with time. One issue pointed out in [94], is that most of the research regarding data variability due to changes in EOC was carried out in laboratories, where basic signal processing techniques were enough to solve the damage detection problem [95]. Unfortunately, these techniques are not considered enough to be employed in an OWT during operation.

Scour effect on the natural frequency of OWT was studied in [96], where it was proved that while scour increases, the natural frequencies of the support structure, and therefore the WT, decrease. This phenomenon represents a threat for the turbine as the natural frequency gets closer to the rotor's frequency of rotation [59]. Therefore, continuous monitoring of WTs’ dynamics variations due to scour is recommended as it is expected to be a useful tool for developing maintenance plans regarding scour protection [96].

Another type of modal monitoring called resistance-based damage detection method has been found to be revolutionary due to the fact that it has the capability of detecting local damage. It uses piezoelectric materials which, by monitoring their electrical impedance, can detect the presence of structural damage. According to [83], only local response of the structure will be transmitted to the sensor in case the excitation frequency is big enough. Damage detection using this monitoring technique has been proven to be effective in different types of structures, including composite structures [97,98].

2.2.2.5 Strain monitoring

Strain monitoring is the technique that detects microscopic length variations in a component at pre-established locations, which does not necessarily mean damage detection. However, these length variations are known to be directly related to stresses and loads applied to the material [99]. Due to the fact that total deformations of large components, i.e. WT blades, are large because they are the sum of all the local deformations, they give no indication of local damage. For that reason, strain sensors have to be positioned at points of particular interest, where large deformations are expected. This limits their applicability to overall component damage sensing applications [100]. Strain monitoring has been proven to be useful in continuous operational WT monitoring as it was successfully employed in a 4.5 MW turbine [101]. However, in order to predict WT failures in blades, tower and foundation, prior knowledge of their component's stress field is required so that sensors can be mounted on critical areas.

Another SHM technology for strain monitoring is the strain memory alloys method, which relies on an irreversible crystallographic transformation for their smart properties. The transformation consists of the change, due to the strain, from one crystal state to another. The parent austenitic crystal structure is paramagnetic, while the product martensitic phase is ferromagnetic. Any SHMS related to this group of smart materials is considered as a passive system, as both full-time power supply and data storage facilities are not necessary. Instead, power is only needed during the sensor's interrogation, being the actual reading stored within the sensor element itself [102].

2.3 Operational Evaluation

2.3.1 Offshore wind turbines damage definition and detection

Damage definition constitutes a very important stage of the SPR paradigm as the boundaries of the problem are defined within it. Moreover, damage features have high variability among fields and structures. Therefore, identification of damage causes, consequences and features must be carried out at the beginning of any SHMS design phase. Several risk analysis techniques can be employed. Failure Mode, Effects and Criticality Analysis is considered one of the most widely used technique for this purpose [103,104]. Different reviews of OWT failure modes have been made in [17,58,105].

One of the main concerns regarding OWT damage detection is to identify the best way to detect structural damage. Usually the change in modal properties is used for this purpose [47]. However determining the best methodology constitutes a much broader field than what can be expected at first sight, as numerous different choices are available. Proof of this is the review of damage detection methods through the change in modal properties presented in [65]. The relevant method are: natural frequency based methods [106], mode shape based methods [106–110], mode shape curvature based methods [111–115], strain mode shape based methods [85,116–120], dynamically measured flexibility based methods [121–123], and neural network based methods [124–129].

Damage definition in OWT blades is closely related to the one that anisotropic reinforced laminated composites have. Delamination is one of the most common in composites [130], which is responsible for causing stiffness reduction, variation in resonant frequency, and decrease in buckling capacity. Such defects might be caused by poor process control during manufacturing, impact loading, or other hazardous service environments [40]. There are many other failure mechanisms for carbon–fiber composites, such as fiber breakage, matrix cracking, fiber splitting, and delamination, as listed in [131].

The most likely failure mechanisms that an OWT's tower and foundation can experience are corrosion and fatigue due to combined wind and wave loading [132]. Failure of these structures due to the accelerated fatigue produced by the increase of stresses, when natural frequencies are found to be similar to the rotor's frequency, can lead to catastrophic consequences which must be avoided. This phenomenon, known as resonance, has to be dealt early in the design stage of these structures taking into account all operation stages through a structure's service life [133]. In the particular case of pile-foundations, scouring and reduction in the foundation's integrity over time can be problematic. Scour reduces the fundamental structural resonances of the SS. Therefore, it can be considered a damage indicator as it can be correlated to a change in the natural frequency of the tower and an increase in the fatigue damage [93,96,134].

2.3.2 Variation in environmental and operational conditions

According to [135], the system's integrity state is a stochastic function of the initial system's integrity (quality), influenced by the acting loads (e.g. extreme loads, cyclic loads, environmental conditions). Even though a structure is considered to be damaged when at least one of its physical properties (mass, stiffness, etc.) varies, changes in EOC might induce variations in these properties without necessarily meaning that damage exists. In fact, in the majority of the situations, it is extremely difficult to assess whether or not EOC cause sensitive variations in the SHMS measurements [136]. For this reason, this topic has been recognized as an important issue in SHMS and has been identified as a key concern across the research community [29].

SHMS for OWT are particularly relevant in the design phase, during shipping, installation and operation. The application of SHMS in harsh environments is a particularly challenging task. The reasons are not only because these systems need to be prepared to withstand the severity of the environment for a long period, and the ease of installation, ruggedness and reliability of equipment is essential in providing key information about the SS's structural integrity, but also because OWFs are being developed further than ever before from coasts, which is making their OM critical [137].

The consequences that the variations in the EOC have on the dynamic behavior of structures have been assessed in different studies [40,138]. For example, a statistical methodology that propagates variability in measured Frequency response function data and calculates the level of uncertainty of the modal properties is explained in [139]. A good example of the effect of the variation in the EOC is presented in [94], where the turbulence suffered by the rotor affected the operational WT Control System. Other important factors that strongly influence SHMS signals are extreme events, such as earthquakes. SHM technologies are known to have an accurate characterization of input excitations. Seismic excitations are transient in nature, constituting an issue that limits the performance of most SHMS due to the fact that these technologies are based on the stationary stochastic-excitation assumption [40]. Further information regarding this issue can be found in [140]. To conclude, any methodology employed has to be able to distinguish between EOC that affect signals and damage features in order to allow the SHMS to detect only damages in the structure.

2.4 Data acquisition, normalisation and cleansing

2.4.1 Sensor types

As previously mentioned, SHMS for OWT can be used to detect damage in blades, tower and SS. This section aims to introduce the different types of sensors and technologies and in which subsystem these are used. From the top to the base of the OWT, blades constitute a difficult element to integrate SHMS due to the high variety of failure modes that can develop, the high strains they experience, the fact that they are rotating components, and the high variability in their operating conditions [94].

Different sensors can be used in blades, as confirmed by different reviews [141]. Two approaches are followed: active and passive sensing technologies, whereby active sensing, but not passive, needs an external excitation [94]. Tower and foundation constitute two key elements of OWT as they are not replaceable unless a significant cost is assumed. These are components that, once the turbine is installed, should sustain associated loads and their partial failure would carry catastrophic consequences. Therefore, early in the design stage, the intended turbine's service life and the possibility of extending it or repowering it with a new nacelle, must be taken into account [142]. Furthermore, due to the difficulty and sensitivity of fatigue analysis, SHMS should be installed in order to be able to verify the accuracy of the design calculations and implement an optimal OM Strategy. These SHMS will mainly consist of fatigue and modal properties monitoring (such as resonance frequency or modal curvatures), corrosion and scour monitoring. It should be noted that regarding SHMS for operating WTs, not much progress has been made in developing robust applications, especially for OWT blades [143].

Some of the methods that were introduced in Section 2.2 [143–146] include vibration monitoring-based methods (accelerometers, piezo or micro-electromechanical systems (MEMS)), strain (strain gauge or fiber optic cables), ultrasonic waves which are widely applied in composite structures (piezoelectric transducer), As (usually barrel sensors), impedance techniques, laser vibrometry, impedance tomography, thermography (infrared cameras), laser ultrasound, nanosensors, and buckling health monitoring. The necessary sensors for implementation of these techniques are described below.

Structural dynamic responses are usually monitored by embedded strain gauges, piezoceramics or accelerometers [147]. Accelerometers are relatively simple devices whereby the operating principle is the comparison of the acceleration they experience with the acceleration due to gravity. They are commonly provided as MEMS which are very small devices with computing capability. These devices are commonly used for modal parameters and vibration monitoring of blades, tower and foundation of the WT. There are various types of accelerometers available, such as piezoelectric, optical, laser, capacitive, and servo. The selection of an accelerometer for a specific application depends on a number of factors, such as amplitude and frequency range of the response, sensitivity, resolution, etc. [49]. The SHM of civil engineering structures using plastic optical-fiber based accelerometers for estimating the natural frequencies by measuring the dynamic response was carried out in [148]. Other types of sensors that can be used to analyze modal parameters are piezoelectric patches, which were used in [63] at critical locations with the aim of comparing their natural frequency. Velocimeters, on the other hand, operate based on a principle similar to interferometry. In SHM these devices are primarily used to measure displacement by integrating acceleration or velocity measurements of the structural members they are attached to [149].

Two popular sensor groups exist for the purpose of strain measurement: traditional electrical and relatively modern fiber optic [99]. Electrical strain gauges have become so widely applied that they dominate the entire field except for special applications. They are, along with electrical resistances, the most popular types of sensors [150], closely followed by Fiber Bragg Grating (FBG) sensors, which recently have experienced considerable improvements [151].

Several types of electrical sensors are available on the market, including capacitance, inductance, semiconductor and resistance. Each is sensitive to a differing electrical property [150]. Resistance strain gauges record the resistance variation of an electrically conductive wire relative to displacement. This resistance variation occurs due to a change in the cross sectional area and length of the wire as the specimen is elongated. Electrical resistances are generally used for identifying cracks in composite materials and joints. The most suitable material for monitoring using this method is carbon fiber polymermatrix composites as their electrical properties are affected by structural damage. This material is commonly used due to its strong, super-elastic, and piezoresistive properties [152]. These sensors can also be used for identifying failures in conductive bolted joints. A novel method for analyzing the structural health of alumina nanocomposites, by the change in electrical conductivities after indentation, is proposed in [153]. The utility of the electrical resistance method for locating barely visible impact damage in carbon fiber composite structures was explained in [154].

Piezoelectric materials, when subjected to stress, produce an electric field and vice versa when subjected to an electric field. Furthermore, changes in the fundamental properties of the structure, such as mass, stiffness and damping, directly make the mechanical impedance vary, this variation being a clear damage indicator [155]. Damage detection using changes in the electromechanical impedance of piezoelectric wafer active sensors can easily be done by attaching them to the structure [156].

Even though piezoelectric materials are the most common sensor type for stress monitoring, there are many other sensors that can also be applied to this aim, such as: thin film sensors, piezoelectric composite materials, rolling sensors, and optic-based sensors [83]. However, an important drawback of this technology is temperature and ambient vibrations effects in the piezoelectric sensors' performance in composites, as explained in [40]. Temperature effect in blades must be compensated in the results, as they are made from this material. In fact, [157] explained how a rise in temperature and vibrations can jeopardise the detection of the delamination caused by impacts. Other common drawbacks that strain gauges might experience are described in [99]: nonlinearity, hysteresis and zero shift due to cold work [150].

Cracks and displacements can also be monitored by fiber-optic sensors which usually include: spectrometric, interferometric or intensity-modulated. An optical fiber is a glass or plastic fiber designed to guide light along its length. Moreover, FBGs were also proved to be useful as a corrosion transducer and temperature sensor simply by adding a metal coating to one segment of the fiber [158]; as a pH-sensitive corrosion detector [159] and good at delamination identification [160]. Furthermore, fiber-optic sensors are employed in SHMS for OWT in various forms:

1) Plastic fiber-optics can be attached, for example, to the blade of a WT to measure loads it bears. This measurement is carried out by the reduction of the

light source's power that takes place in the plastic fiber-optic depending on the strain to which it is subjected [161]. This concept is used to sense strains in a structure. When loads increase, the measured optical power is reduced being damage detectable. This is due to the fact that the normalized optical power decreases linearly as the strain increases, and drastically once the crack density in a composite laminate specimen increases [161].

2) FBG is made by illuminating the core of an optical fiber with a spatially varying pattern of intense Ultraviolet laser lights that have sufficient energy to break the highly stable silicon–oxygen bonds, which will raise, to some degree, the refractive index [162]. Although the main use of FBG consists of measuring strains crack evolution [161], impact damage can be detected by distributing FBG over the structure [163,164].

3) Optical fuses transversally positioned in laminated composites have been proven to be useful in damage detection [165]. For example, if short length optical fibers are embedded through the thickness of a graphite/epoxy laminate during the manufacturing process, the fibers act as optical fuses, which will break in areas of low energy impact damage [166].

2.4.2 Data collection and storage

It is widely recognized that data acquisition is a complex, tedious and costly process [167]. The recent development of wireless monitoring has brought a big advance in SHM and infrastructure asset management as it integrates wireless communications and mobile computing with sensors. The result is a more economic sensor platform that has three functions: acquisition of structural response data, local interrogation of collected measurement data, and wireless transmission of that data or analysis results to a Wireless Sensor Network (WSN), which comprises other wireless sensing units [46]. As explained in [168], a WSN is composed of four mean stages: communication, data acquisition, processing, and fusion stages. Moreover, WSNs encompass many fields: wireless communication, network technology, integrated circuits, sensor technology, MEMS, among many others. WSNs are composed of data acquisition systems which have numerous design parameters: a number of channels, a maximum sampling rate, and resolution, among others; a computational core, where all the data acquired are stored and which possess processing capabilities; and the wireless communication channel.

A real WSN application is presented in [167], where three WTs (instrumented with WSN) proved their efficacy in operational conditions. While in the first turbine instrumented, the aim was to prove the accuracy in the collection and transmission of vibrational data from the turbine's tower, in the second turbine instrumented, several strain gauges were also included at its base. In both turbines, wireless communication channels' performance was assessed and their data was used for offline output-only towers modal analysis.

The acquired data from WTs contains key features for future developments in the wind energy Industry. For that reason, operators are now appreciating the importance of investing in SHMS [169]. However, even though monitoring has many proven advantages, it is expensive and its costs are one of the causes why only a few operational turbines have extensive sensor instrumentation [167],. An assumption usually made, is that traditional cable based monitoring systems are cheaper and easier to install. Nevertheless, this technology is not only more costly to install, but also introduces difficulties in the installation process due to the cables. On the contrary, wireless sensors are substantially cheaper and easier to install than traditional cable-based systems [170]. In the case of turbine blades, wireless communication eliminates the necessity of moving data through a slip ring interface, which is difficult and costly.

Wireless sensors are not, exactly, cable-based sensor replacements; without wires, wireless sensors usually depend on internally stored power for operation. Inefficient use of wireless sensors will deplete this precious energy source rapidly, making frequent battery replacement necessary. Among the three different types of WSN topologies (Star, Cluster tree, and Mesh [168]) there are several important issues for WSN use in SHMS. These were summarized in [167], as follows: compatibility issues between different types of sensors, their sampling frequencies, the problem of transmission bandwidth and real-time ability variance, the selection of a wireless transmission frequency, topology choice, data fusion method, and the contrast between the energy consumption requirements of different applications to that of each different device.

Even though WSN have been proven to be applicable to OWFs [80], their major disadvantage is that high amount of power is needed by the sensors, which had been tried to be diminished with an increased interest in data telemetry with energy harvesting [171,172]. In order to provide enough power to the sensors without using batteries, piezoelectric, thermoelectric and photovoltaic energy harvesting techniques were assessed in [173], on a cross section of a CX-100 WT blade. The aim was to determine the feasibility of powering individual nodes that would compose the sensor network. In another study [174], a 4-channel AE wireless node was powered by structural vibration and wind energy harvesting modules.

2.4.3 Data normalisation and cleansing

The ability to normalize the measured data with respect to varying EOC is a key aspect of SHMS in order to avoid false positive indications of damage [31]. One example of the when the normalization process needs to be carried out to the measured inputs is when modal parameters are being extracted. Two strategies can be employed for normalizing these data: when the EOC are available and are not available.

The most important aspect regarding accuracy of data normalization comes with the damage sensitive features that must be extracted from these data. Those damage sensitive features must not be lost or diluted by the normalization process. There are different data normalization techniques. Some examples are: the subtraction of the mean value of a measured time history for direct current off-sets removal from the signal, the division by the standard deviation of the signal for normalizing varying amplitudes in the signal, curve fitting of analytical forms of the frequency response function to measured frequency response functions in experimental modal analysis, among others. If the structure is linear, this normalization procedure removes the influence of the input from the parameter estimation procedure.

Data normalization constitutes a very important part of the damage identification process as it affects significantly Neural Network (NN) performance [175]. Even though not all sources of variability in the data acquisition mechanism can be eliminated, they need to be identified and minimized as much as possible [176]. Therefore, appropriate measurements need to be carried out in order that such sources of variability can be statistically quantified [31]. An example of data normalization in OWT is explained in [177], where a non-linear regression model was used to perform data normalization in real-life data obtained from the Monopile (MP) structure of an OWT. Further research on this topic will be carried out in the future as, in order to achieve successful SHM goals, data normalization procedures need to be able to discriminate whether measurement variations are motivated by damage in the structure, or by changes in the EOCs [178].

Data cleansing is the procedure of selectively choosing data to pass on or to reject from the feature selection process or, in other words, is the procedure of selectively discarding data that might not represent the system's behavior [32]. Data cleansing is a difficult process due to the fact that it is commonly based on experts' knowledge gained in previous data acquisition processes. An example of data cleansing could be when a sensor is discovered to be loose and, therefore, based on the judgment of the experts; the measurements carried out by that sensor are not accurate and can jeopardise the accuracy of the data set. For this reason, the whole set might be discarded from the feature selection process. Signal processing techniques, such as filtering and resampling, can also be thought of as data cleansing procedures [37,46,179,180].

2.5 Feature extraction and information condensation

Feature extraction constitutes the methodology that refers to the identification of the damage sensitive physical characteristics. It is usually determined by the data obtained from the structure and is application specific [181]. Many methods can be used for damage feature identification, the most basic one being comparison of SHMS output data with similar data obtained when the same structure has experienced a damaging event. This methodology is based on the fact that damaging events have already occurred. Another process for feature identification is the numeric simulation of the damaged system's response to postulated inputs, which is currently the most used technique in several industries, e.g. the automotive industry. Another option for recognizing these sensitive features would be testing the structure or a representative specimen in a laboratory, introducing the expected damage. Damage-accumulation testing, during which structural components of the system under study are subjected to a realistic loading, can be used also to identify appropriate features [40]. As Farrar and Worden explain in [32], this methodology might involve induced-damage testing, fatigue testing, corrosion growth or temperature cycling to accumulate certain types of damage. As such, numerous articles in this theme issue are devoted to the feature extraction portion of SHM [33,34,182,183].

Data condensation constitutes an inherent part of the feature extraction procedure. The different types and quantity of sensors needed to make any SHMS work efficiently and accurately usually produce huge amounts of data. Therefore, data condensation is, most of the time, a necessary stage occurring before the analysis of the extracted data through the statistical models. One possibility of data condensation is to summarize all the damage sensitive features into feature vectors of small dimension. This constitutes an accurate way of estimating the feature's statistical distribution [40]. Moreover, data condensation is not only beneficial due to the savings in computational power, but also necessary in case of comparisons of many data sets over the lifetime of the structure. Even though the more data condensation is achieved, the more computational power is saved; the sensitivity of the chosen features to the structural changes under a certain level of variability in the EOC has to be ensured by the employment of robust data reduction techniques (such as, principal components analysis [184], discriminant analysis [185], regression analysis [186], etc. [187]).

Another option for data condensation in AE is proposed in several studies such as [17,188]. This technique is based on the use of Structural Neural Systems, a highly distributed sensor concept that mimics the signal processing in the biological neural system [62]. This methodology is employed in situations when a great level of accuracy in the damage evaluation is needed, as both the number of sensors and the amount of power needed for condensing and processing the data increase considerably. Moreover, an improvement in this technology is presented in [189] by the connection in series or array pattern of multiple piezoceramic patches. This connection decreases the amount of channels necessary for data collection of AEs or high strains.

2.6 Statistical Model Development

Statistical model development is the Pattern Recognition section that addresses the applicability of the algorithms that operate on the extracted features, identifying and quantifying damage in a structure. There are two main types of algorithms: supervised and unsupervised learning [23–25]. These categories of algorithms correspond to SHMS that do contain and do not contain data from the damaged structure, respectively. Supervised learning approaches are preferable, as by their application, damage can be classified and quantified, while damage identification is the further level of damage, according to Rytter's damage states of a system [190], that unsupervised learning algorithms allow [40].

2.6.1 Supervised Learning

When supervised learning approaches are employed, very high demand of data is associated with them, as data from every conceivable damage situation must be available [191]. The two possible sources of damage data come from: physics-based modelling (i.e. from Finite Element Analysis (FEA)), and experiments. Difficulty in obtaining these data in some fields jeopardises the applicability of this approach (e.g. aviation). Moreover, to accumulate enough training data, copies of the system of interest that can be intentionally damaged in different ways, might be necessary. The different analyses that can be categorised as supervised learning algorithms are introduced below.

2.6.1.1 Response Surface Analysis

Response surface analysis obtains the approximation relationship between the resonance frequencies and other damage parameters (i.e. damage location, and size). An example of this technique is explained in [192], where damages were satisfactorily identified in beams and plates made of carbon fiber reinforced plastic. The technique was applied to data simulated in analytical models. Nevertheless, the applicability of this technique, experimentally, is low as numerous data from various damage conditions are required.

2.6.1.2 Fisher's Discriminant

This method introduces a linear transformation of the original multivariate distributions into univariate distributions whose means are as far apart as possible, while the variances of those transformed distributions are as small as possible [40]. It was satisfactorily applied in [18] where linear and quadratic discrimination methodologies were implemented to measurements taken from a concrete bridge column subjected to static and dynamic testing. No relevant applications of this methodology have been found for OW; however in [193] a new co-training algorithm based on modified Fisher's linear discriminant analysis was proposed for semi-supervised learning, which is meant to be very useful in applications such as brain-computer interface design.

2.6.1.3 Neural Networks (NN)

Neural Networks (NN) are commonly used in SHMS for identifying, locating, and quantifying damage in structures. This methodology is nowadays very well known as substantial textbooks and monograph accounts exist [194]. NN are the group of statistical learning models inspired by biological NN. The reason NN are extremely useful in SHM applications is the fact that they are used to estimate or approximate functions that can depend on a large number of inputs and are generally unknown [190].

Some of the studies that have employed NN in the past for assessing structural damage include: the evaluation of two NNs for damage assessment, namely the Multilayer Perceptron Network and the Radial Basis Function Network [195];

and the damage detection and location in a numerical simulation of a two-dimensional truss structure by using a feed-forward NN [184]. Other studies employed NN for assessing the integrity of bridges as the auto-associative NN employed in [196,197] where NN were trained with FEA data of the bridge.

NNs were also used for structural damage detection in plate truss structures, where damage was assessed by evaluating different learning rates, network types, reduction techniques of network topologies, and dimension analysis [198]. Different reports [124,199,200] assess the benefits and drawbacks of using sensors and NN to detect impact in composite materials, which could be a possibility for SHM of OWT blades.

2.6.1.4 Genetic Algorithms

Ruotolo and Surace did most of the research related to this field between 1996 and 2001 [201–204]. In 1997 they formulated a problem for choosing the location and depth of cracks in beams employing measured modal parameters, which afterwards will be optimized by a genetic algorithm [203,205]. Nevertheless, there are some practical issues because, as the structure's complexity increases either size or geometry, the optimization becomes prohibitive [40]. The same authors carried out a similar study in 1998 where genetic algorithms, simulated annealing, and eigensensitivity analyses were compared in order to identify several damage scenarios in a FEA of a frame structure [206]. Similar studies were carried out in [207] for detecting damage in a composite beam.

2.6.1.5 Support Vector Machine

Support Vector Machines constitute a powerful framework for general classification and regression problems; as many different types of discriminant functions, such as linear, nonlinear, neural network, and radial-basis discriminant functions, can be put in this tool with no real modifications [208]. While in [209], a Support Vector Machines is applied to damage classification problems in ball bearings and truss structures, in [178], nonlinear principal component analysis based on the unsupervised support vector machine is introduced and incorporated for data normalization.

2.6.2 Unsupervised Learning

Unsupervised learning constitutes an alternative to Supervised Learning when no damage state data is available. However, the drawback of the unsupervised learning algorithms is that they can only be used for detection and possibly locating the damage [210]. For that reason, they have perhaps received less attention than Supervised Learning approaches. A common type of unsupervised learning algorithms is known as novelty detection or anomaly detection method [211–213]. The idea of novelty detection is that only training data from the normal EOC of the structure or system are used to establish the diagnostic. To do so, a model of the normal EOC is created with the aim of comparing it with the one made with the newly acquired data. When significant deviations are detected, the algorithm indicates novelty, which means that the system has departed from the normal condition and, therefore, acquired damage. Unsupervised learning algorithms can be roughly categorized into three groups, namely Control Chart Analysis, Outlier Detection, and Neural Networks (NN).

2.6.2.1 Control Chart Analysis

This methodology continuously monitors the features extracted from the measurements, for anomalies. When the observations fluctuate outside the control limits, the monitoring system alarms the abnormality of the system's condition [40]. In [18], Control Chart Analysis for monitoring a reinforced concrete bridge column was used. It has also been frequently used for process control of chemical plants, manufacturing facilities, and nuclear power plants.

2.6.2.2 Outlier Detection

Outlier, or novelty detection, is the primary class of algorithms applied in unsupervised learning applications. These algorithms assess statistical distributions of the measured or derived features to enhance the damage identification process [214]. When applied in an unsupervised learning mode, statistical models are typically used to answer questions regarding the existence and location of damage. When applied in a supervised learning mode and coupled with analytical models, the statistical procedures can be used to better determine the type of damage, the extent of damage and remaining useful life (RUL) of the structure. The statistical models are also used to minimize false indications of damage (both false-positive and false-negative), as these are undesirable.

Outlier detection methodologies use changes in the rank of a matrix as a damage indicator [206]. Firstly, a matrix is composed by putting the feature vectors in columns, measured during various EOC of a structure, without any damage state. Singular value decomposition is used to estimate the rank of this matrix. After that, the same matrix is increased by adding an additional column containing a new feature vector, this time corresponding to a potential damage state of the structure. In case this new feature vector corresponds to a damaged structure, it will be independent from the previously measured vectors and, therefore, the rank of the matrix will increase [215].

The basic principle of novelty detection is that a model of the system is built using training data only acquired from normal EOC of the structure. While the monitoring of the structure takes place, newly acquired data are compared with the model. In the case that significant deviations are found, the algorithm indicates novelty, which means that the system has deviated from the normal condition and, therefore, is damaged [216]. Three different novelty indices to detect damage in composite plates where introduced in [217]. Thus, a stochastic subspace approach to determine damage existence in a structure was used in [218].

2.6.2.3 Neural Networks

NNs in the Unsupervised Learning mode work in the same way as in the Supervised, apart from the fact that no data from damaging events are available. A good example is the adaptive NN model proposed in [219]. In the model, data obtained from FEA simulations are used to train the NN; being the modal parameters from the FEA simulations used as inputs. The NN output will consist of structural parameters. Once modal parameters from the actual structure become available, the NN is used to calculate the associated structural parameters. Finally, the FEA model is updated using these new structural parameters, calculating the associated modal parameters. Training will stop when the measured modal parameters are acceptably not so different from those calculated from the FEA model. In [220] a discussion of delamination detection within composites applying a similar methodology can be found. Good agreement between experimental and analytical results was achieved. In [221], synthetic damage patterns are introduced in the FEA models. These models' structural responses to the damage patterns are calculated, analyzed, and archived in a "damage catalogue" which was used for posterior deteriorations and damage assessment of the WT structure, in near-real time. The most recent NN application to WT blades is explained in [95], where the different NN types that can be used are identified.

2.7 Discussion

Previous sections have reviewed the different SHM technologies that could be employed for OWT. A summary of related critical aspects, such as cost-effectiveness, capabilities and limitations can be found in Table 2-1, based on a structured survey aiming to map current practice within the industry. Responses have indicated high levels of interest and engagement in this topic obtaining responses from multiple industrial stakeholders including sensor providers, equipment providers, consultancies and designers, and developers/operators.

Some of the conclusions derived from the data collection process can be summarized below:

- First generation of WF were equipped with sensors after their deployment. The technologies mostly used were strain and fatigue and modal properties monitoring.
- The percentage of instrumented turbines within a WF is between 3% and 12%, showing a wide discrepancy in best practice.
- Strain gauges, accelerometers and inclinometers are the technologies mostly used for SHM. Linear Variable Differential Transducer (LVDTs) are of interest as they can measure displacements with high reliability and accuracy, however at the expense of cost.

- To date, natural frequency analysis is considered to be the most commonly applied practice for detecting deviations from the design intent in WT foundations, as other techniques are either very expensive, low maturity or of low accuracy.
- Fiber optics technology for strain measurement is considered a promising future technology due to the numerous benefits it brings. However, this option has not been costed or implemented in any case and installation needs to be carefully assessed.
- A necessity of the development of new methodologies to collect, review, purify and analyze the data collected by CM and SHM solutions has been pointed out by most of the interviewees.

Table 2-1 Technology assessment: capabilities and limitations

Technology	Capabilities	Limitations
Acoustic Emission Monitoring Type of sensors: - Piezoelectric Transducers	• Very effective detecting failure mechanisms up to microscale. • Allows a simple, rapid and cost-effective inspection or monitoring of a structure. • Good response at low frequencies. • Multifunctional character of piezoelectric sensors.	• Limited application offshore • Variable damage characterization and assessment effectiveness depending on the algorithm. • Optimization of data processing needed as it still takes up much time and computational effort. • High sensitivity to background noise. • AE systems can only qualitatively gauge how much damage is contained in a structure. • Determining acoustic signature of the structure is very difficult
Thermal Imaging Method Type of sensors: - Impedance tomography - Thermography (infrared cameras)	• Fast. • Cost effective. • Trials using drones are currently being conducted, which will detect cracks up to 0.3mm based on technology limitations, avoid the necessity of having personnel inside the turbine and be even more cost effective. Moreover, time required would be less than traditional sensors.	• Limited implementation in offshore structures. • Camera resolution for detecting cracks • Laborious Image processing • Cracks detection needs more automation from footage.

Ultrasonic Methods Type of sensors: - Piezoelectric Transducers	• It is sensitive to both surface and subsurface discontinuities. • The depth of penetration for flaw detection or measurement is superior to other NDT methods. • Only single-sided access is needed when the pulse-echo technique is used. • It is highly accurate in determining reflector position and estimating size and shape. • Minimal preparation is required. • Electronic equipment provides instantaneous results. • Detailed images can be produced with automated systems. • It has other uses, such as thickness measurement, in addition to flaw detection.	• • Surface must be accessible to transmit ultrasound. • Skill and training required is more extensive than other methods. • Coupling medium to promote the transfer of sound energy into the test specimen is required. • Difficulty of inspection of rough, irregular, very small, exceptionally thin or not homogeneous materials. • Difficulty of inspection of cast iron and other coarse grained materials. • Linear defects oriented parallel to the sound beam may go undetected. • Reference standards are required for both equipment calibration and the characterization of flaws.
Fatigue and Modal Properties Monitoring Type of sensors: - Accelerometers. - MEMS. - Plastic optical-fiber based accelerometers. - Velocimeters.	• High reliability, mature technology • Easy installation. • There are many different techniques available for this purpose. • Recent developments in Operational Modal Analysis solve some limitations. • Stable performance.	• Difficult analysis in operating conditions. • High number of uncertainties when applied in the offshore environment. • Environmental and Operational Conditions changes have to be accounted in the results. • Difficulties in wind and wave loads measuring.
Strain Monitoring Type of sensors: - Strain gauge (capacitance, inductance, semiconductor and resistance). - Fiber optic cables. - Fiber Bragg Grating (FBG).	• Easy installation process once appropriate training has been undertaken. • Mature technology. • Optical fiber might be the future of strain monitoring as it is less prone to fatigue, eliminates wiring issues and allows more points to be monitored with the same cable.	• Not very robust system. • The installation is very sensitive to misalignments. • Reduced service life. • Distance between the sensor and the Data Acquisition System influences accuracy and limits sensor location. • Mechanical properties limitations • Can be affected by EMI noise.

2.8 Conclusions

In this publication, a review of the SPR paradigm for SHMS for OWT was carried out. It is expected that by the assessment of each one of the stages present in this paradigm, SHMS can contribute in the development of an appropriate Condition Based Maintenance Strategy. The optimization of this strategy will lead to reducing labor costs of WT inspection, preventing unnecessary replacement of components, discovering design weaknesses before failure, improving the availability of power while preventing WTs overloading, and maximizing return in WF investments [50]. Increasing efficiency in OM will contribute towards achieving United Kingdom's 2020 and 2050 targets, through ultimately reducing the LCoE [222].

2.9 Acknowledgements

This work was supported by grant EP/L016303/1 for Cranfield University, Centre for Doctoral Training in Renewable Energy Marine Structures (REMS) (http://www.rems-cdt.ac.uk/) from the United Kingdom Engineering and Physical Sciences Research Council (EPSRC).

3 PARAMETRIC FINITE ELEMENT ANALYSIS MODELLING OF OFFSHORE WIND TURBINE SUPPORT STRUCTURES: TOWARDS SCALING-UP AND CAPEX REDUCTION

Maria Martinez-Luengo, Athanasios Kolios and Lin Wang

Centre for Offshore Renewable Energy Engineering, School of Water, Energy and Environment, Cranfield University, Bedford, Bedfordshire, United Kingdom

Submitted 30th November 2016, Accepted 24th May 2017

Published in the International Journal of Marine Energy, 2017, 19, 16-31

DOI: 10.1016/j.ijome.2017.05.005

Statement of contributions of joint authorship

Maria Martinez-Luengo conducted the literature review on the subject, developed the parametric model, planned and performed the validation and analyses for the case studies, calculated the loads and soil-structure interaction, drafter and critically reviewed this manuscript. Also, María analysed the results and produced figures and tables in this paper. Athanasios Kolios and Lin Wang proof-read and critically commented the manuscript before its submission to the International Journal of Marine Energy.

Abstract

Parametric Finite Element Analysis (FEA) modelling is a powerful design tool often used for Offshore Wind (OW). It is so effective because Key Design Parameters (KDPs) can be modified directly within the python code, to assess their effect on the structure's integrity, saving time and resources. A parametric FEA model of an Offshore Wind Turbine (OWT) support structure (SS) (consisting of MP, soil-structure interaction, transition piece (TP), Grouted Connection (GC) and tower) has been developed and validated. Furthermore, the different KDPs that impact on the design and scaling-up of OWT SS were identified. The aim of the analyses is determining how different geometry variations will affect the structural integrity of the unit and if these could contribute to the turbine's scale-up by either modifying the structure's modal properties, improving its structural integrity, or reducing capital expenditure (CAPEX). To do so, three design cases, assessing different KDPs, have been developed and presented. Case A investigated how the TP's and GC's length influences the structural integrity. Case B evaluated the effect of size and number of stoppers in the TP, keeping a constant volume of steel; and Case C assessed the structure's response to scour development. It is expected that this paper will provide useful information in the conceptual design and scale-up of OWT SS, helping in the understanding of how KDPs can affect not only the structure's health, but also its CAPEX.

Keywords: offshore wind turbines; structural health monitoring; key design parameters, structural integrity.

3.1 Introduction

In 2007 the European Union set particular and challenging goals to all Member States, establishing that by 2020 the United Kingdom (UK) must produce 15% of its energy consumption from renewable energy sources. Wind energy is probably the most promising technology contributing to decarbonisation within the UK; in fact, its growth over the last decade confirms this. According to Renewable UK [15], 1.4 GW were installed offshore in 2015 in the UK, making the total Wind Energy capacity 13.3 GW. In other words, wind energy alone provides more renewable electricity than all other sources combined.

According to [223], OW deployment could reach 20-55 GW by 2050. Nowadays and for the next few years mature fixed-bottom technology will dominate, exploiting shallow and close-shore sites, which can be installed at low cost. Beyond 20 GW, fixed-bottom turbines will be forced to move further from shore to access suitably shallow waters, creating numerous challenges. Floating wind (FW) would mitigate some of these challenges, making deep water sites close to shore suitable. In fact, a contribution between 8 and 16 GW of floating is expected if the 40GW of OW deployment is reached. Despite all the advantages, FW technology has yet to be demonstrated at large scale and to face the challenge of driving costs down. A number of cost projections suggest that FW can reach cost parity with fixed-bottom during the 2020s if adequate support is provided by government. Another study [224] suggests that leading FW concepts could achieve a Levelised Cost of Electricity (LCoE) of £85-95/MWh in large-scale commercial projects, with further cost reduction possible over time.

This trend in increasing Wind Farm (WF) capacity will not only be maintained in the following years, but also a progressive increase in OWT size is expected [14]. OWT capacity has grown by 41.1% from 2010 to 2015. In 2015, the average capacity of new OWT installed was 4.2 MW, a significant increase from 3.0 MW in 2010, reflecting a period of continuous development in turbine technology to increase energy yields offshore. The deployment of 4-6 MW turbines seen in 2015 will be followed by the gradual introduction of 6-8 MW turbines closer towards 2018 [16].

With this rapid growth in capacity and size, the scale-up of OWT presents some issues that need to be assessed. A couple of these are the interference between the structure's modal frequencies, with the rotor and environmental excitations and the trade-off between the increase in power and its economic cost. Designing OWT is challenging due to the dynamic sensitivity of the structures. The reason is the proximity of these structures' natural frequencies to those of the wind, wave and 1P (rotor frequency) and 3P (blade shadowing frequency) [225]. Typically a soft-stiff design where the structure's frequency is between 1P and 3P would be targeted. Nevertheless, this gap is very small, which may result in a design prone to dynamic amplification of responses [226]. This enhances the fatigue damage and reduces the intended design life [227]. Furthermore, bigger, more efficient turbines will help drive costs down 30% by 2020 [228], which will help OW to compete with more conventional energy sources. An example of this is the recently upgraded V164-8.0 MW OWT, which enables an 8 MW platform to reach 9 MW depending on specific site conditions. It set a new record for power production at Østerild, generating 216,000 kWh over a 24 hour period. Torben Hvid Larsen, MHI Vestas CTO stated that this OWT will play an integral part in enabling the OW industry to drive LCoE down.

A trade-off between durability of structures and the CAPEX costs needs to be made. Durability is the resistance to age-related deterioration, in particular corrosion and fatigue due to operational and environmental loads. Certain structures have less structural redundancy or may be inherently designed to resist higher stresses [229]. CAPEX is taken to mean an expenditure whose benefit extends beyond one year, and refers here to the costs associated with building and installing the plant. CAPEX mostly comprises material and labour costs for turbines, foundations, and inter-array cabling, but also includes construction financing, development costs, and operating capital [230]. According to [231], 32%

and 14% of the CAPEX will be spent on turbine and foundation costs respectively, in offshore projects. Cost modelling of OWT constitutes a broad field; however, it is safe to say that by bringing the cost of the turbine and foundation down and not posing additional difficulty in installation and manufacturing, CAPEX will decrease [232]. This reduction in CAPEX will have a positive impact in the LCoE, which represents the Key Performance Indicator (KPI) that allows OW to be compared to other, more conventional, energy sources. Wind energy and its further growth is hindered by wind's intermittent nature. Moreover, increasing OW generation influences the reliability of electric power grids. Thus, there is a demand for new technical units providing ancillary services. Non-dispatchable renewable energy sources can be balanced by energy storage devices [233]. Despite near future levels of curtailment and intermittency, will not exclusively refinance additional storage but can aid reducing offshore connection charges representing around 20% of total CAPEX costs [234]. The design and control of OWT require in-depth analysis in order to ascertain their energy capabilities and operation boundaries.

Today, as OW is considered to be a relatively mature technology, operators are progressively feeling more comfortable with it and are willing to balance structural risks with a CAPEX reduction. The use of design methods and standards, and their combination with high fidelity FEA modelling, is considered a powerful and cost effective tool in the design of offshore structures. This paper identifies KDPs for the design and scale-up of OWT SS and analyses the potential impact that the implementation of engineering design decisions in these KDPs, will suppose structurally and economically.

3.2 Design Provisions and parametric modelling of offshore wind turbine monopile structures

3.2.1 Key Design Parameters of OWT support structures

The KDPs of OWT SS are identified through analysis of the relationships among its structural behaviour and economic parameters. Main input data to the model comprise parameters related to the environmental and site conditions, mainly related to the wind, wave and hydrodynamic loads. These will influence the WT's geometry and material properties, which constitute the KDPs of the model. These KDPs can be modified for cost optimisation, or scale-up the OWT SS which, combined with the scale-up of the OWT's rotor size, can be used to capture more wind. The effects of wind turbine (WT) size on the aerodynamic characteristics of a rotor blade were examined by [235], using CFD simulation. KDPs directly affect the KPIs of the system such as LCoE, capacity, availability, etc. For example, a minimum stiffness and thickness (KDPs) are necessary to meet structural integrity requirements, in order to operate at nominal capacity (KPI) [227,236–238].

Environmental conditions play an important role in the design of OWT SS, and a detailed study needs to be conducted in order to assess wind speed ranges, turbulence level, main wind and wave directions and how the structure will behave under their different interactions. Mean water level also plays an important role as the hydrostatic pressure can contribute towards stabilising the structure but also can pose design complications when moving to deep waters.

Since foundations constitute the pillars that sustain the whole structure, site investigation is crucial. Soil layer composition, depth and material properties, such as their strength, together with the environmental conditions, will determine the necessary pile depth. Pile thickness will not only be influenced by the site conditions, but also by the environmental excitations that will strongly determine the dynamics of the structure.

Although for a given rotor and nacelle dimensions, the weight and thrust force (KDPs) cannot be optimised from a structural point of view, their efficiency (aerodynamics combined with pitch and yaw control mechanisms) will make an impact on the turbine’s power production (KPI). Moreover, environmental conditions will also have an impact on this matter. Additionally, for optimised power production that accelerates the RoI, a minimum tower length needs to be reached. Tower length, diameter and thickness are connected to ensure that not only safety limits (Ultimate Limit State (ULS), Fatigue Limit State (FLS) and buckling) are maintained, but also that enough stiffness is achieved so that natural frequencies are within the safety limits (1P and 3P frequencies), ensuring no resonance occurs.

Furthermore, the TP is a crucial part that interconnects the tower and the MP. Its KDPs would be the diameter and thickness, which need to be compatible with those of the tower and foundation. Thus, the number, size and volume of stoppers, which are the contact point between the TP and the MP, will strongly depend on the load excitations. Moreover, these KDPs can also influence the modal frequencies of the structure and become a dangerous risk in the event of extreme loading, leading to the loss of one or more of these stoppers; therefore, the structural integrity of the unit will be strongly compromised. Lastly, the TP’s length and the volume of the stoppers could be optimised in terms of stiffness, natural frequencies and mass. Mass reduction is an important aspect of WTs’ design as it can strongly affect CAPEX and therefore the LCoE of a project. The soil-structure interaction constitutes an important aspect of OWT SS design. Soil profile properties make an important impact on the foundation’s KDPs, which will vary depending on the type of foundation employed. Diameter, thickness and length constitute the main KDPs of Monopile (MP) foundations. However, other KDPs, such as joints in jacket structures, flooded members and Marine Growth, among others, would have to be considered for other foundation types [239].

3.2.2 Geometry

This study analyses how different variations of the geometry can contribute to the scalability and CAPEX reduction of OWT SS. The reference site is located in the North of the UK. The reference turbine used for this analysis consists of a 3.6MW Siemens turbine, connected to an 80m tower, a TP and is sustained by a MP foundation. The MP is 31m long and is embedded 18m into the soil and submerged 11m into the ocean. Figure 3-1a shows a schematic of the OWT SS 3D model. The TP (Figure 3-1b) is 24m in length and joins together the MP and the tower. Six stoppers located in the internal surface of the TP, would allow it to rest on top of the MP. The GC, located between the TP and the MP, is used for the appropriate transmission of loads and stresses. This assembly can be seen in Figures 3-1c and d. The OWT SS was modelled using Abaqus, which is a widely used FEA software.

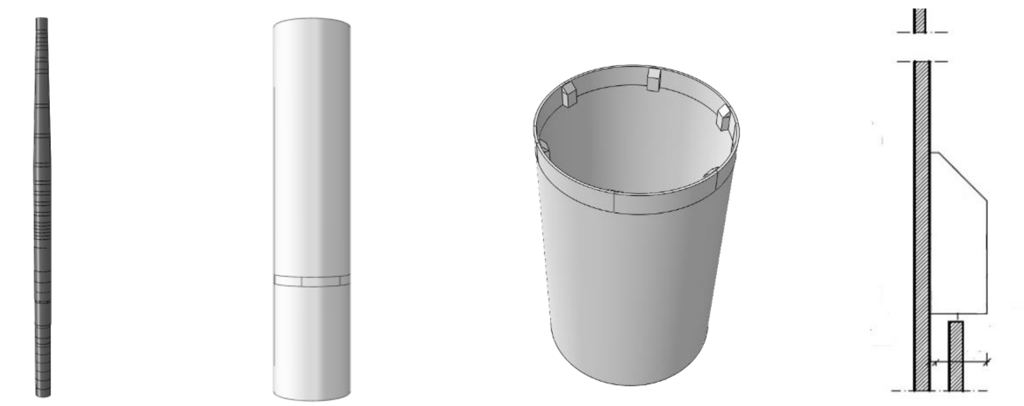

a) b) c) d)

Figure 3-1 a) Assembly of OWT SS b) TP c) Stoppers within TP d) TP-GC-MP assembly

3.2.3 Materials

3.2.3.1 Structural Components

MP, TP, stoppers and the tower are made of steel S355 with a density of 7850 kg/m^3, a Young's modulus of 210 GPa, a Poisson's ratio of 0.3 and a nominal yield strength of 355 MPa. The GC's material properties are characterised by a density of 2740 kg/m^3, a Young's modulus of 88 GPa, a Poisson's ratio of 0.19 and friction coefficient of 0.6 [240].

3.2.3.2 Soil Profile

Apart from the OWT SS, an important part of the detailed parametric model is composed by the soil-structure interaction, which is a design factor of critical importance for the structural response of the pile-monopile-tower assembly. Paradoxically, the soil-structure interaction is an aspect often not considered in OWT SS modelling [239]. The soil profile considered in this analysis consists of one layer of sand and three layers of clay. Composition of soil profiles strongly depends on the geographical emplacement; the soil profile utilised in this analysis corresponds to that of the North West of the UK. Table 3-1 shows the profile's soil parameters used in the simulations, which are based on site measurements. Winkler's approach was used to represent the soil profile. This method is widely used to model the soil-structure interaction by replacing the elastic soil medium with closely spaced and independent elastic springs [241,242]. Furthermore, it is recommended by DNV-GL [227], where the stiffness of the linear springs used in the Winkler's approach, is calculated from the p-y curves [243]. This method is used for the design of horizontal loaded piles by the American Petroleum Institute (API) code [236], and calculates the lateral soil resistance (p) as a function of lateral soil displacement (y). This empirical method is based on test results of laterally loaded piles and depends on the pile diameter, soil strength and loading conditions, although other factors such as layered soils or the space between piles have considerable influence [244] [245].

where $\gamma'$is the submerged unit weight, $S_u$is the undrained shear strength, δ is the characteristic interface friction angle, ɸ is the characteristic angle of internal friction, E is the Young's modulus, ε_{50} is the strain which occurs at one-half of the maximum stress in the laboratory undrained compression test, t_c is the unit skin friction under compression, t_t is the unit skin friction under tension and q is the unit tip resistance under compression.

Table 3-1 Soil properties based on site measurements

	Depth (m)	ɣ' KN/m^3	S_u KPa	δ deg	ɸ deg	E MPa	ε_{50} (%)	t_c kPa	t_t kPa	q (MPa)
SAND	2.4	11	0	37	42	22.7	0	8	8	1.1
	5.4	11	0	37	42	33.3	0	25.9	25.9	3.7
	8.0	11	0	37	42	44.3	0	44.4	44.4	6.3
CLAY	8.4	10	750	0	0	300	0.2	220.7	220.7	6.8
	11.0	10	750	0	0	300	0.2	229.1	229.1	6.8
	13.0	10	575	0	0	230	0.2	198.0	198.0	5.2
	18.0	10	800	0	0	320	0.1	273.1	273.1	7.2

Although this approach is widely used and recommended in design standards, it was developed for up to 2m diameter piles [246]. Therefore, pile deformations might be underestimated [247]. Although a cyclic version of the p-y curve was introduced in [248], it is neither cycle nor amplitude dependent, and provides only a lower bound on the soil-pile lateral stiffness. This shortcoming is overcome in [249] by the utilisation of the quasi-static p-y degradation model of [250]. Continuum modelling of the soil in an Finite Element Analysis constitutes a different approach, where the soil is modelled as a large volume. This approach is more accurate when dynamic studies are carried out; however, it also requires significantly more computational resources. Therefore, for the iterative process required for this paper, a more computationally intensive approach was considered beyond the scope of the aims set to this publication. Besides, as steel is an elastic material, the relationship between its stresses and deformations is linear, making Winkler's approach accurate enough for the purpose of this study.

3.2.4 Mesh Sensitivity Analysis

A mesh sensitivity analysis was performed in order keep a balance between the computational time of the simulations and the accuracy of the results. In the process, it was found that the structure's eigenfrequencies were especially sensitive to the size of the mesh. After the analysis, a mesh size of 0.1m was found to be adequately accurate as results had already converged. This mesh size will therefore save unnecessary computational time in comparison to a further mesh refinement of 0.05m.

3.2.5 Validation

This model has been validated by comparing the results of the modal analysis of both the structure and the tower, against data from the reference OWT. Among these data, it was specified that the eigenfrequencies of the system and the tower must be within the range of 0.275-0.320Hz and around 0.506Hz respectively. Results of the modal analysis can be seen in Table 3-2, where it can be appreciated that the first eigenfrequency of the model is within this range that typically represents the 3P frequency of the rotor. Moreover, the eigenfrequency of the tower is 0.533Hz, which represents a 5.3% of relative difference from the one suggested by the manufacturer. This difference is considered to be acceptable as internal platforms and secondary steel assets have not been included in the simulation.

Table 3-2 Validation of eigenfrequencies: System and Tower

	FEA Model	Real Data
Tower	0.533Hz	0.506Hz
System	0.291Hz	0.275-0.320Hz

3.3 Load Calculations for Offshore Wind Turbine Support Structures

The design's environmental conditions approach followed in this study, is based on the use of the highest extreme conditions likely to occur in a return period of 50 years [251,252] for ULS and buckling limit states and normal operating conditions for the FLS limit state, which are introduced in Section 3.4. Wind, wave and current loads are manually calculated under this premise and then introduced in the FEA parametric model. Although many load cases need to be considered for the design, according to the above mentioned standards, the structure needs to be able to withstand the simultaneous combination of these three loads, acting in the same direction, which is considered the worst static load case scenario.

3.3.1 Wind

For representation of wind climate, a distinction is made between normal and extreme wind conditions. The former generally concern cyclic structural loading conditions, which are important for fatigue assessment, while the latter are wind conditions that can lead to extreme loads, which might lead to the collapse of the structure due to excessive loading. Accurate estimation of the occurrence of extreme wind speeds is an important factor in achieving an affordable level of risk and balance between safety considerations and "over-design" of the structure [253]. Both normal and extreme wind conditions used in this analysis were calculated in accordance with IEC 61400-1 [251], and are summarised in Table 3-3.

Table 3-3 Normal and extreme wind parameters

Subject	Issue	Unit	Value
Normal Conditions	Mean air density, ρ	kg/m^3	1.23
	Mean wind speed (80m), V_{ave}	m/s	8.4
	Maximum flow inclination	deg	0
Extreme Conditions	Air density at extreme wind, ρ_e	kg/m^3	1.225
	Maximum wind speed at hub height, V_{max}	m/s	45.2

Calculating wind loads along the structure can be done applying the following formula:

$$V(h) = V_{ref} * \frac{ln\left(\frac{h}{z_0}\right)}{ln\left(\frac{h_{ref}}{z_0}\right)} \qquad \textbf{3-1}$$

where z_0 is the roughness coefficient, which can be taken from [227]. Once the wind speed profile has been generated, the force in the horizontal direction affecting the tower, TP and nacelle, produced by the wind can be calculated as:

$$F_x = \frac{1}{2} * C_D * \rho_e * (V_{max})^2 * A * \cos\alpha \qquad \textbf{3-2}$$

where:

C_D = drag coefficient of a cylinder in the case of the tower and TP and a plate in the case of the nacelle. Blades are not taken into consideration in this study.

A = area being pushed by the wind.

α = inclination angle of the wind with the horizontal axis

3.3.2 Wave

Wave loading is another environmental load that influences the structural integrity of OWT SS. Wave forces are calculated using Morrison's Equation, which is composed of two terms, representing the inertia and drag [254]. These terms can be identified by the inertia and drag coefficients (C_m and C_D respectively). Morrison's Equation can be expressed as:

$$F = \frac{1}{2}\rho\, C_D\, D\, |U|\, U + C_m\, \rho\, \frac{\pi D^2}{4} \frac{dU}{dt} \qquad \textbf{3-3}$$

where:

U = undisturbed fluid velocity

$\frac{dU}{dt}$ = acceleration of the fluid

ρ = water density

D = diameter of the cylinder

As explained at the beginning of this section, the design wave approach is based on the use of the highest wave likely to occur in a given return period (50 years in this case). Waves are characterised in terms of height (H) and wave period (T). These parameters are summarised in Table 3-4 and were estimated at the offshore emplacement where the turbine is installed in the North of the UK.

Table 3-4 Summary of extreme metocean conditions

Return period (years)	Water level LAT (m)	Hs (m)	Hmax (m)	Tz (s)	Tpeak (s)
1	10.05	4.90	9.2	9.8	13.5
10	10.48	5.90	11.0	11.5	14.8
50	10.93	6.60	12.1	12.7	15.5

where H_s is the significant wave height, H_{max} is the maximum wave height, T_z is the zero up-crossing period and T_{peak} is the peak-to peak-period.

In order to calculate the wave's velocity and acceleration, linear wave theory for shallow water was employed. Airy wave theory was developed by the mathematician and astronomer G.B. Airy in 1845. This wave theory is summarised in the Airy velocity potential formula:

$$\Phi(x,y,t) = -ac\,\frac{\cosh k(y+d)}{\sinh(k+d)}\cos(kx-wt) \qquad \textbf{3-4}$$

where:

a = amplitude (m)
c = celerity (m/s)
k = wave number
d = depth
x, y = horizontal and vertical coordinates
w = wave frequency
t = time

From the Airy velocity potential, the fluid's velocity $\left(U(x,t)\right)$ and acceleration $\left(\dot{U}(x,t)\right)$ in shallow waters can easily be calculated as:

$$U(x,t) = \frac{\partial\Phi(x,y,t)}{\partial x} = \frac{wa}{kd}\sin(wt-kx) \qquad \textbf{3-5}$$

$$\dot{U}(x,t) = \frac{dU(x,t)}{dt} = \frac{w^2a}{kd}\cos(wt-kx) \qquad \textbf{3-6}$$

After the fluid's velocity and acceleration are calculated, the wave loads can be calculated from Morrison's Equation. Mass and drag coefficients, C_m and $C_{D,}$ are usually estimated according to the offshore standards [227] by firstly, deriving the drag coefficient for steady-state flow (C_{DS}) from Equation 3-7, then reading off the wake amplification factor ($\psi(K_c/C_{DS})$), which depends on the Keulegan-Carpenter number (K_c) and C_{DS} and calculating C_D and C_m from Equations 3-10 and 3-11 [255].

$$C_{DS} = \begin{cases} 0.65 & for\ k/D < 10^{-4} \quad (smooth) \\ \dfrac{29 + 4\log_{10}(k/D)}{20} & for\ 10^{-4} < k/D < 10^{-2} \\ 1.05 & for\ k/D > 10^{-2} \quad (rough) \end{cases} \tag{3-7}$$

$$K_c = \frac{U_{max} T_p}{D} = 17.7 \tag{3-8}$$

$$\psi\left(\frac{K_c}{C_{DS}}\right) = 1.2 \quad \text{from [255]} \tag{3-9}$$

$$C_D = C_{DS} * \psi\left(\frac{K_c}{C_{DS}}\right) = 0.78 \tag{3-10}$$

$$C_m = max\{2.0 - 0.044\ (K_c - 3); 1.6 - (C_{DS} - 0.65)\} = 1.6 \tag{3-11}$$

3.3.3 Tidal and current induced loads

Tidal currents and wind driven currents are two environmental loads that even though they do not represent major hazards to the structure's integrity in shallow waters, they contribute to other major excitations such as those produced by the wind and waves. The tidal current profile can be represented as the current speed $(v\ (z))$ at distance z, from still water level (positive upwards), which is the exponential variation of the current at still water level v_0 through the distance to the top of the water column z.

$$v\ (z) = v_0\ \left(\frac{h + z}{h}\right)^{\frac{1}{7}} \qquad for\ z \leq 0 \tag{3-12}$$

where *h* is the water depth.

The extreme tidal current takes place approximately at mean water level, with zero tidal current at high and low tide. Once the tidal current profile is calculated, it will be modelled as a constant over depth current. Wind driven currents are due to wind imposed shear forces on the water surface and are, therefore, likely to be oriented in the same direction as the wind. The wind driven current at the sea surface is estimated in accordance with IEC61400-3 [252], as:

$$U_{wind} \approx 0.01\ U_{1h,10min} \quad \textbf{3-13}$$

where $U_{1h,10min}$ is the hourly mean at 10m height.

3.3.4 Hydrostatic Pressure

Hydrostatic pressure is referred to as the pressure of the water column applied to the submerged parts of the MP and TP. It can be calculated from a control volume analysis of an infinitesimally small cube of fluid and simplified, as density and gravity are constant through depth.

$$p(z) - p(z_0) = \frac{1}{A}\int_{z_0}^{z} dz' \iint \rho\,(z')\,g(z')\,dA = \int_{z_0}^{z} dz' \rho\,(z')\,g(z') = \rho g h \quad \textbf{3-14}$$

where:

$p(z)$ = pressure at a given height z

$p(z_0)$ = pressure at z_0, which is the top of the water column

Therefore $p(z_0) = p_{atm}$

ρ = water density (kg/m^3)

g = gravity (m/s^2)

$h = (z - z_0)$ = height of the liquid column between the test volume and the zero reference point of the pressure

3.3.5 Nacelle's and Rotor's weight

Since the nacelle's and rotor's (composed of the hub and blades) detailed modelling is not part of the parametric model, they are included in the FEA as concentrated or distributed masses in order to be able to reproduce accurately the OWT's structural behaviour. According to [256], there is no need to model the blades due to the fact that, aside from the mass added to the tower top, parked and feathered blades have minimal impact on the natural frequency of OWT. The nacelle's and rotor's weights are 125 and 95 tons respectively, which makes a total of 220 tons that are accounted as a cylinder three metres high and with the same diameter as the top of the tower. The density was increased accordingly in order to account for the total weight. The nacelle's and rotor's weights were found in the official Siemens SWT-107 3.6 MW brochure [257].

3.4 Limit States Formulation

Structural integrity of the system is checked according to DNV-OS-J101 [227], which is the most widely used standard in the design of OWT. According to this standard, four limit states have to be considered in the design: ULS, FLS, Accidental Limit State and Serviceability Limit State. The modifications in the design carried out in the design cases considered were checked upon ULS and FLS. Accidental Limit State was not considered as this limit state is used for the assessment of structural damage in the structure, caused by accidental loads or to re-assess the ultimate resistance and structural integrity after damage. Similarly, Serviceability Limit State was not taken into account as it considers tolerance criteria applicable to normal use of the OWT SS. Furthermore, the structural performance of the system was also checked upon buckling and natural frequencies.

3.4.1 ULS

ULS analysis is carried out considering extreme environmental conditions the worst case scenario for a 50 year return period. This is when wind, wave, tides and wind driven currents are aligned in the principal direction of the wind (SW). The load factor to be used when different loads are combined to form the design load is 1.35 [227]. This load factor is also applicable in operational loading; however, as an extreme loading case is being considered, the turbine cannot be operating due to safety reasons. Therefore, parked conditions apply.

In Section 3.3, extreme loads were calculated with a load factor of 1.35. From the combination of these loads, the utilisation factors are derived. Table 3-5 shows the Maximum Utilisation Rates (MUR) and therefore the Maximum Stresses Allowed (MSA) for the MP and the TP in the baseline case, which will be use to assess the loss or gain of the structural integrity of the different design cases considered. MUR and MSA are related by the following expression:

$$MUR\ (\%) = \frac{MSA}{\sigma_{yield}} * 100 \qquad \textbf{3-15}$$

Table 3-5 Maximum utilization rate for MP and TP in the baseline case

MP		TP	
MUR (%)	MSA (MPa)	MUR (%)	MSA (MPa)
68	227.8	52	174.2

3.4.2 FLS

FLS refers to the cumulative damage in the structure due to cyclic loads. The fatigue design of OWT SS is governed by dynamic responses from simultaneous aerodynamic and hydrodynamic loads [258]. The structure must be able to resist expected fatigue loads, which may occur during temporary and operational design conditions. The load factor in the FLS is 1.0 for all load categories [227]. Normal sea state conditions (significant wave height and peak spectral period) were used for the calculation of wave loading [252]. Wind loads were taken from [259], where the fatigue thrust load for the tower of a 3.6MW OWT with 100m hub height are 143kN.

The two most commonly used fatigue assessment techniques are the stress life (S–N) approach and the fracture mechanics approach. The S–N curve approach is the one recommended by standards [227] and [252]. A review of the currently used S–N curves is provided in [260]. Furthermore, the equivalent stress range ΔS can be determined from the parametric FEA model subjected to the previously mentioned fatigue loads. Having obtained the equivalent stress range, the number of loading cycles to crack initiation can then be determined from the S–N curve in Equation 3-16:

$$\log N = A - m \log \Delta S \qquad \textbf{3-16}$$

where *A* is the intercept, *m* is the slope of the S–N curve in the log–log plot.

The selection of the S–N curve plays a massive role in the results obtained. These are generally classified in: air, seawater with adequate cathodic protection or free corrosion conditions, and are taken from DNV-RP-C203 “Fatigue Strength Analyses of Offshore Steel Structures” [261]. Offshore structures are prone to corrosion development due to the harsh marine environment, which leads to significant levels of damage to the structures and hence a reduction in service life [20]. For that reason, curve D in seawater with adequate cathodic protection is used in service life calculations.

3.4.3 Buckling

Buckling is a failure mechanism, to which slender structures are prone. It is caused by a bifurcation of static equilibrium equations solution [262]. Buckling is characterised by the sudden failure of a structural member subjected to high compressive stress. During this phenomenon, the compressive stress at the point of failure is less than the ultimate compressive stress of the material. When the applied load is increased on a slender structure, such as a column, there is the possibility that it becomes large enough to cause the structure to lose its stability and buckle. Any further load will cause significant and somewhat unpredictable deformations, possibly leading to complete loss of the member's load-carrying capacity.

Eigenvalue linear buckling analysis is generally used to estimate the critical buckling load of the analysed structure. The buckling loads are calculated relative to the base state of the structure, which can include preloads (e.g., bolt preload). In an eigenvalue buckling problem we search for the loads for which the model stiffness matrix becomes singular, so that the problem has non-trivial solutions [263]. The buckling stability of shell structures is often checked according to DNV-RP-C202 [237] or Eurocode 3/ EN 1993-1-1 [264] and Eurocode 3/ EN 1993-1-6 [265]; in this analysis Abaqus Computer-Aided Engineering (CAE) is used to assess it.

3.4.4 Natural Frequencies

Resonance is a phenomenon in which a vibrating system or external forces (in this case environmental and operational loads experienced by the OWT SS) drive another system to oscillate with greater amplitude at a specific preferential frequency. These amplified oscillations produce higher than expected deformations, a rise in stress within different parts of the turbine, which will lead to crack initiation, and generally a decrease in the fatigue life of the structure. Furthermore, the fact that wave loading and the turbine's operating loads are cyclic loads, makes the design of these structures particularly difficult.

A classic aspect of good structural design lies in optimizing stiffness-to-mass ratio through material and shape choices. Natural frequencies' sensitivity analyses are carried out for the different case studies with the aim of detecting patterns of change in the characteristic natural frequencies of the structure that could potentially be employed for its scale-up or to monitor a particular failure mechanism.

Modal frequencies monitoring is a common Structural Health Monitoring (SHM) technique implemented in OWT that identifies their modal frequencies whose deviations are a damage symptom [266]. This is carried out by the installation of accelerometers either in the nacelle of the turbine or along the tower and SS. However, because the wind and wave loading applied to the structure cannot be measured accurately in a continuous manner, Operational Modal Analysis (OMA) needs to be employed. This technique allows identification of the resonance frequencies every 10 min without any human interaction [267] based on the assumption that the structure is subjected to unknown random loads [59,268].

3.5 Sensitivity Analysis and Results

In Section 3.2.1, a number of KDPs of OWT SS were identified. In this section, three KDPs have been chosen based on their preliminary capacity of impacting on the design of OWT SS in terms of scaling-up and CAPEX reduction. The cases considered in this study are: TP's and GC's length, effect of size and number of stoppers, and scour development.

3.5.1 Design Case A: TP's and GC's length

Case study A checks the sensitivity of the length of the TP and GC, which comprises from where the stoppers are assembled, to the bottom of the TP. The grout, not only enhances the correct transmission of loads and stresses from the TP to the MP, but also contributes to the accurate positioning of the two components. In the baseline turbine this length is 7.8m. Variations of one and two metres have both been added and subtracted from this baseline length of 7.8m to complete the analysis.

Depending on the variation in the natural frequencies of the OWT, once it has been scaled-up to a bigger turbine, modifications to its geometry can be applied to intentionally increase or decrease the turbine's natural frequency. Furthermore, savings or additions in material will make an economic impact on the CAPEX, as the cost of materials is an important driver [230], [231] and [232]. To that aim, sensitivity analyses of natural frequencies, ULS, FLS and buckling checks have also been carried out. The benefit of these checks is not only to scale-up the turbine (ensuring the health of the structure), but also to potentially save a considerable amount of material and therefore money.

Table 3-6 shows the variation in the first six natural frequencies. From this sensitivity analysis it can be appreciated that the variation of the first two natural frequencies, which are those that are dangerously close to the 1P and 3P rotor frequencies, is low. This suggests that reducing the TP's and GC's length will not necessarily enhance scalability, as natural frequencies change at a low rate. However, this brings up the possibility of saving materials and therefore reduce CAPEX. In order to be able to do that, ULS, FLS and buckling checks will have to support this reduction in length.

Table 3-6 Case A: Percentage of variation of modal frequencies

Modal frequencies	Transition Piece Length				
	5.8 m	6.8 m	7.8 m	8.8 m	9.8 m
1	-1.01%	-0.52%	0.29089 Hz	0.54%	1.10%
2	-1.05%	-0.54%	0.29615 Hz	7.41%	7.75%
3	0.84%	0.39%	1.6776 Hz	-0.35%	-0.65%
4	0.77%	0.36%	1.7211 Hz	-7.30%	-7.90%
5	-1.17%	-0.53%	1.9516 Hz	0.41%	0.75%
6	-1.11%	-0.50%	2.0637 Hz	0.40%	0.71%

Tables 3-7 and 3-8 present the results from the ULS and buckling checks, being the buckling frequency for a particular load combination, the inverse of the utilization factor for the structure to buckle. Table 3-7 shows that no major changes in the MUR occur due to this length variation. Moreover, buckling frequency does not change due to this length reduction, although it has a slight tendency to decrease when the length of the TP is increased. These results show in the case of the TP length reduction (5.8m and 6.8m), that because of the decrease in the weight of material, an increase in the buckling frequency could be expected. The lack of variation in results suggests that this reduction must have been compensated by a loss of support produced by a reduction of the GC length.

Table 3-7 Case A: ULS check: MURs (%) of the OWT SS

MUR (%)	Transition Piece's Length				
	5.8 m	6.8 m	7.8 m	8.8 m	9.8 m
MP	64.72%	64.73%	64.73%	64.72%	64.70%

TP	21.84%	22.17%	22.39%	22.60%	22.76%

Table 3-8 Case A: buckling check

	Transition Piece's Length				
Buckling frequency (Hz)	5.8 m	6.8 m	7.8 m	8.8 m	9.8 m
	1.5316	1.5316	1.5316	1.5291	1.5296

The FLS check shows no rise in the effective stress range (ΔS), when the TP's and GC's lengths are reduced. This indicates that fatigue life will be maintained and therefore, as ULS and buckling checks also allowed it, almost 20 tons of material could be saved and therefore material costs will be reduced.

Table 3-9 Case A: FLS analysis

Transition Piece's Length					
TP length	5.8 m	6.8 m	7.8 m	8.8 m	9.8 m
ΔS (MPa)	33.9	33.9	33.9	34.5	35.0
Fatigue life (yr)	32.9	33.0	33.1	29.9	28.1

3.5.2 Design Case B: Effect of size and number of stoppers

Case study B evaluates the effect of adding or suppressing stoppers in the integrity of the structure and its natural frequencies. The six stoppers of the reference turbine were increased to eight and 12 and then decreased to four. The volume of steel utilised in the stoppers is continuous, therefore modification in the number of stoppers necessarily implies a variation in the stopper dimensions. This assumption implies that no cost in materials will be added or saved and the results will just impact on the integrity of the structure. Table 3-10 shows the stoppers' dimensions. As can be observed below, the dimensions of the stopper's base (B2) have been maintained in all cases. This is due to the fact that the relative position between the TP and the MP does not change throughout Design Case B.

Table 3-10 Stopper's dimensions keeping a constant volume of steel

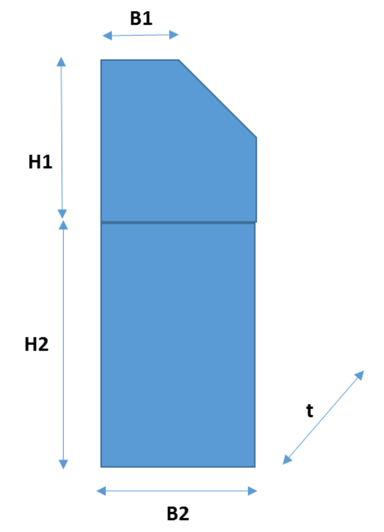

Dimension (m)	Number of Stoppers			
	4	6	8	12
B1	0.02	0.02	0.02	0.02
B2	0.21	0.21	0.21	0.21
H1	0.20	0.18	0.17	0.15
t	0.407	0.316	0.290	0.260
H2	0.50	0.42	0.33	0.23

From the frequencies' sensitivity analysis (see Table 3-11), the large variation that the number and distribution of stoppers produces in the natural frequencies can be observed. A dramatic drop in the natural frequencies occurs when just four stoppers are used, making the first two frequencies fall into the boundaries of resonance with the rotor frequencies. In the case of eight stoppers, a slight drop also occurs, although not as severe as for the four stoppers. This sensitivity analysis shows that the distribution of stoppers every 90 and 45 degrees produces a drop in natural frequencies, as opposed to 60 and 30 degrees distribution, as these frequencies are higher for a TP with six and 12 stoppers than for four and eight.

From the buckling analysis (Table 3-12) it is clear that the four stopper distribution is not a safe alternative, due not only to its first two natural frequencies being very close to resonance, but also to the moderate reduction of the buckling frequency from 1.53Hz to 1.12Hz, which means that for the same amount of material being spent in the stoppers, the OWT SS can take 1.12 times the extreme loads instead of 1.53 times. This will compromise the integrity of the structure. Furthermore, buckling would take place between the TP and MP, which is not the case in the six, eight and 12 stopper distributions. The eight stopper distribution slightly improves the buckling capacity, which is marginally reduced in the 12 stopper distribution. Nevertheless, this reduction is within reasonable limits that do not threaten the integrity of the structure.

Table 3-11 Case B: sensitivity analysis of modal frequencies

Case B: Stopper Configuration				
Mode	4 Stoppers	6 Stoppers	8 Stoppers	12 Stoppers
1	-17.11%	0.29089 Hz	-1.54%	0.11%
2	-17.61%	0.29615 Hz	-0.93%	0.11%
3	-5.07	1.6776 Hz	-2.24	0.12%
4	-5.18%	1.7211 Hz	-1.53%	0.12%
5	-5.38%	1.9516 Hz	0.16%	0.16%
6	-5.56%	2.0637 Hz	0.38%	0.38%

Table 3-12 Case B: buckling analysis

	4 Stoppers	6 Stoppers	8 Stoppers	12 Stoppers
Buckling frequency (Hz)	1.12	1.53	1.55	1.50

Results of the ULS analysis are summarised in Table 3-13. The four stopper distribution is again characterised by bad results, showing much higher MURs than the six stopper configuration, which are very close to the yielding point of the steel and therefore, not safe. The eight and 12 stopper configurations appear to considerably improve the MURs for both the MP and the TP.

Table 3-13 Case B: ULS check: MURs (%) of the OWT SS

MUR (%)	Stopper Configuration			
	4 Stoppers	6 Stoppers	8 Stoppers	12 Stoppers
MP	81.42%	64.73%	58.54%	54.57%
TP	96.99%	22.39%	8.67%	8.86%

In the fatigue check, the four stopper configuration presents similar results to the other structural checks performed, with an increase in ΔS of 42.5%, which makes a considerable reduction in service life. Other configurations results, shown in Table 3-14, present a non-existent or very low rise (1.8%) in ΔS of the eight and 12 stopper configurations, in comparison to the six stopper's, respectively.

Table 3-14 Case B: FLS analysis

	Stopper Configuration			
No. of stoppers	4 Stoppers	6 Stoppers	8 Stoppers	12 Stoppers
ΔS (MPa)	48.3	33.9	33.9	34.5
Service life (yr)	5.6	33.1	32.8	30.2

3.5.3 Design Case C: scour development

Case study C assesses the effect that scour development has not only on the natural frequencies of the structure, but also on its integrity. Scour is one of the biggest issues currently being faced by operators. This phenomenon occurs around the foundations of structures when these are placed into a marine environment and exposed to water currents and tides. Due to the presence of the structure itself, different changes affect the natural flow regime at the sea bed around the foundation, which lead to increased sediment mobility [269]. Depending on the foundation type and the environmental conditions, scour depths of several metres around the OWT SS could be observed even within short periods [270].

Rambabu et al. [271] stated that the fluid flow, geometry of foundation and seabed conditions are the governing factors for seabed scouring. The characteristics of fluid flow include the current velocity, Reynolds number of the model and Froude number of the flow. Therefore, for different foundation types, different scouring patterns will develop [272]. The scour development around MP structures has been studied extensively for the foundation of OWT in the past few decades [273].

This design case was selected in order to make a structural analysis of how the whole OWT SS will be affected by scour development. This FEA model includes not only the tower of the OWT, which is the common focus of FEA modelling [53-57]; but also the SS and MP-soil interaction with multi-layered soil composed of layers of both clay and sand, which is not present in most of the studies, due to the difficulty of modelling sand layers [247,279,280]. However, this analysis does not take into account the process or the mechanism of the scour development, as it is considered beyond the scope of this study. Therefore, the structural analysis carried out in this publication assumes the scour has already developed. These analyses were carried out by recalculating the value of the springs' stiffness used to model the soil, assuming that the first one, two and three meters of soil had disappeared due to the scour process.

From previous research, a significant impact on the structure's integrity was anticipated because as scour develops, a lesser percentage of the MP is embedded in the soil, producing eigenfrequency reductions and therefore, leading to resonance. Table 3-15 corroborates this prediction; however, surprisingly, not for the first natural frequency. As can be observed, changes in the natural frequencies occur mainly in the second and fourth modes. Because the first and the second natural frequencies are very close to each other, the fact that there is significant variation in the second mode still poses a threat to the structure.

It seemed reasonable to believe that as scour develops, the MP's MUR would increase, due to the loss of support from the soil. However, results do not show significant changes in MURs (Table 3-16), which remain practically unaltered. Furthermore, the more the scour is developed, the lower buckling capacity the OWT SS presents (Table 3-17), which could become a threat to its integrity if the process continues, although the capacity remains within safety limits in this design case.

Table 3-15 Case C: sensitivity analysis of modal frequencies

Case C: Scour Development				
Mode	No Scour	1m Scour	2m Scour	3m Scour
1	0.29037 Hz	0.00%	0.00%	0.00%
2	0.29594 Hz	-0.42%	-0.74%	-0.97%
3	1.6755 Hz	0.00%	0.00%	0.00%
4	1.7203 Hz	-0.57%	-1.02%	1.34%
5	1.9519 Hz	0.00%	-0.01%	-0.02%
6	2.0642 Hz	0.00%	0.00%	0.00%

Table 3-16 Case C: ULS check: MURs (%) of the OWT SS

MUR (%)	Scour Development			
	No Scour	1m Scour	2m Scour	3m Scour
MP	64.73%	64.74%	64.75%	64.76%
TP	22.39%	22.43%	22.43%	22.43%

Table 3-17 Case C: buckling analysis

	No Scour	1m Scour	2m Scour	3m Scour
Buckling frequency (Hz)	1.53	1.51	1.46	1.43

Furthermore, Table 3-18 shows how scour development increases the stress range, making the service life of the OWT SS shorter. It is also worth bearing in mind that particular soil types with low cohesion will be more prone to scour development, which can be a quick phenomenon if it is not mitigated. Furthermore, given the moderate rate of change (7.7%, 11.2% and 23.6% in 1m, 2m and 3m scour respectively) of the stress range that scour produces, special effort should be put either into frequent and costly inspections, or into scour mitigation and prevention measures. Additionally, it is recommended to take account of the scour development into the reliability assessment of OWT SS, providing more accurate reliability assessment results for reliability-based inspection of OWT SS.

Table 3-18 Case C: FLS analysis

Scour Development				
Level of Scour	No Scour	1m Scour	2m Scour	3m Scour
ΔS (MPa)	33.9	36.5	37.7	41.9
Service life (yr)	33.1	22.7	19.3	11.4

3.6 Discussion

Case A was proved to be effective in materials cost reduction but not in modal frequencies control. The reduction in length of the TP and GC of the OWT SS produced low variation in modal frequencies, which will be reduced within safety limits. Furthermore, as ULS, FLS and buckling are not compromised by these modifications, a lower safety factor could be employed in the future for TP and GC design, reducing their length. As a consequence, material costs could be reduced, as more than 20 tons of steel could be removed per turbine.

No material reduction is allowed in Case B due to the constant volume of steel employed in the stoppers. However, the interest in this case study remains in its potential to decrease the fatigue damage and to improve the buckling capacity and MUR of the OWT SS just by changing the number (and therefore the dimensions) of the stoppers and their distribution. Within this case study, it was proved that the distribution of the stoppers plays an important role in the structural integrity of the unit. Besides the fact that the four stopper distribution was not structurally safe in terms of natural frequency, stability, buckling capacity and fatigue life, results show that eight stopper distribution produces a minor decrease in natural frequencies (between 0.1% and 1.5% depending on the mode), and a moderate and major decrease in the MP's and TP's MUR (9.6% and 86% respectively). Furthermore, the stress range remains almost equal to the baseline's. These results show that, although the eight stopper configuration fails in the enhancement of fatigue life, it has a very positive effect on the structure's behaviour against extreme loads.

Although the results for the 12 stopper distribution are generally good, (minor rise (between 0.1% and 0.4%) in natural frequencies, minor reduction in buckling capacity without safety repercussion and great improvement (15.7% and 86% respectively) in the MP's and TP's MURs, the cost of installation (welding to the TP) will inevitably be higher and take longer to be completed. Therefore, special consideration of this rise in costs and the benefits to the turbine's structural integrity, will have to be considered. Furthermore, FLS results present a slight increase in the stress range, which leads to a reduction in the service life from 33.1 years to 30.2 years.

Case C highlights the importance of scour monitoring and the impact that its development can have on the structure's integrity [96]. From the natural frequencies' sensitivity analysis it can be concluded that, although the first mode does not present variation due to scour, modes two and four could potentially be used to detect the development of this phenomenon. The behaviour of the structure against extreme loading is not compromised due to scour development, presenting a minimal increase in the MP's and TP's MURs. A remarkable reduction of 6.5% in the buckling capacity takes place when the scour reaches 3m. Furthermore, given the moderately high rate of change (7.7%, 11.2% and 23.6% in 1m, 2m and 3m scour respectively) of the stress range and therefore expected service life (from 33.1 to 22.7, 19.3 and 11.4 years, respectively) that scour produces, special effort should be put either into frequent and costly inspections, or into scour mitigation and prevention measures.

The design of scour protection should be integrated into the foundations' design [281]. In order to carry out an effective design, sediment properties, seabed's geotechnical composition, environmental conditions and turbine specifications, among others, have to be taken into account and must accurately predict the maximum scour that would occur in the absence of this protection [282].

3.7 Conclusion

A good understanding of how geometrical modifications to the structure will affect its structural integrity and end of life is vital to adapt these structures to harsher environments further from shore [142]. To this end, a sensitivity analysis of three KDPs of OWT SS was carried out, in order to analyse whether these KDPs could contribute to the turbine's scale–up by either modifying its modal properties, improving structural integrity, or saving in CAPEX. Three case studies were considered for this analysis: Case A: reduction of the TP's and GC's length, Case

B: stoppers optimisation and Case C: scour development. The following conclusions can be drawn from the present study:

- A reduction in the TP's and GC's length was proven to maintain the structure's integrity within safety limits. Therefore, although reducing the TP and GC's length will not necessarily enhance their scaling-up, due to the minimal change in natural frequencies, it will save almost 20 tons of steel per turbine. This measure will provide a considerable reduction in CAPEX, when applied to all the units within a WF.
- Increasing the number of stoppers while maintaining the volume of steel, was proven to have a positive impact on the structure's integrity for both the eight and the 12 stopper configurations. However, as cost of installation (welding the stoppers to the TP) will inevitably be higher and take longer to be completed, special consideration of the trade-off between this rise in costs and the benefits to the structural integrity, will have to be made. The eight stopper configuration may constitute a good compromise between the six and 12 stopper configurations without reducing the expected service life of the structure.
- Scour is one of the biggest issues currently being faced by operators, which was proven to compromise the buckling capacity and fatigue life of OWT SS. Modes two and four showed special sensitivity to the development of this phenomenon. For that reason it is believed that Integrity Monitoring could become a good alternative to monitor them in order to detect and control this phenomenon. However, before the installation of the instrumentation, no overlapping between failure mechanisms, that would also affect modal properties, must be ensured in order to avoid misleading information about the threat and its extent at that particular time.

3.8 Acknowledgements

This work was supported by grant EP/L016303/1 for Cranfield University, Centre for Doctoral Training in Renewable Energy Marine Structures (REMS) (http://www.rems-cdt.ac.uk/) from the UK Engineering and Physical Sciences Research Council (EPSRC) and Innogy SE.

DATA MANAGEMENT FOR STRUCTURAL INTEGRITY ASSESSMENT OF OFFSHORE WIND TURBINE SUPPORT STRUCTURES: DATA CLEANSING AND MISSING DATA IMPUTATION

Maria Martinez-Luengo, Mahmood Shafiee and Athanasios Kolios

Centre for Offshore Renewable Energy Engineering, Department of Energy and Power, Cranfield University, Bedfordshire, MK43 0AL, UK

Submitted 20 May 2018, Accepted 2 January 2019

Published in Ocean Engineering 173 (2019) 867-883

DOI: https://doi.org/10.1016/j.oceaneng.2019.01.003.

Statement of contributions of joint authorship

Maria Martinez-Luengo conducted the literature review on the subject, developed the framework, planned and performed the analyses, drafter and critically reviewed this manuscript. Also, María analysed the results and produced figures and tables in this paper. Athanasios Kolios and Mahmood Shafiee proof-read and critically commented the manuscript before its acceptance in Ocean Engineering.

Abstract

Structural Health Monitoring (SHM) and Condition Monitoring (CM) Systems are currently utilised to collect data from Offshore Wind Turbines (OWT), to enhance the accurate estimation of their operational performance. However, industry accepted practices for effectively managing the information that these systems provide have not been widely established yet. This paper presents a four-step methodological framework for the effective data management of Structural Health Monitoring Systems (SHMS) of OWTs and illustrates its applicability in real-time continuous data collected from three operational units, with the aim of utilising more complete and accurate datasets for fatigue life assessment of SS. Firstly, a time-efficient synchronisation method that enables the continuous monitoring of these systems is presented, followed by a novel approach to noise cleansing and the posterior Missing Data Imputation (MDI). By the implementation of these techniques those data-points containing excessive noise are removed from the dataset (Step 2), advanced numerical tools are employed to regenerate missing data (Step 3) and fatigue is estimated for the results of these two methodologies (Step 4). Results show that after cleansing, missing data can be imputed with an average absolute error of 2.1%, while this error is kept within the [+15.2% to −11.0%] range in 95% of cases. Furthermore, only 0.15% of the imputed data fell outside the noise thresholds. Fatigue is found to be underestimated both, when data cleansing does not take place and when it takes place but MDI does not. This makes this novel methodology an enhancement to conventional structural integrity assessment techniques that do not employ continuous datasets in their analyses.

Keywords: Structural health monitoring (SHM), offshore wind, data synchronisation, noise cleansing, missing data imputation, neural network (NN).

4.1 Introduction

SHMS have become relevant in the last decade for the OM of OWT due to their damage detection and continuous fatigue life assessment capabilities. Operation and Maintenance (O&M) related costs are a significant contributor to the Levelised Cost of Electricity (LCoE) [283–285]. While in the past SHMS were installed as a way to abide by the German regulations (imposing a 10% of assets instrumented across an Offshore Wind Farm (OWF)) and not exploited to their full potential, nowadays operators have realized how these technologies could result in an increase in electricity production and thereby a reduction in LCoE [286,287]. Over the past decades, many researchers from the SHM community have developed an extensive amount of methods based on a variety of physically interpretable structural features [288]. At this point in time there is no widely accepted practice with respect to the specification of monitoring systems, as industry is still exploring WTs' potential, making every Wind Farm (WF) different in terms of technologies implemented, number and location of the sensors, redundancies, etc. Most of these fatigue assessment methods rely on collected data from either accelerometers, strain gauges or the combination of both from selected instrumented units [9,142]. Numerous authors have carried out different ways of analysing SHMS' data – for example, a vibration-based damage localization and quantification method, based on natural frequencies and mode shapes extracted by means of Operational Modal Analysis (OMA) combined with Finite Element Analysis (FEA) of the test structure [288].

Another approach to fatigue assessment is by the extrapolation of the dynamic behaviour of OWTs from a limited set of sensors. Existing monitoring strategies for monopiles are based on physical models or artificial intelligence [289]. Model-based time-domain algorithms require accelerometers and sometimes strain gauges on the structure. These try to reproduce the time history of dynamic response parameters, such as acceleration or strain, of the whole structure for different operational regimes. This was carried out by employing Kalman filters [290,291], joint input-state estimation [292] and modal expansion algorithms [292–294]. Even though accelerometers might be placed in the WT's nacelle for Supervisory Control and Data Acquisition (SCADA) or CM purposes, they are not so often placed at different levels of the SS, unless there is a particular interest in its vibration monitoring. However, installing these accelerometers at different levels of the turbine is more expensive. Besides, accelerometers alone do not cover all the necessary frequencies needed for modal expansion algorithms as [292] explains, making strain gauges also necessary. Furthermore, sometimes WTs are only instrumented with strain gauges, especially those commissioned more than five years ago.

Most fatigue-sensitive spots (called hot spots) in OWTs are inaccessible for direct measurements, i.e. at welds or mudline [295]. Different methods have been utilised to accurately predict the structure's response at these important locations where strain gauges cannot be installed. This is achieved by combining measurements from sub-optimal locations with FEA [10,289,294–296], to extrapolate to the critical locations.

Sometimes datasets at accessible locations are not complete due to failure in acquiring or recording the data, full storage space, high noise, etc. The issue of limited information due to limited availability of operational data could be mitigated by these FEAs. This hypothesis has been supported in different articles, where accurate load estimation is believed to be best carried out with data driven models requiring only a short period of mechanical strain measurements [297]. However, this approach of using incomplete SHM datasets is questionable, not only for deriving service life estimations from reduced time intervals, but also for introducing uncertainty in the estimations and wasting costly SHM data that could potentially be utilised for damage detection and quantification strategies.

As mentioned earlier, OMA introduces uncertainty in the estimations. According to Banfi and Carassale, the available mathematical OMA techniques have the common feature that the unmeasured excitation is modelled as a random process specified by some probabilistic models [298]. In practical applications, the length of the measurement is limited and the probabilistic model adopted to represent the excitation does not necessarily apply. This, together with measurement errors, leads to uncertainties of a different nature that affect the estimation of the modal parameters. Finally, it seems impractical to install multiple sensors and dedicate resources to analysing their measurements, without obtaining a long-term view of how the system behaves and degrades.

Noise is inherent to data acquisition. Signals in realistic applications are inevitably contaminated with measurement noise, as well as other sorts of variabilities and uncertainties, such as calibration issues, transmission or de-synchronisation between the real and the recorded time-stamp. As a result, the SHM features extracted from the contaminated data, such as damage equivalent loads (DELs), power spectrum and frequency response function, are also noisy [299,300]. Uncertainty could contaminate the extracted SHM features dramatically if the data quality is poor, and thereby causes ambiguity in interpreting the features [301]. Usually the uncertainty will raise false alarms in the damage detection, i.e. non-damage-induced feature deviation from the undamaged baseline. Therefore, noise identification and quantification in SHMS′ data should not be ignored and, ideally, should take place before fatigue assessment. Besides, a systematic approach to the effective data management of these SHMS installed in OWTs’ prior fatigue assessment, has not been established yet either in the literature or by regulations.

This paper aims to develop a methodological framework for the effective data management of SHMS of OWTs by addressing the issues of missing data and noise in the acquired data, which influence the effective fatigue assessment of Offshore Wind (OW) energy assets. This is achieved through a four-step process (including synchronisation, cleansing, imputation and fatigue assessment) that enables the continuous analysis of the unit's structural integrity and remaining service life throughout the years, as highlighted in Figure 4-1. This novel framework is implemented by utilising real and continuously monitored, 50 Hz strain data collected from three different OWTs currently in operation, for over three years. These turbines were instrumented with SHMS during their commissioning. Therefore, it is assumed that no previous fatigue damage from the commissioning phase was undertaken by the turbine without being captured and that the noise/calibration error present in the measurements, used to derive the dynamic structural behaviour of the units, is minimum.

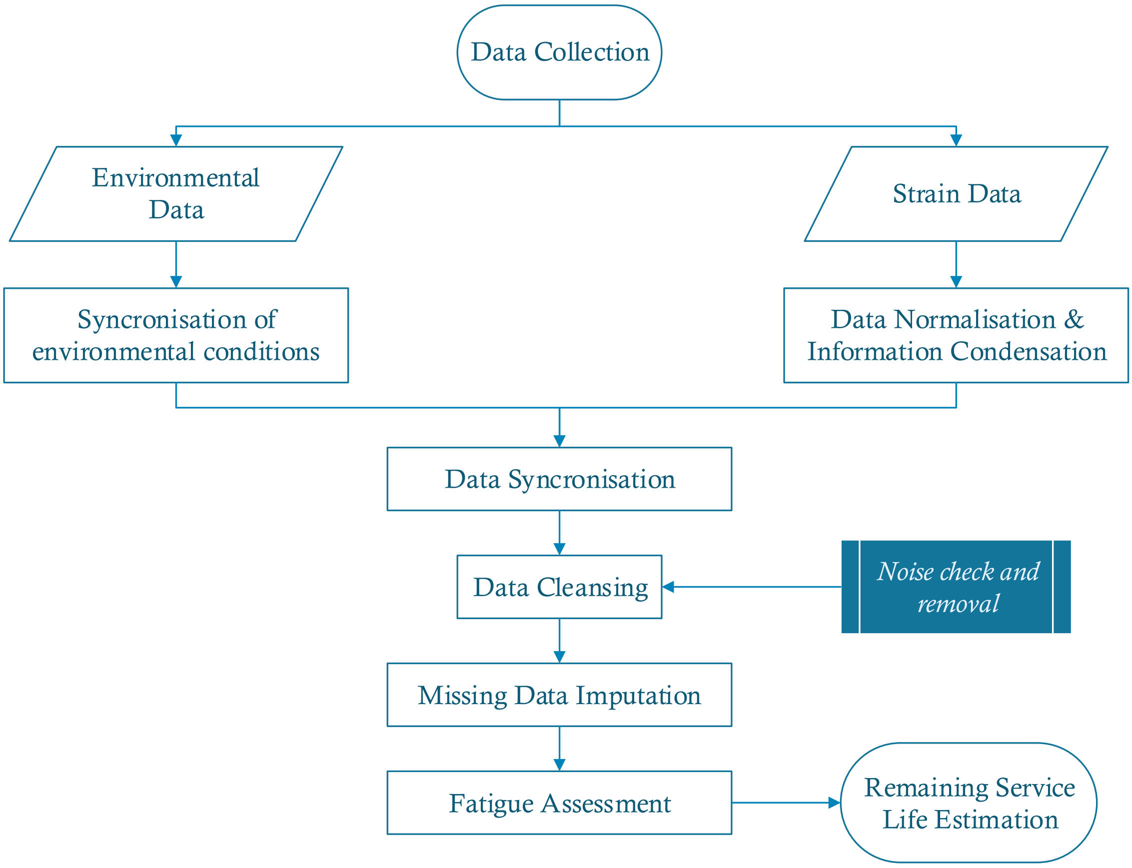

Figure 4-1 Framework for the effective data management of SHMS of OWT

This article highlights the importance of appropriate data handling of SHMS for the continuous fatigue assessment of an OWT's SS. The four-stage methodology proposed in Figure 4-1 is implemented in Section 4.2 and its results discussed in Section 4.3. After data synchronisation takes place, noise cleansing and MDI are applied. Their efficiency for the better assessment of the structure's integrity is analysed in Section 4.3, where the impact that noise cleansing has in the accuracy of MDI is shown. During the noise cleansing stage, the inherent dynamic relationships between different parts of the support structure (SS) are derived and those dynamic responses significantly deviating from them are cleansed. In the third stage, missing data present in these datasets is imputed for both the non-cleansed and the cleansed scenarios. The accuracy of the imputation is shown by the comparison between the imputed and the exact data values. Finally, fatigue is estimated for four different scenarios: without cleansing/without MDI, without cleansing/with MDI, with cleansing/without MDI and with cleansing/with MDI.

Results show that the proposed data management framework could help the OW industry to derive more accurate fatigue life estimations to help push the boundaries of current operational periods and make the technology more competitive by reducing its LCoE.

4.2 Development of a framework for data management of offshore wind applications

4.2.1 Data Synchronisation

Modern WTs are equipped with sophisticated SCADA control systems, spreading, on a 10 min time basis, a vast amount of information, including: details on the wind flow and meteorological conditions, on turbine alignment to the wind, on the conversion of wind kinetic energy into active power, on the vibrational and mechanical status of the machine, on thermal conditions at relevant parts of the turbines, and so on [302]. SHMS′ data are physically collected from time to time (at the discretion of the operator) from the OWT as the local storage capacity is limited. This often coincides with regular inspection activities. Once data have been collected, environmental data (from both SCADA and metmast) are synchronised by having one measurement for each time-step. Typically, wind measurements are recorded every 10 min, and metmast measurements every 30 min. As a result, two synchronisation approaches could be considered: every 10 min by keeping wave measurements constant for the 30-min interval or every 30 min by averaging wind conditions. In this analysis the 10-min interval dataset is chosen as wind is considered to be the environmental factor contributing most to the overall loading that the structure is subject to, in comparison to wave's loading. Therefore, by having 10-min intervals, wind variability is more accurately captured. Strain data would typically need to be temperature normalized. Each strain gauge that required compensation has an associated temperature channel and set of apparent strain coefficients. Therefore, the temperature compensated strain would be the actual measured strain minus the apparent strain, which depends on the temperature and the sensor material properties. The apparent strain (ε_A) is calculated as:

$$\varepsilon_A = C_0 + (C_1 * T) + (C_2 * T^2) + (C_3 * T^3) + (C_4 * T^4) \qquad \textbf{4-1}$$

where T is the value of the temperature (°C) and C_0 to C_4 are the coefficients for the gauge batch.

The length of the dataset also needs to be reduced as handling 50 Hz strain data is neither time- nor cost-efficient. Furthermore, its synchronisation with environmental conditions would be problematic as there would be 30,000 strain measurements per each 10-min measurement of environmental conditions. A solution to this issue consists of the calculation of the DELs for 10-min intervals [303–305]. DELs are equivalent to the single load that would cause the same damage than the cumulative effect of the loads for the established interval, which in this case is 10 or 30 min. The expression is calculated with the following formula [303–305]:

$$DEL = \left(\sum_{i-1} \frac{n_i \sigma_i^m}{N_{eq}} \right)^{\frac{1}{m}} \qquad \textbf{4-2}$$

where n_i is the current cycle, σ_i is the stress range, N_{eq} is a fixed number of cycles and m is the slope of the S-N curve. Values for N_{eq} and m can be obtained from standards such as the volume dedicated to fatigue design of offshore steel structures from DNVGL-RP-C203 [306]. Once the DELs are calculated, resulting in a single dataset containing 18 months of continuous data, strain data can be synchronised with environmental data (provided that environmental data was previously synchronised at the same frequency than the strain data). The result is a single dataset containing SCADA, environmental (wind, wave and generator's active power) and strain data for every 10 min. Any redundant data will be identified and removed during this process, reducing the length of the dataset and avoiding double-counting fatigue cycles.

4.2.2 Data Cleansing

Before these datasets can be used for fatigue analysis and following the Statistical Pattern Recognition (SPR) Paradigm (for more information see [9]), data cleansing must take place. In the OW energy context, cleansing is understood as two phenomena:

- The removal of abnormal data, which are believed to be abnormal not due to damage, but due to external conditions, i.e. the malfunctioning of a sensor.
- Removal of noisy data. This occurs when sensors record noisy measurements.

Strain gauges generally record noisy measurements in the presence of electric and/or magnetic fields, which can superimpose electrical noise on the measurement signals. If not controlled, the noise can lead to inaccurate results and incorrect interpretation of the strain signals [307]. Even though sensors for SHM of OWT SS are placed way below the nacelle and therefore not exposed to their electric and magnetic fields, interferences could occur if they are placed close to the J-tube in the transition piece (TP). Other noise sources that could potentially introduce noise in the train measurements are: transformers, relays, generators, rotating equipment, radio transmitters, electrical storms, poor insulation of the sensor during installation, transient vibrations, etc. In summary, any electrical device that generates, consumes, or transmits power is a potential source for causing noise in strain gage circuits. In general, the higher the voltage or current level, and the closer the strain gage circuit to the electrical device, the greater will be the induced noise [307]. It is difficult to know if a sensor is recording noise and how much the magnitude of this noise is individually, but due to the embedded redundancy in the SHMS, the relative noise can be accounted for by comparing the readings of two correlated sensors at each time-stamp.

The concept of correlating sensors lies in the premise that, depending on wind direction, different pairs of sensors will exhibit behaviour of a similar trend. This is illustrated in Figure 4-2 and 4-3. While in Figure 4-2, for that particular day, sensors A and C were correlated and therefore, exhibit the same trend in DELs measurements (even though there is some offset between them), Figure 4-3 shows that these same two sensors (A and C) were not exhibiting the same trend on another day when the wind direction did not make them in correlation. When two sensors are not in correlation at a particular moment, it does not necessarily mean that there is noise in their measurements. It only implies that the parts of the SS where these two sensors are placed are not experiencing physically the same trend of stress, and therefore, sensors are not measuring the same trend of strains (for a particular direction). This correlation between sensors allows us to understand the offset between DELs measurements when two sensors are in correlation and therefore, it can be employed to cleanse the dataset whenever the noise between a pair of sensors is higher than a particular level previously established.

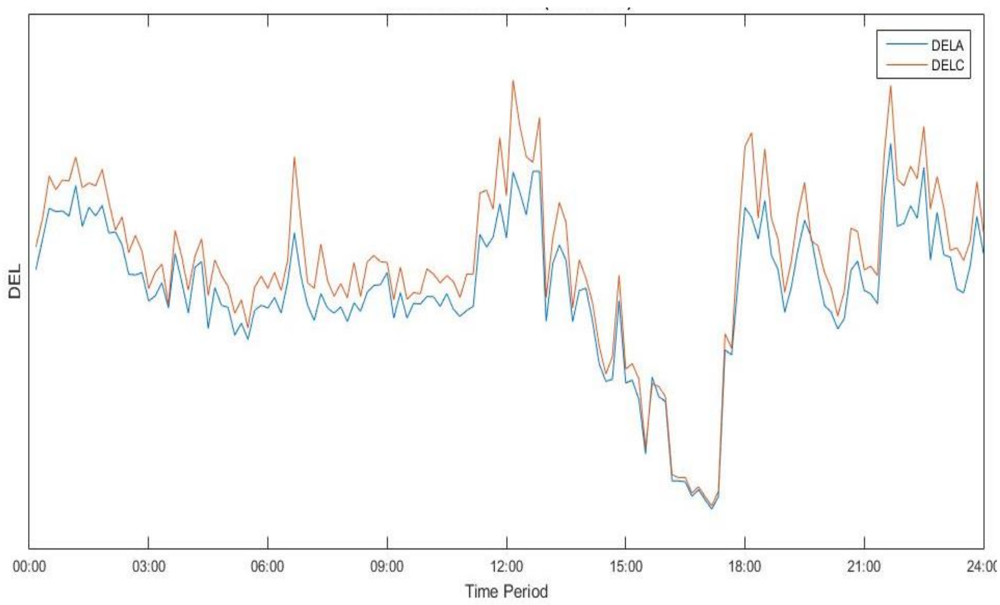

Figure 4-2 Low level of noise: Sensors in perfect correlation

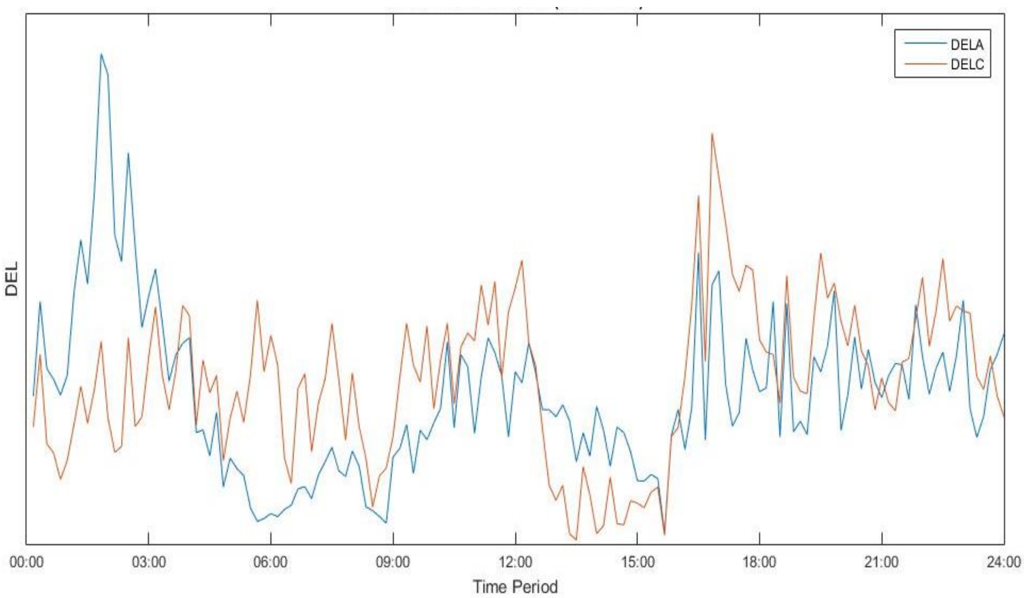

Figure 4-3 Unknown level of noise: Sensors not in correlation

In this paper, we propose a novel approach for noise identification and removal. For that approach, analysis of the sensors that are in correlation for particular intervals, depending on the wind direction, is carried out. The term "correlation" is understood to be two sensors following the same behaviour or trend in measurements, even though there might be an offset between the two.

Initially, in order to determine which sensors are in correlation at different wind directions, the dataset was divided into 20deg intervals (18 in total) and DELs were plotted for each wind direction angle (see Figure 4-4 where DELs from different sensors are plotted). As it can be appreciated in this figure, sensors 1 and 3 seem to be following a similar uniform trend in Orientation 2 (between 20 and 40 deg of wind direction); however, for Orientation 15 (280–300 deg) it seems that their measurements are much more distorted. This procedure was repeated several times to find which sensors would correlate at each Orientation.

Nevertheless, these graphs do not show precisely the differences between sensor readings and their evolution. For this reason they are not an accurate way of determining whether a new point would be within reasonable limits of noise. To solve that, noise thresholds have to be defined in a way that, when the noise level of a particular measurement happens to fall above a predefined threshold, the data-point is automatically excluded from the final dataset.

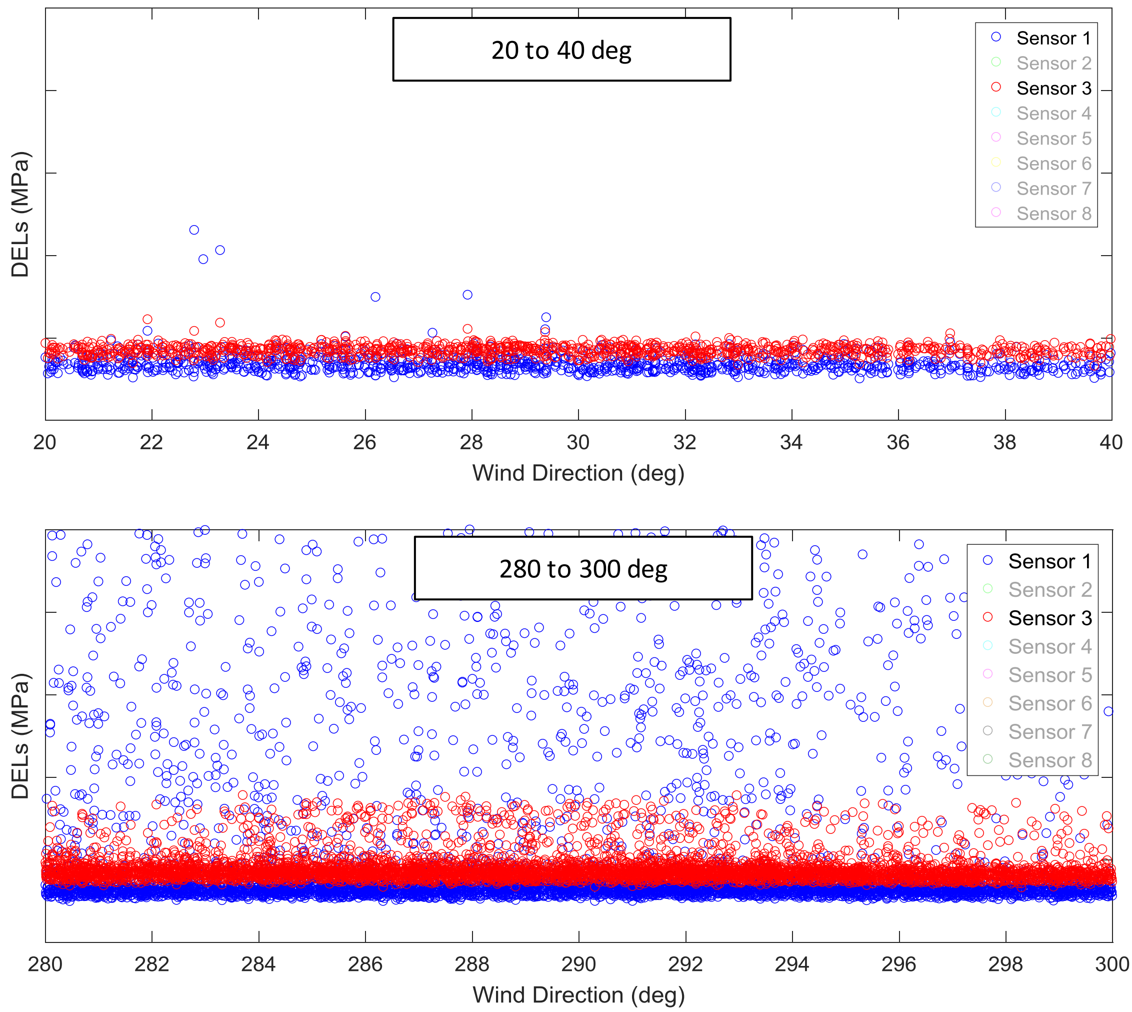

Figure 4-4 Sensors 1 and 3 in full and not complete correlation (above and below respectively)

Noise thresholds are determined by calculating the difference between two sensors' measurements, for all wind directions. The value of this difference tends to be a stable value or offset, which may be zero when the pair of sensors are in perfect correlation. This means that, even if the difference (the offset) is constant around a certain value (statistical distribution's mean value), the standard deviation would be significantly lower whenever the sensors are in correlation and higher when they are not. In order to be exhaustive, all possible sensor combinations for each one of the 18 orientations were analysed. For each orientation there is a total possible number of combinations ‘C’ of:

$$C = \sum_{i=1}^{n} (n-1) = 28 \qquad \textbf{4-3}$$

‘n’ being the number of sensors, which in this case is eight. Afterwards, a normal distribution was fitted to all computed values of the 28 sensor combinations for every orientation. The mean of the normal distribution determines the offset between the measurements. This offset constitutes the difference between dynamic responses of the two sensors of the combination being analysed. The best indicator of the correlation between two sensors is the standard deviation of the difference between their measurements. The smaller this is, the more correlated these measurements are, as this means that these sensors' measurements follow a more similar trend. In order to automatize data cleansing throughout the life of a structure, firstly the noise thresholds need to be set. This would be achieved by analysing the correlation between sensors for small intervals of wind direction right at the beginning of the operation of the analysed asset. Five degree intervals were selected for this purpose for two reasons in order to not only to capture the slightest variability of these correlations with enough accuracy but also to have enough data-points to posteriorly define the polynomials that will constitute the noise thresholds.

In order to define the noise thresholds, the dataset is divided into intervals according to wind direction, which results in a total of 72 intervals (360/5=72). Also, for each data-point the 28 sensor combinations are computed. If for each sensor combination (among 28 possible combinations), the mean and standard deviation at all orientations (72) are plotted into a graph, and a polynomial is fitted into the points, the boundaries of the admissible noise can be set. This can be observed in

Figure 4-5, where the mean value (blue line) and mean value plus and minus the standard deviations (black dashed lines) of the difference between sensors' readings, every five degrees, are plotted. Fifth order polynomials were fitted to the points. The order of these polynomials was determined after the optimisation of the fitting error was carried out. Figure 4-5 shows the particular case of the sensor 2–6 combination.

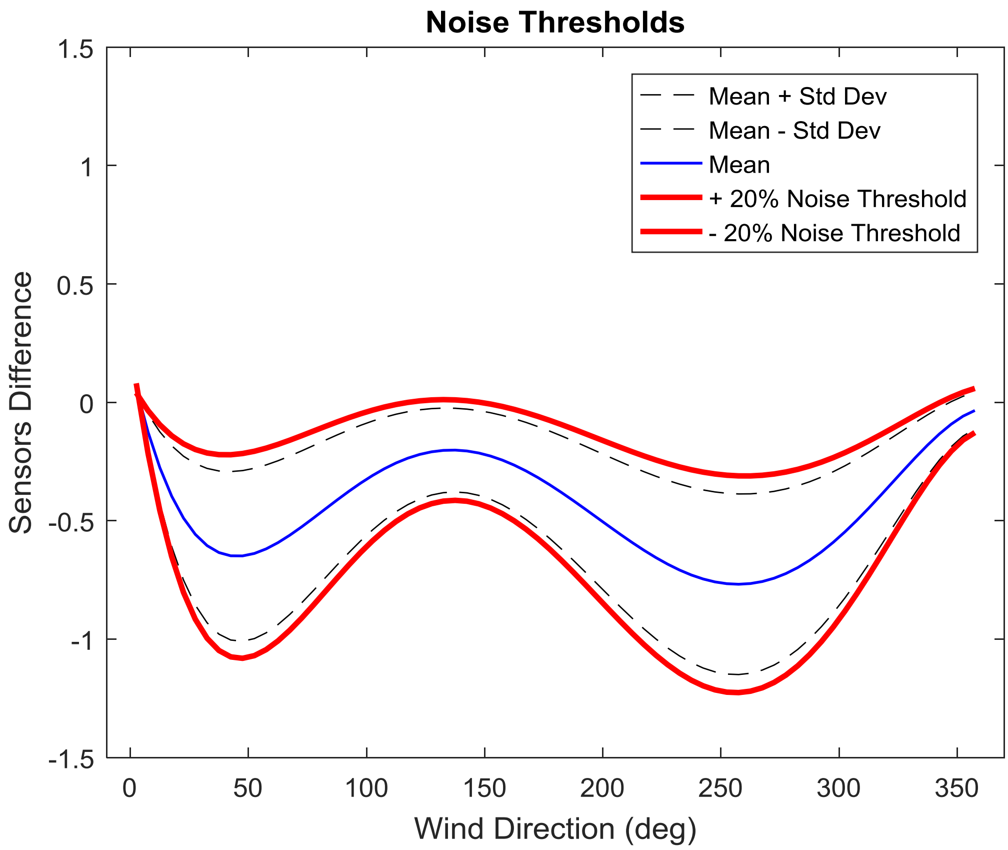

Figure 4-5 Sensor 2-6 noise thresholds

Furthermore, the two red polynomials represent a 20% noise allowance. This noise allowance is set to be 20% of the standard deviation at each orientation. For each new measurement, if the deviation of the difference between sensors' measurements is higher or lower than the thresholds (red lines), the data-point is considered to have excessive noise and is therefore excluded from the dataset. In

Figure 4-5, the mean value of the difference in DELs measured by sensors 2 and 6 is shown in blue. This difference is:

$$\Delta DELs_{2-6} = DELs_2 - DELs_6 \qquad \textbf{4-4}$$

This mean value represents the offset of the measurements due to both the measurement of different physical states of the structure and difference in calibration when these sensors were installed. The closer that $\Delta DELs_{2-6}$ for a particular data-point gets to the mean, for a given wind direction, the less noise this sensor's readings will have. A certain noise or variation in $\Delta DELs_{2-6}$ will still be expected and its magnitude will be dependent upon the level of correlation these two sensors experience throughout the wind directions. This is measured by the standard deviation, which determines how spread the values are in a normal distribution and accounts for 95% of the values (99.7% within 3 standard deviations of the mean). The closer that the $mean \pm Std.deviation$ is to zero, the more correlated the sensors are and, therefore, the more similar trend of measurements these will record.

When a dataset is cleansed, the 28 different sensor relationships (at each time-step) are computed. Thus, the wind direction is used to extract the upper and lower noise thresholds for each combination, which will be compared to the computed values of the combinations. A noise matrix will be filled for each data-point of the set. Whenever the computed value is within the established thresholds, a 1 would be filled in the noise matrix. If the measured difference of values falls outside the thresholds, the noise in the measurement is considered 'too high'. Therefore a 0 would be placed in the noise matrix, which is composed of the following relationships:

$$\begin{bmatrix} \Delta DELs_{1-1} & \Delta DELs_{1-2} & \Delta DELs_{1-3} & \Delta DELs_{1-4} & \Delta DELs_{1-5} & \Delta DELs_{1-6} & \Delta DELs_{1-7} & \Delta DELs_{1-8} \\ \Delta DELs_{2-1} & \Delta DELs_{2-2} & \Delta DELs_{2-3} & \Delta DELs_{2-4} & \Delta DELs_{2-5} & \Delta DELs_{2-6} & \Delta DELs_{2-7} & \Delta DELs_{2-8} \\ \Delta DELs_{3-1} & \Delta DELs_{3-2} & \Delta DELs_{3-3} & \Delta DELs_{3-4} & \Delta DELs_{3-5} & \Delta DELs_{3-6} & \Delta DELs_{3-7} & \Delta DELs_{3-8} \\ \Delta DELs_{4-1} & \Delta DELs_{4-2} & \Delta DELs_{4-3} & \Delta DELs_{4-4} & \Delta DELs_{4-5} & \Delta DELs_{4-6} & \Delta DELs_{4-7} & \Delta DELs_{4-8} \\ \Delta DELs_{5-1} & \Delta DELs_{5-2} & \Delta DELs_{5-3} & \Delta DELs_{5-4} & \Delta DELs_{5-5} & \Delta DELs_{5-6} & \Delta DELs_{5-7} & \Delta DELs_{5-8} \\ \Delta DELs_{6-1} & \Delta DELs_{6-2} & \Delta DELs_{6-3} & \Delta DELs_{6-4} & \Delta DELs_{6-5} & \Delta DELs_{6-6} & \Delta DELs_{6-7} & \Delta DELs_{6-8} \\ \Delta DELs_{7-1} & \Delta DELs_{7-2} & \Delta DELs_{7-3} & \Delta DELs_{7-4} & \Delta DELs_{7-5} & \Delta DELs_{7-6} & \Delta DELs_{7-7} & \Delta DELs_{7-8} \\ \Delta DELs_{8-1} & \Delta DELs_{8-2} & \Delta DELs_{8-3} & \Delta DELs_{8-4} & \Delta DELs_{8-5} & \Delta DELs_{8-6} & \Delta DELs_{8-7} & \Delta DELs_{8-8} \end{bmatrix} \quad \textbf{4-5}$$

where the relationships between the same sensor are not considered (the difference is zero by definition). Therefore these are marked as NAN ("Not A Number") in the matrix below. Furthermore, inverse relationships are considered as if the first sensor of the difference is always the lowest number (i.e. $\Delta DELs_{2-1}$will never be computed because it has similar characteristics to $\Delta DELs_{1-2}$, therefore $\Delta DELs_{2-1}$ is substituted for $\Delta DELs_{1-2}$ in the matrix). This procedure makes the matrix symmetric, which facilitates the procedure of determining which of the sensors for a particular combination is the one presenting noise (or if both are). Equation 4-6 shows the resultant noise matrix.

$$\begin{bmatrix} NAN & 1-2 & 1-3 & 1-4 & 1-5 & 1-6 & 1-7 & 1-8 \\ 1-2 & NAN & 2-3 & 2-4 & 2-5 & 2-6 & 2-7 & 2-8 \\ 1-3 & 2-3 & NAN & 3-4 & 3-5 & 3-6 & 3-7 & 3-8 \\ 1-4 & 2-4 & 3-4 & NAN & 4-5 & 4-6 & 4-7 & 4-8 \\ 1-5 & 2-5 & 3-5 & 4-5 & NAN & 5-6 & 5-7 & 5-8 \\ 1-6 & 2-6 & 3-6 & 4-6 & 5-6 & NAN & 6-7 & 6-8 \\ 1-7 & 2-7 & 3-7 & 4-7 & 5-7 & 6-7 & NAN & 7-8 \\ 1-8 & 2-8 & 3-8 & 4-8 & 5-8 & 6-8 & 7-8 & NAN \end{bmatrix} \quad \textbf{4-6}$$

Note: For clarity, the matrix above only shows the sensors' combinations.

When a dataset is being cleansed, the 28 different sensors' relationships at each time-step are computed and compared to the noise thresholds to determine whether or not the noise they present is admissible or not (admissible=1, inadmissible=0). For each time-step, the noise matrix will be filled in binary. Once the noise matrix is complete for a particular time-step, each sensor of the combination is checked whenever noise is detected for that particular combination. For example, if the combination 1–2 (shown in red in Figure 4-6) has noise, either sensor 1, sensor 2, or even both of them, could have noise. The criteria used to decide which one or if both of the sensors have noise is to check the overall performance of the sensors at a given time-step. Therefore, for this case all the relationships involving sensor 1 (first row) and sensor 2 (second column) are checked with three potential outcomes:

- Majority of sensor 1's combinations have noise but not sensor 2's combinations (sum(NoiseMatrix(1,:)>=4). Therefore, sensor 1's value is deleted due to excessive noise, but not sensor 2's value.
- Majority of sensor 2's combinations have noise but not sensor 1's combinations (sum(NoiseMatrix(:,2)>=4). Therefore, sensor 1's value is deleted due to excessive noise, but not sensor 2's value.
- Both sensors' combinations have noise (sum(NoiseMatrix(1,:)>=4 && sum(NoiseMatrix(:,2)>=4) Therefore, both sensors' values are deleted.

$$
\begin{array}{ll}
\left[\begin{array}{cccccccc}
NAN & 1-2 & 1-3 & 1-4 & 1-5 & 1-6 & 1-7 & 1-8 \\
1-2 & NAN & 2-3 & 2-4 & 2-5 & 2-6 & 2-7 & 2-8 \\
1-3 & 2-3 & NAN & 3-4 & 3-5 & 3-6 & 3-7 & 3-8 \\
1-4 & 2-4 & 3-4 & NAN & 4-5 & 4-6 & 4-7 & 4-8 \\
1-5 & 2-5 & 3-5 & 4-5 & NAN & 5-6 & 5-7 & 5-8 \\
1-6 & 2-6 & 3-6 & 4-6 & 5-6 & NAN & 6-7 & 6-8 \\
1-7 & 2-7 & 3-7 & 4-7 & 5-7 & 6-7 & NAN & 7-8 \\
1-8 & 2-8 & 3-8 & 4-8 & 5-8 & 6-8 & 7-8 & NAN
\end{array}\right]
&
\begin{array}{l}
\rightarrow X_1 \\ \\ \\ \\ \\ \\ \\ \\
\end{array}
\\
\begin{array}{cccccccc}
 & \downarrow X_2 & & & & & &
\end{array}
&
\end{array}
$$

Figure 4-6 Noise Criteria

4.2.3 Missing Data Imputation

After noise is removed, data is checked using the criterion of completeness, making sure that information is not corrupted. Missing data is a challenge faced in almost every empirical analysis but especially in engineering applications employing sensing technologies. These technologies are by no means infallible as they can present different types of failure modes in the data collection. Some of these are: calibration, noise, transmission and data storing issues, and also those related to the reliability and failure mechanisms of the data acquisition system (composed of the sensing technologies, transmission and storage of the measurements). Current practice in the OW industry would ignore the missing data and select reduced intervals of complete time series that are believed to be representative, to carry out their analysis. This approach is practical for time-consuming studies; however, precious data are discarded in the process. Having complete datasets free of noise would, without doubt, enhance the confidence in the fatigue life analysis and allow more realistic remaining service life estimations.

An effective way of dealing with missing data from SHMS of OWTs is through employing artificial Neural Networks (NN). This method was chosen as the best approach due to its applicability, accuracy and consistency with the analytic software used for other data management activities during this project [308–310]. Other relevant methods for MDI are: mean imputation [311], K-nearest neighbour, Maximum Likelihood [52,312,313] and Multiple Imputation methods [314,315]. Figure 4-7 shows the methodology followed for MDI using ANN.

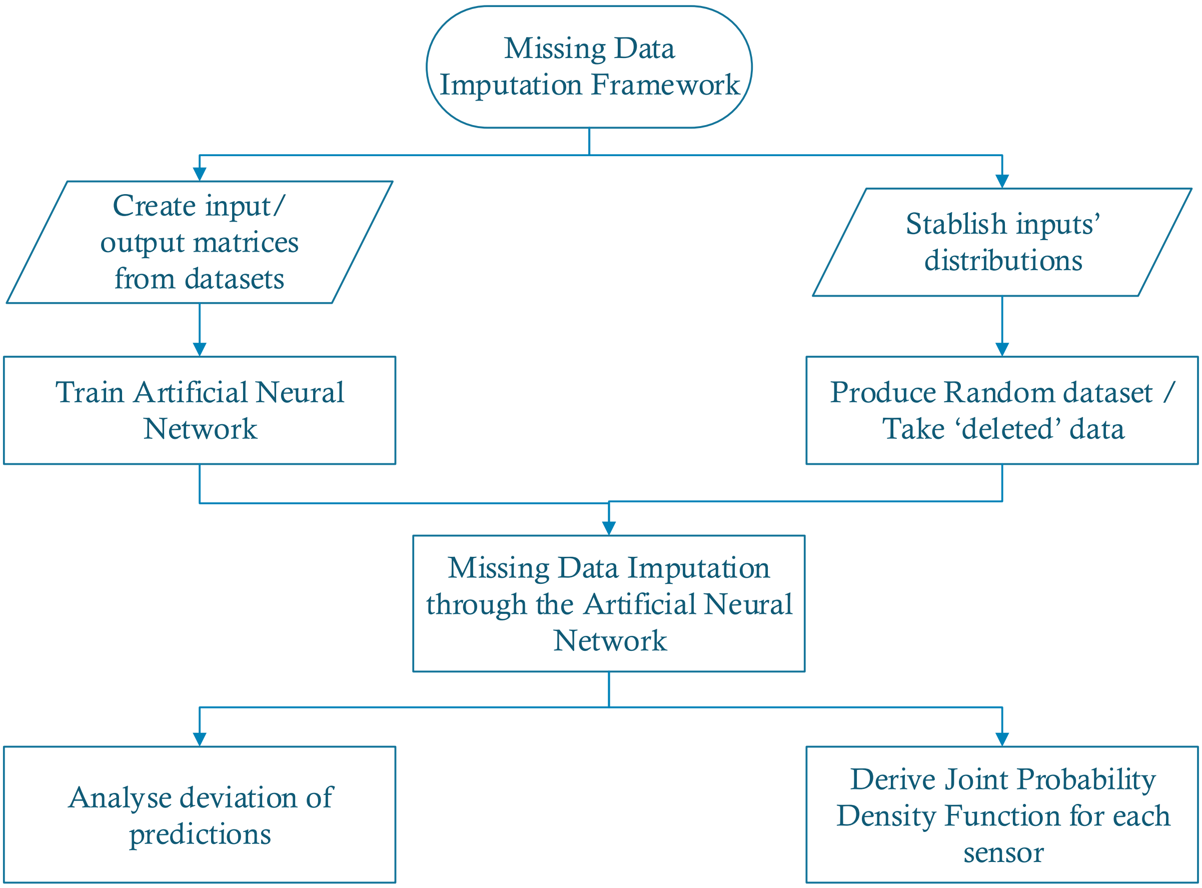

Figure 4-7 Missing Data Imputation Framework

In order to train the ANN, input and output matrices need to be specified. This process might seem trivial but often one of the most recurrent issues with SHM is the excess of non-necessary data and how to determine which data should/should not be analysed. For this application the relevant input variables include: wind speed, wind direction, generator active power, significant wave height and wave direction. Output data is constituted by the eight sensors previously utilised for data cleansing. These sensors are located at the TP of the turbines. Once the input matrices for each dataset are created, the statistical distributions of each input are derived. As can be appreciated from Figure 4-8, normal, Rayleigh and kernel distributions were fitted to the inputs – kernel distribution being the best fit, among others, to the available empirical data. A kernel distribution is a nonparametric representation of the probability density function of a random variable [316]. Kernel distributions are used when a parametric distribution cannot properly describe the data, also when assumptions about the distribution of the data are better to be avoided. Kernel distributions are defined by a smoothing function and a bandwidth value, which control the smoothness of the resulting density curve.

Furthermore, from the initial dataset, a similar percentage to the one of the data removed during the cleansing would be deleted from both the original and the cleansed datasets. These removed data are imputed with the ANNs described later and their results compared to the originals in order to assess the level of confidence that can be given to these estimations. Further details are explained in Section 4.3.2.

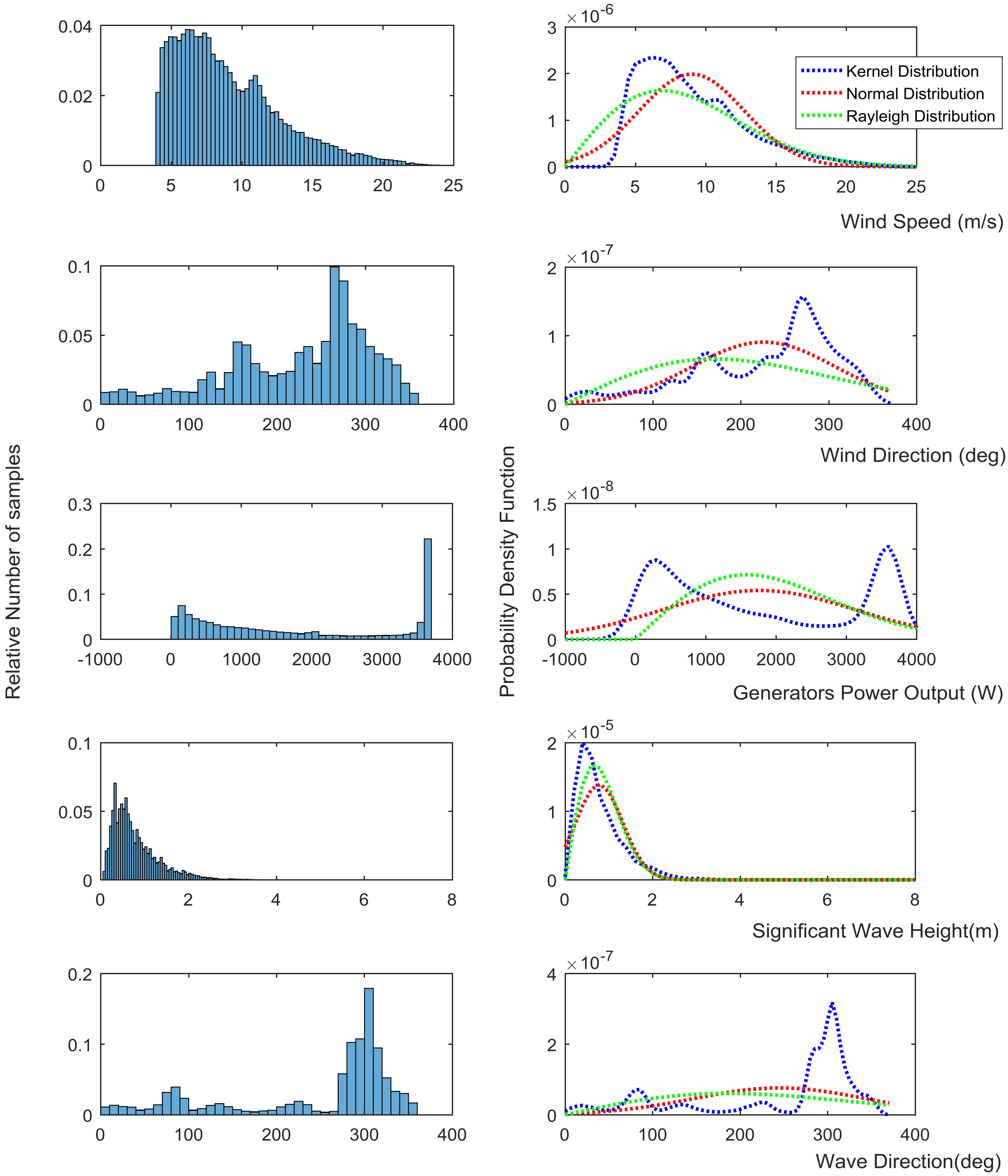

Figure 4-8 a) Histogram of real input datab) statistical distributions fitted to real input data

4.2.4 Fatigue Assessment

The ultimate aim of this framework is to develop a data management tool that supports fatigue calculations for SS of OWT. In order to do so, data cleansing and MDI techniques were applied to real SHM data from three WTs, obtained from a continuous monitoring campaign. Therefore, the fatigue that these three turbines are subject to during the monitoring campaign, is assessed for the four possible scenarios, as summarised in Figure 4-9. An initial dataset without any other manipulation than eliminating missing data, is used for Case A (without cleansing/without MDI scenario). Case A is utilised to train the Artificial neural networks (NN) mentioned in Section 4.2.3, which imputes the missing data from the original dataset, constituting Case B (without cleansing/with MDI scenario).

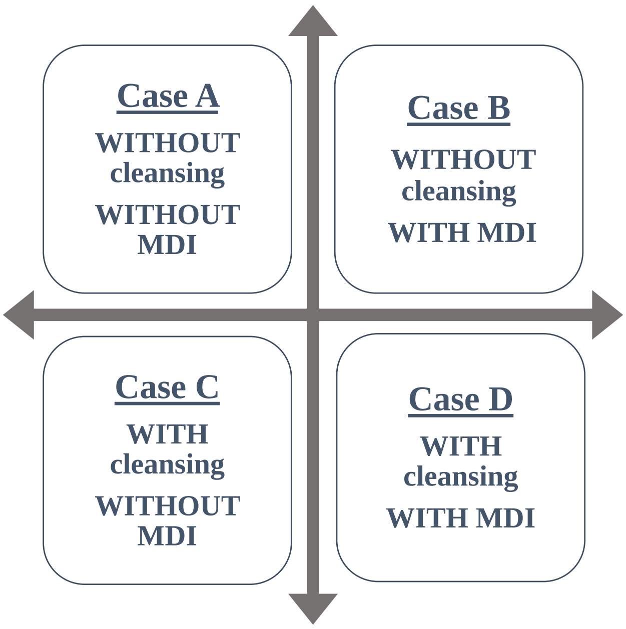

Figure 4-9 Scenarios for fatigue assessment

On the other hand, Case C (with cleansing/without MDI scenario) is made when data are cleansed and missing data removed from the dataset afterwards. This has the implication that only high quality data (without noise) are used for the calculation. However, the length of the dataset is significantly reduced, which also diminishes the confidence in the remaining service life estimations. Lastly, Case D (with cleansing/with MDI scenario) is made by employing Case C's dataset to train an ANN, which imputes the previously removed missing data after the cleansing took place.

The two most commonly used fatigue assessment techniques are the stress life (S–N) approach and the fracture mechanics approach [10]. The S–N curve approach is the one recommended by DNV and IEC standards (see [255] and [252]) due to its straight forward implementation. A review of the currently used S–N curves is provided in [260]. Furthermore, the equivalent stress range ΔS is determined from the four different datasets, previously mentioned, by calculating the DEL of the whole dataset in the same way as in Section 4.3.1. Having obtained the equivalent stress range, the number of loading cycles to crack initiation, in Equation 4-7, can then be determined from the S–N curve, expressed as:

$$\log N = A - \log \Delta S \tag{4-7}$$

where A is the intercept 'm' in the slope of the S–N curve in the log–log plot .

The selection of the S–N curve plays a massive role in the results obtained. These are generally classified in air, seawater with adequate cathodic protection or free corrosion conditions, and are taken from DNV-RP-C203 ''Fatigue Strength Analyses of Offshore Steel Structures" [261]. Offshore structures are prone to corrosion development due to the harsh marine environment, which leads to significant levels of damage to the structures and hence a reduction in service life [20]. For that reason, curve D in seawater with adequate cathodic protection is used in service life calculations with an intercept $A = 15.6$ and a slope $m = 5$.

4.3 Results and Discussion

In this Section, the results of the analyses described in Section 4.2 are presented. This analysis was performed on three WTs from the same OWF, which from now on are called 'Turbines 1, 2 and 3' for clarity purposes. Metocean, SCADA and strain data were available for the three turbines and synchronised, as explained in the previous section, before the data cleansing started. Also, all the data-points where the turbine should have been in operation (wind speeds of 4–25 m/s), but according to SCADA was shut down, were deleted from the dataset. This deletion is carried out so these non-operational intervals do not affect the data cleansing process. Figure 4-10 shows how this filtered dataset follows the power curve.

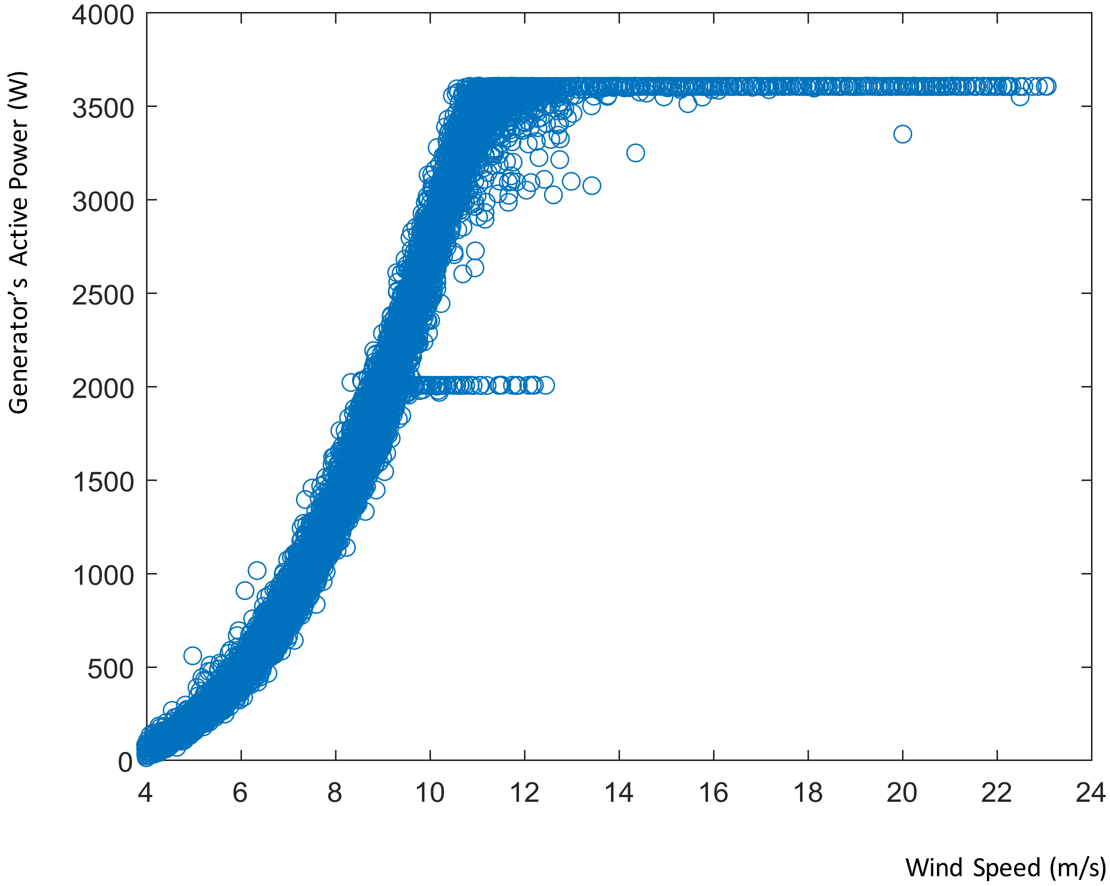

Figure 4-10 Filtered dataset follows power curve

4.3.1 Data Cleansing

In order to capture the dynamic response of each turbine better, the synchronised datasets are divided into five intervals of wind speed. These intervals consist of three operational and two not-operational regimes (0–4 m/s and>25 m/s being the intervals of the non-operational regime and 4–11 m/s, 11–18 m/s and 18–25 m/s the intervals of the operational regime). This approach was chosen as it provides a good compromise between capturing well the behaviour of the turbines and having enough data in each interval for the statistical analysis. The interval corresponding to wind speed greater than 25 m/s had to be discarded due to the lack of samples, which made the statistical analysis of this interval not possible. The only data-point of this interval remained 'uncleansed' in the final dataset, as it was impossible to determine whether it had noise or not. Therefore, the assumption of no noise present in this data-point was made.

During the analysis, the different polynomials, which constitute the noise thresholds for each interval for each one of the 28 sensor combinations, are extracted. Figure 4-11a and b shows an example of how these different noise thresholds may look, while Figure 4-11a shows the great level of physical correlation that sensors 1–2 have for low wind speeds (0–4 m/s) with a very steady mean and standard deviation values. A constant mean value of difference between sensors implies that these sensors are physically exposed to the same type of physical excitations, as the average offset between these sensors does not have significant variation across the different wind directions. A constant value of the standard deviation implies that the pair of sensors is continuously correlated, as the deviation of their sensor readings from the mean value (definition of standard deviation) is constant across wind directions; Figure 4-11b shows a different situation, where the correlation of sensors 3–7 is strongly influenced by the wind direction in a pattern similar to a sinusoidal wave. Furthermore, the standard deviation also exhibits a higher degree of variation than in Figure 4-11a, by reaching local maximums in the valleys of the mean distribution and local minimums at the hills of the mean value distribution.

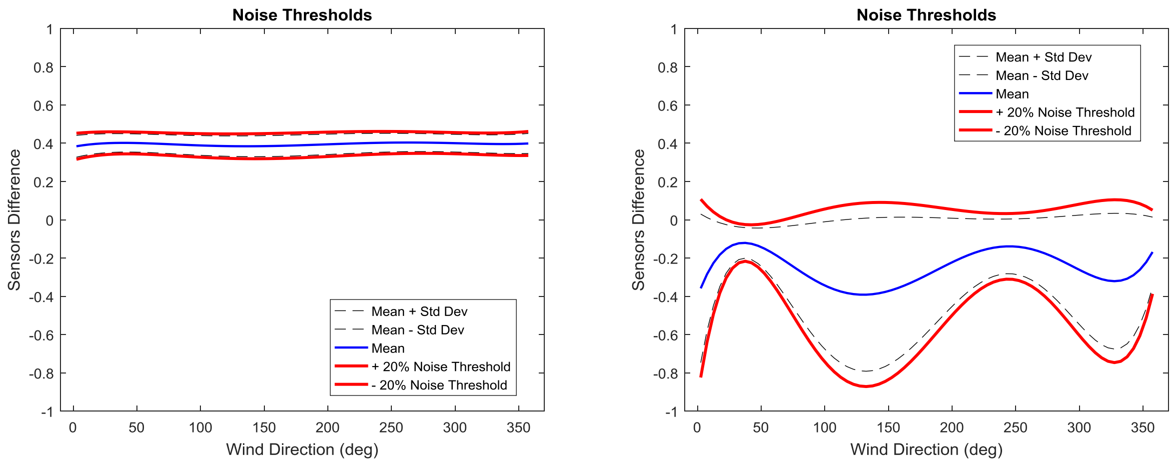

Figure 4-11 Noise Thresholds for 0-4 m/s. a) Sensors 1-2 b) Sensors 3-7

The noise thresholds are set to be 20% of the standard deviation of the difference between sensors. Although this percentage might seem high, it was set to be a reasonable trade-off between cleansing excessive noise and capturing diversions from the expected behaviour of the asset that could potentially lead to an acceleration of fatigue damage. Excessive cleansing would result in the removal of expected phenomena such as vibrations and sudden excitations that could locally affect the turbine (wind gusts, local impact of waves, propagation effects, or even localized damage). This percentage ensures that not too much data are discarded for further analysis; however, it may vary depending on the level of risk that each operator is willing to take. Figure 4-12 shows the percentage of deleted data for each sensor, at the three turbines and for the different wind classes, which correspond to the operational regimes previously mentioned (1: 0–4 m/s, 2: 4–11 m/s, 3: 11–18 m/s and 4: 18–25 m/s).

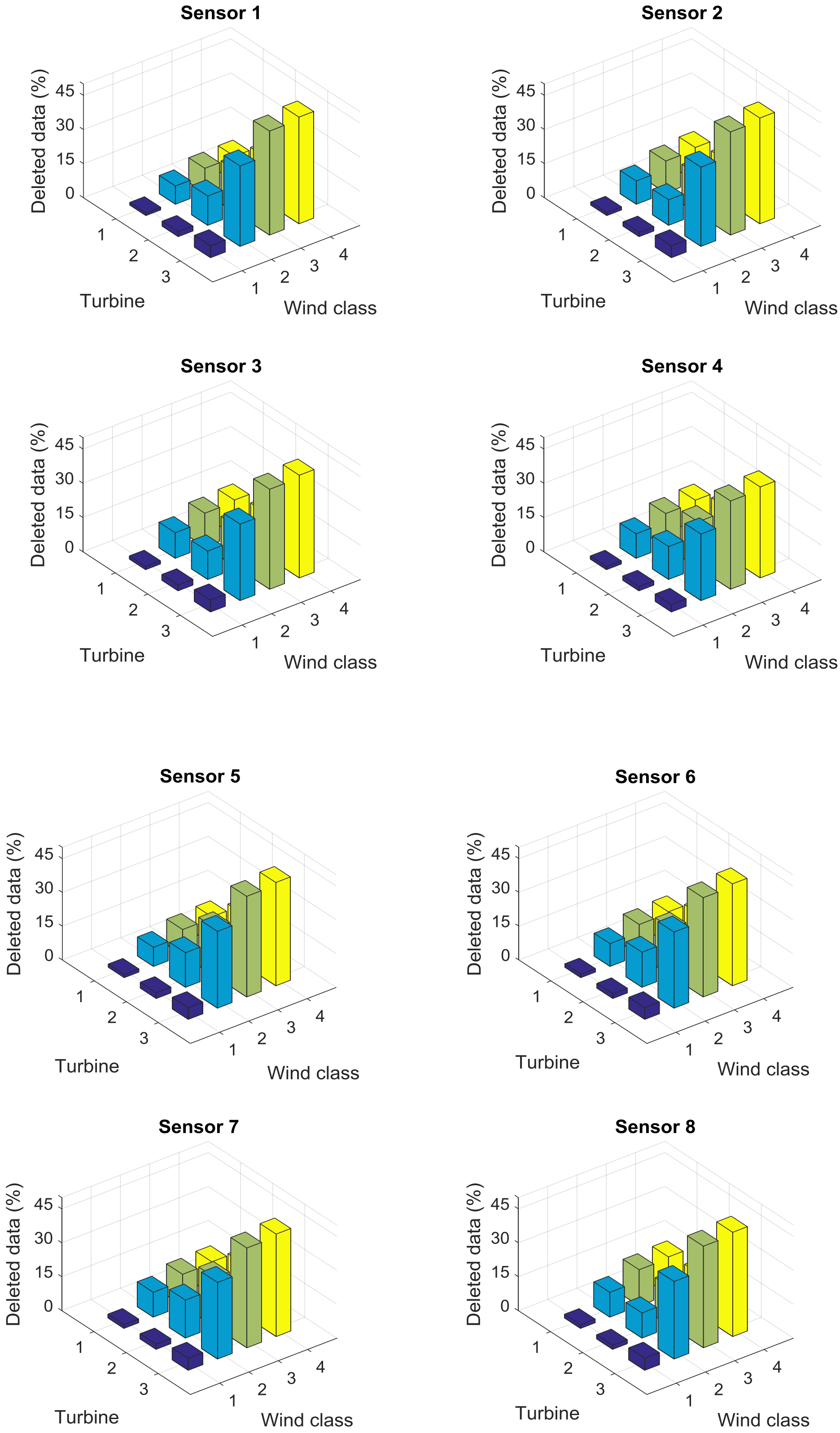

Figure 4-12 Sensors' percentage of cleansed data

4.3.2 Missing Data Imputation

After data cleansing has taken place, the missing data from the reduced but more accurate datasets are imputed with the aim of obtaining more complete datasets for the fatigue assessment. Artificial neural networks (NN) with different structures are developed to perform this imputation and to determine whether the imputation becomes more accurate due to the data cleansing. Therefore, following the MDI framework, the three filtered and cleansed datasets from Turbines 1, 2 and 3 were used as inputs and outputs to train the artificial NNs. The artificial NN employed was a two-layer feedforward network, with a sigmoid transfer function in the hidden layer and a linear transfer function in the output layer. The number of hidden neurons was optimised for each turbine. After the training was done, a removed from each sensor of both the original and the already cleansed datasets. A record of these randomly deleted data was kept for later on, when computing the deviation of the prediction from the real value (verification process).

Three different algorithms for artificial NN training were utilised: Scaled Conjugate Gradient, Levenberg-Marquardt and Bayesian Normalisation. Levenberg-Marquardt is recommended by [316] for most problems, but for some noisy and small problems Bayesian Normalisation can take longer but obtain a better solution [317,318]. For large problems, however, Scaled Conjugate Gradient is recommended as it uses gradient calculations which are more memory efficient than the Jacobian calculations the other two algorithms use [319]. Finally Levenberg-Marquardt was chosen for outperforming the others in terms of Error (minimum squared error (MSE) and residuals (R)), training performance, regression, number of iterations and training time needed. Figure 4-13 and 4-14 show an example of the error histogram and regression chart.

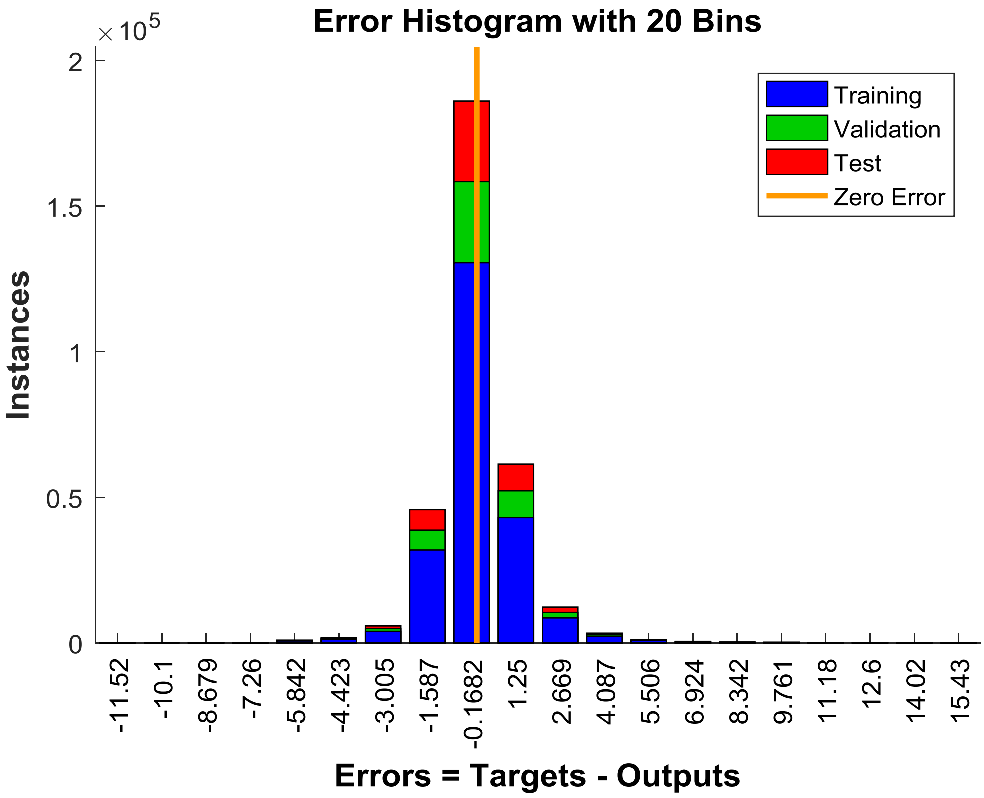

Figure 4-13 ANN's Error Histogram for Turbine 1

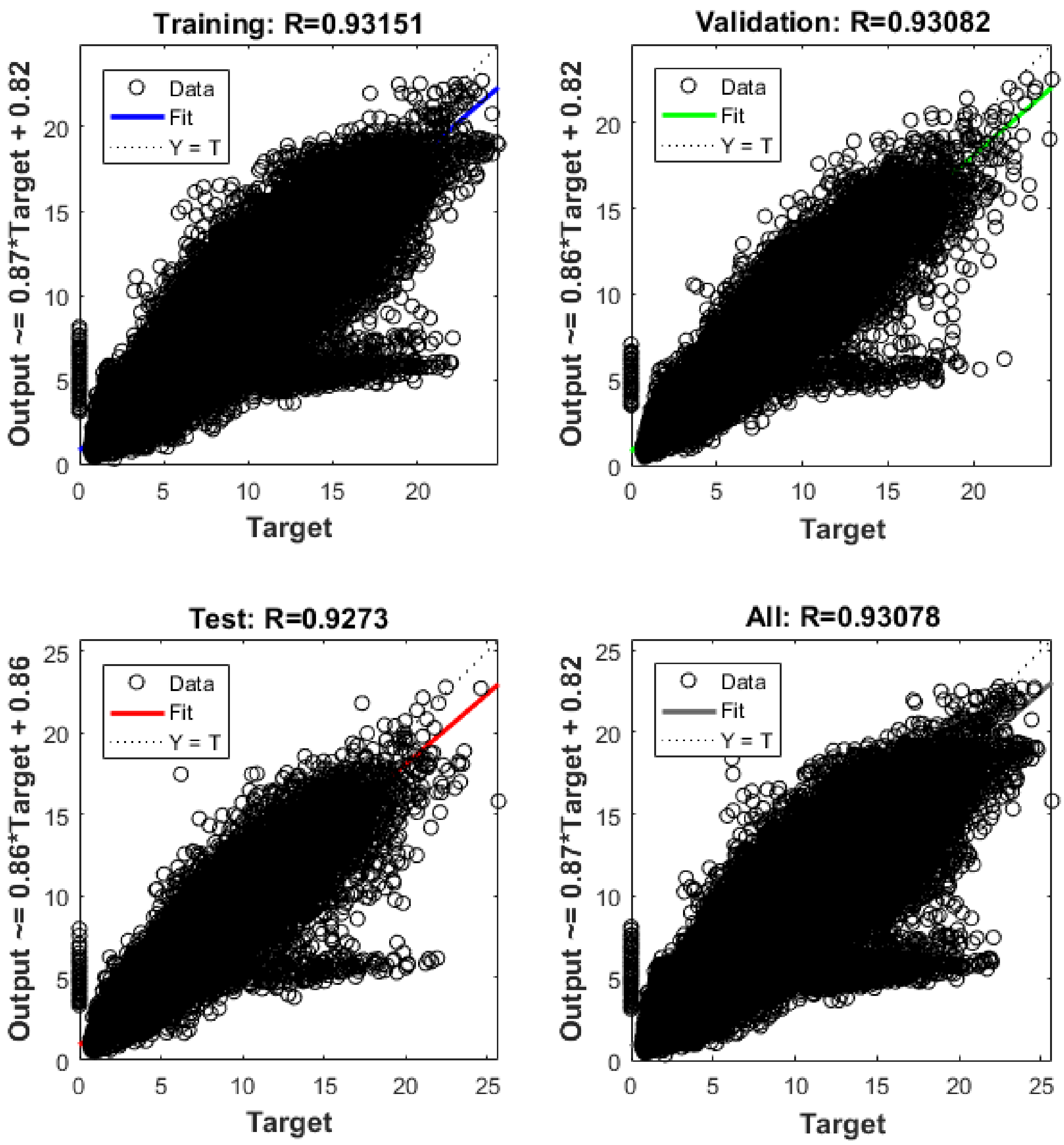

Figure 4-14 ANN's Regression plots for Turbine 1

Missing data were imputed through a number of stochastic input values to the ANN. A problem often presented in artificial NN is overfitting. Overfitting occurs when the network has memorized the training examples, but has not learned to generalize to new situations. This could be the case when the performance on the training set is good, but the test set performance is significantly worse. The solution in this case would be reducing the number of neurons. An example of overfitting can be the artificial NN employing 1000 neurons for Turbine 2, where the error is considerably higher than that of the 400 neurons artificial NN (see Figure 4-16). In order to avoid overfitting but optimise the results, the best performing architectures were chosen for each turbine. These were the 200, 400 and 1000 neurons for Turbines 1, 2 and 3 respectively. The following figures show the performance of the different artificial NN architectures for both with and without cleansing cases (see Figure 4-15, 4-16 and 4-17).

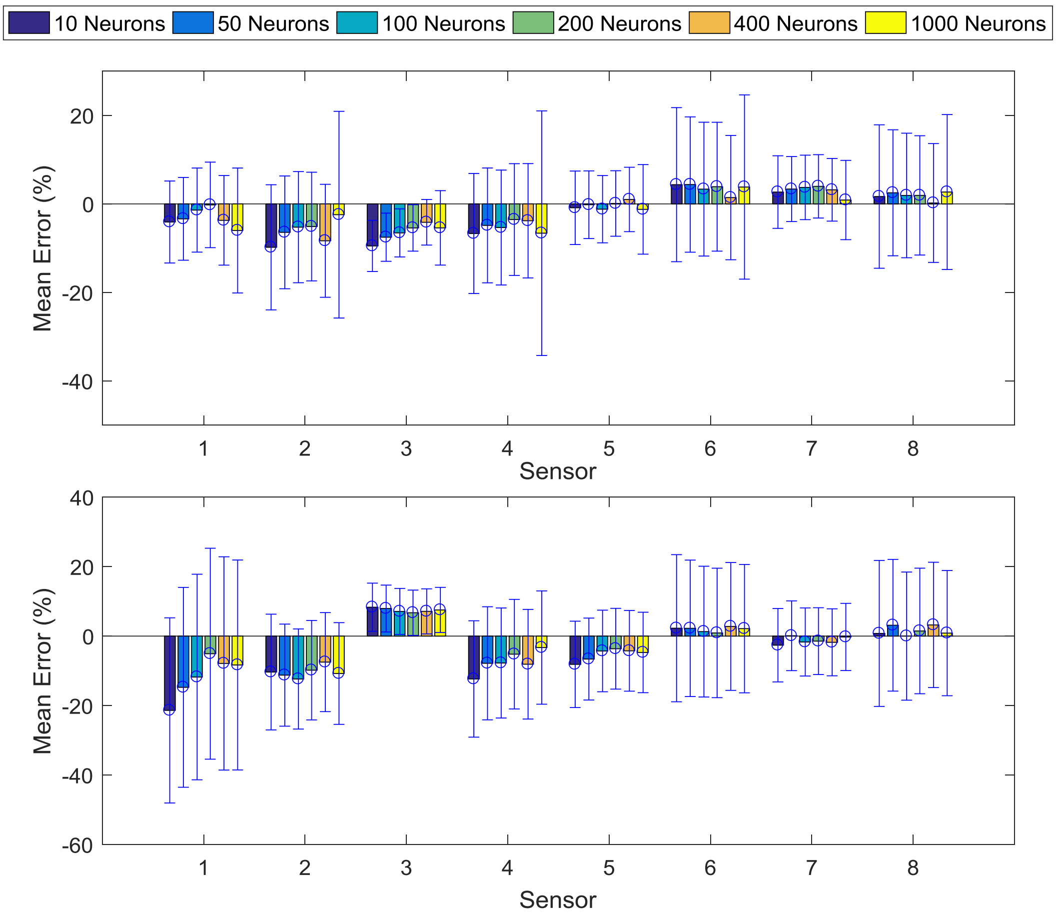

Figure 4-15 Artificial NN selection with (above) & without (below) data cleansing: turbine 1

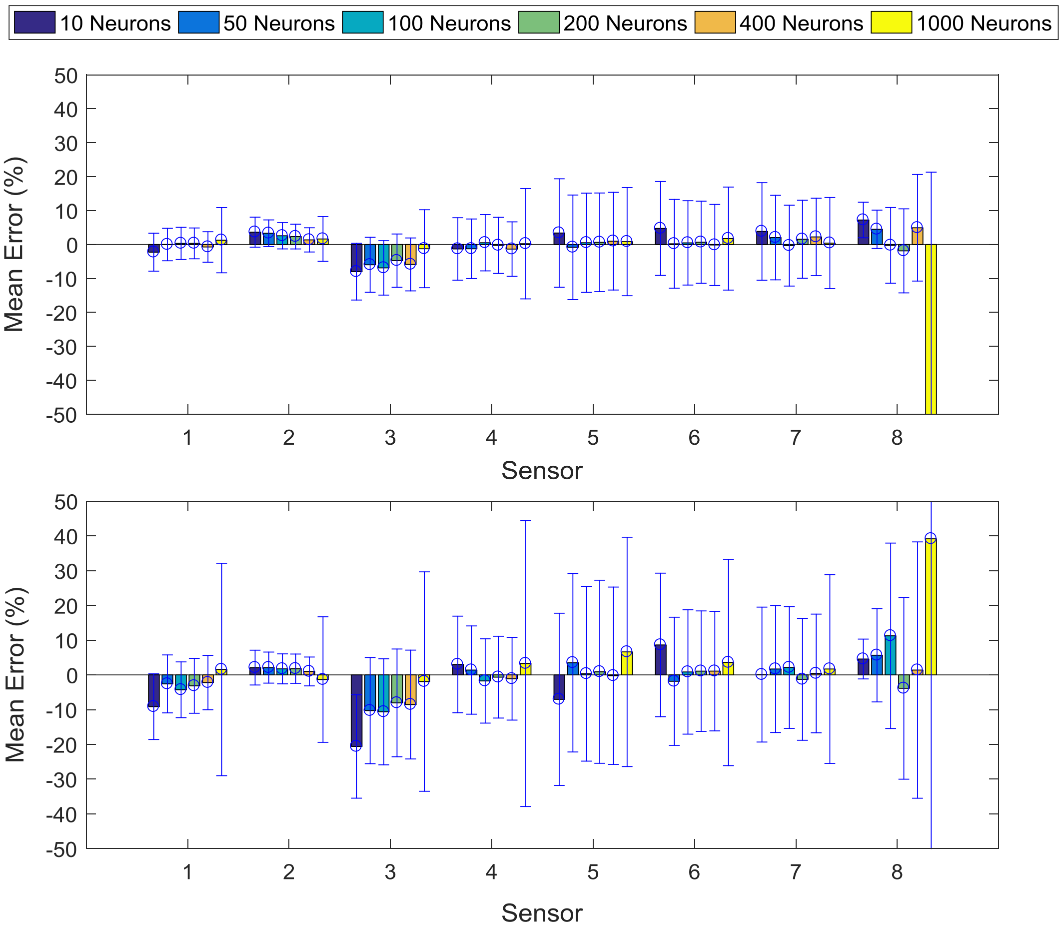

Figure 4-16 Artificial NN Selection with (above) & without (below) Data Cleansing: Turbine 2

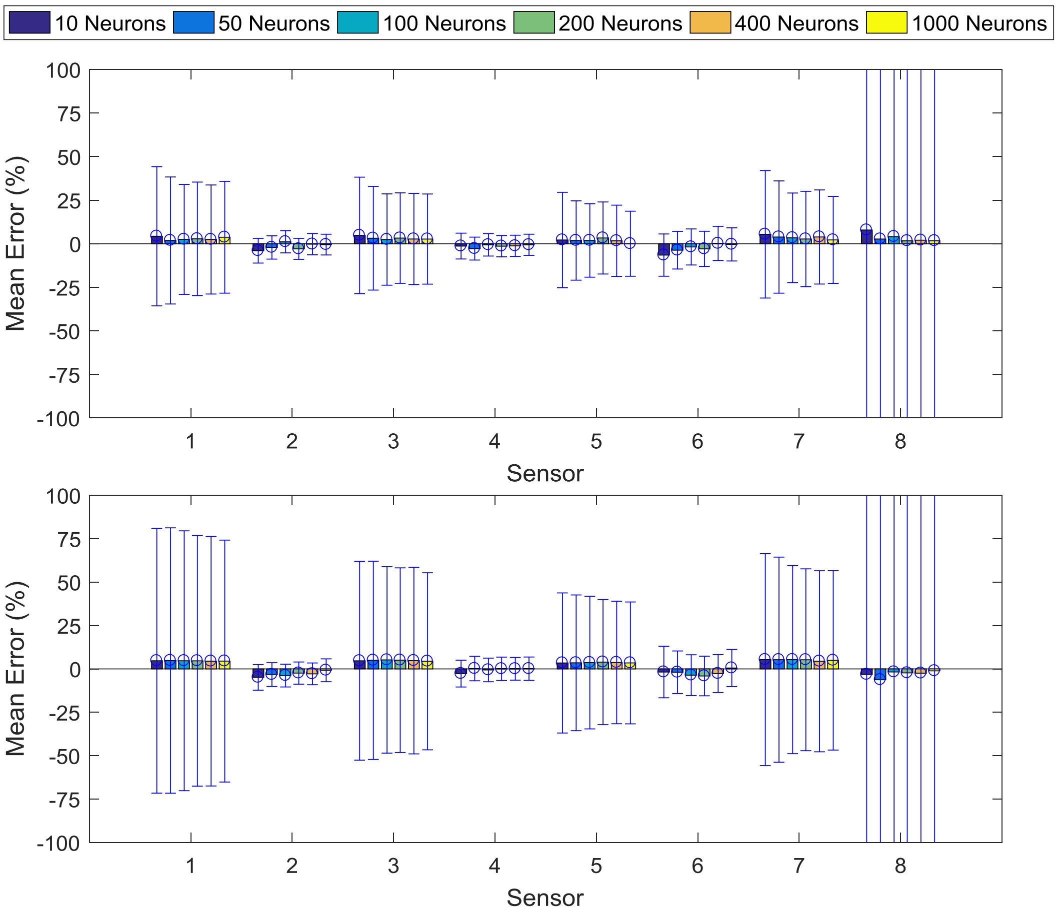

Figure 4-17 Artificial NN Selection with (above) & without (below) Data Cleansing: Turbine 3

Another aspect noticed during the cleansing process of Turbine 3 was that all measurements from sensor 8 were compromised as they appeared to be two orders of magnitude lower than the expected values. Therefore, the level of mismatching in the MDI is not surprising. Furthermore, the results of Turbine 3 show that for no apparent reason, axial sensors 1, 3, 5 and 7 present a higher challenge for the imputation, which appears to be mitigated with the cleansing, but is still noticeable.

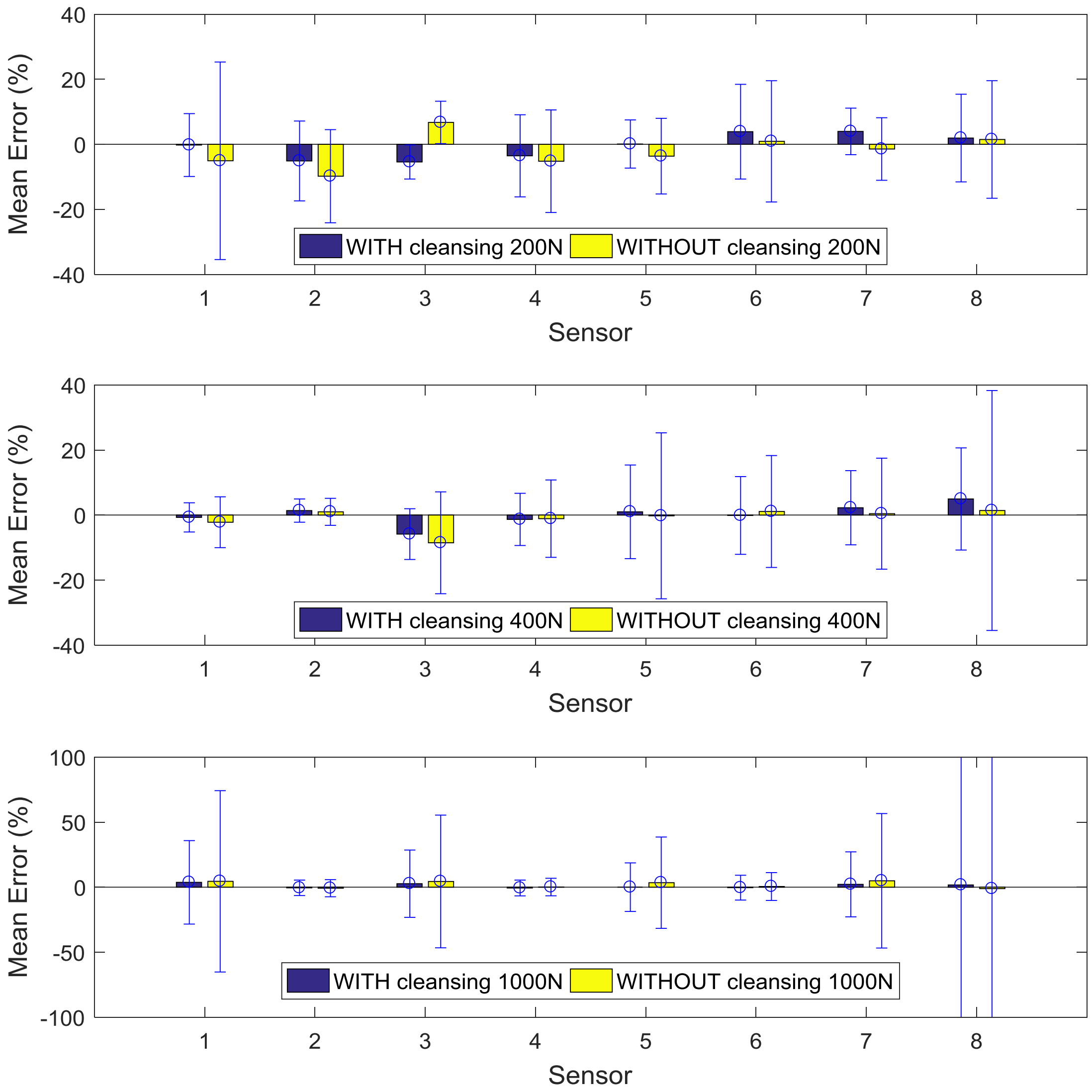

Figure 4-18 Missing Data Imputation comparison for Turbines 1, 2 and 3 respectively

Figure 4-18 represents a comparison between the best performing ANNs trained with and without cleansed data for the three turbines. This figure shows that MDI is performed more efficiently after data cleansing has taken place, as this reduces not only the mean error of the imputation, but also the standard deviation of this error. Thus, for the few cases where the mean imputation error of the dataset with previous data cleansing exceeded the one without it (Turbine 1: Sensors 6, 7 and

8; Turbine 2: Sensors 7 and 8), the absolute error is still smaller with data cleansing.

When the comparison of the performance is made (see Figure 4-19), results show that the average absolute error is 2.1%. Furthermore, in 95% of the cases (i.e.±2 standard deviations) the error is within the range [+15.2%−11.0%]. This estimation was carried out by averaging mean value and standard deviation errors across the eight sensors for the three turbines (excluding Sensor 8 from Turbine 3 as mentioned before). Besides, Turbine 3 presents the highest challenge to input data to, having standard deviations that exceed the 20% of error in the imputation.

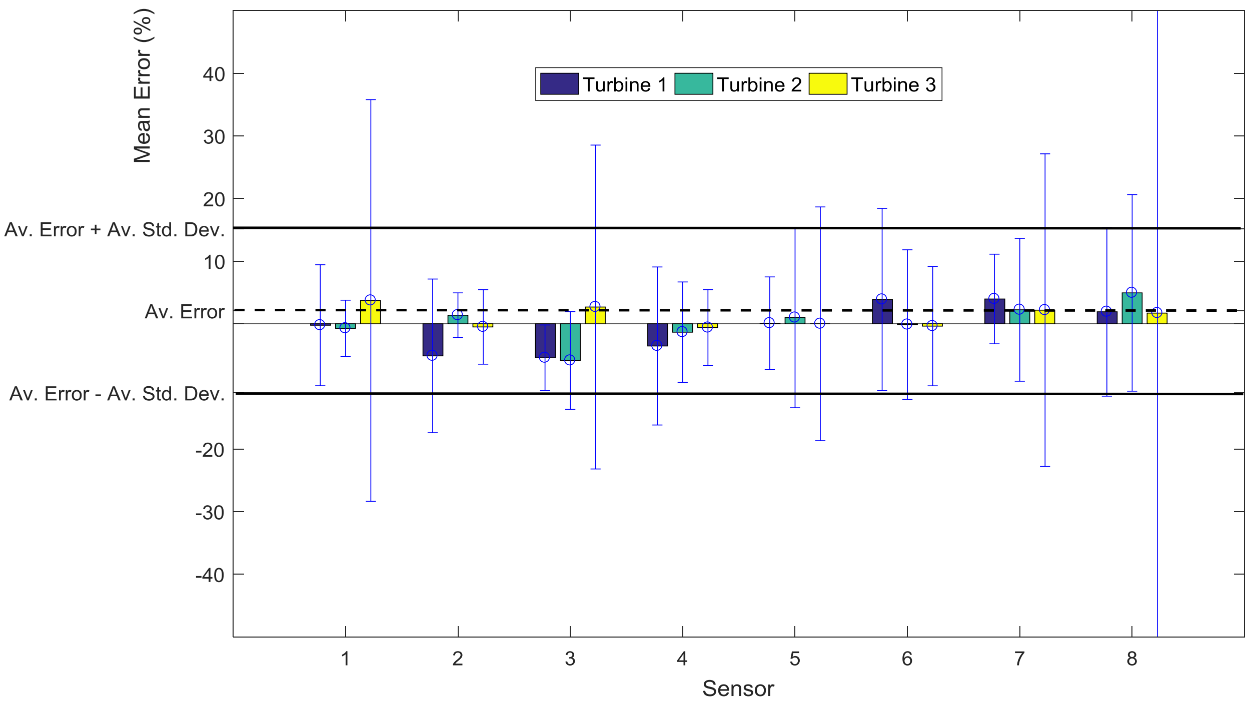

Figure 4-19 Comparison of Missing Data Imputation results between turbines

Furthermore, the errors presented in this section were calculated from the difference between the imputation and the exact value of DELs. Nevertheless, errors reduce considerably by checking when the imputed values are within the noise thresholds previously defined. These errors are presented in Table 4-1.

Table 4-1 Imputation Error within Noise Thresholds

Imputation Error within Noise Thresholds			
Data Cleansing	Turbine 1	Turbine 2	Turbine 3
YES	0.05 %	0.16 %	0.24 %
NO	5.28 %	10.51 %	32.17 %

4.3.3 Fatigue Assessment

Fatigue assessment constitutes the last step of the proposed methodology and the fundamental reason for its development. This section analyses the effect that data cleansing and MDI have on the current fatigue damage estimation. Fatigue assessment is normally based on uncomplete datasets, hence being able to impute missing data enhances the confidence in residual fatigue life estimations, as the number of samples increases and can become more accurate. However, this imputation needs to be precise by not introducing noise or amplifying biases in the estimations. Data cleansing is key in keeping noise away from the datasets. Figure 4-20, 4-21 and 4-22 show, for each of the three turbines under consideration, the effect that the four different combinations of cleansing and MDI scenarios have in fatigue calculations. This analysis takes Case D as its baseline, due to the positive results obtained in the previous section where missing data were proven to be imputed to the exact real value with an average absolute error of 2.1% and within the range of [+15.2%−11.0%], for 95% of the times.

According to Figures 4-20 and 4-22, fatigue is underestimated when data cleansing and MDI are not performed. This can be appreciated, especially in Case A (without cleansing/without MDI) and Case B (without cleansing/with MDI). The cause is believed to be an excess of noise, which contributes to the collection of lower measurements, and makes stress ranges lower for the rainflow-counting algorithm.

When data cleansing is not carried out but the MDI is, there is occasional overestimation of stresses (see Case B, sensors 1 and 6 in Figure 4-20 and sensors 3 and 5 in Figure 4-21). The reason is that the noise is picked up in the algorithm and reproduced, making the cumulative effect to considerably increase the overall fatigue of the structure. On the opposite side, Case C, where data cleansing is carried out but MDI is not, is found to underestimate fatigue for the three turbines. The explanation for this phenomenon is the dramatic reduction in the number of samples considered for the fatigue calculation (see Table 4-2).

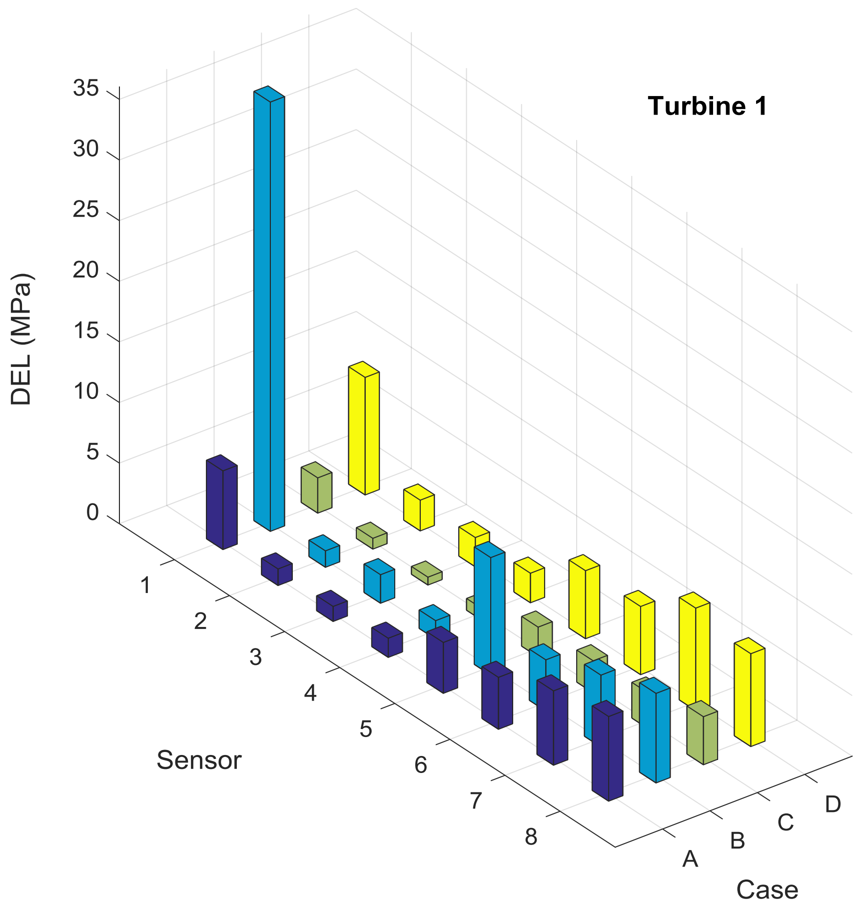

Figure 4-20 Fatigue scenarios: Turbine 1

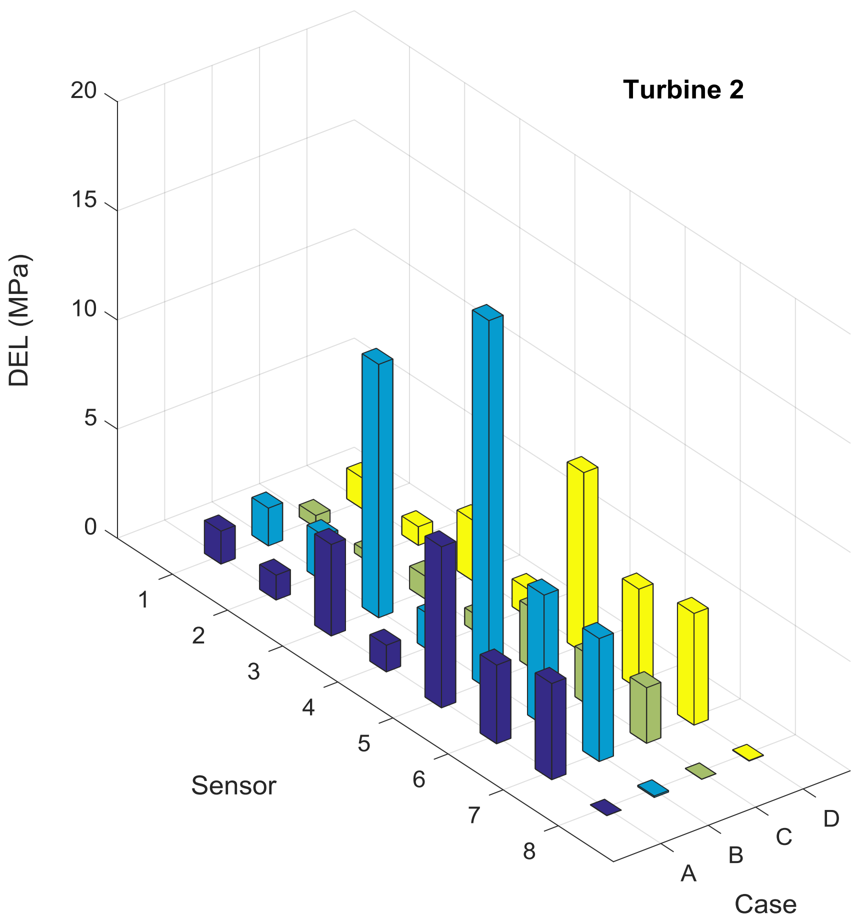

Figure 4-21 Fatigue scenarios: Turbine 2

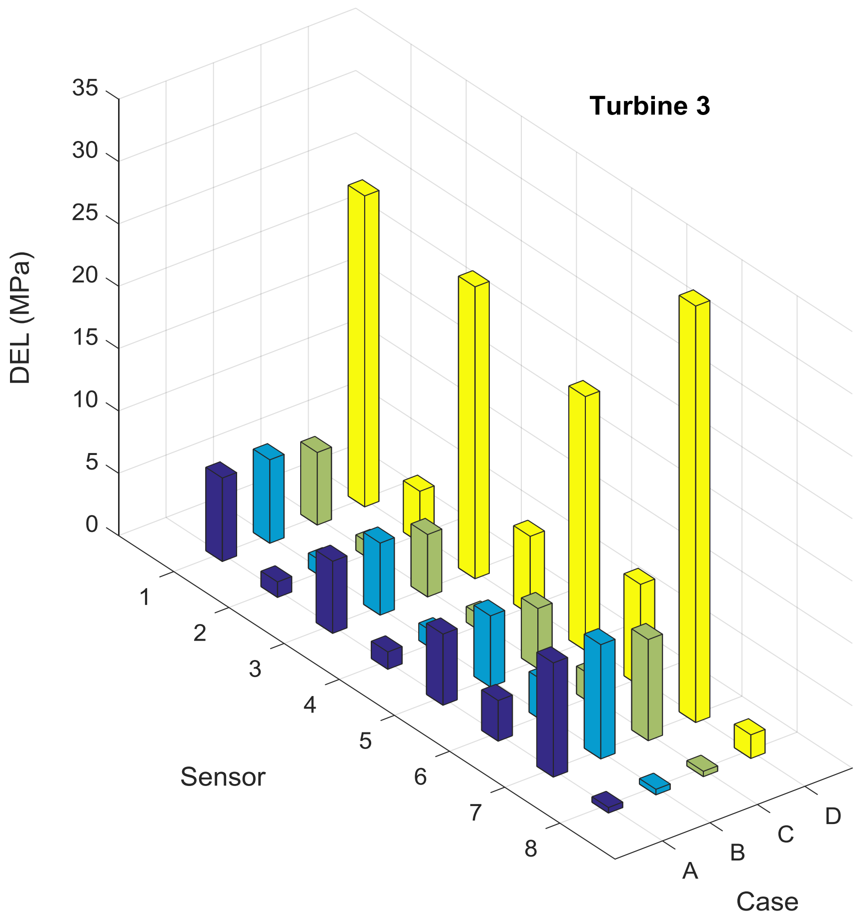

Figure 4-22 Fatigue scenarios: Turbine 3

The underestimation of fatigue when data cleansing is not carried out is particularly concerning. The implications of the underestimation of fatigue loads may seem small at this stage; however, these estimations have been made after two years of operation and at not critical locations. This means that while the difference in fatigue damage is currently not an issue, after ten years of operation it could make a difference to the remaining service life calculations, when an underestimated stress range is introduced in the S-N curve. Furthermore, sensors are not installed at turbine's hot-spots, meaning that the measurements they collect are potentially

5–10 times smaller than they could be at hot-spots [10]. The underestimation of fatigue could potentially make a big impact at these hot-spots and in the remaining service life of the structure.

Table 4-2 Number of samples for fatigue estimations according to different scenarios

Scenario	Turbine	# of Samples	Scenario	Turbine	# of Samples
Case A WITHOUT/ WITHOUT	1	64765	Case C WITH/ WITHOUT	1	40007
	2	28170		2	15888
	3	61254		3	29097
Case B WITHOUT/ WITH	1	195149	Case D WITH/ WITH	1	195149
	2	179981		2	179981
	3	168976		3	168976

4.4 Conclusion

In this study, a framework for the effective data management of SHMS was developed enabling the continuous analysis of OWT' structural integrity throughout the life cycle. The synchronisation between environmental data (SCADA and metocean) and real, continuously monitored, 50 Hz strain data collected from three different OWTs currently in operation in the Irish Sea, led to datasets over three years long; however, these three datasets were incomplete. Noise cleansing and MDI were carried out with the purpose of determining their benefits in continuous fatigue assessment of OWT.

Two scenarios were considered for each WT: with and without noise cleansing. Our results confirmed that in those cases where data cleansing was carried out, the average imputation error was about 2.1%. Furthermore, in 95% of the cases the error was within the range [+15.2%−11.0%]. The results indicated that noise cleansing and MDI could successfully be employed together to produce more complete datasets containing real low-disturbed strain data. Furthermore, fatigue was estimated for the four different cases, namely (i) without cleansing/without MDI (Case A), (ii) without cleansing/with MDI (Case B), (iii) with cleansing/without MDI (Case C), and (iv) with cleansing/with MDI (Case D). Results showed that for the wind turbines 1 and 3, fatigue was underestimated when data cleansing had not been performed. The cause is believed to be an excess of noise, which contributes to the collection of more uniform cycles of fatigue. In Case C, where data cleansing was carried out but MDI was not, fatigue was found to be underestimated for all the three turbines. Also, there was an overestimation of fatigue in some sensors when data cleansing was not carried out but MDI was. The reason is that the noise is picked up in the MDI algorithm and reproduced, making the cumulative effect to considerably increase the overall fatigue of the structure.

Currently, fatigue analyses are often performed based on incomplete datasets. The methodology presented in this research provides the possibility of enhancing the confidence in fatigue life estimations by increasing the length of the datasets through firstly, data cleansing and secondly, MDI. The results obtained validate our two novel methodologies, making it a suitable tool for better evaluation of OWT' structural integrity. We are exploring some opportunities to implement the proposed approaches in the wind energy sector with the aim of deriving more accurate fatigue life estimations to help push the boundaries of current operational periods and make the technology more competitive by reducing its LCoE. Further work could potentially focus on accounting for the degradation in the accuracy of sensor readings (increase in noise) across the years, comparing different periods across the life of a windfarm. A comparison between the performance of the proposed artificial NN method and some other techniques such as random forest, support vector machine and Gaussian process regression is in our research agenda.

4.5 Acknowledgements

This work was supported by grant EP/L016303/1 for Cranfield University, Centre for Doctoral Training in Renewable Energy Marine Structures (REMS) (http://www.rems-cdt.ac.uk/) from the United Kingdom Engineering and Physical Sciences Research Council (EPSRC) and Innogy SE.

5 GUIDELINES AND COST-BENEFIT ANALYSIS OF STRUCTURAL HEALTH MONITORING IMPLEMENTATION IN OFFSHORE WIND TURBINE SUPPORT STRUCTURES

Maria Martinez-Luengo and Mahmood Shafiee

Centre for Offshore Renewable Energy Engineering, School of Water, Energy and Environment, Cranfield University, Bedford, Bedfordshire, United Kingdom

Submitted 14th February 2019, Accepted 18th March 2019

Published in Energies 12 (2019) 1176

DOI: https://doi.org/10.3390/en12061176

Statement of contributions of joint authorship

Maria Martinez-Luengo conducted the literature review on the regulations and standards, developed the guidelines, Structural Health Monitoring (SHM) strategy and inspection strategy, planned and performed the cost-benefit analysis, drafter and critically reviewed this manuscript. Also, María analysed the results and produced figures and tables in this paper. Mahmood Shafiee supervised the work, reviewed and critically commented on the manuscript before its submission to Energies.

Abstract: This paper investigates how the implementation of Structural Health Monitoring Systems (SHMS) in the support structures (SS) of Offshore Wind Turbines (OWT) affects Capital and Operational Expenditure (CAPEX and OPEX) of Offshore Wind Farms (OWF). In order to determine the added value of Structural Health Monitoring (SHM), the balance between the reduction in OPEX and the increase in CAPEX is evaluated. In this paper, guidelines for SHM implementation in OWF are developed and applied to a baseline scenario. The application of these guidelines consist of a review of present regulations in the United Kingdom and Germany, the development of SHM strategy, where the first stage of the Statistical Pattern Recognition (SPR) paradigm is explored, failure modes that can be monitored are identified, and SHM technologies and sensor distributions within the turbines are described for a baseline scenario. Furthermore, an inspection strategy where the different structural inspections to be carried out above and below water is also developed, together with an inspection plan for the lifetime of the structures, for the aforementioned baseline scenario. Once the guidelines have been followed and the SHM and inspection strategies developed, a cost-benefit analysis is performed on the baseline case (10% instrumented assets) and three other scenarios with 20%, 30% and 50% of instrumented assets. Finally, a sensitivity analysis is conducted to evaluate the effects of SHM hardware cost and the time spent in completing the inspections on OPEX and CAPEX of the Wind Farm (WF). The results show that SHM hardware cost increases CAPEX significantly, however this increase is much lower than the reduction in OPEX caused by SHM. The results also show that an increase in the percentage of instrumented assets will reduce OPEX and this reduction is considerably higher than the cost of SHM implementation.

Keywords: Offshore wind; Structural Health Monitoring (SHM), Offshore inspection; guidelines; Cost-benefit analysis; Operational expenditure (OPEX), Capital Expenditure (CAPEX)

5.1 Introduction

Over the past 15 years, wind energy has experienced a remarkable growth in Europe. This is partially due to the long-term goal set by the European Commission (EC) to lower greenhouse gas emissions by 80–95% by 2050, compared to levels in the 1990's. This target has had significant implications for renewable energy development, which has experienced a rapid growth in the past few years. Wind power technologies (including onshore and offshore) play a crucial role in reaching Europe's renewable energy targets. The Offshore Wind (OW) industry in Europe is moving fast to being a mainstream supplier of low-carbon electricity [320]. In 2017 alone, about 3150 MW new OW power capacity was connected to the grid. This is twice more than in 2016 and 13% higher than in 2015, which was until now the record year for OW power installation [7]. This rapid development is not only due to the targets set by the EC in 2006 for all Member States [13], but also due to the scalability of wind energy with units of larger capacity been deployed in larger farms, further offshore [14].

The United Kingdom (U.K.) currently has 36 large WF, generating 20.8 TWh of electricity, which supplies on average 6.2% of the nation's electricity demand [321]. Furthermore, by the end of 2017, 2923 turbines were either operational or under construction, reaching a cumulative installed capacity of 5.83 GW, which will soon reach 10.4 GW once turbines being commissioned are energised [321]. Moreover, in February 2018 the 7 GW milestone was reached, which highlights the industry's progression. With all this growth taking place, areas close to shore and with good wind resource are running out and WF tend to be developed further from shore, which usually implies deeper waters. As was reported by WindEurope [7], the average water depth of OWF with grid connections in 2017 was 27.5 m, whereas the average distance-to-shore was 41 km.

A key factor in the rapid development of the OW industry is the substantial reduction in the Levelised Cost of Electricity (LCoE) experienced in the past few years, which enhanced and stimulated investors' interest in the industry. In 2013, the LCoE for OW energy was €140/MWh [322], but over the last few years this has cost plummeted, surpassing the 2020 target of €100/MWh. Vattenfall's OW price bid of €49.9/MWh in 2016 for the Kriegers Flak project set a record LCoE forecast of €40/MWh [323]. In order to achieve and maintain the expected cost reductions and ensure the cost-competitiveness of OW in the energy sector, OW operators are currently investigating ways to optimise CAPEX and OPEX, which will lead to an LCoE reduction. An alternative route to reduce OPEX, and subsequently LCoE, is through the optimisation of the inspection and maintenance strategies. This optimisation is carried out by switching periodic or risk-based inspection regimes to a condition-based regime. In order to do so, periodic inspections can be postponed or directly taken out of the scope of works whenever the condition of the assets is proven to be appropriate. SHMS are currently the best approach to gain confidence in the assets' integrity without actually deploying offshore. Furthermore, depending on the country, regulations about inspection regimes and monitoring of offshore assets may differ.

Today, a few technical guidelines for SHM exist and these are mainly focused on civil infrastructure, such as bridges [324]. These were developed and published by national or international scientific or technical organizations [325–329]. In the OW field, Germanischer Lloyd — one of the leading certification organizations — published a guideline for the certification of Condition Monitoring (CM) systems for WT [330]. This guideline focusses mainly on the rotating parts of an OWT (CM Systems), but also includes requirements for SHM of the SS. Nevertheless, guidelines for SHM implementation in a holistic way constitute a research gap in the academic literature. For the sake of clarity, a distinction needs to be made between "guidelines for the implementation of SHM technologies" and "guidelines for SHM implementation". The former refers to the process of determining how a particular technology would be applied into a given turbine. It will involve different aspects, such as the number of sensors, where these sensors will be located, their distribution, redundancies, number of channels for the data acquisition unit (DAU), the data transmission system and data storage, among others. The latter refers to the integration of different SHM technologies to optimise the structural integrity of an asset holistically and the understanding of the environmental and geographic challenges, design weaknesses and the expected failure mechanisms associated with this asset. It involves the development of a SHM strategy that increases confidence in the structural integrity of the assets as a whole, complying with local legislation and aiming for an economic benefit.

This paper aims to deliver guidelines for the correct SHM implementation to the SS of a baseline OWF. An increase in implementation of these systems will enhance operators' confidence in the structural integrity of OWT SS and reduce the number of inspections they need during their lifetime. An example of the application of these guidelines is also provided for the baseline scenario, which is employed later in Section 5.3. An economic analysis is performed for the baseline WF to evaluate the benefits of SHM implementation in terms of reduction in OPEX, based on the previously developed guidelines. Furthermore, a comparison is made between the achieved OPEX reduction and the incurred cost of SHM implementation. The organisation of this paper is as follows. Section 5.2 presents the guidelines for SHM implementation, which when installed from the beginning of the operation on the WF, could be used to adopt a condition-based inspection strategy for reducing OPEX. In Section 5.3, a cost-benefit analysis of the impact of SHMS implementation in OPEX reduction is carried out based on the applied guidelines developed in Section 5.2. These results are presented and discussed in Section 5.4 and followed by general conclusions in Section 5.5.

5.2 Guidelines for structural integrity monitoring of offshore wind turbine support structures

This section presents the process to be followed for the implementation of SHMS in OWF's SS from the design stage. The reason why SHM needs to be considered early during design is to consistently capture the loading conditions of the turbines throughout the life of the structures (not only operational life, but also during the installation-energisation and stop-of production and decommissioning) and to determine whether the structural integrity of the units is as good as expected, or if anything is compromising it. SHM not only provides confidence in the condition-based inspection and maintenance strategy but can also be used in the structural integrity evaluation process of the assets in order to obtain certification and permits from governmental authorities. If SHMS are designed, installed and their data analysed appropriately, OPEX could be reduced, even though their implementation would have a slight increase in CAPEX associated with the commissioning stage. Nevertheless, this increase in CAPEX would be justified by the higher decrease in OPEX experienced throughout the operational life of the units. The proposed guidelines for SHM implementation consist of five stages:

I. To obtain a clear understanding of the legislation regulating the territory where the OWF will be developed.
II. To perform an analysis of the design drivers and challenges (i.e., sand banks that make the structures prone to scour development or a high tidal range that compromises accessibility) and failure mechanisms expected for the preferred design concept.
III. To develop a SHM strategy based on the failure mechanisms that can be monitored.
IV. To develop an inspection strategy that takes into consideration points I, II, and III and that becomes an economic justification for SHM implementation.
V. To verify the economic feasibility of the proposed SHM strategy implementation. If the SHM implementation does not achieve a higher OPEX reduction than the associated CAPEX increase, either the SHM and inspection strategies should be reconsidered, or an alternative justification for the aforementioned implementation should be found (ie., an OWF is already in operation and SHMS are being implemented after there is the risk of a failure mechanism occurring).

In the following subsections, the different stages of the SHM implementation guidelines are developed and applied to a baseline. The regulations concerning the inspection and maintenance of OW assets in the United Kingdom and Germany are reviewed (Section 5.2.1). A methodology for the development of a SHM strategy at a WF level is presented (Section 5.2.2), and an inspection strategy for a baseline scenario is provided (Section 5.2.3) for the posterior cost-benefit analysis carried out in Section 5.3.

5.2.1 Regulations and standards

In the offshore industries, operations often take place within the limits of territorial waters and a state's Exclusive Economic Zone (EEZ). Legislative frameworks that are applicable to OW assets depend on the coastal state in whose waters they are installed. All states regulate the activities on their EEZ, however, international law must also be observed. The United Kingdom and Germany have been chosen as examples of the two European countries with the highest installed wind power capacity in 2017 [7]. The regulations concerning inspection and maintenance of OW assets in these two countries have been reviewed and compared below.

In the United Kingdom, The Department for Energy and Climate Change [331] has overall responsibility for offshore energy projects, though some responsibilities in England and Wales are delegated to the Marine Management Organisation and powers are devolved to the Scottish Executive for Scottish projects. The Maritime and Coastguard Agency (MCA), as an executive agency of the Department for Transport and the Health and Safety Executives of Great Britain and Northern Ireland, hold the main responsibilities for Health and Safety (H&S) regulations in the United Kingdom's OW industry. While floating structures are regulated by the MCA, fixed-bottom structures on the U.K. continental shelf are regulated by the Health and Safety Executive of Great Britain.

In terms of inspection requirements, there is no entity or regulatory body imposing periodic inspection intervals. It is up to the operator to take care of the integrity of its assets. However, in order to get the appropriate insurance, the assets need to be certified by a certification body (i.e., DNV GL (Det Norske Veritas Germanischer Lloyd), Lloyds Register, etc.). Technical evidence proving that the assets have been designed, inspected and maintained following best practices and regulations (when applicable) must be provided to these certification authorities by the operators.

In contrast to the United Kingdom, Germany has a more complicated process for obtaining the consent for installation and operation of OWF. The Bundesamt für Seeschifffahrt und Hydrographie (BSH) [332] is the regulating authority for OW projects in German waters. All inspection and maintenance performed on the OW assets (WT, substation, array cables, onshore base and port, etc.) must be done in accordance with the requirements set out in the corresponding standards in their current version, as well as current state-of-the-art requirements for certification. BSH standards are listed in Table 5-1.

Table 5-1 BSH regulations to be abided for the development and operation of OWF in Germany

Regulating authority	Standard document	Ref
BSH	Minimum requirements concerning the constructive design of offshore structures within the EEZ	[333]
	Design of offshore wind turbines	[334]
	Minimum requirements for geotechnical surveys and investigations into offshore wind energy structures, offshore stations and power cables.	[335]
	Investigation of the impacts of OWT on the marine environment (StUK4)	[336]

One of the key requirements imposed by the BSH for the development of OW projects is that the design of these projects is certified by a certification authority (e.g. DNVGL, Lloyds Register, etc.). In order to acquire this certification some technical codes of practice that shall be taken into account in the design and marine operations of the WF. These are listed in Table 5-2.

Table 5-2 Technical standards for the design and operation of OWF

Standard document	Regulated subject	Ref
ISO 19901-6	Petroleum and natural gas industries – Specific requirements for offshore structures, Part 6: marine operations	[337]
ISO 19905-1	Petroleum and natural gas industries – Site-specific assessment of mobile offshore units – Part 1: Jack-ups	[338]
ISO/DIS 29400	Ships and marine technology – Offshore wind energy – Port and marine operations	[339]
EN 1990	Basis of structural design	[340]
EN 1997	Eurocode 7: Geotechnical design	[341]
EN 1993	Eurocode 3: Design of steel structures	[265]
DNV-OS-H101	DNV offshore standard – marine operations, general	[342]
GL-IV-7	GL rules for the certification and construction, IV industrial services, Part 7: Offshore substations	[343]
GL-IV-6	GL rules for the certification and construction, IV industrial services, part 6: Offshore technology	[344]
API RP-2A-WSD	American Petroleum Institute, Recommended Practice – Planning, designing and constructing fixed offshore platforms – working stress design	[345]
GL-IV-2	GL rules and guidelines, IV industrial services, Part 2 Guideline for the certification of offshore wind turbines	[346]
DNV-OS-J101	DNV offshore standard – Design of offshore wind turbine structures	[255]
DNV-OS-J201	DNV offshore standard – Offshore substations for wind farms	[347]

Furthermore, there are two special consent approvals to be obtained. These concern the inspection and maintenance regimes of the Grouted Connection (GC) in both the offshore substation and WT. Maintenance of the equipment installed on the offshore assets is to be carried out with consideration of the original equipment manufacturer's recommendations and particular warranty conditions, as well as any applicable statutory requirement related to the certification of the equipment as listed below. Nevertheless, as this paper is focused on OW assets' SS, inspection and maintenance of this equipment is considered out of scope. Aside from the standards listed above, the Periodic Inspection Concept needs to meet the outstanding conditions from the certification reports. These conditions are:

Table 5-3 Minimum requirements for the periodic inspection of SS according to the BSH [8]

Test object	Test basis and intervals
Functionality of the anodes or impressed-current system	During the first 2 years: annually After the first 2 years: depending on the condition (recommended every 4 years)
Substructure: welded seams (subject to cyclic loads), intactness of the surface of the structural elements	In accordance to the life cycle calculations and inspection plan
Composition of the seabed surface, scouring	During the first 2 years: annually After the first 2 years: depending on the condition (recommended every 4 years)
Corrosion protection (visual inspection): • Underwater area of the structure • Alternating load • Underwater area of the substructure • Operational structure (SS)	• Depending on the condition (recommended every 4 years) • Depending on the condition (recommended every 2 years) • Depending on the condition (recommended every 4 years) • Depending on the condition (recommended every 4 years)
Operational structure: welded seams (subject to cyclic loads), bolts	In accordance to the life cycle calculations and inspection plan

The areas and locations to be subjected to periodical inspections are to be selected based on a risk-based prioritisation. Based on standard recommendations [34], the interval between inspections of critical items should not exceed one year. For less critical items, longer intervals are acceptable. All the structural assets should be inspected at least once every five-year period. This could be taken as one single inspection in that period, or as the inspection of a certain percent of the total number of assets on a regular basis. The latter is considered a more sensible approach, as it enables the operator to have a continuous record of the integrity of the structural assets, e.g., 20% of OWT foundations on an annual basis.

Ultimately, the risk-based SHM of the structural assets shall be used to reduce the scope of structural inspections in some cases, upon demonstration of the appropriate integrity level of the assets. These methods are meant to be employed for the entire operational life of the SS, modifying the scope of inspections and their periodicity, based on the findings and real condition of the assets. These periodic inspections shall provide evidence that the SS continues to comply with the design assumptions and that findings and observations are within the operational limits. If the periodical inspections or continuous SHM on selected locations reveal that degradation mechanisms are not developing as expected, unscheduled inspections or remedial works may be required. Unscheduled activities can be also triggered following an incident or event likely to have affected the structural integrity.

5.2.2 SHM strategy

As previously mentioned, the SHM strategy for the through-life of an OWF should, ideally, be built during the design stage. This means that while some design milestones are settled (foundation type, pile depth, stiffness, natural frequency, different welds criticality, etc.), SHMS can be designed to cover risky aspects of the design and to optimise the inspection intervals. The way SHMS are designed and implemented follows the SPR paradigm, which is widely used across different industries for the implementation of damage detection strategies [23,348]. This paradigm was initially introduced in the SHM field by Farrar and Sohn [349] and later on adapted to the OW industry by Martinez-Luengo et al. [11,266]. The SPR paradigm consists of four stages, which are intensively described in [266]. These stages are presented in Figure 5-1.

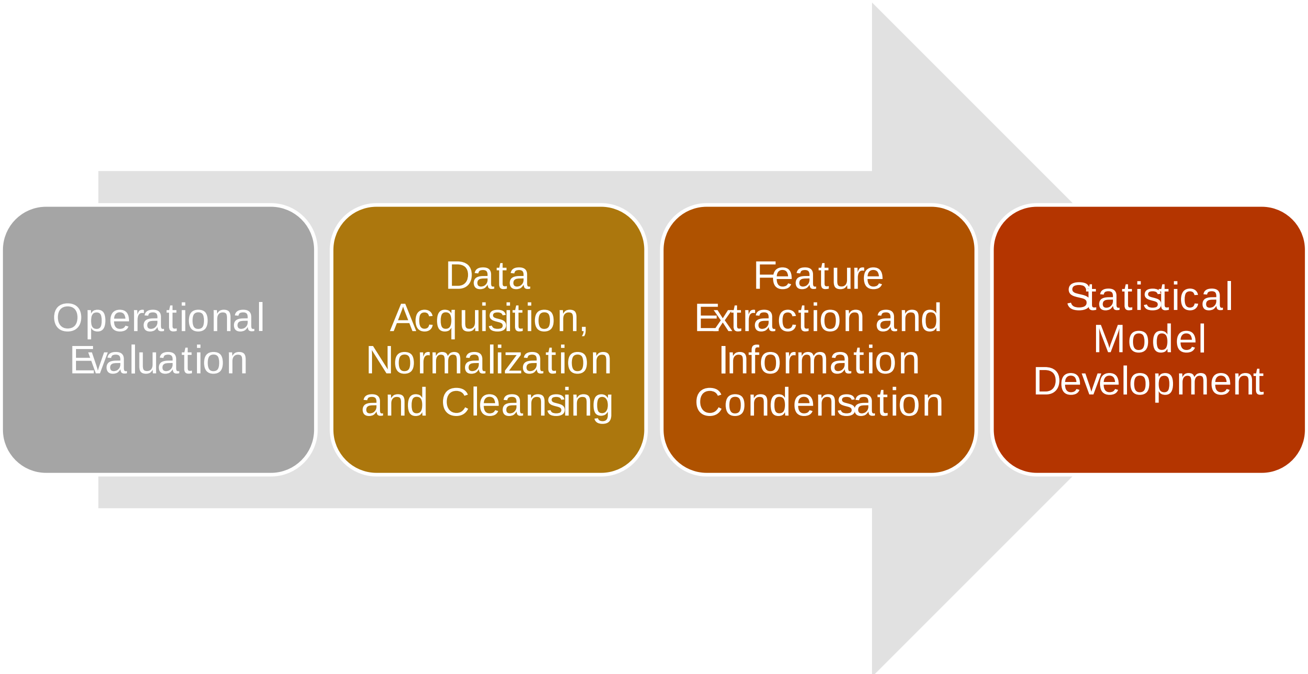

Figure 5-1 Statistical Pattern Recognition stages

Operational evaluation is the first stage of the SPR paradigm and the one to be approached first during the design stage, as it sets the boundaries of the damage identification problem. This subsection focuses on the operational evaluation stage in order to give an example of the process and set the basis of the cost-benefit analysis carried out in Section 5.3. This stage aims to answer four questions concerning the implementation of the damage detection strategies. These questions relate to the following:

A. The motivation and economic justification for implementing the SHMS: while the motivation for the implementation of SHMS is to gain certainty in the structural integrity of the monitored assets, extend the service life and increase the WF revenue, the economic justification is covered in the next Section with the cost-benefit analysis.

B. The different systems' damage definitions.

C. The Environmental and Operational Conditions (EOC) in which the SHMS are used.

Operational evaluation, which is often disregarded in the literature, is crucial for the development of SHM strategies. It identifies the different failure mechanisms that are potentially worth monitoring and establishes damage thresholds. These damage thresholds are later employed to determine whether something is compromising the structural integrity of the assets, and therefore an unscheduled inspection is required to verify the extent of the damage and potentially carry out repair works, or everything is behaving as expected, and therefore a future scheduled inspection may not be required. The EOC in which the SHMS are operating also needs to be set in the operational evaluation stage (part C), as depending on the technologies employed, issues may arise with the damage sensitive features obtained (i.e., modal analysis).

In order to perform the operational evaluation, the basis for the next section's cost-benefit analysis needs to be set. For this purpose, a baseline scenario for an OWF is defined. The main characteristics of this baseline case are given in Table 5-4.

Based on these characteristics, the failure modes of the SS (foundation, GC and transition piece (TP)) are identified. After the failure mode identification, those failure modes that could potentially be monitored are analysed and their condition-based inspection strategy is optimised [142]. Table 5-5 shows the effect that these failure modes may have on the structural integrity of the assets.

Table 5-4 WF baseline scenario and EOC

Characteristic	Unit	Value
Number of WTs	-	100
Turbine capacity	MW	5
WF area	km^2	50
Average distance to port	km	50
Average water depth	m	30
Foundation type	-	Monopile
Number of offshore substations	-	1
Average wind speed	m/s	10.0 m/s (at hub height)
Tidal conditions	s	0.5m (HAT to LAT)
50 year wave	m	6.5
Current	m/s	1.0
Number of export cables	-	1

Table 5-5 Failure modes of offshore wind turbine support structures and their effects on structure integrity.

Failure mode	Impact on structural integrity	Can be monitored?	SHMS
Excessive loading	Accelerated fatigue	YES	Accelerometers and/or strain gauges
Cracks in welds	Accelerated fatigue	YES	Accelerometers and/or strain gauges
Corrosion	Loss of material leading to over-utilisation	YES	Impressed currents corrosion protection (ICCP)
Excessive fouling or marine growth	Corrosion and modification of modal properties and loading conditions	NO	Could be monitored by accelerometers but difficult to estimate the root cause of the modification in natural frequencies. Therefore it deems not worth monitoring
Scour	Loss of bearing capacity and modification of modal frequencies	YES	Accelerometers (not first mode), cameras or sonar
GC displacement	Loss of structural integrity	YES	linear variable differential transformer (LVDT)

Accelerated fatigue can lead to collapse of the structure before its decommissioning, which is the reason why some OWF were intentionally overdesigned. However, this overdesign implies a potential loss of revenue due to the decommissioning of an asset that may still be able to operate safely. Maximising return of investment (RoI) while optimising LCoE through the asset's life extension could be achieved when the structural integrity of the aforementioned asset is well known. This is when continuous SHM becomes necessary. Fatigue and modal property monitoring are among the most important SHM techniques for SS of OWF, as the consequences of structural damage may be catastrophic. Modal properties can be monitored though the variation that modal parameters, such as resonance frequency, damping coefficient and modal curvatures, among others, experience with the change in different physical properties (i.e., reduction in mass or stiffness) [23,349]. In order to carry out modal property monitoring and analyse the structure's dynamic response, several accelerometers must be installed [266]. Operational Modal Analysis allows modal parameters in operational conditions to be estimated based only on vibration responses, without measuring the excitation forces [59,350].

Corrosion is one of the failure modes that most compromises the integrity of the SS of OWT, as it attacks any unprotected metal surface. This failure mechanism can be avoided by the protection of these surfaces in contact with the sea water [20]. Contact between dissimilar metals must also be avoided to prevent galvanic corrosion. This is achieved by the introduction of isolating elements and washers between the two metals [351]. The corrosion protection system of the SS of OWT comprises corrosion allowance, paint coating and cathodic protection by means of sacrificial anodes (SACP) or impressed currents corrsion protection (ICCP). All primary steelwork surfaces of the Monopile (MP) and TP, the secondary steelwork and the main access platform elements are coated according to ISO 12944 [352]. The SACP consists of stand-off sacrificial anodes made of Al-Zn-In, cast onto a steel insert, which are welded onto the MP structure. Corrosion is generally not monitored, although it can be done via ICCP. ICCP is an innovative method where direct current is used to regulate the cathodic protection of a structure based on the potential in the water [353]. Therefore, the use of an external power supply enables the operator (who must be constantly monitoring the voltage requirement) to adapt the current to the voltage requirements at any time. ICCP also generates significantly higher current output with fewer, longer lasting anodes than a conventional SACP system [353]. The main benefit ICCP possess is that anode depletion can be monitored and controlled. Therefore, the chances of failure of the cathodic protection of the asset are minimised [354].

ICCP costs are complicated to estimate. For that reason, ICCP has not been included in the SHM strategy for the baseline scenario of the cost-benefit analysis presented in Section 5.3. Only SACP, coating and corrosion allowances have been utilised for the corrosion protection of the assets. Typically, MPs are designed with the intent of preventing internal corrosion, as wall thickness (and therefore CAPEX) would significantly increase if corrosion allowance was to be provided internally as well as externally. A way of preventing internal corrosion would be by sealing the internal compartments to eliminate the influence of oxygen and corrosive substances [355]. However, in the case of MPs, this sealing strategy is challenged in several areas:

- The sealing around the cable entry and exit.
- The edges around the post-mounted airtight platform sealing the upper part of the MP.
- The GC between the MP and TP.

Due to these challenges, corrosion protection inside the MP for this case study will be carried out by the implementation of SACP as opposed to coating, as SACP systems can be easily designed to last for the whole life of the structure (including decommissioning), whereas the expected lifetime of the coating is usually around 15 years.

One of the main challenges in the design and operation of OWT arises from the uncertainty of maximum scour depth around their foundations. Scour action can lead to excessive excavation of the surrounding seabed and is considered a major risk for OWF developments [356]. However, real-time scour data is currently not being collected by operators due to the lack of available instrumentation and monitoring techniques. New scour monitoring technologies for OWT installations are currently being investigated [10,357,358].

GC displacement is a dangerous failure mechanism as it compromises the overall integrity of the OWT SS but also the ability of the turbine to produce electricity. GC displacement occurs when the axial capacity of the connection between the grout and the TP or the grout and the MP is insufficient, leading to a relative displacement between these elements and ultimately to the TP sliding down the MP to the seabed. The cause of the lack of axial capacity potentially stems from a number of possible failure modes, which are described and analysed in [359]. GC displacement can be easily detected by the use of displacement sensors (i.e., LVDT), indicating loss of capacity in the GC. The extent of the loss of axial capacity can also be determined by the installation of strain gauges in the stoppers of the TP. These stoppers are used temporarily during the installation of the TP. In the event that there is a loss of axial capacity, the TP would slide down until its stoppers rest on the MP and carry some, or all, of the axial and bending loads from the WT, which would be captured by the strain gauges.

According to BSH regulations, 10% of the SS in any German WF must be equipped with permanent SHMS or CM Systems. These systems should be planned in accordance to the risk identification and prioritisation previously carried out. Other aspects to be taken into account in the selection of the locations to be monitored include:

- Even monitoring of different structures within the OWF. Sometimes in an OWF not all the turbines have the same design or even the same manufacturer. This may occur when there is a high variation of water depths across the OWF, or a very high number or assets to be commissioned. Therefore, enough assets within each group of structures must be monitored in order to be able to ascertain whether SHM data represents a single turbine, a group of assets or the entire WF.

- Minimisation of the potential loss of production due to failure and consequent turned-off turbines close to the offshore substation, affecting the whole production of the array.
- Maximum water depth location due to highest seabed stresses produced by wave loading.
- Critical locations in accordance to manufacturing or installation deviations. Sometimes fabrication and installation do not happen as expected. When deviations occur, a better assessment of the asset's integrity is recommended. Aside from the requirement specified in BSH standards, a higher number of assets may be equipped with permanent SHMS or CM Systems if deemed necessary.

Ideally all turbines (or as many as possible) should have the same SHMS or CM Systems installed so that conclusions and trends can be derived across the WF [11]. These SHMS or CM Syestems must be reliable and have a relatively high service life. They should also be able to collect data for long time periods without the necessity of inspection and maintenance on site. Therefore, sufficient redundancy shall be provided at the hardware, the software and the data storage. For the SHM systems, Table 5-6 details the necessary hardware to be installed. This SHMS strategy is comprised of acceleration, inclination and temperature sensors. Ten out of the 100 locations have the base case SHMS complemented by strain gauges. This arrangement of sensors serves to evaluate the dynamic and static behaviour of the SS under the actual site conditions, acknowledging temperature effects.

Table 5-6 SHM strategy: number, type and hardware location

Sensor Type	Sensors/WT	At levels	Sensors/10

			WT
2D accelerometer	3	Top of TP, 2/3 of Tower height and Top of Tower	30
2D inclinometer	1	Top of TP	10
Displacement sensor (LVDT)	3	Bottom of TP at the stoppers	30
Strain gauges	12	4 sensors per level: Top of TP (external), bottom TP (stoppers), top of MP	120
Temperature sensor	3	Top and Bottom of TP	30
Data acquisition unit	1	Inside TP	10

5.2.3 Inspection strategy

A structural inspection strategy for the SS service life at the WF level is developed in this subsection, following the requirements of the BSH. BSH legislation has been chosen as it is more restrictive than the one applying in the United Kingdom. This inspection strategy is fundamentally divided into two types of work—above water and below water—which is strongly related to the three different types of periodical inspections described in DNVGL-ST-0126 [360]. This division concerns the different personnel, equipment and logistics needed. The following activities are believed to be necessary in order to have confidence in the structural integrity of the assets.

5.2.3.1 Above water

<u>General visual inspection (GVI) of primary and secondary steel:</u> The aim of this inspection is to provide a general overview of the integrity of the part of the SS that

is above water. This involves a general inspection passing around the MP and access systems from a crew transfer vessel (CTV). The objective is to identify any obvious mechanical, fatigue or corrosion damage. These damages could be manifested as cracks, plastic deformation, buckling, denting, generalised galvanic corrosion, pitting, dents in the coatings or excessive Marine Growth (MG). Once the access systems have been cleared, the personnel must check the main access platform and TP.

Close visual inspection (CVI) of primary and secondary steel: The aim of this inspection is to detect corrosion or fatigue damage in the inspected areas of the TP, main access platform and access systems above water and determine whether non-destructive testing (NDT) would be necessary to inspect any of the welds. This inspection is carried out closer to the structure (at a meter distance), therefore detecting smaller defects.

Detailed Visual Inspection (DVI) of primary and secondary steel: The aim of this inspection is to determine the extent of fatigue damage when cracks are detected at pre-selected welds. In order to achieve that, NDT is employed. This inspection is carried out as a reactive measure when there is either a strong suspicion, or evidence of fatigue damage being present at welds.

5.2.3.2 Below water

Subsea GVI of primary and secondary steel: The aim of this inspection is to provide a general overview of the integrity of the part of the SS that is below water, in the same way than for the above water. This inspection can be carried out by divers or by a remotely operated vehicle (ROV).

Subsea CVI of primary and secondary steel: The aim of this inspection is to identify corrosion or fatigue damage in the inspected areas of the TP and MP below water, and determine whether NDT would be necessary to inspect any of the welds. This inspection is carried out at a meter distance. For these analyses, MG cleaning as well as good visibility and environmental conditions are required. The necessary equipment to carry out this inspection is an ROV, a water jet to clean the MG, a length measuring device and a camera to document findings.

Subsea DVI of primary and secondary steel: The aim of this inspection is to determine the extent of fatigue damage when cracks have been detected at pre-selected welds using NDT techniques. This inspection would be carried out as a reactive measure when there is either a strong suspicion, or evidence of fatigue damage being present at welds.

CVI of the GC: The aim of this inspection is to assess the integrity of the GC between the TP and the MP. Eight o-clock positions around the circumference of the bottom of the GC will be inspected and measurements of the level of the grout with regards to the bottom of the TP, taken. Any evidence of grout material loss or surface crack shall be reported. This inspection will be carried out by divers or an ROV.

Marine growth survey: The aim of this inspection is to estimate the coverage, thickness and type of MG colonisation on the MP and sacrificial anodes and to compare its thickness against the one assumed in the design basis. Loading issues that could potentially arise from a significant deviation between the measurements and the design assumptions must be established [361]. Any MG formations on structural parts accessed by personnel, i.e., boat landings and access ladders, must be removed. This activity will be carried out either by divers or an ROV.

Cathodic protection survey: The aim of this inspection is to confirm if there is adequate global cathodic protection from the water table to the seabed. Potential readings are to be made to every anode. Two methodologies can be followed to perform these readings: proximity readings using a reference electrode and contact readings. Both of these methods consist of a cathodic protection probe to be mounted on an ROV. No cleaning of MG needs to be performed during this task as this would disturb the measurements to be taken.

Scour survey: The aim of this inspection is to monitor changes in the seabed topology around the MP foundation to account for both local and global scour. Seafloor objects and debris close to the structure must be identified and removed. Two different methods can be used: Multi Beam Echo Sounder Bathymetry Survey and Side Scan Sonar Survey.

5.3 Cost-Benefit analysis

This Section investigates the potential impact that implementation of the SHM strategy presented in Section 5.2.2 will have on OPEX and the reduction of LCoE. For this reason, the variation in the scope of works of the inspection and maintenance plan throughout the life of the WF is estimated for three different scenarios (optimistic, average and pessimistic). For these scenarios, the reduction in OPEX of the OWF achieved by SHMS is assessed. OPEX accounts for any necessary expense incurred in the inspection, Operation and Maintenance (O&M) of the offshore assets. OPEX usually consists of fixed costs that do not depend on the WF uptime and variable costs that depend on the time the WF operates [362]. Operations represent activities associated with high-level management of the plant, whereas inspection and maintenance are the tasks that entitle more effort, cost and risk. Inspection and maintenance can be preventive (carried out proactively before the system or component fails) or corrective (carried out once there has already been a failure that needs repair/replacing or the suspicion this failure is/will be developing). Unscheduled inspections and corrective maintenance take longer time to perform due to planning and logistics, the acquisition of spare parts, complexity of the repair and weather downtime. The longer these take to be performed, the higher the degradation of the system and the loss of production will be. One of the benefits of SHMS is that early onset of failures can potentially be detected, sometimes enabling preventive maintenance to be carried out, and other times enabling the mitigation of the consequences of such failures.

Inspection is the process where the assets are verified to be fit for purpose. For SS of OWT, these inspections check that none of the failure modes described in Table 5-5 pose a risk to the integrity of the structure. Offshore inspections are costly due to a number of factors, but mainly due to difficulties in the accessibility of the assets. That is the reason why relying on SHMS as an identification and diagnosis tool for failure mechanisms could help operators reduce the number of these inspections, and therefore OPEX. This Section calculates the potential saving in OPEX achieved by implementation of the SHM strategy in SS of OWF.

5.3.1 Scenarios

The main benefit of SHMS is that these systems, when applied effectively, can detect early stages of failure mechanisms being developed in the assets. The ability to react quickly to SHMS alarms helps mitigate these failure mechanisms and enables operators to have greater confidence in the structural integrity of their assets. This principle is explored in this section, where the added value of the implementation of SHMS in WTs is calculated. For this, the scenario presented in Section 5.2.2, where according to BSH only 10% of the assets are instrumented, is chosen as the baseline case. Furthermore, three other scenarios, including 20%, 30%, and 50% of instrumented assets, are considered. For all the scenarios, the inspection frequency is estimated depending on the number of instrumented assets, which is related to the operator's confidence in the structural integrity of their assets. It should be noted that this confidence in the integrity status of the assets can be influenced by a number of factors, such as the global safety factor considered in their design, the operator's experience in OW O&M activities and the operator's risk appetite.

The above-mentioned scenarios are presented in Table 5-7, where the number of inspections performed on each one of the assets during their service life is specified following BSH regulations. This implies that for some of the activities, all the assets must be inspected in the first couple of years, with the interval between inspections able to be increased afterwards. Also, a higher number of instrumented turbines implies an increase in CAPEX due to the extra instrumentation and installation. The aim of this section is to calculate the added value of the implementation of SHMS in SS of OWF. This is achieved by the comparison of the reduction in OPEX versus the increase in CAPEX due to the implementation of higher percentages of SHMS from the three scenarios presented in Table 5-7.

Table 5-7 Scenarios of SHM implementation

Activity	Baseline Scenario		Scenario 1		Scenario 2		Scenario 3	
	SHMS in 10% of WTs	**Inspection frequency during service life**	**SHMS in 20% of WTs**	**Inspection frequency during service life**	**SHMS in 30% of WTs**	**Inspection frequency during service life**	**SHMS in 50% of WTs**	**Inspection frequency during service life**
GVI of primary and secondary steelwork	100% every year	25	100% every year	25	50% every year	12.5	20% every year	5
CVI of primary and secondary steelwork	25% every year	6.25	20% every year	5	15% every year	3.75	5% every year	1.25
DVI of primary and secondary steelwork	25% every year	6.25	20% every year	5	15% every year	3.75	5% every year	1.25
Seabed scour survey	100% the 2 first years and then 25% every year	7.75	100% the 2 first years and then 20% every year	6.6	100% the 2 first years and then 15% every year	5.45	100% the 2 first years and then 5% every year	3.15
Subsea marine growth survey	25% every year	6.25	20% every year	5	15% every year	3.75	5% every year	1.25
Cathodic protection potential survey	100% the 2 first years and then 25% every year	7.75	100% the 2 first years and then 20% every year	6.6	100% the 2 first years and then 15% every year	5.45	100% the 2 first years and then 5% every year	3.15
CVI of the GC	25% every year	6.25	20% every year	5	15% every year	3.75	5% every year	1.25
GVI of primary and secondary steelwork	25% every year	6.25	20% every year	5	15% every year	3.75	5% every year	1.25
CVI of primary and secondary steelwork	25% every year	6.25	20% every year	5	15% every year	3.75	5% every year	1.25
DVI of primary and secondary steelwork	25% every year	6.25	20% every year	5	15% every year	3.75	5% every year	1.25

5.3.2 CAPEX increase due to SHM implementation

This sub-section evaluates the increase in CAPEX costs ($\Delta CAPEX$) incurred due to implementation of the SHM strategy under three scenarios of 20%, 30% and 50% of instrumented assets. The cost of implementation of the SHM strategy (φ_{SHM}) is given by:

$$\Delta CAPEX = \varphi_{SHM} = \varphi_H + \varphi_V + \varphi_I + \varphi_M + \varphi_{PM} \quad \textbf{5-1}$$

Hardware costs (φ_H) are related to the sensors, cabling, and DAUs required for the implementation of these systems. The cost of the necessary hardware for applying the SHM strategy (developed in Section 5.2.2) to the Baseline case under the scenarios 1, 2 and 3 is detailed in Table 5-8.

Table 5-8 Hardware costs in Baseline scenario

Sensor Type	Sensors/ WT	Average unit rate (€)	Ref.	Total number of sensors	Average Cost
2D Accelerometer	3	621.5	[363,364]	30	36000
2D Inclinometer	1	661.5	[365,366]	10	10000
Displacement sensor (LVDT)	3	167.5	[367,368]	30	6450
Strain gauges	12	105.25	[369,370]	120	12000
Temperature Sensor	3	182.25	[371,372]	30	4200
DAU	1	6988.5	[373,374]	10	115000

Installation and calibration cost (φ_I) is another cost incurred by the implementation of SHMS. This cost account for installation and calibration activities that are typically subcontracted to either the hardware supplier or a service provider. Personnel costs are also accounted by φ_I. When third parties are involved, there are other costs associated with SHMS, such as the mobilisation/demobilisation cost (φ_M), vessel cost (φ_V), and project management costs (φ_{PM}). φ_M is related to the cost incurred by the third party for travelling personnel and transporting goods for the duration of the works. This is highly variable with the duration of the installation, the number of personnel taking part in the works and the geographic location of the WF. Table 5-9 shows the number of people considered to take part in the installation of the hardware. φ_I and φ_M are estimated by using the following equations:

$$\varphi_I = 0.3\ \varphi_H \tag{5-2}$$

$$\varphi_M = 350 \frac{€}{person * day} \tag{5-3}$$

Depending on the nature of the monitoring campaign, the installation could be carried out either onshore or offshore. Typically, performing the same type of work could be up to ten times more expensive if performed offshore rather than onshore [8]. Therefore, given the fact that these systems are implemented from the commissioning stage, their installation would be carried out onshore. Therefore, no φ_V is incurred this time.

Table 5-9 Mobilisation / demobilisation costs for the different scenarios

Scenario	People	Days	Cost (k€)
Baseline	4	10	14
Scenario 1	8	10	28
Scenario 2	12	10	42
Scenario 3	20	10	70

φ_{PM} is related to all administration and coordination activities to make the installation of the SHMS possible. These costs tend to vary depending on the supplier and therefore have been estimated from the following formula extracted from [375]:

$$\varphi_{PM} = 0.03 * (\varphi_H + \varphi_V + \varphi_I + \varphi_M) \tag{5-4}$$

5.3.3 OPEX reduction due to SHM implementation

This sub-section investigates the reduction in OPEX achieved by implementation of the SHMS strategy. As the number of instrumented turbines increases, the knowledge and certainty about the structural integrity of the assets also rise. This enables the operators to reduce number of inspections carried out ono the assets throughout their service life. It is believed that the decrease in OPEX due to the reduction in the number of inspections exceeds the increase in CAPEX due to the cost associated with instrumenting the units. In this sub-section, the OPEX reduction due to SHM implementation is calculated. Inspection costs are influenced by the following aspects:

- Cost of accessibility (φ_A): how many turbines can be inspected in a day depending on the type of inspection to be carried out, type of vessel to be used (φ_V), commuting time to the WF and back, fuel consumption of the vessels, price of fuel, etc.
- Equipment costs depending on each activity (φ_E).
- Personnel costs (φ_P): how many people intervene, their daily rate and their shifting patterns.
- Project management costs (φ_{PM}): to account for logistics organization and reporting.

Accessibility has a great influence on the cost of inspections. Depending on where the activity is carried out (above water or below water), a certain type of vessel is employed. Typically, there are two options: CTV and service vessel (SV). CTVs are designed to be efficient and effective. They are specially designed to work in the OW sector. CTVs are generally small aluminium catamarans employed to transfer personnel in and out offshore sites on a daily basis [376]. Their carrying capacity is usually 12 crew, which will do 12hr shifts, meaning that the CTV would come back to port by the end of the day. Transit speeds range between 15 and 30 knots [376]. SVs are boats designed, modified, or equipped to carry out sea mapping. SVs come generally equipped with Sidescan Sonar and/or Multibeam Echosounder. They are employed for subsea operations as generally CTVs do not have the capability of launching an ROV or enough dynamic positioning redundancies to keep still during the ROV operation. These vessels have a capacity of around 10 passengers and they perform 24hr operation, which means that they would only come back to port approximately once every two weeks [377]. They are bigger and slower than CTVs with cruising speeds around the 20 knots when they are half-loaded [378]. Table 5-10 shows mobilization / demobilisation costs and daily rates for both CTVs and SVs.

Table 5-10 Vessel costs

Vessel cost (φ_V)	CTV	SV	Reference
mob / demob (€)	0	70000	[286]
day rate (€/day)	3700	5000	

Regarding the amount of turbines that can be inspected in a day, the actual number not only depends on the inspection to be carried out, but also on the transit time to the site for above water works and on the transit time between turbines for both above and below water works. These transfers have been estimated and are shown in Table 5-11. Table 5-12 shows equipment costs and their daily rates for inspection of SS in OWF.

Table 5-11 Equipment costs

Average transit time to OWF (hr)	1.5
Average transit time to turbine (hr)	0.25
Average fuel consumption (L/ Nautical Mile)	25
Average cost of fuel (€/L)	0.6

Table 5-12 Average transit times and cost

Equipment cost (φ_E)	Day rates (€/day)	Source
Mechanical toolkit	50	[379]
ROV	2750	
measuring toolkit	500	
NDT equipment	700	
Water jet	0	[380]

Table 5-13 shows the estimation of time that each one of the inspections takes, and the number of turbines that can be inspected by the end of the day. It must be noted that this time is subject to variations depending on the details of inspection activities, technicians' experience, environmental conditions, etc. Table 5-13 shows the amount of personnel required for each inspection and the necessary equipment to be deployed. It should be noted that "solo working" is not permitted due to H&S considerations. Also, to account for the 24hr works below water without returning to port for periods of sometimes up to two weeks, the working crew would be on average of 10 passengers [381]. Personnel salary highly depends on the project, geographic location and qualifications. In [286], personnel salary (φ_P) is reported to be of 270£/day (around 310€/day), however, from the authors' point of view, this salary might be up to twice as much.

Table 5-13 Activities specifications: vessel type, personnel, working time and equipment

Work Package	Activity	Vessel Type	personnel	Shift Type	hr/WT (average)	Equipment	WT/day (average)
AW	GVI of primary and secondary steelwork	CTV	2	12	1.5	Mechanical toolkit	5
AW	CVI of primary and secondary steelwork	CTV	2	12	2.5	Mechanical toolkit	3
AW	DVI of primary and secondary steelwork	CTV	2	12	4	NDT equipment	2
SB	Seabed scour survey	SV	10	24	1.75	Geophysical survey equipment	11
SB	Subsea marine growth survey	SV	10	24	1.5	ROV and measuring toolkit	12
SB	Cathodic protection potential survey	SV	10	24	3	ROV and measuring toolkit	7
SB	CVI of the GC	SV	10	24	2	ROV and measuring toolkit	9
SB	Subsea GVI of primary and secondary steelwork	SV	10	24	2	ROV	9
SB	Subsea CVI of primary and secondary steelwork	SV	10	24	7	ROV, measuring toolkit, water jet and NDT equipment	3
SB	Subsea DVI of primary and secondary steelwork	SV	10	24	6	ROV, measuring toolkit and water jet	3

5.3.4 Sensitivity analysis

Inspection costs are subject to uncertainties due to the large number of factors and stakeholders involved in these activities. To this aim, a sensitivity analysis is performed to evaluate the effect of two factors on CAPEX and OPEX. These two factors are: cost of SHM hardware and inspection time. Nowadays, various sensors with a range of prices are available in the OW energy market. Table 5-14 presents an optimistic, average and pessimistic range of hardware prices. As it can be observed, for a sensor with similar specifications, there might be up to 100% increase in price due to slight modifications in its design. The effect of these fluctuations on the increase of CAPEX due to the instrumentation of a higher percentage of assets is investigated.

Table 5-14 Sensitivity analysis of hardware price

Sensor type	Unit price (€) (optimistic)	Unit price (€) (average)	Unit price (€) (pessimistic)
2D Accelerometer	160	621.5	1083
2D Inclinometer	293	661.5	1030
Displacement sensor (LVDT)	95	167.5	240
Strain gauges	43	105.25	167.5
Temperature sensor	110.5	182.25	254
DAU	1037	6988.5	12940

Inspection time is another variable aspect that strongly influences the cost of inspection campaigns. Inspection time is susceptible to weather conditions, sea state, technicians' experience, condition of the asset, etc. An increase in inspection time leads to an increase in the number of offshore days within a campaign. This may seem not crucial however, this time-increase has other associated costs such as: deploying of a vessel, personnel, and equipment offshore. Furthermore, inspection times may vary depending on the supplier performing the activities. A 30% weather downtime has been considered in these analyses. Table 5-15 shows the optimistic, average and pessimistic scenarios used for the sensitivity analysis of this case study and how the increase or decrease in time to perform the different inspections influence the number of assets to be inspected in a single working day.

Table 5-15 Sensitivity analysis of inspection time

Activity	hrs/WT (optim.)	hrs/WT (av.)	hrs/WT (pessim.)	WT/day (optim.)	WT/day (av.)	WT/day (pessim.)
GVI of primary and secondary steelwork	1	1.5	2	8	6	5
CVI of primary and secondary steelwork	1.5	2.5	3.5	6	4	3
DVI of primary and secondary steelwork	3	4	5	3	3	2
Seabed scour survey	1	1.75	2.5	17	11	8
Subsea marine growth survey	1	1.5	2	17	13	10
Cathodic protection potential survey	2	3	4	10	7	5
CVI of the GC	1	2	3	17	10	7
Subsea GVI of primary and secondary steelwork	1	2	3	17	10	7
Subsea CVI of primary and secondary steelwork	6	7	8	4	3	3
Subsea DVI of primary and secondary steelwork	4	6	8	5	4	3

5.4 Results and discussion

In this Section, the results of the cost-benefit analysis are reported. The aim is to quantify the added value of SHMS when implemented from the installation of the OWF. The total CAPEX is £1.68 billion (around €1.87 billion), while the annual OPEX was estimated £56.6 million (around €63 million) [286]. With the implementation of SHM, Table 5-16 shows the CAPEX increase due to the SHM implementation for the baseline scenario and scenarios 1, 2 and 3. Furthermore, the results of the sensitivity analysis performed with regards to the highly variable hardware prices are given in Table 5-16. As it can be appreciated, the hardware cost variation plays an important role in the overall cost of implementation and subsequent CAPEX increase. This is observed that CAPEX increase in an "optimistic scenario 3" (SHMS in 30% of the assets) is 25% cheaper than an "average Baseline scenario" (SHMS in 10% of the assets).

Table 5-16 SHMS cost and CAPEX % for hardware sensitivity analysis

Scenario	SHM cost and hardware cost sensitivity analysis					
	Optimistic		Average		Pessimistic	
	Cost (M€)	CAPEX %	Cost (M€)	CAPEX %	Cost (M€)	CAPEX %
Baseline	0.04	0.003	0.16	0.009	0.28	0.016
Scenario 1	0.08	0.006	0.32	0.019	0.55	0.031
Scenario 2	0.12	0.009	0.48	0.028	0.83	0.047
Scenario 3	0.20	0.014	0.79	0.046	1.39	0.078

These results suggest that hardware selection and acquisition constitutes a very important aspect of SHM implementation. Figures 5-2, 5-3 and 5-4 show the amount of increase in CAPEX due to SHM implementation in Scenario 3 for three cases of optimistic, average and pessimistic hardware costs respectively. As can be seen in the figures, the cost of SHM implementation accounts for a small proportion of the total CAPEX.

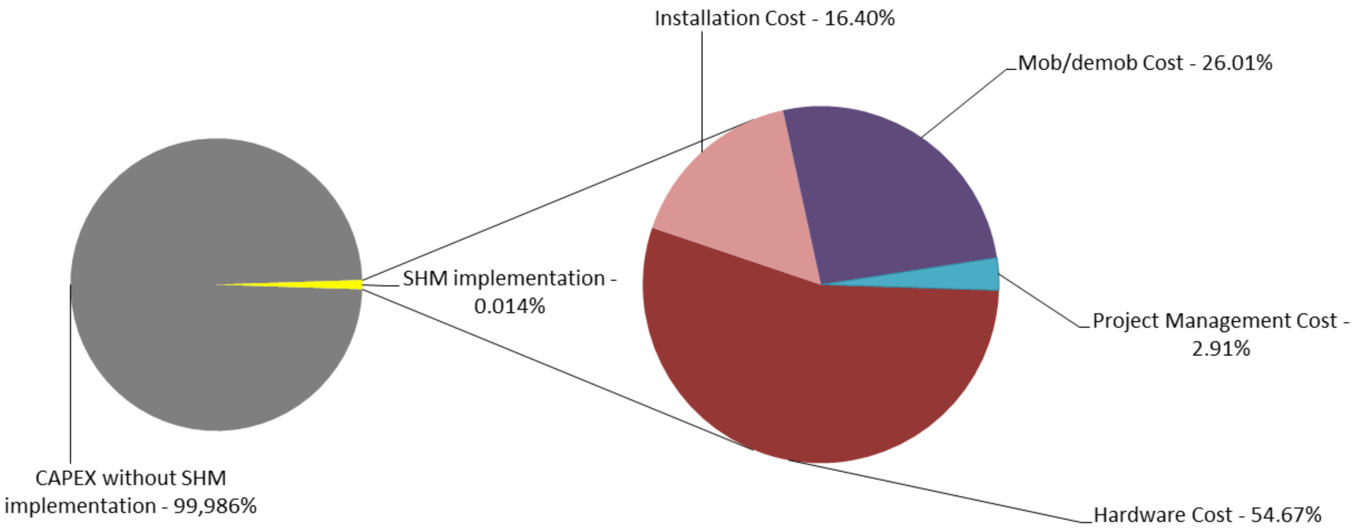

Figure 5-2 CAPEX increase due to SHM implementation in scenario 3, optimistic case of hardware costs

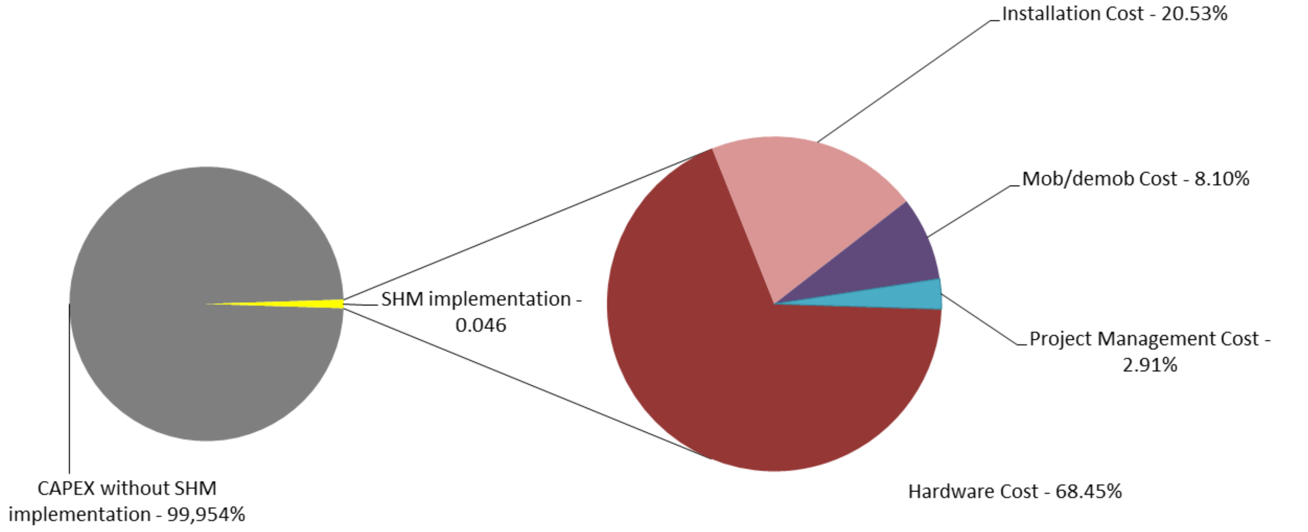

Figure 5-3 CAPEX increase due to SHM implementation in scenario 3, average case of hardware costs

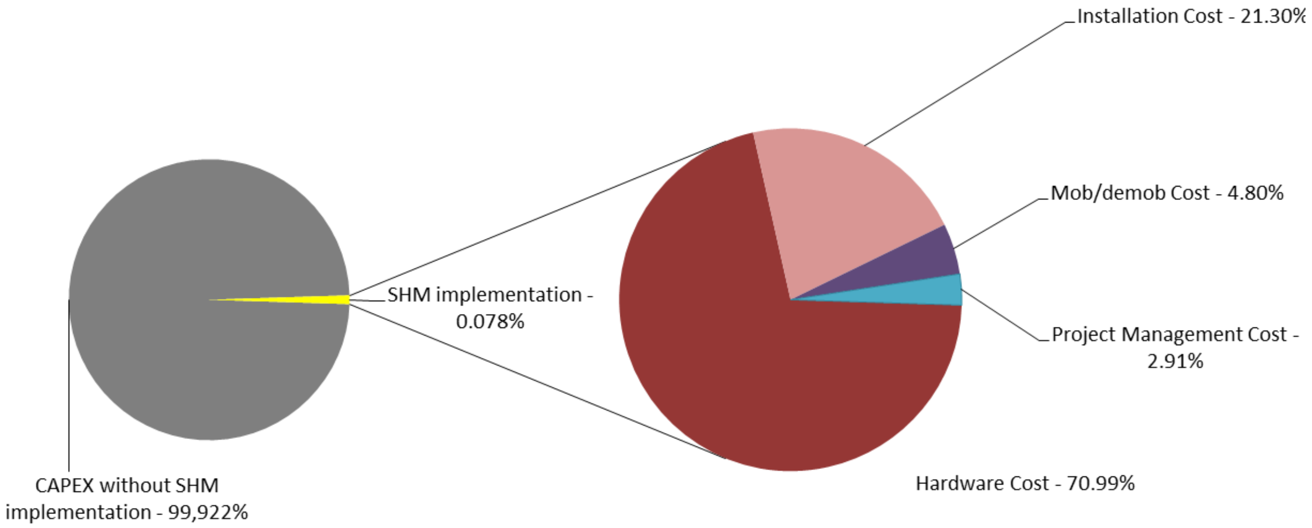

Figure 5-4 CAPEX increase due to SHM implementation in scenario 3, pessimistic case of hardware costs

Overall, it can be concluded that the percentage of CAPEX increase when SHMS are installed onshore is less than 0.1% of the CAPEX. The quantification of the OPEX percentage dedicated to structural inspections of the assets throughout their lifetime is given in Table 5-17 and is graphically shown in Figure 5-5. The results of the sensitivity analysis performed on the effect of inspection time in the cost of inspections and OPEX are also presented in Table 5-17.

Table 5-17 Lifetime inspection costs and inspection-time sensitivity analysis for Baseline case, Scenario 1, 2 and 3

Scenario	Inspection time sensitivity analysis					
	Optimistic		Average		Pessimistic	
	Cost (M€)	OPEX %	Cost (M€)	OPEX %	Cost (M€)	OPEX %
Baseline	15.6	1.2	19.9	1.6	24.4	1.9
Scenario 1	13.1	1.0	16.8	1.3	20.5	1.6
Scenario 2	9.5	0.8	12.1	1.0	14.9	1.2
Scenario 3	3.8	0.3	4.9	0.4	6.1	0.5

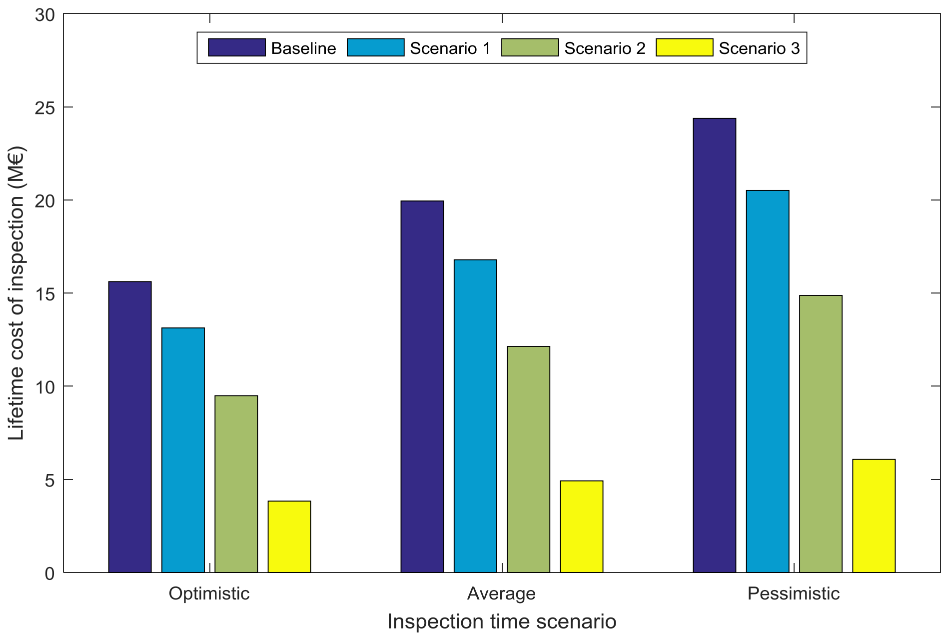

Figure 5-5 Graphical comparison of lifetime cost of structural inspections under different scenarios

Furthermore, Table 5-18 shows the OPEX percentage reduction in terms of structural inspection costs for the three cases of optimistic, average and pessimistic inspection time under different SHM implementation scenarios when compared to the baseline case. Even though the percentages are low (below 2%), they represent up to 18,3M€. It is worth mentioning that these savings took into account scheduled inspections but unscheduled maintenance was ignored, which given their often urgent nature will increase OPEX considerably. The reason why unscheduled maintenance has not been considered in the study is the lack of available data in the literature.

Table 5-18 Lifetime OPEX reduction due to SHM implementation and inspection time

Scenario	OPEX reduction for different inspection-time scenarios					
	Optimistic		Average		Pessimistic	
	M€	%	M€	%	M€	%
Scenario 1	2.5	0.2	3.2	0.3	3.9	0.3
Scenario 2	6.1	0.5	7.8	0.6	9.5	0.8
Scenario 3	11.8	0.9	15.0	1.2	18.3	1.5

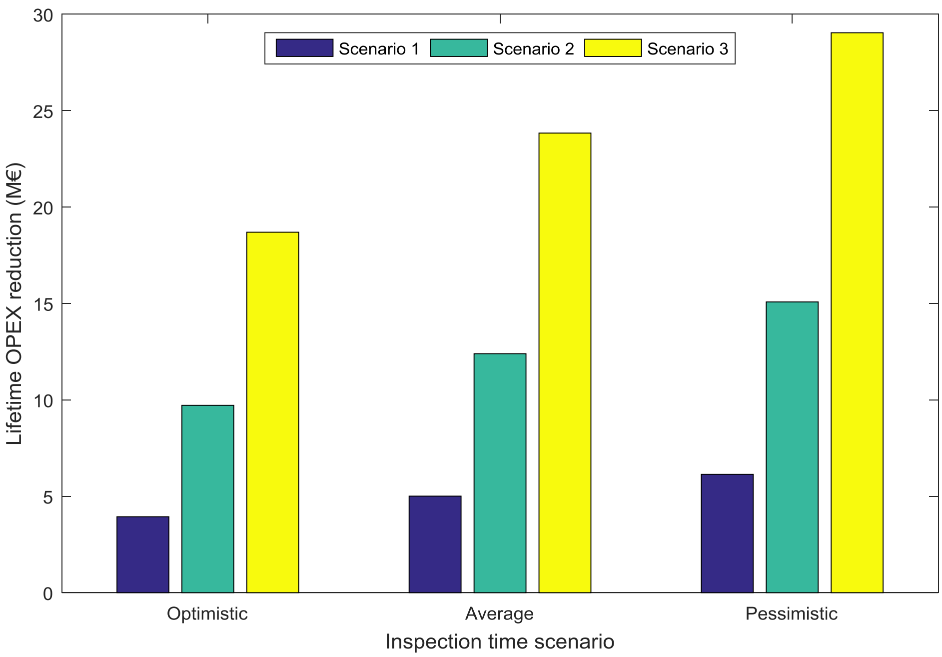

Figure 5-6 Lifetime OPEX reduction from baseline case

Table 5-18 and Figure 5-6 show the reduction of OPEX due to the implementation of SHMS in the WF. Furthermore, Figure 5-6 presents graphically how the lifetime cost of each one of the different inspections decreases with the number of times such inspections are performed to all the assets in their lifetime. This is related to the different scenarios presented in Table 5-7, where a higher percentage of SHM implementation enhanced the confidence in the structural integrity of the assets, enabling a smaller frequency of inspection. Thus, in Figure 5-7, while average inspection-time scenarios are represented by different symbols in the legend, optimistic and pessimistic scenarios are shown by dashed lines. These optimistic and pessimistic inspection-time scenarios represent the upper and lower bound of the cost interval, respectively. Furthermore, Figure 5-7 shows the cost reduction when the number of lifetime inspections is reduced due to SHM implementation. Slope change between above/below water inspections can be observed.

Lastly, Table 5-19 summarizes the increase in CAPEX versus the decrease in OPEX that different SHM implementation scenarios have for the optimistic, average and pessimistic cases of both sensitivity analyses for SHM hardware cost and inspection time. As can be appreciated, SHM implementation makes sense in all of the cases, as the OPEX reduction is much higher than the CAPEX increase due to the implementation of the SHMS. From Table 5-19 it can be concluded that the added value of SHM implementation ranges from 1.93–18.11 M€ for the presented scenarios and sensitivity analyses. Therefore, it can be concluded that SHM implementation can help WF operators reduce LCoE and maximise RoI.

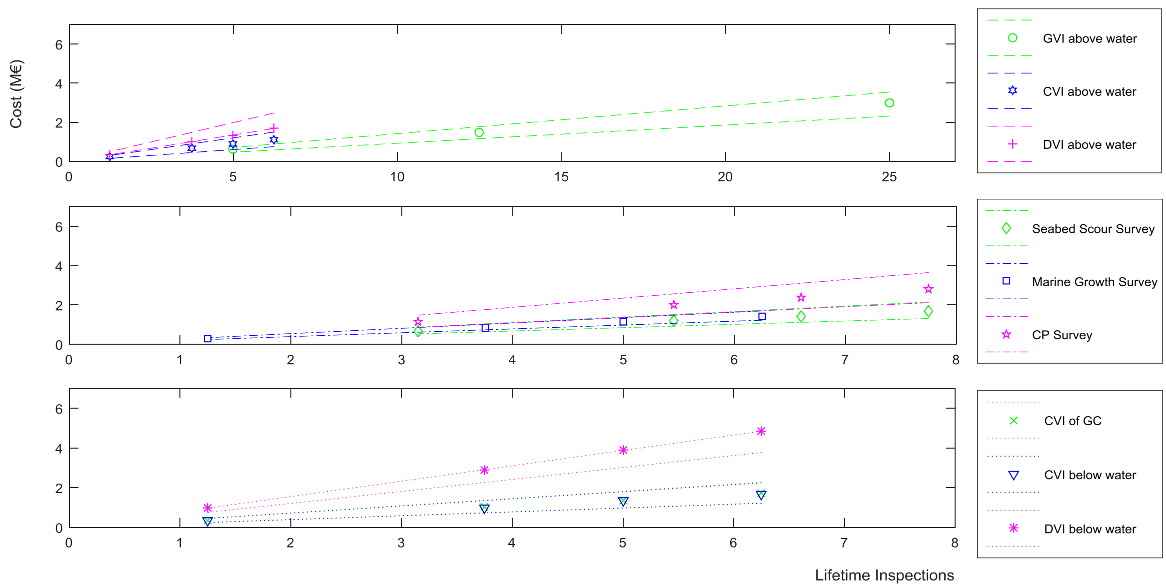

Figure 5-7 Lifetime cost of inspection depending on the lifetime inspection frequency

Table 5-19 CAPEX increase versus OPEX reduction due to SHMS implementation

SHM implementation scenario	Hardware cost sensitivity analysis	Inspection-time sensitivity analysis					
		Optimistic		Average		Pessimistic	
		CAPEX increase (M€)	OPEX reduction (M€)	CAPEX increase (M€)	OPEX reduction (M€)	CAPEX increase (M€)	OPEX reduction (M€)
Scenario 1	Optimistic	0.08	2.48	0.08	3.16	0.08	3.87
	Average	0.32		0.32		0.32	
	Pessimistic	0.55		0.55		0.55	
Scenario 2	Optimistic	0.12	6.12	0.12	7.81	0.12	9.51
	Average	0.48		0.48		0.48	
	Pessimistic	0.83		0.83		0.83	
Scenario 3	Optimistic	0.20	11.78	0.20	15.03	0.20	18.31
	Average	0.79		0.79		0.79	
	Pessimistic	1.39		1.39		1.39	

5.5 Conclusions

In this paper, guidelines for the implementation of an SHMS were developed and applied to a case study. SHMS, when installed from the beginning of operation of the WF, can be used to adopt a condition-based inspection strategy for reducing OPEX. The regulations to be adhered to for the specific cases of the United Kingdom and Germany were extensively described and then the process to be followed by operators for the development of a SHM strategy together with an inspection strategy was explained and applied to a baseline case study. This baseline case study was used to perform the economic analysis of the benefits of SHMS implementation in the reduction of OPEX based on the developed guidelines.

Results back up the hypothesis that when implemented from the beginning of the service life, SHMS help WF operators reduce the number of necessary inspections required, thereby reducing OPEX. This reduction was found to be much greater than the cost associated with the implementation of these systems. Furthermore, hardware selection and acquisition constitute a very important aspect of SHM implementation, whilst this cost remains significantly lower than the total CAPEX. Thus, the percentage of CAPEX increase due to SHMS implementation remains less than 0.1% of CAPEX, whereas the percentage of OPEX reduction is estimated to be in the 0.2–1.5% range. Finally, the added value of SHM implementation was estimated to be between 1.93–18.11 M€ for the presented scenarios and sensitivity analyses.

An aspect that has not been taken into account due to the high variability and lack of economic data available was the unscheduled inspections and repairs in the structure of the OWT. The main benefit and the reason why inspections are scheduled less often when SHMS are implemented is that these systems are able to detect and sometimes predict failures. Therefore, by the implementation of these systems, unscheduled repairs with a subsequent loss of production are less likely to occur, which would be translated into a further reduction in OPEX. This idea is expected to be researched in further works.

5.6 Acknowledgements

This work was supported by the United Kingdom Engineering and Physical Sciences Research Council (EPSRC) grant EP/L016303/1 for Doctoral Training in Renewable Energy Marine Structures (REMS).

6 GENERAL DISCUSSION AND LIMITATIONS

In the past years Offshore Wind (OW) Energy has become a mature technology able to compete with non-renewable sources and a significant contributor to the reduction of CO_2 emissions [382]. OW has rapidly reduced costs, which enables it to play a central role in Europe's power mix going forward, as from the 14th of June 2018 the European Parliament and Member States agreed to increase the European Union's renewable energy target for 2030 to 32% with a possibility for upward revision in 2023 [383].

With this agreement the European Union stays in the race for Global competitiveness on renewables, which gives developers and operators confidence to include this technology within their mainstream portfolios. Combating Climate Change also encourages developers and operators to keep investing in improving Offshore Wind's (OW)'s technology readiness. In order to do so, there are few challenges to overcome. Increasing availability of farms and reliability of units, decreasing scheduled and unscheduled inspection and maintenance, eliminating unexpected catastrophic failures and extending operational lives of the assets, are some of the targets that attract focus towards deploying the next generation of WF [384]. Meeting these targets and at the same time reducing Levelised Cost of Electricity (LCoE) are the biggest challenges OW aims to achieve [384]. In order to do so, both Capital Expenditure and Operational Expenditure (CAPEX and OPEX) need to be optimised. Structural Health Monitoring (SHM) contributes to increasing confidence in the monitoring performance of the assets against certain failure modes and reducing the necessary inspections to be carried out in the Offshore Wind Farm (OWF) throughout the lifetime.

Structural Health Monitoring Systems (SHMS) have become a useful method to enhance OM and enhance inspection and maintenance activities, as the information gathered can be employed in the development of a tailored condition-based inspection and maintenance program. This aims to reduce the necessary downtime and inspection cost (number of offshore visits), prevent repairs and failures and increase availability.

A detailed review of SHM technologies for Offshore Wind Turbines (OWT) and how these could enhance inspection and maintenance activities is presented in Chapter 2 (Publication 1). The aim of this review is to understand how SHM data is collected and how it needs to be handled, pre-processed, analysed and interpreted. Furthermore, technological implementation of SHMS was investigated through the adaptation of the Statistical Pattern Recognition (SPR) paradigm to the OW Industry. The SPR paradigm's stages are:

I. Operational evaluation

II. Data acquisition, normalisation and cleansing

III. Feature extraction and information condensation

IV. Statistical model development

All SPR paradigm's stages can be applied to every SHM technology however, these do not always have the same impact on them. Furthermore, these stages are not a linear sequence, which means that, depending on the application, each one of the stages will take place in different order. This is shown in Chapter 4 (Publication 3), where information condensation and synchronisation take place before cleansing, for the particular case of strain monitoring.

The ability to normalise the measured data with respect to varying Environmental and Operational Conditions (EOC) is a key aspect of a SHMS in order to avoid false positive indications of damage. The most important aspect regarding accuracy of data normalisation comes with the damage sensitive features that must be extracted from these data. Those damage sensitive features must not be lost or diluted by the normalisation process. Even though not all sources of variability in the data acquisition mechanism can be eliminated, they need to be identified and minimised as much as possible.

An example of the variable impact that each one of the SPR paradigm's stages has in the different SHM technologies manifests with data normalisation. Whereas data normalisation is an important and difficult process in vibration monitoring, having to employ OMA techniques; it is a straight forward and well known procedure in strain monitoring, where the only variable to normalise against is temperature (as explained in Publication 3).

Data cleansing is the procedure of selectively choosing data to pass-on or to reject from the feature selection process. In other words, data cleansing is the procedure of selectively discarding data that might not represent the system's behaviour. In Chapter 2 (Publication 1), the difficulty in performing data cleansing was placed in the fact that this process is commonly based on experts' knowledge gained in previous data acquisition processes. By the identification of outliers, experts should be able to determine whether these are noise-free measurements, and therefore utilised in future assessments; or if these measurements contain a level of noise higher than the allowable and therefore should be erased from the dataset. This process was investigated in Chapter 4 (Publication 3), where a novel data cleansing methodology was developed with real SHM data for the particular case of continuous strain monitoring. This new methodology could potentially enable operators to rely less on expert's experience for data cleansing and more on the data analysis.

As part of this methodology the relationships between multiple sensor responses to complex cyclic loading were established according to wind speed and wind direction. An important limitation of this work is in the fact that only these two variables were used to derive the aforementioned relationships, leaving the influence of other important variables, such as turbulence, wave height, direction and period, out of these relationships. Including these variables in the proposed methodology would not require much computational effort, however, it would considerably increase the amount of data required and also make more difficult the visualisation of the resulting "noise thresholds" and the definition of noise due to the high number of variables.

These sensor relationships at the beginning of the operational life of the turbine were set as the baseline behaviour. The reason why this is carried out right after the turbine's commissioning is because this is when the calibration of the systems takes place. The sensors are therefore meant to record the most accurate readings and be more reliable. Once the baseline behaviour is set, it is used to cleanse future measurements and establish changes in the structure's behaviour. These changes may be punctual (due to a sudden change in the environmental conditions or an specific operational configuration), or permanent (due to a permanent change in loading conditions or modal conditions, like stiffness). The effect that the aforementioned limitation (of not considering all environmental variables to set the baseline behaviour) has in the percentage of data removal due to noise is high. Currently this percentage can reach between 15-30% in some cases. This percentage is deemed to be higher than expected in some cases and could potentially be labelling good data as "noisy" due to the lack of relationships with other variables in the methodology. Future work could potentially focus in including the rest of environmental variables in the methodology in order to reduce the percentage of removed data.

As concluded in Chapter 4 (Publication 3), this procedure could be beneficial not only for removing noise sources and improving missing data imputation at a later stage, but also in identifying outliers. In this chapter, two scenarios were considered for three different turbines: with and without noise cleansing. For those cases where data cleansing had been performed, the average imputation error was 2.1%. Furthermore, in the 95% of cases the error is within the range [+15.2% to –11.0%]. These results are fairly positive considering the high variability of EOC at an OWF. Results from the applied methodologies of noise cleansing and Missing Data Imputation (MDI) to strain monitoring data indicate that these techniques could successfully be employed together to produce more complete datasets containing real low-disturbed strain data.

Before SHM started to be extensively used in the OW industry, fatigue estimations where extrapolated from a relatively small time-series dataset of strain measurements. Nowadays sensors tend to be left offshore for longer periods, if not for the whole service life of the asset, and therefore much longer datasets are collected. Due to this extensive data extraction, robust data reduction techniques have to be developed to preserve feature sensitivity to the changes of interest. Data condensation constitutes an inherent part of the Feature Extraction procedure. The different types and quantity of sensors needed in order to make any SHMS work efficiently produce big volumes of data. For this reason, data condensation is, most of the times, a necessary stage occurring before the analysis of the extracted data through the statistical models. However, a smart trade-off between data condensation and loss of information must always be maintained.

In the particular case of fatigue analysis through strain monitoring, collected information comes always in the form of time series of strains at the points where the strain gauges are placed. Generally, the time series are collected at high frequencies (i.e. 50Hz) and processed into condensed formats. These processed formats lose information as condensation takes place. Loss of information is always risky in engineering as it may lead to miscalculations in service life estimations. In order to deal with information loss, three approaches could be followed:

- Smart data fusion: SHM data needs to be synchronised with environmental conditions/Supervisory Control and Data Acquisition (SCADA) data at the beginning of the data assessment. Data is generally collected at different frequencies and therefore, the ability to appropriately synchronise all of them will reduce information loss. An example of smart data fusion can be found in Chapter 4 (Publication 3) where 50Hz strain measurements were synchronised with 30 min wave data and 10 min SCADA data.

- More conservative designs: are common practice utilised to counteract information loss and the uncertainties this produces. This may lead to over-dimensioned structures, which have a negative impact on CAPEX and make OW less competitive in comparison to other energy sources.

- Missing data imputation (MDI): can be an effective mitigation strategy to information loss produced not only by data reduction, but also by data cleansing or potential issues in data collection. Provided that MDI is carried out effectively, reproducing the data accurately, it enhances the confidence in fatigue life estimations, as these are based in much longer datasets. Chapter 4 (Publication 3) developed a methodology for the MDI of strain monitoring data in OWT. This chapter argues that the accuracy in the missing data estimations is higher when data cleansing has previously taken place.

However, this increase in accuracy may be also influenced by the sometimes high percentage of data removed through cleansing.

Fatigue estimations were carried out for four different cases:

1) Case A: without cleansing/without MDI
2) Case B: without cleansing/with MDI
3) Case C: with cleansing/without MDI
4) Case D: with cleansing/with MDI

Results showed:

- In Case A and B, when data cleansing did not take place, fatigue was underestimated in Turbines 1 and 3. The reason of this underestimation being an excess of noise contributing to the collection of more uniform cycles of fatigue.
- In Case C, when data cleansing took place but MDI did not, fatigue was again underestimated for Turbines 1, 2 and 3.
- In Case B, when data cleansing did not take place but MDI did, fatigue was overestimated in some sensors. The reason of this overestimation is the replication of noise by the MDI algorithm, making the cumulative effect to considerably increase the overall fatigue of the structure.

Another scope limitation of this project is the fatigue estimation in other critical locations through the extrapolation of stresses. This task was not carried out due to time constraints, but also due to the fact that it has already been given attention by other sources. For more information regarding extrapolation of strain measurements in OWTs, please refer to the following articles [385–388].

Finally, it should be noted that the term “correlation” used in Chapter 4, is not the most appropriate term to be used in the context that has been used, as it can be easily mistaken by the traditional “correlation” term used in a linear model with an offset and a slope. In Chapter 4, “correlation” is evaluated by the standard deviation of the difference between sensor readings. Therefore, this is closer to a measurement of “equality”. Equality constitutes a particular case of correlation, as, in a linear model, it would be represented by a slope equal to one and zero offset, whereas correlation in a linear model would be defined as any slope and offset and measured by a correlation coefficient.

Aiming to understand the response of OW monopile support structures (SS) to complex loading, a parametric FEA model was developed and validated with the SHM data provided by an offshore wind operator. This validation is shown in Chapter 3, where the natural frequencies of the whole turbine and just the tower obtained through modal analysis were validated with the industrial data provided by the sponsor.

Despite the fact that the parametric FEA model developed and validated in Chapter 3 was fairly complete, not all verifications were done. For example, all the analyses performed were either static or model and there was no dynamic analysis carried out. Also, several of the load cases detailed in [252] were not modelled, (i.e, the load case with extreme load effects under normal operation). This constitutes the main limitation of the resented parametric FEA model. Despite this limitation, the model provided an understanding of how OWT SS behave, which was useful later on during the project. Furthermore, the PYTHON coding of the model could be developed further to perform dynamic analyses.

The understanding obtained from this parametric model was used in the analysis of some of the SPR paradigm’s stages. From this model, Key Design Parameters were identified and two of them (Case A and B from Publication 2) were assessed to see their influence in the structural integrity of the OWT. These two case studies aimed to reduce CAPEX costs either by lowering the amount of steel needed in the turbines or by controlling their natural frequencies and stability. Furthermore, another two case studies were developed to understand failure mechanisms affecting OWT: scour development and marine growth.

Case C from Chapter 3 (Publication 2) studied the effect of scour development. The fourth case study assesses the effect of marine growth in the structural integrity of OWTs. The focus of the analysis is to determine how different growth rates and patterns of zonation of MG affect the structural integrity of the system. This case study was developed and presented in the Marine Structures international conference that took place in Lisbon during May 2017 [361]. Because this is a conference paper, it has not been included as a core contribution to the thesis (as a chapter). Instead it shall be considered as a “Complimentary Publication”. For further details about this case study, please refer to Appendix A.

Results from Case A, B and C showed:

- Case A was effective in materials cost reduction but not in modal frequencies control. The reduction in transition piece’s (TP) and Grouted Connection’s (GC) length of the OWT SS produced low variation in modal frequencies, which would be reduced within safety limits. According to the results, Ultimate Limit State, Fatigue Limit State and buckling were not compromised by these length modifications in the grouted connection and TP, so a lower safety factor could be employed in the future for TP and GC design, reducing their length. As a consequence, material costs could be reduced, as more than 20 tons of steel could be removed per turbine. However, an important aspect of the design of grouted connections that was not verified during this analysis is the resistance of the grout material to the increased loading due to the length reduction in grouted connection. This constitutes an important limitation of the case study. Furthermore, different failure modes of the grouted connection could have potentially been considered, such as the debonding of grout from the monopile or the TP.
- Case B involved a constant volume of steel to be employed in the stoppers, changing their number, dimensions and distribution. Results showed that the distribution of the stoppers plays a critical role in the structural integrity of the unit and therefore strain and/or vibration monitoring is recommended for design verification due to the criticality of the transmission of loads from the TP to the MP, through the GC.
- Case C studied the structural response of an OWT SS to scour development. Results showed the significant detrimental impact that scour can have on the structure’s integrity. This detrimental impact of scour on natural frequencies and buckling capacity has a negative effect on the structure’s fatigue life. For that reason, scour development should be prevented, monitored, or accounted by the design.

- Natural frequencies monitoring of scour might be possible, as shown in Publication 2. Although the first natural frequency mode does not detect scour development, modes two and four could potentially be used to this purpose.

Through the understanding of how failure mechanisms develop, monitoring and mitigation strategies can be applied early on in the service life or even from the assets' commissioning, keeping OPEX costs down. Understanding and identifying failure and damage modes is a crucial part of the holistic implementation of SHMS in OWT SS and also the first stage of the SPR paradigm: operational evaluation. As discussed in Chapter 5 (Publication 4), operational evaluation needs to be approached from the design phase of a Wind Farm (WF). Guidelines for SHM design and implementation were developed and presented. These guidelines are based on the SPR paradigm's stages and contribute to the development of efficient SHM and inspection strategies. Through the optimisation of these two strategies, CAPEX and OPEX can be reduced, making OW a more competitive technology.

An economic analysis was carried out with the aim to assess the benefits of SHM implementation in terms of reduction in OPEX based on the implementation of the previously developed guidelines for the baseline OWF. For this analysis, the reduction in required inspections due to the implementation of SHMS was not based in failure rates, but estimated. This estimation was carried out due to the unavailability of data detailing how these failure rates would evolve due to SHM implementation. This estimation constitutes a limitation of the economic analysis, but also constitutes a potential topic for future work.

After the aforementioned economic analysis, a comparison was made between the achieved OPEX reduction and the incurred cost of SHM implementation. Results validated the hypothesis of SHM implementation aiding the reduction of OPEX and necessary visits to the assets when carried out from the beginning of service life. This reduction is found to be much higher than the cost of implementation of the SHMS: the percentage of CAPEX increase due to SHMS implementation remains less than 0.1% of CAPEX, whereas the percentage of OPEX reduction is estimated to be in the 0.2-1.5% range. Finally, the added value of SHM implementation was found to be positive with higher added value associate with an increase in percentage of SHM implementation. This is estimated to be between 1.93 -18.11 M€ for the presented scenarios and sensitivity analyses. The results of the cost-benefit analysis performed show the added value that SHM has in lowering OPEX costs through the reduction of planned inspection and maintenance.

Something not considered in this analysis is the added value that could be achieved through the early detection and prevention of damages, which would reduce unplanned offshore works and make OPEX savings much higher than the current forecasted values. Another aspect not considered is the effect of the reliability of the SHMS, which has not been modelled in Chapter 5. This is related to the amount of false positives or false negatives in the SHM technology. False positive occurs when the SHMS identify that the conditions for a damage to be present, have been wrongly recorded. If the rate of false positives is high, the use of SHMS could lead to performing more inspections than without using SHMS. Thus, false negative occurs when damage has happened and the SHMS have not been able to identify it. A high rate of false negatives (low damage detection rate) would translate in damages been disregarded for longer periods of time and more failure failures could be seen compared to the scenario with higher number of inspections.

The reason why the reliability of SHMS has not been modelled is due to the lack of data regarding the performance of these systems. This constitutes one of the limitations of Chapter 5, which could potentially be explored in the future, when reliability data of SHMS is available.

If explored in the future, it would have to build on the findings from "The COST Action TU1402 on Quantifying the Value of SHM". This EU-funded project aims to develop and describe a theoretical framework, together with methods, tools, guidelines, examples and educational activities, for the quantification of the value of information from SHM, even before its implementation [389,390].

Operational evaluation is the first stage of the SPR paradigm adapted to the OW Idustry in Chapter 2 (Publication 1). This stage needs to be approached first during the design stage, as it sets the boundaries of the damage identification problem. In this stage, the motivation and economic justification for SHM implementation are investigated and agreed. While the motivation for SHM implementation is to increase confidence in the structural condition of the monitored assets, extend the service life and increase the WF revenue, the economic justification is to reduce OPEX and LCoE in order to make OW a more competitive source of energy. Another aspect of Operational Evaluation is the investigation of the systems' damage definitions. This task was performed partially in Chapter 5 (Publication 4), where the different failure modes that can potentially be monitored by SHMS, were identified. However, a more thorough investigation was carried out in Publication 2, where a parametric Finite Element (FE) model of an OWT SS was developed and validated with industrial data. The understanding of asset's structural response help the investigation of the other stages of the SPR paradigm, which led to Publication 3.

In Chapter 4 (Publication 3) a framework for the effective data management of SHMS is presented and implemented in a real case study for the particular case of strain monitoring. Stages two, three and four of the SPR are combined in order to develop methodologies for data synchronisation, data cleansing and MDI. The results obtained from this case study indicate that the developed methodologies can enhance data management of SHMS of OWT. These results combined with added value of SHM implementation due to OPEX reduction, indicate the suitability of SHMS to make the OW industry price-competitive with non-renewable sources and keep growing at the same rate of the past few years.

Next Chapter summarises the conclusions extracted from the work presented in this EngD thesis, the contribution to knowledge of the work developed for the fulfilment of the aim and objectives and the recommendations for future research derived from this work.

7 GENERAL CONCLUSION AND RECOMMENDATIONS

7.1 Summary

The aim of this research is to develop advance structural health monitoring strategies that enhance the condition-based inspection and maintenance of offshore wind turbine support structures. The focus is on the selection of technologies to be employed, the sequence of tasks to be carried out for the implementation of these technologies, the understanding of the structural response of the asset under complex loading, the economic justification for such implementation and how Structural Health Monitoring (SHM) data is managed and analysed effectively. This aim was achieved by meeting the objectives set in Section 1.2:

Objective I: Conduct a detailed review of SHM technologies and their application in Offshore Wind Turbines (OWT). Provision of a comprehensive study of the utilisation of SHM technologies in the Offshore Wind (OW) Industry.

Objective II: Develop a parametric Finite Element (FE) model of an OWT support structure and validate it with data from an operational wind farm.

Objective III: Evaluate an OWT support structure's response under complex loading in order to understand how design changes and failure mechanisms affect the structure's condition.

Objective IV: Formulate a framework for the effective data management of Structural Health Monitoring Systems (SHMS) for OWT support structures and validate it for a real case study utilising industrial data.

Objective V: Create guidelines for the implementation of SHMS from the design stage of a Wind Farm.

Objective VI: Evaluate the economic impact that of the implementation of SHMS in Offshore Wind Farm (OWF) support structures through the proposed guidelines.

To meet the established aim and objectives, this EngD project employed a number of engineering methods that ranged from structural modelling and simulation using commercial software (Abaqus Computer-Aided Engineering (CAE)), unsupervised learning algorithms (NN), deterministic and probabilistic methods for SHM data analysis and the cost-benefit analysis. The main conclusion drawn from this EngD project is that the implementation of SHMS in OWT, when carried out effectively following the Statistical Pattern Recognition (SPR) paradigm (technology implementation) and the guidelines developed in Chapter 5 (holistic implementation), has the potential to reduce Operational Expenditure (OPEX).

As mentioned in Chapter 1 and discussed in Chapter 6, the scope of this research project was too broad for the duration and resources of the project. For that reason there are some limitations in it. These were shown in Figure 1-2 and discussed in Section 6.

Some key findings of the project are:

- The four stages of the SPR paradigm are not consecutive, or a sequence, which means that depending on the application, each one of the stages can take place in different order.
- While the first generation of WFs was equipped with SHMS after their deployment, nowadays installation of SHM hardware will preferably be carried out onshore before offshore installation of the assets. This reduces the installation costs and allows monitoring the structures from the beginning of their service life.
- Strain and modal properties monitoring continue to be the most used SHM techniques.
- In order to apply some of the SPR paradigm stages, parametric FE modelling was identified as an appropriate tool to understand the response of OWT support structures (SS) under complex loading and failure mechanisms.

- From the parametric FE model validated with industrial data:
  - Case A was effective in materials cost reduction but not in modal frequencies control. The reduction in transition piece transition piece's (TP) and Grouted Connection's (GC) length of the OWT SS produced low variation in modal frequencies, which would be reduced within safety limits. According to the results, Ultimate Limit State, Fatigue Limit State and buckling were not compromised by these modifications in the grouted connection and TP, so a lower safety factor could be employed in the future for TP and GC design, reducing their length. As a consequence, material costs could be reduced, as more than 20 tons of steel could be removed per turbine. As explained in Section 6, this case study does not verify the resistance of the grout material to the increased loading due to the length reduction in grouted connection, which constitutes a limitation of the case study.
  - Case B involved a constant volume of steel to be employed in the stoppers, changing their number, dimensions and distribution. Results showed that the distribution of the stoppers plays a critical role in the structural integrity of the unit and therefore strain and/or vibration monitoring is recommended for design verification due to the criticality of the transmission of loads from the TP to the MP, through the GC.
  - Case C studied the structural response of an OWT SS to scour development. Results showed the significant detrimental impact that scour can have on the structure's integrity. This detrimental impact of scour on natural frequencies and buckling capacity has a negative effect on the structure's fatigue life. For that reason, scour development should be prevented, monitored, or accounted by the design.
  - Natural frequencies monitoring of scour might be possible, as shown in Publication 2. Although the first natural frequency mode does not

detect scour development, modes two and four could potentially be used to this purpose.

- Effective data management of SHMS requires a wide understanding of the asset's response under complex loading and the location and distribution of the monitoring hardware.
- Monitoring from the beginning of service life enhances data cleansing and Missing Data Imputation (MDI). The ability to calibrate SHM thresholds with an undamaged scenario (unless the asset has not been manufactured, transported and installed correctly) is crucial for the post-processing of SHM data throughout the lifetime of the structure.
- Regarding the two scenarios considered for each turbine in Chapter 4 (with and without noise cleansing), for those cases where data cleansing had been performed, the average imputation error was 2.1%. Furthermore, in the 95% of cases the imputation error is within the range [+15.2% –11.0%]. These results are fairly positive considering the high variability of Environmental and Operational Conditions (EOC) at an OWF. However, this increase in accuracy may be also influenced by the, sometimes high, percentage of data removed through cleansing.
- Results from the applied methodologies of noise cleansing and MDI to strain monitoring data indicate that these techniques can successfully be employed together to produce more complete datasets containing real low-disturbed strain data. Results could possibly be improved if the influence of other important variables, such as turbulence, wave height, direction and period, were utilised for defining the noise thresholds for data cleansing. Including these variables would calibrate noise thresholds better and could potentially avoid considering "good data" as noisy data. As discussed in Section 6, including all these variables would considerably increase the amount of data required and also make more difficult the visualisation of the resulting "noise thresholds" and the definition of noise due to the high number of variables.

- For the four different cases where fatigue was estimated (without cleansing/without MDI (Case A), without cleansing/with MDI (Case B), with cleansing/without MDI (Case C) and with cleansing/with MDI (Case D)):
    - When data cleansing did not take place, fatigue could be underestimated in Turbines 1 and 3. The reason of this underestimation being an excess of noise contributing to the collection of more uniform cycles of fatigue.
    - When data cleansing took place but MDI did not, fatigue could be again underestimated for Turbines 1, 2 and 3.
    - When data cleansing did not take place but MDI did, fatigue could be overestimated in some sensors. The reason of this overestimation is the replication of noise by the MDI algorithm, making the cumulative effect to considerably increase the overall fatigue of the structure.
- The data synchronisation, cleansing and MDI methodologies developed in Chapter 4 increase the confidence in fatigue life estimations by increasing the length of the datasets employed, as opposed to the incomplete datasets currently utilised.
- In Chapter 5, guidelines for the implementation of SHMS from the design stage of a WF based on the SPR paradigm’s stages contribute to the development of efficient SHM and inspection strategies. The application of these guidelines from the installation of the assets was verified to save both Capital Expenditure and Operational Expenditure (CAPEX and OPEX), as offshore installation is considerably more expensive than onshore installation (CAPEX savings) and the number of inspections throughout the lifetime of the assets can potentially be reduced due to the increased confidence in the assets’ structural integrity (OPEX savings).
- After utilising the guidelines for developing a SHM and inspection strategy for the baseline WF in Chapter 5, an economic analysis was carried out to verify the benefits of SHM implementation. The reduction in OPEX based on the developed guidelines was quantified.
- Hardware selection and acquisition was proven to be an important factor in SHM implementation.

- The results of the cost-benefit analysis aforementioned back-up the hypothesis that, when implemented from the beginning of the service life, SHMS help WF operators reduce the number of necessary inspections required, thereby reducing OPEX.
- OPEX reduction was found to be much greater than the cost associated with the implementation of these systems. The percentage of CAPEX increase due to SHMS implementation was quantified to be less than 0.1% of CAPEX, whereas the percentage of OPEX reduction was estimated to be in the 0.2-1.5% range. The added value of SHM implementation was estimated to be between 1.93 -18.11 M€ for the presented scenarios and sensitivity analyses. As explained in Section 6, for this analysis, the reduction in required inspections due to the implementation of SHMS was not based in failure rates, but estimated. This estimation was carried out due to the unavailability of data detailing how these failure rates would evolve due to SHM implementation. This estimation constitutes a limitation of the economic analysis, but also constitutes a potential topic for future work.

7.2 Contribution to knowledge

Throughout this EngD project research was conducted with the purpose of fulfilling the six objectives detailed in Section 1.2. Table 7-1 summarises the contribution to knowledge of this project with regards to novelty, scientific soundness and value of each research objective. The contents provided in Table 7-1 are discussed in Chapters 2, 3, 4 and 5.

Objective	Novelty	Scientific Soundness	Value / Stakeholder
I) Provision of a detailed review of SHM technologies and their application in OWT. Comprehensive study of the implementation of SHM technologies in the OW Industry.	- Interpretation and adaptation of the SPR paradigm to the offshore wind industry. - Provision of capabilities and limitations of the SHM technologies utilised in offshore wind. - First technology mapping of SHM practices conducted to industrial stakeholders.	- Application of an existing, industry- and research-proven paradigm to a new industry. - Involvement of key industrial stakeholders. - Based on thorough literature review and experience from similar industries.	- Relevant for a wide community (WT OEMs, developers, operators, investors, academia, CM Systems developers and providers, equipment suppliers). - A more comprehensive way for the technological implementation of SHMS.
II) Develop a parametric FE model of an OWT support structure and validate it with data from an operational wind farm.	- First parametric FE model in the field. - High-detail FE model combining all the elements of an OWT support structure including the soil-structure interaction, as a first. - Provision of Key Design Parameters of OWT support structures.	- Combination of existing tools and methodologies for a new problem. - Structural modelling and simulation using commercial software (Abaqus CAE). - Verification of methodology and results through involvement of industrial stakeholders.	- High level of disclosed information with regards to the modelling and load calculation. - Methodological contribution to the academic community in offshore wind. Reproducibility and reusable validation case.

Objective	Novelty	Scientific Soundness	Value / Stakeholder
III) Evaluation of an OWT support structure' response under complex loading in order to understand how design changes and failure mechanisms affect the structure's integrity.	- Quantification of impact of design changes in the structural integrity of OWT support structures. Two case studies. - Quantification of the effect that two failure modes have changes in the structural integrity of OWT support structure: scour development and marine growth development. - Development of an understanding of the structure's response, which aided data analysis afterwards.	- Use of validated and verified methods for assessing the impact quantitatively. - Combination of existing tools and method for a quantifying the impact of the case studies.	- Quantified results that can be used in design of OWT support structures and in the development of an SHM strategy.
IV) Formulation of a framework for the effective data management of SHMS for OWT support structures. Validation of the framework for a real case study utilising industrial data.	- First of its kind research in the field. - Provision of a methodology for data synchronisation of environmental conditions and strain measurements. - Provision and validation of a methodology for noise identification and removal in strain data. - Incorporation of noise criteria for strain measurements. - Provision and validation of a methodology for missing data imputation. - Quantification of potential implications towards accuracy in fatigue assessment of OWT support structures.	- Use of the previously developed parametric model to obtain an understanding of the structure's response. - Combination of existing tools and methods for a new problem. - Use of unsupervised learning algorithms (Neural Networks) to perform missing data imputation.	- Provision of a sound methodology for data cleansing that can still be used in case that the allowable noise threshold is updated. - The data cleansing methodology enables operators to rely less on experts for data cleansing and more on the data analysis. - Provision of a sound methodology for missing data imputation. - Methodological contribution both for academia and industry about effective data management of SHMS.

Objective	Novelty	Scientific Soundness	Value / Stakeholder
V) Provision of guidelines for the implementation of SHMS from the design stage of a WF	- First guidelines for the holistic implementation of SHM technologies in the field. - Provision of a methodologies for the development of SHM and inspection strategies in the offshore wind industry, as a first. - Detailed comprehensive review of legal inspection requirements in UK and Germany.	- Extensive and comprehensive literature review for the development of the guidelines and their application into the baseline case.	- Significant insight into offshore inspection planning and logistics. - Provision of sound guidelines for the holistic SHM implementation that may be applied in other industries. - Relevant for a wide community (WT operators, investors, academia, CM Systems developers, maintenance providers and equipment providers)
VI) Quantification of the economic impact that the implementation of SHMS in OWT support structures through the proposed guidelines.	- First of its kind research in that field. - Quantification of SHM implementation cost at a Wind Farm level, as a first. - Quantification of OPEX reduction due to SHM implementation in an offshore wind farm, as a first.	- Extensive and comprehensive literature review for data acquisition. - Liaison with industry experts to perform the quantification of costs and develop an understanding of time implications.	- High level of disclosed information. - Economic justification of SHM implementation provided, which can be applied in other locations/systems and even in other industries. - Relevant for a wide community (WT operators, investors, academia, CM Systems developers, maintenance providers and equipment providers)

Table 7-1 Summary of research novelty, scientific soundness and value

7.3 Recommendations for future work

The work carried out during this EngD project has significantly contributed to the scientific body of knowledge of SHM of OWT, which is proven via the project outputs published in four high impact factor peer-reviewed journal papers. Despite these contributions, the scope of this reseach project was too broad for the available time and resources. For that reason, numerous topics could have been explored further, or differently.

Previous sections of this thesis have described some of the limitations related to the works undertaken in the project however, there are also some topics not previously described in detail in the thesis that could also been expanded in the future. This section presents these limitations encountered as part of this work and possible future paths for research in these areas.

7.3.1 Confidence in SHM and model updating

Chapter 5 proved that the implementation of SHMS has a significant impact in reduction of OPEX through the reduction of number of inspections during life time of SS in OWF. The reason why inspection frequencies can be reduced is that through the monitoring of the structure's condition, more confidence in the structural integrity of the assets can be obtained. This confidence in the structural integrty of the assets is gained by the analysis of the monitored data obtained from the structures.

Holistic monitoring is carried out by combining data from the different sensors installed to reproduce the structure's response under certain loadings. This process involves post-processing SHM data with the aim to accurately evaluate the system's response over time under real site conditions. FE models can be used as part of the data post-processing. The FE models used at the design stage would be updated based on the results from SHM data and the measured EOC in order to develop dynamic models that truly represent the behaviour of the SS. These updates are carried out by adapting the model parameters, such as materials, flexural and spring stiffness, masses, inertia moments, etc. of the individual elements composing the FE model. Once these updated models are built they are compared to the actual behaviour of the structure and refined as much as possible, so eventually they would almost mimic its behaviour. This practice is called "digital twin" and it is currently carried out by different consultancy companies in the sector. Some examples are: WindGEMINI, developed by DNV GL's wind energy experts [391], the Veristar AIM3D Digital Twin, which is a colaboration between Bureau Veritas (BV) and Offshore Renewable Energy (ORE) Catapult. This will be tested at ORE Catapult's 7MW Levenmouth Offshore Wind Demonstration Turbine in Fife, Scotland [392]. But GE is not behind with their Predix Platform and the first Wind Farm Twin [393].

As these private companies are not likely to share their software and methods, the research gap of developing the first academic digital twin built with free software is still required to be investigated in order to keep research centres familiar with the state-of-the-art in the OW industry.

7.3.2 Optimisation of O&M through inspections and SHM

- Chapter 4 justified that the implementation of SHM in OWT SS is economically beneficial, as it reduced OPEX in OWF. This OPEX reduction was purely quantified by the reduction of planned maintenance activities. However, the quantification of OPEX savings, due to SHM implementation, in unscheduled inspections and repairs has not been carried out during this project due to the lack economic data available. The reason why inspections can be scheduled less often when SHMS are implemented is that these systems are able to detect changes in the structure's behaviour that alert and sometimes predict changes in the condition of the structure. Therefore, by the implementation of these systems, unscheduled repairs with a subsequent loss of production are less likely to occur, which would be translated into a further reduction in OPEX.

- Drones for visual inspections. At the moment, visual inspections of OWT support structures are carried out by people. The main challenge associated to these inspections is accessibility. This can manifest in the ability of transferring personnel to the turbine, or in the ability of accessing difficult parts of the asset for the visual inspection (outside handrails or underneath the access platform). The transfer process from the Crew Transfer Vessel (CTV) to the turbine is commonly done by the vessel pushing onto the boat landing and personnel moving from the edge of the vessel to the access ladder and climbing up to the access platform. This process can only be undertaken when the environmental conditions are below a certain threshold. Carrying out visual inspections with drones will eliminate these challenges, as drones can be piloted from the CTV without the need of personnel accessing difficult areas of the structure via rope access or even the need of transferring personnel to the asset. Drone inspection has a the potential of great reduction of OPEX through the decrease in time for visual inspections, increase availability and decrease Health and Safety risk for personnel. However, further developments in image pattern recognition for corrosion identification are yet to be developed. Furthermore, as drones are piloted from a vessel subject to wave motion, motion sickness of the pilots must be prevented.

7.3.3 SHM data analysis

Future work in the SHM field could potentially focus on accounting for the degradation in the accuracy of sensor readings (increase in noise) across the years, comparing different periods across the life of a windfarm. Furthermore, developments in sensor reliability would also be welcomed in the sector.

8 References

[1] Nations U. Paris Agreement Signing Ceremony n.d. https://www.un.org/sustainabledevelopment/parisagreement22april/#programme (accessed February 27, 2019).

[2] EUCOM. Communication from the Commission to the European Parliament, the Council, the European Economic and Social Committee and the Committee of the Regions. 2011.

[3] Commission E. Energy efficiency targets for 2020 and 2030 n.d. https://ec.europa.eu/energy/en/topics/energy-efficiency (accessed February 27, 2019).

[4] Joseph Salvatore. World Energy Perspective - Cost of Energy Technologies. 2013. doi:ISBN: 978 0 94612 130 4.

[5] Ilas A, Ralon P, Rodriguez A, Taylor M. Renewable Power Generation Costs in 2017. vol. Abu Dhabi. 2018. doi:10.1007/SpringerReference_7300.

[6] Offshore wind investment , policies and job creation Review of key findings. Halifax, Canada: n.d.

[7] Europe W. Offshore Wind in Europe: key trends and statistics 2017. n.d.

[8] Röckmann C, Lagerveld S, Stavenuiter J. Operation and Maintenance Costs of Offshore Wind Farms and Potential Multi-use Platforms in the Dutch North Sea. In: Buck BH, Langan R, editors. Aquac. Perspect. Multi-Use Sites Open Ocean Untapped Potential Mar. Resour. Anthr., Cham: Springer International Publishing; 2017, p. 97–113. doi:10.1007/978-3-319-51159-7_4.

[9] Martinez-Luengo M, Kolios A, Wang L. Structural health monitoring of offshore wind turbines: A review through the Statistical Pattern Recognition Paradigm. Renew Sustain Energy Rev 2016;64:91–105. doi:10.1016/j.rser.2016.05.085.

[10] Martinez-Luengo M, Kolios A, Wang L. Parametric FEA modelling of Offshore Wind Turbine Support Structures: towards scaling-up and CAPEX

reduction. Int J Mar Energy 2017;19:16–31.

[11] Martinez-Luengo M, Shafiee M, Kolios A. Data management for structural integrity assessment of offshore wind turbine support structures: data cleansing and missing data imputation. Ocean Eng 2019;173:867–83.

[12] Martinez-Luengo M, Shafiee M. Guidelines and Cost-Benefit Analysis of the Structural Health Monitoring Implementation in Offshore Wind Turbine Support Structures. Energies 2019;12:1–26. doi:10.3390/en12061176.

[13] European Commission. Communication from the Commission to the European Parliament, the Council, the European Economic and Social Committee and the Committee of the Regions n.d. http://ec.europa.eu/europe2020/pdf/europe2020stocktaking_en.pdf (accessed August 3, 2017).

[14] EWEA Business Intelligence. Aiming high: Rewarding Ambition in Wind Energy. n.d. doi:10.1021/nn700402d.

[15] RenewableUK. Wind Energy in the UK. State of the Industry Report Summary 2015 2015:1–43.

[16] Ho A, Mbistrova A, Corbetta G. EWEA. The European Offshore Wind Industry: Key Trends and Statistics 2015. European Wind Energy Asociation: n.d.

[17] Ciang CC, Lee J-R, Bang H-J. Structural health monitoring for a wind turbine system: a review of damage detection methods. Meas Sci Technol 2008;19:122001. doi:10.1088/0957-0233/19/12/122001.

[18] Farrar CR, Sohn H. Pattern Recognition For Structural Health Monitoring. Work. Mitig. Earthq. Disaster by Adv. Technol., 2000.

[19] Ghoshal A, Sundaresan MJ, Schulz MJ, Pai PF. Structural health monitoring techniques for wind turbine blades. J Wind Eng Ind Aerodyn 2000;85:309–24. doi:10.1016/S0167-6105(99)00132-4.

[20] Adedipe O, Brennan F, Kolios AJ. Review of Corrosion Fatigue in Offshore

Structures: Present Status and Challenges in the Offshore Wind Sector. Renew Sustain Energy Rev 2016;61:141–54.

[21] Larsen FMF, Sorensen T. New Lightning Qualification Test Procedure for Large Wind Turbine Blades. … Int Conf Light … 2003;36:1–10.

[22] Kim H, H. Melhem. Damage detection of structures under earthquake excitation using discrete wavelet analysis. Eng Struct 2004;26:347–62.

[23] Farrar CR, Worden K. An introduction to structural health monitoring. Philos Trans R Soc A Math Phys Eng Sci 2007;365:303–15. doi:10.1098/rsta.2006.1928.

[24] Bently DE, Hatch CT. Fundamentals of rotating machinery diagnostics. New York: ASME Press; 2003.

[25] Shull PJ. Nondestructive evaluation theory, techniques, and applications. New York: Marcel Dekker, Inc; 2002.

[26] Montgomery DC. Introduction to statistical quality control. New York: John Wiley & Sons Inc; 1997.

[27] Farrar CR, Lieven NAJ. Damage prognosis: the future of structural health monitoring. Philos Trans A Math Phys Eng Sci 2007;365:623–32. doi:10.1098/rsta.2006.1927.

[28] C.R. Farrar, Sohn H, Hemez FM, Anderson MC, Bement MT, Cornwell PJ, et al. Damage Prognosis : current status and future needs. 2003.

[29] Farrar CR, Doebling SW, Nix DA. Vibration-based structural damage identification. Philos Trans A Math Phys Eng Sci 2001;359.

[30] Fassois SD, Sakellariou JS. Time-series methods for fault detection and identification in vibrating structures. Philos Trans R Soc A Math Phys Eng Sci 2007;365:411–48. doi:10.1098/rsta.2006.1929.

[31] Farrar CR, Sohn H, Worden K. Data Normalization : A Key For Structural Health Monitoring. 2001.

[32] Farrar CR, Worden K. An introduction to structural health monitoring. Philos Trans A Math Phys Eng Sci 2007;365:303–15. doi:10.1098/rsta.2006.1928.

[33] Friswell MI. Damage identification using inverse methods. Philos Trans R Soc A Math Phys Eng Sci 2007;365:393–410. doi:10.1098/rsta.2006.1930.

[34] Mal A, Banerjee S, Ricci F. An automated damage identification technique based on vibration and wave propagation data. Philos Trans R Soc A Math Phys Eng Sci 2007;365:479–91. doi:10.1098/rsta.2006.1933.

[35] Staszewski WJ, Robertson AN. Time-frequency and time-scale analyses for structural health monitoring. Philos Trans A Math Phys Eng Sci 2007;365:449–77. doi:10.1098/rsta.2006.1936.

[36] Hayton P, Utete S, King D, King S, Anuzis P, Tarassenko L. Static and dynamic novelty detection methods for jet engine health monitoring. Philos Trans R Soc A Math Phys Eng Sci 2007;365:493–514. doi:10.1098/rsta.2006.1931.

[37] Sohn H. Effects of environmental and operational variability on structural health monitoring. Philos Trans A Math Phys Eng Sci 2007;365:539–60. doi:10.1098/rsta.2006.1935.

[38] Worden K, Manson G. The application of machine learning to structural health monitoring. Philos Trans A Math Phys Eng Sci 2007;365:515–37. doi:10.1098/rsta.2006.1938.

[39] Doebling S, Farrar C, Prime M, Shevitz D. Damage identification and health monitoring of structural and mechanical systems from changes in their vibration characteristics: a literature review. 1996. doi:10.2172/249299.

[40] Sohn H, Farrar CR, Hemez FM. A Review of Structural Health Monitoring Literature: 1996-2001. Masachusets, USA: 2002.

[41] Randall RB. State of the Art in Monitoring Rotating Machinery – Part 1. J Sound Vib 2004;38:10–6.

[42] C.S. Byington MJR. Prognostic enhancements to diagnostic systems for

improved condition-based maintenance [military aircraft]. Aerosp. Conf. Proceedings, IEEE, 2002, p. Volume: 6, Pages: 2815-2824.

[43] Bao P, Yuan M, Dong S, Song H, Xue J. Fiber Bragg grating sensor fatigue crack real-time monitoring based on spectrum cross-correlation analysis. J Sound Vib 2013;332:43–57. doi:10.1016/j.jsv.2012.07.049.

[44] Woike M, Abdul-Aziz A, Oza N, Matthews B. New sensors and techniques for the structural health monitoring of propulsion systems. Sci World J 2013;2013:1–11. doi:10.1155/2013/596506.

[45] Brownjohn JMW. Structural health monitoring of civil infrastructure. Philos Trans Math Phys Eng Sci 2007;365:589–622.

[46] Lynch JP. An overview of wireless structural health monitoring for civil structures. Philos Trans A Math Phys Eng Sci 2007;365:345–72. doi:10.1098/rsta.2006.1932.

[47] Carden EP. Vibration Based Condition Monitoring: A Review. Struct Heal Monit 2004;3:355–77. doi:10.1177/1475921704047500.

[48] Grafe H. Model Updating of Large Structural Dynamics Models Using Measured Response Functions. Imperial College of Science, Technology and Medicine, University of London, UK, 1998.

[49] Wang, M.L., Lynch, J.P. and Sohn H. Sensor technologies for civil infrastructures. Cambridge, UK: 2014.

[50] Montalvão D, Maia NMM, Ribeiro AMR. A review of vibration-based structural health monitoring with special emphasis on composite materials. Shock Vib Dig 2006;38:295-324.

[51] Kaewunruen S. Monitoring structural deterioration of railway turnout systems via dynamic wheel/rail interaction. Case Stud Nondestruct Test Eval 2014;1:19–24. doi:10.1016/j.csndt.2014.03.004.

[52] Eason TJ, Bond LJ, Lozev MG. Ultrasonic thickness structural health monitoring photoelastic visualization and measurement accuracy for internal

pipe corrosion. Proc. SPIE 9439, Smart Mater. Nondestruct. Eval. Energy Syst. , n.d.

[53] Jacques R, Clarke T, Morikawa S, Strohaecker T. Monitoring the structural integrity of a flexible riser during dynamic loading with a combination of non-destructive testing methods. NDT E Int 2010;43:501–6. doi:10.1016/j.ndteint.2010.05.005.

[54] Kolios AJ, Chahardehi A, Brennan FP. Experimental determination of the overturning moment and net force generated by a novel VAWT – Experiment design under load uncertainty. Exp Tech n.d.;37:7–14.

[55] Borg M, Collu M, Kolios AJ. Offshore floating vertical axis wind turbines, dynamics modelling state of the art. Part II: Mooring Line & Structural Dynamics. Renew Sustain Energy Rev n.d.;39:1226–1234.

[56] Brennan FP, Kolios AJ. Structural integrity considerations for the H2Ocean multi modal wind-wave platform. Sci. Proc. Eur. Wind Energy Assoc. Annu. Event, Barcelona, Spain: n.d.

[57] Liu WY, Tang BP, Han JG, Lu XN, Hu NN, He ZZ. The structure healthy condition monitoring and fault diagnosis methods in wind turbines: A review. Renew Sustain Energy Rev 2015;44:466–72. doi:10.1016/j.rser.2014.12.005.

[58] García Márquez FP, Tobias AM, Pinar Pérez JM, Papaelias M. Condition monitoring of wind turbines: Techniques and methods. Renew Energy 2012;46:169–78. doi:10.1016/j.renene.2012.03.003.

[59] Devriendt C, Magalhaes F, Weijtjens W, Sitter G De, Cunha A, Guillaume P. Structural Health Monitoring of offshore wind turbines using automated operational modal analysis. Struct Heal Monit 2014;13:644–59. doi:10.1177/1475921714556568.

[60] Smarsly K, Hartmann D, Law KH. A computational framework for life-cycle management of wind turbines incorporating structural health monitoring. Struct Heal Monit An Int J 2013;12:359–76. doi:10.1177/1475921713493344.

[61] Kolios AJ, Martinez Luengo M. Operational management of offshore energy

assets. J Phys Conf Ser 2016;687. doi:10.1088/1742-6596/687/1/012001.

[62] Schulz MJ, Sundaresan MJ. Smart Sensor System for Structural Condition Monitoring of Wind Turbines. Denver, Colorado, USA: 2006.

[63] Sundaresan MJ, Schulz MJ, Ghoshal A. Structural Health Monitoring Static Test of a Wind Turbine Blade. Denver, Colorado, USA: 2002.

[64] Chang PC, Flatau A, Liu SC. Review Paper: Health Monitoring of Civil Infrastructure. Struct Heal Monit An Int J 2003;2:257–67. doi:10.1177/1475921703036169.

[65] Doebling SW, Farrar CR, Prime MB, Shevitz DW. Damage identification and health monitoring of structural and mechanical systems from changes in their vibration characteristics: A literature review. 1996. doi:10.2172/249299.

[66] Doebling S, Farrar CR, Prime M. A summary review of vibration-based damage identification methods. Shock Vib Dig 1998:1–34.

[67] Ghoshal A, Sundaresan MJ, Schulz MJ, Frank Pai P. Structural health monitoring techniques for wind turbine blades. J Wind Eng Ind Aerodyn 2000;85:309–24. doi:10.1016/S0167-6105(99)00132-4.

[68] Butterfield S, Sheng S, Oyague F. Wind energy’s new role in supplying the world’s energy — what role will structural health monitoring play. Proc. 8th Int. Work. Struct. Heal. Monit. 7th Int. Work. Struct. Heal. Monit., Stanford, CA, USA.: DEStech Publications Inc; 2009.

[69] Sutherland H, Beattie A, Hansche B, Musial W, Allread JM, Johnson J. The application of non-destructive techniques to the testing of a wind turbine blade. Sandia National Laboratories, USA: 1994.

[70] Joosse PA, Blanch MJ, Dutton AG, Kouroussis DA, Philippidis TP, Vionis PS. Acoustic emission monitoring of small wind turbine blades. Proc. 21st ASME Wind Energy Symp. conjunction with 40th AIAA Aerosp. Sci. Meet., Reno, USA: 2002, p. pp 1–11.

[71] A.A. Anastassopoulos, Kouroussis DA, Nikolaidis VN, Proust A, Dutton AG,

Blanch MJ, et al. Structural integrity evaluation of wind turbine blades using pattern recognition analysis on acoustic emission data. 25th Eur. Conf. Acoust. Emiss. Test. EWGAE 2002, Prague, Czech Republic: 2002.

[72] Beattie A, Beattie A. Acoustic emission monitoring of a wind turbine blade during a fatigue test. 35th Aerosp. Sci. Meet. Exhib., Reston, Virigina: American Institute of Aeronautics and Astronautics; 1997. doi:10.2514/6.1997-958.

[73] Jørgensen ER, Borum KK, Mcgugan M, Thomsen CL, Jensen FM, Debel CP, et al. Full scale testing of wind turbine blade to failure - flapwise loading. vol. 1392. Denmark: 2004.

[74] Wells R, Hamstad MA, Mukherjee AK. On the origin of the first peak of acoustic emission in 7075 aluminum alloy. J Mater Sci 1983;18:1015–1020.

[75] Dutton AG. Thermoelastic Stress Measurement and Acoustic Emission Monitoring in Wind. Eur. Wind Energy Conf. EWEC 2004, London: 2004.

[76] Dutton AG. Acoustic Emission Condition Monitoring of Wind Turbine Rotor Blades : Laboratory Certification Testing To Large Scale in-Service Deployment. Eur. Wind Energy Conf., 2003, p. 1–11.

[77] Rantala J, Wu D, Busse G. Amplitude-modulated lock-in vibrothermography for NDE of polymers and composites. Res Nondestruct Eval 1996;7:215–28. doi:10.1007/BF01606389.

[78] Hahn F, Kensche CW, Paynter RJH, Dutton AG, Kildegaard J, Kosgaard C. Design, fatigue test and NDE of a sectional wind turbine rotor blade. J Thermoplast Compos Mater 2002;15:267–77.

[79] Walle G, Abuhamad M, Toma E NU. Defect indications in sono-thermography in relation to defect location and structure. Proc. Quant. infrared Thermogr. Conf., Rhode Saint Genèse, Belgium: 2004.

[80] Rantala J, Wu D, Busse G. Amplitude modulated lock-in vibrothermography for NDE of polymers and composites. J Res Nondestruct Eval 1996;7:215–28.

[81] Walle G, Abuhamad M, Toma E, Netzelmann U. Defect indications in sono-thermography in relation to defect location and structure. Proc. Quant. Infrared Thermogr. Conf., Rhode Saint Gen` Ese, Belgium: 2004.

[82] Li S, Shi K, Yang K, Xu J. Research on the defect types judgment in wind turbine blades using ultrasonic NDT. IOP Conf Ser Mater Sci Eng 2015;87:012056. doi:10.1088/1757-899X/87/1/012056.

[83] Sørensen BF, Lading L, Sendrup P, McGugan M, Debel CP, Kristensen OJDD, et al. Fundamentals for Remote Structural Health Monitoring of Wind Turbine Blades - a Preproject. vol. 1336. 2002. doi:Risø-R-1336(EN).

[84] Park B, An Y-K, Sohn H. Visualization of hidden delamination and debonding in composites through noncontact laser ultrasonic scanning. Compos Sci Technol 2014;100:10–18.

[85] Farrar CR, Doebling SW. Damage Detection and Evaluation II: field applications to large structures. Modal Anal Test NATO Sci Ser 1999;363:pp 345-378.

[86] Zhang H, Schulz MJ, Ferguson F, Pai PF. Structural health monitoring using transmittance functions. Mech Syst Signal Process 1999;13:765–87.

[87] Gross E, Simmermacher T, Rumsey M, Zadoks RI. Application of damage detection techniques using wind turbine modal data. Am. Soc. Mech. Eng. Wind Energy Symp., Reno, NV, USA: 1999.

[88] Jang J-H, Yeo I, Shin S, Chang S-P. Experimental Investigation of System-Identification-Based Damage Assessment on Structures. J Struct Eng 2002;128:673–82. doi:10.1061/(ASCE)0733-9445(2002)128:5(673).

[89] Carne TG, James GH. The inception of OMA in the development of modal testing technology for wind turbines. Mech Syst Signal Process 2010;24:1213–26. doi:10.1016/j.ymssp.2010.03.006.

[90] Hermans L, Van Der Auweraer H. Modal Testing and Analysis of Structures Under Operational Conditions: Industrial Applications. Mech Syst Signal Process 1999;13:193–216. doi:http://dx.doi.org/10.1006/mssp.1998.1211.

[91] Cauberghe B. Applied frequency-domain system identification in the field of experimental and operational modal analysis. Vrije Universiteit Brussel, Vakgroep Werktuigkunde, Faculteit Toegepaste Wetenschappen, 2004.

[92] Devriendt C, Guillaume P. Identification of modal parameters from transmissibility measurements. J Sound Vib 2008;314:343–56. doi:10.1016/j.jsv.2007.12.022.

[93] Devriendt C, El-kafafy M, Sitter G De, Guillaume P. Damping Estimation of Offshore Wind Turbines on a Monopile Foundation Using State-of-the-Art Operational Modal Analysis Techniques. Int. Conf. noise Vib. Eng., Leuven: 2012, p. 2647–62.

[94] Antoniadou I, Dervilis N, Papatheou E, Maguire AE, Worden K, Sheffield S. Aspects of structural health and condition monitoring of offshore wind turbines. Philos Trans A Math Phys Eng Sci 2015;373.

[95] Dervilis N, Choi M, Taylor SG, Barthorpe RJ, Park G, Farrar CR, et al. On damage diagnosis for a wind turbine blade using pattern recognition. J Sound Vib 2014;333:1833–50. doi:10.1016/j.jsv.2013.11.015.

[96] Weijtjens W, Verbelen T, De Sitter G, Devriendt C. Foundation structural health monitoring of an offshore wind turbine: a full-scale case study. Struct Heal Monit 2015. doi:10.1177/1475921715586624.

[97] Peairs DM, Park G, Inman DJ. Improving Accessibility of the Impedance-Based Structural Health Monitoring Method. J Intell Mater Syst Struct 2004;15:129–39. doi:10.1177/1045389X04039914.

[98] Pitchford C, Grisso BL, Inman DJ. Impedance-based structural health monitoring of wind turbine blades. Proc SPIE 2007;7293:72930X-72930X – 12. doi:10.1117/12.715800.

[99] Schubel PJ, Crossley RJ, Boateng EKG, Hutchinson JR. Review of structural health and cure monitoring techniques for large wind turbine blades. Renew Energy 2013;51:113–23. doi:10.1016/j.renene.2012.08.072.

[100] Balageas D, Fritzen C-P, Guemes A. Structural health monitoring. ISTE Ltd.

London, UK: 2006.

[101] Schroeder K, Ecke W, Apitz J, Lembke E, Lenschow G. A fibre Bragg grating sensor system monitors operational load in a wind turbine rotor blade. Meas Sci Technol 2006;17:1167. doi:10.1088/0957-0233/17/5/S39.

[102] Li X, Levy C, Li M, Keshri AK, Agarwal A. A multifunctional MWCNT composite: Strain sensing, damping and application to structural vibration control. ASME Int. Mech. Eng. Congr. Expo. Proceedings., n.d., p. 323–34.

[103] Stamatis DH. Failure Mode and Effect Analysis: FMEA from Theory to Execution. 2nd ed. AS. Milwaukee, WI, USA: 2003.

[104] Sinha Y, Steel JA. A progressive study into offshore wind farm maintenance optimisation using risk based failure analysis. Renew Sustain Energy Rev 2015;42:735–42. doi:10.1016/j.rser.2014.10.087.

[105] Li D, Ho S-CM, Song G, Ren L, Li H. A review of damage detection methods for wind turbine blades. Smart Mater Struct 2015;24:033001. doi:10.1088/0964-1726/24/3/033001.

[106] Salawu OS, Williams C. Bridge Assessment Using Forced-Vibration Testing. J Struct Eng 1995;121:161–73. doi:10.1061/(ASCE)0733-9445(1995)121:2(161).

[107] Allemang RJ, Brown DL. Correlation Coefficient for Modal Vector Analysis. Proc. Int. Modal Anal. Conf. Exhib., Union Coll; 1982, p. 110–6.

[108] Ren W-X, De Roeck G. Structural Damage Identification using Modal Data. I: Simulation Verification. J Struct Eng 2002;128:87–95. doi:10.1061/(ASCE)0733-9445(2002)128:1(87).

[109] Ren W-X, De Roeck G. Structural Damage Identification using Modal Data. II: Test Verification. J Struct Eng 2002;128:96–104. doi:10.1061/(ASCE)0733-9445(2002)128:1(96).

[110] Araújo dos Santos JV, Mota Soares CM, Mota Soares CA, Pina HLG. A damage identification numerical model based on the sensitivity of

orthogonality conditions and least squares techniques. Comput Struct 2000;78:283–91.

[111] Ratcliffe CP, Bagaria WJ. Vibration technique for locating delamination in a composite beam. AIAA J 1998;36:1074–7.

[112] Abdel Wahab MM, De Roeck G. Damage Detection in Bridges Using Modal Curvatures: Application To a Real Damage Scenario. J Sound Vib 1999;226:217–35. doi:10.1006/jsvi.1999.2295.

[113] Sampaio RPC, Maia NMM, Silva JMM. Damage detection using the frequency response function curvature method. J Sound Vib 1999;226:1029–42. doi:10.1006/jsvi.1999.2340.

[114] Oh BH, Jung BS. Structural damage assessment with combined data of static and modal tests. J Struct Eng 1998;124:956–65.

[115] Abdel Wahab MM. Effect of Modal Curvatures on Damage Detection Using Model Updating. Mech Syst Signal Process 2001;15:439–45. doi:10.1006/mssp.2000.1340.

[116] Kim J-T, Stubbs N. Model-Uncertainty Impact and Damage-Detection Accuracy in Plate Girder. J Struct Eng 1995;121:1409–17. doi:10.1061/(ASCE)0733-9445(1995)121:10(1409).

[117] Worden K. An experimental appraisal of the strain energy damage location method. Key Eng Mater 2001:35–46.

[118] Kim J-T, Stubbs N. Improved Damage Identification Method Based. J Sound Vib 2002;252:223–238. doi:10.1006/jsvi.2001.3749.

[119] Stubbs N, Kim J-T. Damage localization in structures without baseline modal parameters. AIAA J 1996;34:1644–9. doi:10.2514/3.13284.

[120] Park G. Self-monitoring and self-healing jointed structures. Key Eng Mater 2001:75–84.

[121] Li G-Q, Hao K-C, Lu Y, Chen S-W. A flexibility approach for damage identification of cantilever-type structures with bending and shear

deformation. Comput Struct 1999;73:565–72. doi:10.1016/S0045-7949(98)00295-8.

[122] D. Bernal. Load Vectors for Damage Localization. J Eng Mech 2002;128:7–14.

[123] Zhao J, DeWolf JT. Sensitivity study for vibrational parameters used in damage detection. J Struct Eng 1999;125:410–6.

[124] Feng M, Bahng E. Damage Assessment of Bridges with Jacketed RC Columns Using Vibration Test. Smart Struct. Mater. 1999 Smart Syst. Bridg. Struct. Highw. Proc. SPIE, 1999, p. 316–327.

[125] Mangal L, Idichandy VG, Ganapathy C. ART-based multiple neural networks for monitoring offshore platforms. Appl Ocean Res 1996;18:137–43. doi:10.1016/0141-1187(96)00024-7.

[126] Waszczyszyn Z, Ziemianski L. Neural networks in mechanics of structures and materials -new results and prospects of applications. Comput Struct 2001;79:2261–76. doi:10.1016/S0045-7949(01)00083-9.

[127] Zubaydi A, Haddara MR, Swamidas ASJ. Damage identification in a ship's structure using neural networks. Ocean Eng 2002;29:1187–200. doi:10.1016/S0029-8018(01)00077-4.

[128] Barai SV, Pandey PC. Time-delay neural networks in damage detection of railway bridges. Adv Eng Softw 1997;28:1–10. doi:10.1016/S0965-9978(96)00038-5.

[129] Marwala T, Hunt HEM. Fault Identification Using Finite Element. Mech Syst Signal Process 1999;13:475–90.

[130] Zak A, Krawczuk M, Ostachowicz W. Vibration of a laminated composite plate with closing delamination. J Intell Mater Syst Struct 2001;12:545–51. doi:10.1106/9PFK.-LXAD-9WLL-JXMG.

[131] Marín JC, Barroso A, París F, Cañas J. Study of fatigue damage in wind turbine blades. Eng Fail Anal 2009;16:656–68.

doi:10.1016/j.engfailanal.2008.02.005.

[132] Adedipe O, Brennan F, Kolios AJ. Corrosion Fatigue Load Frequency Sensitivity Analysis. Mar Struct n.d.;42:115–136. doi:10.1016/j.marstruc.2015.03.005.

[133] Van Der Tempel J. Design of support structures for offshore wind turbines. TU Delft, Delft, 2006., 2006.

[134] Gomez HC, Gur T, Dolan D. Structural condition assessment of offshore wind turbine monopile foundations using vibration monitoring data 2013;8694:86940B. doi:10.1117/12.2018263.

[135] Adams D, White J, Rumsey M, Farrar CR. Structural health monitoring of wind turbines: method and application to a HAWT. Wind Energy 2011;14:603–23. doi:10.1002/we.

[136] Cross EJ. On Structural Health Monitoring in Changing Environmental and Operational Conditions. University of Sheffield, 2012.

[137] Faulkner P, Cutter P, Owens A. Structural Health Monitoring Systems in Difficult Environments - Offshore Wind Turbines. 6th Eur Work Struct Heal Monit 2012:1–7.

[138] Hu W, Thöns S, Rohrmann RG, Said S, Rücker W. Vibration-based structural health monitoring of a wind turbine system Part II: Environmental / operational effects on dynamic properties 2015;89:273–90.

[139] Doebling SW, Farrar CR. Using Statistical Analysis to Enhance Modal-Based Damage Identification in Structural Damage Assessment Using Advanced Signal Processing Procedures. Proc. DAMAS '97, University of Sheffield, UK: 1997, p. 199–210.

[140] Sakellariou JS, Fassois SD. Parametric output error based identification and fault detection in structures under earthquake excitation. Proc. Eur. COST F3 Conf. Syst. Identif. Struct. Heal. Monit., 2000, p. 323–32.

[141] Taylor SG, Farinholt K, Choi M, Jeong H, Jang J, Park G, et al. Incipient

crack detection in a composite wind turbine rotor blade. J Intell Mater Syst Struct 2014;25:613–20. doi:10.1177/1045389X13510788.

[142] Martinez Luengo M, Kolios A. Failure Mode Identification and End of Life Scenarios of Offshore Wind Turbines: A Review. Energies 2015;8:8339–54. doi:10.3390/en8088339.

[143] Overgaard LCT, Lund E, Thomsen OT. Structural collapse of a wind turbine blade. Part A: Static test and equivalent single layered models. Compos Part A Appl Sci Manuf 2010;41:257–70. doi:10.1016/j.compositesa.2009.10.011.

[144] Kirikera G, Sundaresan M, Nkrumah F, Grandhi G, Ali B, Mullapudi S, et al. Wind Turbines. Encycl. Struct. Heal. Monit., 2009, p. 1–23.

[145] Sørensen FB, Jørgensen E, Debel PC, Jensen MF, Jensen MH, Jacobsen KT, et al. Improved design of large wind turbine blade of fibre composites based on studies of scale effects (Phase 1) - Summary Report (Risø-R-1390(EN)). vol. 1390. 2004. doi:Risø-R-1390(EN).

[146] Zhou HF, Dou HY, Qin LZ, Chen Y, Ni YQ, Ko JM. A review of full-scale structural testing of wind turbine blades. Renew Sustain Energy Rev 2014;33:177–87. doi:10.1016/j.rser.2014.01.087.

[147] Kessler S. Damage detection in composite materials using frequency response methods. Compos Part B Eng 2002;33:87–95. doi:10.1016/S1359-8368(01)00050-6.

[148] Antunes PC, Dias JM, Varum H, André P. Dynamic structural health monitoring of a civil engineering structure with a POF accelerometer. Sens Rev 2014;34:36–41. doi:10.1108/SR-04-2013-656.

[149] Ahlborn TM, Shuchman R, Sutter LL, Brooks CN, Harris DK, Burns JW, et al. The State-of-the-Practice of Modern Structural Health Monitoring for Bridges: A Comprehensive Review. Burns 2010;48105:70.

[150] Dally JW, Riley WF. Experimental Stress Analysis. J Appl Mech 1996;33. doi:10.1115/1.3625012.

[151] Bogue R. Uk start up poised to take the fibre optic sensor marked by storm. Sens Rev 2005;25:24–7.

[152] Wang S, Chung DDL, Chung JH. Impact damage of carbon fiber polymer-matrix composites, studied by electrical resistance measurement. Compos Part A Appl Sci Manuf 2005;36:1707–15. doi:10.1016/j.compositesa.2005.03.005.

[153] Inam F, Bhat BR, Vo T, Daoush WM. Structural health monitoring capabilities in ceramic-carbon nanocomposites. Ceram Int 2014;40:3793–8. doi:10.1016/j.ceramint.2013.09.039.

[154] Swait TJ, Jones FR, Hayes SA. A practical structural health monitoring system for carbon fibre reinforced composite based on electrical resistance. Compos Sci Technol 2012;72:1515–23. doi:10.1016/j.compscitech.2012.05.022.

[155] Mascarenas DL, Todd MD, Park G, Farrar CR. Development of an impedance-based wireless sensor node for structural health monitoring. Smart Mater Struct 2007;16:2137–45. doi:10.1088/0964-1726/16/6/016.

[156] Hamzeloo SR, Shamshirsaz M, Rezaei SM. Damage detection on hollow cylinders by Electro-Mechanical Impedance method: Experiments and Finite Element Modeling. Comptes Rendus - Mec 2012;340:668–77. doi:10.1016/j.crme.2012.07.001.

[157] Staszewski WJ, Biemans C, Boller C, Tomlinson GR. Impact damage detectionin composite structures- Recent advances. Struct. Heal. Monit., Standford University. Palo Alto, California: 2000, p. 754–63.

[158] Yu-Lung Lo and Fu-Yuan Xiao. Measurement of Corrosion and Temperature Using a Single-Pitch Bragg Grating Fiber Sensor. J Intell Mater Syst Struct 1998;9:800–7.

[159] Panova AA, Pantano P, Walt DR. In Situ Fluorescence Imaging of Localized Corrosion with a pH-Sensitive Imaging Fiber. Anal Chem 1997;69:1635–41. doi:10.1021/ac961025c.

[160] Ling H, Lau K, Cheng L, Jin W. Fibre optic sensors for delamination identification in composite beams using a genetic algorithm. Smart Mater Struct 2005;14:287–95. doi:10.1088/0964-1726/14/1/030.

[161] Takeda N. Characterization of microscopic damage in composite laminates and real-time monitoring by embedded optical fiber sensors. Int J Fatigue 2002;24:281–9. doi:10.1016/S0142-1123(01)00083-4.

[162] Doyle C. Fibre Bragg Grating Sensors-An Introduction to Bragg gratings and interrogation techniques. 2003.

[163] Tsuda H, Toyama N, Urabe K, Takatsubo J. Impact damage detection in CFRP using fiber Bragg gratings. Smart Mater Struct 2004;13:719–24. doi:10.1088/0964-1726/13/4/009.

[164] Takeda N, Okabe Y, Kuwahara J, Kojima S, Ogisu T. Development of smart composite structures with small-diameter fiber Bragg grating sensors for damage detection: Quantitative evaluation of delamination length in CFRP laminates using Lamb wave sensing. Compos Sci Technol 2005;65:2575–87. doi:10.1016/j.compscitech.2005.07.014.

[165] Deng L, Cai CS. Applications of fiber optic sensors in civil engineering. Struct Eng Mech 2007;25:577–96. doi:10.12989/sem.2007.25.5.577.

[166] Kolle J.J. Transverse optical fuse for composite damage detection. SAMPE Quaterly 1993;24:35–40.

[167] Swartz R, Lynch J, Zerbst S, Sweetman B, Rolfes R. Structural Monitoring of Wind Turbines Using Wireless Sensor Networks. Smart Struct Syst 2010;6:1–8.

[168] Wang P, Yan Y, Tian GY, Bouzid O, Ding Z. Investigation of Wireless Sensor Networks for Structural Health Monitoring. J Sensors 2012;2012:1–7. doi:10.1155/2012/156329.

[169] Wang F, Liu J. Duty-cycle-aware broadcast in wireless sensor networks. Proc. - IEEE INFOCOM, 2009, p. 468–76. doi:10.1109/INFCOM.2009.5061952.

[170] Lynch JP, Loh KJ. A Summary Review of Wireless Sensors and Sensor Networks for Structural Health Monitoring. Shock Vib Dig 2006;38:91–128. doi:10.1177/0583102406061499.

[171] Song G, Li H, Gajic B, Zhou W, Chen P, Gu H. Wind turbine blade health monitoring with piezoceramic-based wireless sensor network. Int J Smart Nano Mater 2013;4:150–66. doi:10.1080/19475411.2013.836577.

[172] Joyce BS, Farmer J, Inman DJ. Electromagnetic energy harvester for monitoring wind turbine blades. Wind Energy 2014;17:869–76. doi:10.1002/we.

[173] Carlson CP, Schlichting AD, Ouellette S, Farinholt K, Park G. Energy Harvesting to Power Sensing Hardware Onboard Wind Turbine Blade. Proc. of the IMAC- XXVIII, Jacksonville, Florida USA: n.d.

[174] Godinez-Azcuaga VF, Inman DJ, Ziehl PH, Giurgiutiu V, Nanni A. Recent Advances in the development of a self-powered for Wireless Sensor Network for Structural Health Prognosis. Proc. SPIE - Int. Soc. Opt. Eng., vol. 7983, 2011, p. 798325-798325–7. doi:10.1117/12.880249.

[175] Isik F, Ozden G, Kuntalp M. Importance of data preprocessing for neural networks modeling: The case of estimating the compaction parameters of soils. Energy Educ Sci Technol Part A Energy Sci Res 2012;29:463–74.

[176] Asdrubali F, Baldinelli G, D'Alessandro F, Scrucca F. Life cycle assessment of electricity production from renewable energies: Review and results harmonization. Renew Sustain Energy Rev 2015;42:1113–22. doi:10.1016/j.rser.2014.10.082.

[177] Weijtjens W, Verbelen T, De Sitter G, Devriendt C. Data normalization for foundation SHM of an offshore wind turbine: A real-life case study. 2nd Eur. Conf. Progn. Heal. Manag. Soc., Acoustics and Vibrations Research Group (AVRG), Vrije Universiteit Brussel, Brussel, Belgium: 2014, p. 788–95.

[178] Oh CK, Sohn H. Damage diagnosis under environmental and operational variations using unsupervised support vector machine. J Sound Vib

2009;325:224–39. doi:10.1016/j.jsv.2009.03.014.

[179] Park G, Inman DJ. Structural health monitoring using piezoelectric impedance measurements. Philos Trans A Math Phys Eng Sci 2007;365:373–92. doi:10.1098/rsta.2006.1934.

[180] Todd MD, Nichols JM, Trickey ST, Seaver M, Nichols CJ, Virgin LN. Bragg grating-based fibre optic sensors in structural health monitoring. Philos Trans R Soc A Math Phys Eng Sci 2007;365:317–43. doi:10.1098/rsta.2006.1937.

[181] Abe S. Feature Selection and Extraction. Support Vector Mach. Pattern Classification. Adv. Pattern Recognit., 2010, p. 471. doi:10.1007/978-1-84996-098-4.

[182] Fassois SD, Sakellariou JS. Time-series methods for fault detection and identification in vibrating structures. Philos Trans A Math Phys Eng Sci 2007;365:411–48. doi:10.1098/rsta.2006.1929.

[183] Staszewski WJ, Robertson AN. Time-frequency and time-scale analyses for structural health monitoring. Philos Trans R Soc A Math Phys Eng Sci 2007;365:449–77. doi:10.1098/rsta.2006.1936.

[184] Wold S, Esbensen K, Geladi P. Principal component analysis. Chemom Intell Lab Syst 1987;2:37–52. doi:10.1016/0169-7439(87)80084-9.

[185] McLachlan GJ. Discriminant analysis and statistical pattern recognition. 2004.

[186] S. Chatterjee, Simonoff JS. Handbook of Regression Analysis. Wiley. 2012.

[187] Namey E, Guest G, Thairu L, Johnson L. Data reduction techniques for large qualitative data sets. Handb. team-based Qual. Res., 2007, p. 137–63.

[188] Kirikera GR, Shinde V, Schulz MJ, Ghoshal A, Sundaresan M, Allemang R. Damage localisation in composite and metallic structures using a structural neural system and simulated acoustic emissions. Mech Syst Signal Process 2007;21:280–97. doi:10.1016/j.ymssp.2006.01.010.

[189] Ghoshal A, Martin WN, Schulz MJ, Chattopadhyay A, Prosser WH, Kim HS.

Health Monitoring of Composite Plates using Acoustic Wave Propagation, Continuous Sensors and Wavelet Analysis. J Reinf Plast Compos 2007;26:95–112. doi:10.1177/0731684407069965.

[190] Rytter A, Kirgegaard P. Vibration Based Inspection Using Neural Networks. Struct. Damage Assess. Using Adv. Signal Process. Proced. Proc. DAMAS ‘97, University of Sheffield, UK: 1997, p. 97–108.

[191] Farrar CR, Worden K. Chapter 11: Supervised Learning – Classification and Regression. Struct. Heal. Monit. A Mach. Learn. Perspect., 2013, p. 361–401.

[192] Inada T, Shimamura Y, Todoroki A, Kobayashi H, Nakamura H. Damage Identification Method for Smart Composite Cantilever Beams with Piezoelectric Materials. Struct. Heal. Monit. 2000, Stanford University, Palo Alto, California,: 1999, p. 986–994.

[193] Tan X-M, Chen M-Y, Gan JQ. A co-training algorithm based on modified Fisher’s linear discriminant analysis. Intell Data Anal 2015;19:279–92. doi:10.3233/IDA-150717.

[194] Bishop CM. Neural Networks for Pattern Recognition. Cambridge University Press.: 1998.

[195] Rytter A. Vibration based inspection of civil engineering structures. Aalborg University, Denmark., 1993.

[196] Chan TH, Ni YQ, Ko JM. Neural Network Novelty Filtering for Anomaly Detection of Tsing Ma Bridge Cables. Struct. Heal. Monit. 2000, Stanford University, Palo Alto, California: 1999, p. 430–439.

[197] Liu PL, Sun SC. The Application of Artificial Neural Networks on the Health Monitoring of Bridges. Struct. Heal. Monit. Curr. Status Perspect., Stanford University, Palo Alto, California: 1997, p. 103–110.

[198] Hermann H-G, Streng J. Problem-Specific Neural Networks for Detecting Structural Damage. Struct. Heal. Monit. Curr. Status Perspect., Stanford University, Palo Alto, California: 1997, p. 267–278.

[199] Choi MY, Kwon IB. Damage Detection System of a Real Steel Truss Bridge by Neural Networks. Smart Struct. Mater. 2000 Smart Syst. Bridg. Struct. Highw. Proc. SPIE, Newport Beach, California: 2000, p. 295–306.

[200] Maseras-Gutierrez M, Staszewski W, Found M, Worden K. Detection of Impacts in Composite Materials Using Piezoceramic Sensors and Neural Networks. Smart Struct. Mater. 1999 Smart Struct. Integr. Syst. Proc. SPIE, 1998, p. 491–7.

[201] Ruotolo R, Surace C. Diagnosis of damage in a steel frame. Proc. 1998 16th Int. Modal Anal. Conf. IMAC. Part 1, Santa Barbara, CA, USA: 1998, p. 609–15.

[202] Ruotolo R, Surace C, Mares C. Damage identification using simulated annealing. Proc. Int. Modal Anal. Conf. - IMAC, vol. 1, SEM; 1997, p. 954–60.

[203] Ruotolo R, Surace C. Damage Assessment of Multiple Cracked Beams: Numerical Results and Experimental Validation. J Sound Vib 1997;206:567–88. doi:10.1006/jsvi.1997.1109.

[204] Mares C, Ruotolo R, Surace C. Using transmissibility data to assess structural damage. Key Eng Mater 1999;167:236–45.

[205] Mares C, Surace C. An Application of Genetic Algorithms to Identify Damage in Elastic Structures,". J Sound Vib 1996;195:195–215. doi:10.1006/jsvi.1996.0416.

[206] Ruotolo and Surace. Damage Detection Using Singular Value Decomposition. Struct. Damage Assess. Using Adv. Signal Process. Proced. Proc. DAMAS '97, University of Sheffield, UK: 1997, p. 87–96.

[207] Krawczuk M, Ostachowicz W, Kawiecki G. Detection of Delaminations in Cantilevered Beams Using Soft Computing Methods. Eur. COST F3 Conf. Syst. Identif. Struct. Heal. Monit., Madrid, Spain: 2000, p. 243–252.

[208] Vapnik V. Statistical Learning Theory. John Wiley. New York, USA: 1998.

[209] Worden K, Lane AJ. Damage identification using support vector machines. Smart Mater Struct 2001;10:540–547.

[210] Farrar CR, Worden K. Chapter 10. Unsupervised Learning - Novelty Detection. Struct. Heal. Monit. A Mach. Learn. Perspect., 2013, p. 321–60.

[211] Worden K. Structural Fault Detection Using a Novelty Measure. J Sound Vib 1997;201:85–101. doi:10.1006/jsvi.1996.0747.

[212] Markou M, Singh S. Novelty detection: A review - Part 1: Statistical approaches. Signal Processing 2003;83:2481–97. doi:10.1016/j.sigpro.2003.07.018.

[213] Markou M, Singh S. Novelty detection: a review—part 2:: neural network based approaches. Signal Processing 2003:1–26. doi:10.1016/j.sigpro.2003.07.019.

[214] Surace C, Worden K. Novelty detection in a changing environment: A negative selection approach. Mech Syst Signal Process 2010;24:1114–28. doi:10.1016/j.ymssp.2009.09.009.

[215] Basseville M, Abdelghani M, Benveniste A. Subspace-based fault detection algorithms for vibration monitoring. Automatica 2000;36:101–9. doi:10.1016/S0005-1098(99)00093-X.

[216] Farrar CR, Worden K. Chapter 9: Machine Learning and Statistical Pattern Recognition. Struct. Heal. Monit. A Mach. Learn. Perspect., 2013, p. 295–320.

[217] Worden K, Pierce SG, Manson G, Philp WR, Staszewski WJ, Culshaw B. Detection of Defects in Composite Plates Using Lamb Waves and Novelty Detection. Int J Syst Sci 2000;31:1397–1409.

[218] Mevel L, Benveniste A, Basseville M, Goursat M. In Operation Structural Damage Detection and Diagnosis. Eur. COST F3 Conf. Syst. Identif. Struct. Heal. Monit., Madrid, Spain: 2000, p. 641–650.

[219] Chang TYP, Chang CC, Xu YG. Updating Structural Parameters: An

Adaptive Neural Network Approach. Struct. Heal. Monit. 2000, Stanford University, Palo Alto, California: 1999, p. 379–389.

[220] Sanders W, Akhavan F, Watkins S, Chandrashekhara K. Fiber Optic Vibration Sensing and Neural Networks Methods for Prediction of Composite Beam Delamination. Smart Struct. Integr. Syst. Proc. SPIE, 1997, p. 858–867.

[221] Smarsly K, Hartmann D, Law KH. A computational framework for life-cycle management of wind turbines incorporating structural health monitoring. Struct Heal Monit 2013;12:359–76. doi:10.1177/1475921713493344.

[222] European Union Committee. The EU's Target for Renewable Energy: 20% by 2020, 2008. Available online: Http://WwwPublicationsParliamentUk/Pa/Ld200708/Ldselect/Ldeucom/175/175Pdf n.d. http://www.publications.parliament.uk/pa/ld200708/ldselect/ldeucom/175/175.pdf (accessed August 3, 2015).

[223] Energy Technologies Institute. Options. Choices. Actions. UK Scenarios for a low carbon energy system transition 2015.

[224] Carbon Trust. Floating Offshore Wind : Market and Technology Review. 2015.

[225] Bhattacharya S. Challenges in Design of Foundations for Offshore Wind Turbines. IET Eng Technol Ref 2014:1–9. doi:10.1049/etr.2014.0041.

[226] Damgaard M, Zania V, Andersen L V., Ibsen LB. Effects of soil-structure interaction on real time dynamic response of offshore wind turbines on monopiles. Eng Struct 2014;75. doi:10.1016/j.engstruct.2014.06.006.

[227] DNV (Det Norske Veritas). DNV-OS-J101 Design of Offshore Wind Turbine Structures. 2014.

[228] RenewableUK. Offshore Wind Energy in the UK. n.d.

[229] Kolios AJ, Collu M, Chahardehi A, Brennan FP, Patel MH. A Multi-Criteria

Decision Making Method to Compare Support Structures for Offshore Win d Turbines. EWEC 2010 Conf., Warsow, Poland: n.d.

[230] Levitt AC, Kempton W, Smith AP, Musial W, Firestone J. Pricing offshore wind power. Energy Policy 2011;39:6408–21. doi:10.1016/j.enpol.2011.07.044.

[231] Moné C, Smith A, Maples B, Hand M. 2013 Cost of Wind Energy Review. Nrel/Tp-5000-63267 2013:NREL/TP-5000-63267.

[232] Kaiser MJ, Snyder BF. Offshore Wind Energy Cost Modelling. Installation and Decommissioning. Springer L. London, UK: 2012. doi:10.1007/978-1-4471-2488-7.

[233] Koch S, Andersson G. Assessment of revenue potentials of ancillary service provision by flexible unit portfolios. 2012.

[234] Härtel P, Doering M, Jentsch M, Pape C, Burges K, Kuwahata R. Cost assessment of storage options in a region with a high share of network congestions. J Energy Storage 2016;8:358–67.

[235] Giahi MH, Jafarian Dehkordi A. Investigating the influence of dimensional scaling on aerodynamic characteristics of wind turbine using CFD simulation. Renew Energy 2016;97:162–8. doi:10.1016/j.renene.2016.05.059.

[236] API Recommended Practice 2GEO/ISO 19901-4, Geotechnical and Foundation Design Considerations. n.d.

[237] DET NORSKE VERITAS AS. DNV RP-C202 Buckling Strength of Shells. 2013.

[238] DNV. Risk based inspection of o shore topsides static mechanical equipment. RP-G101. 2009.

[239] Shi W, Park H, Han J, Na S, Kim C. A study on the effect of different modeling parameters on the dynamic response of a jacket-type offshore wind turbine in the Korean Southwest Sea. Renew Energy 2013;58:50–9. doi:10.1016/j.renene.2013.03.010.

[240] Densit. Ultra High performance grout - Ducorit Data Sheet n.d. http://www.densit.com/Files/Billeder/Densit_v2/Pdf files/renewable/pro_ducorit_itw-uk.pdf (accessed February 10, 2016).

[241] Winkler E. Die Lehre von Elastizitat und Festigkeit. Prag : Dominicius; 1867.

[242] Koukoura C, Natarajan A, Vesth A. Identification of support structure damping of a full scale offshore wind turbine in normal operation. Renew Energy 2015;81:882–95. doi:10.1016/j.renene.2015.03.079.

[243] Kezdi A. Handbook of soil mechanics. Elsevier. Amsterdam: 1974.

[244] Chen W-F, Duan L. Bridge engineering handbook. USA: CRC Press: 1999.

[245] Gerolymos N, Gazetas G. Winkler model for lateral response of rigid caisson foundations in linear soil. Soil Dyn Earthq Eng 2006;26:347–61.

[246] Heidari M, Naggar H El, Jahanandish M, Ghahramani A. Generalized cyclic p–y curve modeling for analysis of laterally loaded piles. Soil Dyn Earthq Eng 2014;63:138–49. doi:10.1016/j.soildyn.2014.04.001.

[247] Abdel-Rahman K, Achmus M. Finite element modelling of horizontally loaded monopile foundations for offshore wind energy converters in Germany. Hannover: 2005.

[248] H. Matlock. Correlations for Design of Laterally Loaded Piles in soft Clay. 2nd Offshore Technol. Conf., Houston, Texas, USA: 1970.

[249] Carswell W, Arwade SR, DeGroot DJ, Myers AT. Natural frequency degradation and permanent accumulated rotation for offshore wind turbine monopiles in clay. Renew Energy 2016;97:319–30. doi:10.1016/j.renene.2016.05.080.

[250] Rajashree SS, Sundaravadivelu R. Degradation model for one-way cyclic lateral load on piles in soft clay. Comput Geotech 1996;19:289–300.

[251] International Electrotechnical Commission. IEC 61400-1 International Satandard. Wind turbines - Part 1: Design Requirements. Geneva, Switzerland: 2005. doi:10.5594/J09750.

[252] International Electrotechnical Commission. International Standard IEC 61400-3 Wind turbines - Part 3: Design requirements for offshore wind turbines. 2009.

[253] Palutikof J, Brabson B, Lister D, Adcock S. A review of methods to calculate extreme wind speeds. Meteorol Appl 1999;6:119–32. doi:10.1017/S1350482799001103.

[254] Sarpkaya T. Wave Forces on Offshore Structures. Cambridge. Cambridge: 2010.

[255] DNV (Det Norske Veritas). DNV−OS−J101 Design of Offshore Wind Turbine Structures. n.d.

[256] Carswell W, Johansson J, Løvholt F, Arwade SR, Madshus C, Degroot DJ, et al. Foundation damping and the dynamics of offshore wind turbine monopiles. Renew Energy 2015;80:724–36. doi:10.1016/j.renene.2015.02.058.

[257] Siemens. SWT-3.6-107 Wind Turbine. 2010.

[258] Passon P. Damage equivalent wind e wave correlations on basis of damage contour lines for the fatigue design of offshore wind turbines. Renew Energy 2015;81:723–36. doi:10.1016/j.renene.2015.03.070.

[259] LaNier MW. LWST Phase I Project Conceptual Design Study: Evaluation of Design and Construction Approaches for Economical Hybrid Steel/Concrete Wind Turbine Towers. Denver, Colorado, USA: 2005.

[260] Brennan F, Tavares I. Fatigue design of offshore steel monopile wind substructures. Proc Inst Civ Eng - Energy 2014;167:1–7.

[261] (DNV) Det Norske Veritas. Fatigue Design of Offshore Steel Structures. 2005.

[262] Novoselac S, Ergić T, Baličević P. Linear and Nonlinear Buckling and Post Buckling Analysis of a Bar With the Influence of Imperfections. Teh Vjesn 2012;19:695–701.

[263] Życzkowsky M. Post-buckling analysis of non-prismatic columns under general behaviour of loading. Int J Non Linear Mech 2005;40:445–63.

[264] EN 1993-1-1. Eurocode 3: Design of steel structures. 2005.

[265] European Standard. EN 1993-1-6 Eurocode 3 - Design of steel structures - Part 1-6: Strength and stability of shell structures. vol. 6. 2007.

[266] Martinez Luengo M, Kolios A, Wang L. Structural Health Monitoring of Offshore Wind Turbines: A review through the Statistical Pattern Recognition Paradigm. Renew Sustain Energy Rev 2016;64:91–105.

[267] Weijtjens W, Verbelen T, Sitter G De, Devriendt C. Foundation structural health monitoring of an offshore wind turbine — a full-scale case study. Struct Heal Monit 2016;15:389–402. doi:10.1177/1475921715586624.

[268] Devriendt C, Magalhães F, Weijtjens W, Sitter G De, Cunha Á, Guillaume P. Automatic Identification of the Modal Parameters of an Offshore Wind Turbine using state-of-the-art Operational Modal Analysis. 5th Int. Oper. Modal Anal. Conf., Guimarães, Portugal: n.d., p. 1–12.

[269] Stahlmann A. Numerical and Experimental Modeling of Scour at Tripod Foundations for Offshore Wind Turbines 2014;1:1019–26.

[270] Rudolph D, Bos K, Luijendijk A, Rietema K, Out J. Scour Around Offshore Structures, Analysis of Field Measurements. Proc 2nd Int Conf Scour Eros., Meritus Mandarin, Singapore: 2004, p. 400–407.

[271] Rambabu M, Rao SN, Sundar V. Current-induced scour around a vertical pile in cohesive soil. Ocean Eng 2003;30:893–920. doi:10.1016/S0029-8018(02)00063-X.

[272] Chen L, Lam WH. Methods for predicting seabed scour around marine current turbine. Renew Sustain Energy Rev 2014;29:683–92. doi:10.1016/j.rser.2013.08.105.

[273] Mutlu Sumer B. Mathematical modelling of scour: A review. J Hydraul Res 2007;45:723–35. doi:10.1080/00221686.2007.9521811.

[274] Yoshida S. Wind Turbine Tower Optimization Method Using a Genetic Algorithm. Wind Eng 2006;30:453–69. doi:10.1260/030952406779994150.

[275] Daniel Stratton, Martino D, Pasquali FM, Lewis K, Hall JF. A Design Framework for Optimizing the Mechanical Performance, Cost, and Environmental Impact of a Wind Turbine Tower. J Sol Energy Eng 2016;138. doi:10.1115/1.4033500.

[276] Tuan-Cuong Nguyen, Huynh T-C, Kim J-T. Numerical evaluation for vibration-based damage detection in wind turbine tower structure. Wind Struct 2015;21:657–75.

[277] Uys PE, Farkas J, Jármai K, van Tonder F. Optimisation of a steel tower for a wind turbine structure. Eng Struct 2007;29:1337–42. doi:10.1016/j.engstruct.2006.08.011.

[278] Negm HM, Maalawi KY. Structural design optimization of wind turbine towers. Comput Struct 2000;74:649–66. doi:10.1016/S0045-7949(99)00079-6.

[279] Zaaijer MB. Foundation modelling to assess dynamic behaviour of offshore wind turbines. Appl Ocean Res 2006;28:45–57. doi:10.1016/j.apor.2006.03.004.

[280] Sahasakkul W, Nguyen H, Ph D, Sari A, Ph D. An Improved Methodology on Design and Analysis of Offshore Wind Turbines Supported by Monopiles. Offshore Technol. Conf., Houston, Texas, USA: n.d. doi:10.4043/27181-MS.

[281] Negro V, López-Gutiérrez JS, Esteban MD, Matutano C. Uncertainties in the design of support structures and foundations for offshore wind turbines. Renew Energy 2014;63:125–32. doi:10.1016/j.renene.2013.08.041.

[282] Schoesitter P de, Audenaert S, Baelus L, Bolle A, Brown A, Neves L Das, et al. Feasibility of a Dynamically Stable Rock Armour Layer Scour. Proc. ASME 2014 33rd Int. Conf. Ocean. Offshore Arct. Eng. OMAE2014, June 8-13, 2014, San Francisco, California, USA: 2014, p. 1–9.

[283] Dalgic Y, Lazakis I, Dinwoodie I, Mcmillan D, Revie M. Advanced logistics

planning for offshore wind farm operation and maintenance activities. Ocean Eng 2015;101:211–26. doi:10.1016/j.oceaneng.2015.04.040.

[284] Shafiee M, Sørensen J. Maintenance optimization and inspection planning of wind energy assets: Models, methods and strategies. Reliab Eng Syst Saf (In Press 2018.

[285] Shafiee M, Brennan F, Armada Espinosa I. A parametric whole life cost model for offshore wind farms. Int J Life Cycle Assess 2016;21:961–75.

[286] Ioannou A, Angus A, Brennan F. A lifecycle techno-economic model of offshore wind energy for different entry and exit instances. Appl Energy 2018;221:406–24. doi:10.1016/j.apenergy.2018.03.143.

[287] Myhr A, Bjerkseter C, Ågotnes A, Nygaard TA. Levelised cost of energy for offshore fl oating wind turbines in a life cycle perspective. Renew Energy 2014;66:714–28. doi:10.1016/j.renene.2014.01.017.

[288] Hansen JB, Brincker R, López-Aenlle M, Overgaard CF, Kloborg K. A new scenario-based approach to damage detection using operational modal parameter estimates. Mech Syst Signal Process 2017;94:359–73. doi:10.1016/j.ymssp.2017.03.007.

[289] Ziegler L, Smolka U, Cosack N, Muskulus M. Structural monitoring for lifetime extension of offshore wind monopiles: Can strain measurements at one level tell us everything? Wind Energy Sci Discuss 2017:469–476,. doi:10.5194/wes-2017-21.

[290] Maes K, Roeck G De, Iliopoulos A, Weijtjens W, Devriendt C, Lombaert G. Kalman filter based strain estimation for fatigue assessment of an offshore monopile wind turbine. Proceeding ISMA2016 Incl USD2016 2016;77:592–611.

[291] Fallais DJM, Voormeeren S, Lourens E. Vibration-based Identification of Hydrodynamic Loads and System Parameters for Offshore Wind Turbine Support Structures. Energy Procedia 2016:191–198.

[292] Maes K, Iliopoulos A, Weijtjens W, Devriendt C, Lombaert G. Dynamic strain

estimation for fatigue assessment of an offshore monopile wind turbine using filtering and modal expansion algorithms. Mech Syst Signal Process 2016;76–77:592–611. doi:10.1016/j.ymssp.2016.01.004.

[293] Iliopoulos A, Shirzadeh R, Weijtjens W, Guillaume P, Van Hemelrijck D, Devriendt C. A modal decomposition and expansion approach for prediction of dynamic responses on a monopile offshore wind turbine using a limited number of vibration sensors. Mech Syst Signal Process 2016:84–104.

[294] Iliopoulos A, Devriendt C, Guillaume P, Van Hemelrijck D. Continuous fatigue assessment of an offshore wind turbine using a limited number of vibration sensors. Proc 7th Eur Work Struct Heal Monit , EWSHM 2014 2014. doi:10.1117/12.2045576.

[295] Iliopoulos A, Weijtjens W, Hemelrijck D Van, Devriendt C. Full-Field Strain Prediction Applied to an Offshore Wind Turbine. Model Valid. Uncertain. Quantif. Vol. 3, 2017. doi:10.1007/978-3-319-29754-5_34 349.

[296] Gentils T, Wang L, Kolios A. Integrated structural optimisation of offshore wind turbine support structures based on finite element analysis and genetic algorithm. Appl Energy 2017;199:187–204. doi:10.1016/j.apenergy.2017.05.009.

[297] Smolka U, Cheng PW. On the Design of Measurement Campaigns for Fatigue Life Monitoring of Offshore Wind Turbines. Twenty-Third Int Offshore Polar Eng Conf 2013;9:408–13.

[298] Banfi L, Carassale L. Uncertainties in an Application of Operational Modal Analysis. In: S. Atamturktur EA, editor. Model Valid. Uncertain. Quantif., vol. 3, The Society for Experimental Mechanics, Inc.; 2017, p. 112–20. doi:10.1007/978-3-319-54858-6.

[299] Mao Z, Todd M. A model for quantifying uncertainty in the estimation of noise-contaminated measurements of transmissibility. Mech Syst Signal Process 2012;28:470–481.

[300] Mao Z, Todd M. Statistical modeling of frequency response function

estimation for uncertainty quantification. Mech Syst Signal Process 2013;38:333–345.

[301] Sarrafi A, Mao Z. Statistical Modeling of Wavelet-Transform-Based Features in Structural Health Monitoring. Model Valid. Uncertain. Quantif., The Society for Experimental Mechanics, Inc.; 2017.

[302] Castellani F, Astolfi D, Sdringola P, Proietti S, Terzi L. Analyzing wind turbine directional behavior : SCADA data mining techniques for efficiency and power assessment q. Appl Energy 2017;185:1076–86. doi:10.1016/j.apenergy.2015.12.049.

[303] Schutz W. A history of fatigue. Eng Fract Mech 1996;54:263–300.

[304] Ziegler L. Lifetime extension of offshore wind monopiles: Assessment process and relevance of fatigue crack inspection. EAWE PhD Semin Wind Energy Eur 2016.

[305] Cosack N. Fatigue Load Monitoring with Standard Wind Turbine Signals 2010:243.

[306] DNV (Det Norske Veritas). Fatigue Design of Offshore Steel Structures', (DNVGL-RP-C203), p. 176. n.d.

[307] Vishay Precision Group M-M. Noise Control in Strain Gage Measurements. 2013.

[308] Gheyas IA, Smith LS. A neural network-based framework for the reconstruction of incomplete data sets. Neurocomputing 2010;73:3039–65. doi:10.1016/j.neucom.2010.06.021.

[309] Kolios A, Jiang Y, Somorin T, Sowale A, Anastasopoulou A, Anthony EJ, et al. Probabilistic performance assessment of complex energy process systems – The case of a self-sustained sanitation system. Energy Convers Manag 2018;163:74–85. doi:10.1016/j.enconman.2018.02.046.

[310] Lazakis I, Raptodimos Y, Varelas T. Predicting ship machinery system condition through analytical reliability tools and artificial neural networks.

Ocean Eng 2018;152:404–15. doi:10.1016/j.oceaneng.2017.11.017.

[311] Hawthorne G, Elliott P. Imputing cross-sectional missing data: Comparison of common techniques. Aust N Z J Psychiatry 2005;39:583–90. doi:10.1111/j.1440-1614.2005.01630.x.

[312] Dempster AP, Laird NM, Rubin DB. Maximum likelihood from incomplete data via the EM algorithm. J R Stat Soc Ser B Methodol 1977;39:1–38. doi:http://dx.doi.org/10.2307/2984875.

[313] Enders CK. A Primer on Maximum Likelihood Algorithms. Available for Use With Missing Data. Struct Equ Model A Multidiscip J 2001;8:128–41.

[314] Richman MB, Trafalis TB, Adrianto I. Multiple imputation through machine learning algorithms. Fifth Conf Artif Intell Appl to Environ Sci 2007.

[315] Reilly M, Pepe M. The relationship between hot-deck multiple imputation and weighted likelihood. Stat Med 1997;16:5–19. doi:10.1002/(SICI)1097-0258(19970115)16:1<5::AID-SIM469>3.0.CO;2-8.

[316] Mathworks. Matlab: Statistics and Machine Learning Toolbox User’s Guide R2016b. 2016.

[317] Foresee FD, Hagan MT. Gauss-Newton approximation to Bayesian regularization. Proc. 1997 Int. Jt. Conf. Neural Networks, 1997, p. 1930–1935.

[318] Hagan MT, Menhaj M. Training feed-forward networks with the Marquardt algorithm. IEEE Trans Neural Networks 1999;5:989–993.

[319] Moller MF. A scaled conjugate gradient algorithm for fast supervised learning. Neural Networks 1993;6:525–33.

[320] BVG-Associates, WindEurope. Unleashing Europe’s offshore wind potential. 2017.

[321] The Crown Estate. Offshore Wind - Operational report 2017. 2017. doi:10.1016/B978-0-12-410422-8.00003-0.

[322] Leanwind. Driving Cost Reductions in Offshore Wind. 2018.

[323] NewEnergyUpdate. Europe's new record offshore LCoE forecast at 40 euros/MWh 2018. http://newenergyupdate.com/wind-energy-update/europes-new-record-offshore-lcoe-forecast-40-eurosmwh (accessed August 10, 2018).

[324] W. Daum. Guidelines for Structural Health Monitoring. Handb. Tech. Diagnostics, Berlin, Germany: Springer; 2013. doi:https://doi.org/10.1007/978-3-642-25850-3_27.

[325] ISIS Canada—the Canadian Network of Canada. Guidelines for Structural Health Monitoring—Design Manual No. 2. n.d.

[326] SAMCO. F08b Guideline for Structural Health Monitoring. Berlin, Germany: 2006.

[327] University D. Development of a Model Health Monitoring Guide for Major Bridges. Philadelphia, PA, USA: 2003.

[328] Norsok Standard N-005. Condition Monitoring of Loadbearing Structures. 1997.

[329] German _Society_for_Non-Destructive-testing. Automatisierte Dauerüberwachung im Ingenieurbau. Berlin, Germany: 2000.

[330] Lloyd G. Guidelines for the Certification of Condition Monitoring Systems for Wind Turbines. Bereich Windenergie, Hamburg: 2007.

[331] DECC. The Department for Energy & Climate Change. Organ Website 2019. https://www.energy.gov/science-innovation/climate-change (accessed January 30, 2019).

[332] BSH. Bundesamt für Seeschifffahrt und Hydrographie. Organ Website 2019. https://www.bsh.de/DE/Home/home_node.html (accessed January 30, 2019).

[333] Bundesamt für Seeschifffahrt und Hydrographie. Minimum requirements concerning the constructive design of offshore structures within the Exclusive

Economic Zone. 2015.

[334] Bundesamt für Seeschifffahrt und Hydrographie. Design of Offshore Wind Turbines. 2015.

[335] Bundesamt für Seeschifffahrt und Hydrographie. Minimum requirements for geotechnical surveys and investigations into offshore wind energy structures, offshore stations and power cables. 2015.

[336] Bundesamt für Seeschifffahrt und Hydrographie. Investigation of the impacts of Offshore Wind Turbines on the Marine Environment (StUK4). 2015.

[337] ISO 19901-6. Petroleum and natural gas industries — Specific requirements for offshore structures — Part 6: Marine operations. 2009.

[338] ISO 19905-1. Petroleum and natural gas industries - Site-specific assessment of mobile offshore units – Part 1: Jack-ups. n.d.

[339] ISO 29400. Ships and marine technology - Offshore wind energy - Port and marine operations. 2015.

[340] EN 1990. Eurocode - Basis of structural design. 2005.

[341] EN 1997. Eurocode 7 - Geotechnical design. 2008.

[342] DNV-OS-H101. Marine Operations , General. 2011.

[343] GL-IV-7. Rules for certification and construction IV Industrial Services, Part 7 Offshore Substations. 2013.

[344] GL-IV-6. GL Rules for the Certification and Construction, IV Industrial Services, Part 6 Offshore Technology. 2013.

[345] American Petroleum Institute Recommended Practice. API RP-2A-WSD Planning, Designing and Constructing Fixed Offshore Platforms – Working Stress Design, 2014.

[346] Windenergie GL. GL-IV-2. GL Rules and Guidelines, IV Industrial Services, Part 2 Guideline for the Certification of Offshore Wind Turbines, 2005.

[347] DNV-OS-J201. Offshore Substations for Wind Farms. 2013.

[348] Farrar CR, Doebling SW. Damage Detection and Evaluation II. Modal Anal. Test., Dordrecht: Springer Netherlands; 1999, p. 345–78. doi:10.1007/978-94-011-4503-9_17.

[349] Farrar C.R and Sohn H. Pattern Recognition for Structural Health Monitoring. Los Alamos National Laboratory, 2000.

[350] Dong X, Lian J, Wang H, Yu T, Zhao Y. Structural vibration monitoring and operational modal analysis of offshore wind turbine structure. Ocean Eng 2018;150:280–97. doi:10.1016/j.oceaneng.2017.12.052.

[351] Adedipe O, Brennan F, Kolios AJ. Corrosion fatigue crack growth in offshore wind monopile steel HAZ material. MARSTRUCT 2015, 5th Int. Conf. Mar. Struct., Southampton, United Kingdom: n.d.

[352] International Organization for Standardization. ISO 12944 Paints and varnishes. Corrosion protection of steel structures by protective paint systems, 2018.

[353] Kim Y, Seok S, Lee J, Lee SK, Kim J. Engineering Analysis with Boundary Elements Optimizing anode location in impressed current cathodic protection system to minimize underwater electric field using multiple linear regression analysis and artificial neural network methods. Eng Anal Bound Elem 2018;96:84–93. doi:10.1016/j.enganabound.2018.08.012.

[354] Jang S, Han M, Kim S. Electrochemical characteristics of stainless steel using impressed current cathodic protection in seawater. Trans. Nonferrous Met. Soc. China, vol. 19, The Nonferrous Metals Society of China; 2009, p. 930–4. doi:10.1016/S1003-6326(08)60380-5.

[355] DNVGL-RP-0416. Corrosion protection for wind turbines. 2016.

[356] Boon J Den, Sutherland J, Whitehouse R. Scour behaviour and scour protection for monopile foundations of offshore wind turbines. … Eur Wind Energy … 2004:1–14.

[357] Shashank Gupta, Stoddart E, Sanderson D, Morrison A. Condition monitoring of offshore wind turbines with scour and grout damage in monopile foundations. Earthq. Risk Eng. Towar. a Resilient World, Cambridge, UK: n.d.

[358] Michalis P, Saafi M, Judd M. Capacitive Sensors for Offshore Scour Monitoring. Energy 2013;166:189–97.

[359] Schaumann P, Raba A, Bechtel A. Fatigue behaviour of grouted connections at different ambient conditions and loading scenarios. Energy Procedia 2017;137:196–203. doi:10.1016/j.egypro.2017.10.373.

[360] DNVGL-ST-0126. Support Structures for wind turbines. 2016.

[361] Martinez-Luengo M, Causon P, Gill AB, Kolios AJ. The effect of marine growth dynamics in offshore wind turbine support structures. Prog. Anal. Des. Mar. Struct. - Proc. 6th Int. Conf. Mar. Struct. MARSTRUCT 2017, 2017, p. 889–98. doi:10.1201/9781315157368-100.

[362] Ioannou A, Angus A, Brennan F. Stochastic Prediction of Offshore Wind Farm LCOE through an Integrated Cost Model. Energy Procedia 2017;107:383–9. doi:10.1016/j.egypro.2016.12.180.

[363] Omni Instruments Ltd. Subsea Acceleration and Vibration Logger n.d. http://www.omniinstruments.co.uk/subsea-offshore-systems/subsea-logging-systems-and-displays/subsea-acceleration-and-vibration-logger.html (accessed December 5, 2018).

[364] Omni Instruments Ltd. Triple Axis Low Noise MEMS Accelerometer n.d. https://www.omniinstruments.co.uk/catalogsearch/result/index/?dir=asc&limit=25&order=price&q=accelerometer (accessed December 5, 2018).

[365] Omni Instruments Ltd. G-NSDQL-004. DQG Series dual-axis inclinometer n.d. http://www.omniinstruments.co.uk/displacement-position-sensors/tilt-sensors/dqg-series-inclinometer.html (accessed December 5, 2018).

[366] Ltd LD. LSOC-3-A – LSO Inclinometer sensor, ±3°, output ±5V n.d. https://www.leveldevelopments.com/products/inclinometers/inclinometer-

sensors/lsoc-3-a-lso-inclinometer-sensor-3-output-5v/ (accessed December 5, 2018).

[367] Electronics D-K. LVDT Transducers n.d. https://www.digikey.es/products/en/sensors-transducers/lvdt-transducers-linear-variable-differential-transformer/522?utm_adgroup=Sensors+%26+Transducers&mkwid=sPyF8Bumv&pcrid=268479553667&pkw=&pmt=b&pdv=c&productid=&slid=&gclid=EAIaIQobChMIi9etuP7g3gIV77D (accessed December 3, 2018).

[368] Omni Instruments Ltd. Industrial Series LVDT n.d. http://www.omniinstruments.co.uk/displacement-position-sensors/linear-position-and-lvdt-sensors/industrial-series-linear-velocity-displacement-transducers.html#partbuilder (accessed December 3, 2018).

[369] OMEGA Engineering. SGD-2/350-RY51. 3-Element Strain Gauge Rosette Triaxial: 0°/45°/90° n.d. https://www.omega.co.uk/pptst/SGD_TRIAXIAL.html (accessed December 3, 2018).

[370] OMEGA Engineering. SGD-1.5/120-LY11 Linear Strain Gauges n.d. https://www.omega.co.uk/pptst/SGD_LINEAR1-AXIS.html (accessed December 3, 2018).

[371] Omni Instruments Ltd. HC2A-S3. Advanced HygroClip2 n.d. http://www.omniinstruments.co.uk/hc2a-s3.html (accessed December 3, 2018).

[372] Omni Instruments Ltd. HBS/1/6000/1. PT100 Temperature sensor with integral transmitter n.d. http://www.omniinstruments.co.uk/temperature-and-humidity/thermocouples-pt100-sensors-and-temperature-transmitters/hbs6000-pt100-sensors-with-integral-temperature-transmitters.html (accessed December 5, 2018).

[373] Omni Instruments Ltd. AMS42-USB. All-In-One USB Data Acquisition Unit. n.d. http://www.omniinstruments.co.uk/data-acquisition-systems-high-speed-usb-lan/bmcm-all-in-one-measurement-systems-lan-usb/all-in-one-

measurement-system-ams42-usb.html#upsell-product-div (accessed December 5, 2018).

[374] Omni Instruments Ltd. AMS84-LAN16F. All-In-One LAN Acquisition Unit n.d. https://www.omniinstruments.co.uk/all-in-one-measurement-system-ams84-lan16f.html (accessed December 5, 2018).

[375] Shafiee M, Brennan F, Armada Espinosa I. A parametric whole life cost model for offshore wind farms. Int J Life Cycle Assess 2016;21:961–75. doi:10.1007/s11367-016-1075-z.

[376] Offshore 4C. An introduction to Crew Transfer Vessels n.d. https://www.4coffshore.com/news/an-introduction-to-crew-transfer-vessels-aid2.html (accessed December 1, 2018).

[377] NorthernSurvey. M/V FREDERIK Survey vessel specifications. NorthernSurvey: Rønde, Denmark n.d. https://northern-survey.com/wp-content/uploads/2017/12/Northern-Survey-MV-Frederik-pdf.pdf (accessed March 24, 2019).

[378] Marine Brokers with a Global Approach SB. 22m Research Vessel Specifications n.d. http://www.seaboats.net/?function=prodlist&filterflags=0&pointer=0&searchtext=32326D2072657365617263682076657373656C&grpid=0&ingrpid=0&groupmode=0&code=&style=&alwaysrender=0 (accessed December 1, 2018).

[379] ROV day rates 2018. https://uncw.edu/uvp/documents/DAYRATECHARGES.pdf (accessed November 4, 2018).

[380] Specialist Offshore Services Ltd. Water Jetter 420bar n.d. https://www.specialistoffshore.com/product/high-pressure-water-jetting/.

[381] Fulop A. An Overview of Seabed Surveys. Hydrofest, The Hydrographic Society of Scotland; 2015.

[382] InnoEnergy. Innovation Readiness Level Report of Renewable Energy Technologies. Analysis of wind, solar and ocean power. 2018.

[383] European Parliament. Energy: new ambitious targets on renewables and energy efficiency. News Eur Parliam Press Release n.d. http://www.europarl.europa.eu/news/en/press-room/20181106IPR18315/energy-new-ambitious-targets-on-renewables-and-energy-efficiency (accessed February 25, 2019).

[384] IRENA. Offshore innovation widens renewable energy options. Opportunities , challenges and the vital role of international co-operation to spur the global energy transformation. Abu Dhabi: 2018.

[385] Clemens H, Weijtjens W, Rolfes R, Devriendt C. Reliability analysis of fatigue damage extrapolations of wind turbines using offshore strain measurements. J Phys Conf Ser 2018;1037:32–5.

[386] Ziegler L. Probabilistic estimation of fatigue loads on monopile-based offshore wind turbines. NTNU Trondheim and TUDelft, n.d.

[387] Lott S, Wen Cheng P. Load extrapolation based on measurements from an offshore wind turbine at Alpha ventus. J Phys Conf Ser 2016;753.

[388] Michalopoulos V. Simplified fatigue assessment of offshore wind support structures accounting for variations in a farm. TUDelft, 2015.

[389] COST059/14. Memorandum of Understanding for the implementation of a European Concerted Research Action designated as COST Action TU1402: Quantifying the value of structural health monitoring. Brussels: n.d.

[390] Bismut E, Schneider R, Sousa H, Straub D. COST TU1402: Quantifying the Value of Structural Health Monitoring. Framework and Categorization for Value of Information Analysis. 2017.

[391] WindGEMINI - Offshore Wind Turbine Digital Twin. DNV GL n.d. https://www.dnvgl.com/services/windgemini-digital-twin-for-wind-turbine-operations-102853 (accessed January 13, 2019).

[392] Bureau Veritas, ORE Catapult. Press release: Industry collaboration to drive the evolution of the “Digital Twin” for offshore wind n.d. https://marine-offshore.bureauveritas.com/industry-collaboration-drive-evolution-digital-twin-

offshore-wind (accessed January 13, 2019).

[393] General Electric. Building a Digital Twin, bolstering the power of a Wind Turbine n.d. https://www.ge.com/renewableenergy/stories/improving-wind-power-with-digital-twin-turbines (accessed January 13, 2019).

APPENDICES

Appendix A The effect of Marine growth dynamics in offshore wind turbine support structures

Martinez-Luengo, M., Causon, P., Gill, A.B., Kolios, A.J.

Centre for Offshore Renewable Energy Engineering, School of Water, Energy and Environment, Cranfield University, Bedford, Bedfordshire, United Kingdom

6th International Conference on Marine Structures, MARSTRUCT 2017; Lisbon; Portugal; 8 May 2017 through 10 May 2017

Published in Progress in the Analysis and Design of Marine Structures - Proceedings of the 6th International Conference on Marine Structures, MARSTRUCT 2017 2017, Pages 889-898

DOI: 10.1201/9781315157368-100

Abstract

Offshore Wind Turbine support structures are invariably subject to colonisation by marine organisms, which are not spatially or temporally linear. Marine Growth varies based on location and season, and with structural and material characteristics. MG is a major consideration for engineers. As organisms settle on the structure they may increase surface roughness and cross-sectional area, altering drag and inertia coefficients and increasing hydrodynamic loading. Furthermore, the added mass from MG also influences structural integrity. As such, there is considerable uncertainty surrounding the response of OWTs to MG, as this phenomenon is often overlooked in FEA modelling. This paper uses the parametric FEA model of an OWT support structure developed in (Martinez-Luengo, Kolios, and Wang 2017) to analyse how different growth rates and patterns of zonation of MG affect the structural integrity of the system.

The Effect of Marine Growth dynamics in Offshore Wind Turbine Support Structures

M. Martinez-Luengo, P. Causon, A.B. Gill & A.J. Kolios

Centre for Offshore Renewable Energy Engineering, School of Water, Energy and Environment, Cranfield University, Cranfield, MK43 0AL, UK

ABSTRACT: Offshore wind turbine (OWT) support structures are invariably subject to colonisation by marine organisms, which are not spatially or temporally linear. Marine Growth (MG) varies based on location and season, and with structural and material characteristics. MG is a major consideration for engineers. As organisms settle on the structure they may increase surface roughness and cross-sectional area, altering drag and inertia coefficients and increasing hydrodynamic loading. Furthermore, the added mass from MG also influences structural integrity. As such, there is considerable uncertainty surrounding the response of OWTs to MG, as this phenomenon is often overlooked in FEA modelling. This paper uses the parametric FEA model of an OWT support structure developed in [1] to analyse how different growth rates and patterns of zonation of MG affect the structural integrity of the system. MG has a great impact in the fatigue life of the structure, as a reduction of 58.6-59.2% is presented in the baseline scenarios.

1 INTRODUCTION

Offshore wind turbine (OWT) support structures are invariably subject to colonisation by marine organisms, which are believed to have an impact on OWTs structural integrity. Marine growth (MG) refers to the colonisation of submerged structures by marine organisms with sessile life stages, referred to as epibenthic organisms, and is a major challenge for engineers. As organisms settle on the structure they may increase surface roughness and cross-sectional area, altering drag and inertia coefficients and increasing hydrodynamic loading. It can be assumed that variability in MG would lead to fluctuations in corresponding loading and inertia. Furthermore, the added mass from MG also influences structural integrity (i.e. buckling and natural frequency). As such there is considerable uncertainty surrounding the long-term dynamic response of OWTs to MG, as this phenomenon is often overlooked in FEA modelling.

Parametric FEA modelling is a powerful design tool often used in offshore wind. It is so effective because key design parameters (KDPs) can be modified directly in the code, to assess their effect in the structure's integrity, saving time and computational resources.

This paper uses the parametric FEA model of an OWT support structure developed in [1] to analyze how critical the MG effect is in the structural integrity of OWT support structures. A review of how the Oil and Gas Industry has approached this issue in the past and how the Offshore Wind Industry can benefit from their knowledge is presented in Section 2. Section 3 shows a summary of the baseline turbine and parametric FEA model developed in [1], along with the loading conditions presented in Section 4. ULS, FLS, buckling and natural frequencies are investigated against different growth rates and patterns of zonation and presented in Section 5. Finally, results and conclusions can be found in Section 6 and 7.

2 MARINE GROWTH

Settlement of epibenthic organisms is determined and influenced by multiple factors including season, species presence, life cycle and life stage requirements, prevailing environmental conditions, and features and characteristics of the substrate.

Seasonal variation in settlement is evident from a number of studies [3, 4]. In the North Sea biomass has been shown to peak in the summer, with lowest levels observed in the winter and spring [4]. This is supported by [3], who reported that species richness increased from February to July, with densities increasing 10-20 fold, in the southern North Sea. In addition, surveys of a Belgian offshore wind farm in 2008 and 2011 have demonstrated seasonal variability in epibenthic coverage. Down to a depth of -2 m *Mytilus edulis* coverage varied from 0-60% in February, but increased to 90-100% in September [4].

Early research on colonisation stemmed from the observation that, on rocky shores, organisms occupied distinct bands both above the waterline and below. It is now well known that this pattern of zonation is a result of localized environmental characteristics forming small scale habitats resulting to varying levels environmental parameters, such as nutrient transport, current regimes or wave exposure. Indeed exposure to wave action can influence the distribution and morphology of epibenthic organisms. Shell lengths in dogwhelks, *Nucella lapillus*, have been found to be shorter and wider on exposed shores whilst having elongated, narrower spires at sheltered locations [5]. Wave exposure has also been shown to effect growth rates in epibenthic invertebrates. Waves and water flow influence light levels, oxygen and sediment movement and nutrient availability [6]. Maximum growth rates have been found in areas with intermediate levels of exposure, with highly exposed and highly sheltered locations showing a sharp reduction in growth rates [7]. Indeed impact of waves place hydrodynamic forces on epibenthic invertebrates, such as mussels, and may cause them to become damaged or dislodged [9, 13]. Therefore settlement and post settlement survival may be reduced in areas of heavy wave action.

Similar patterns have been found on offshore structures. Zonation in relation to depth has been described in communities colonising offshore oil and gas platforms as well as wind turbine substructures [4]. Southgate and Myers [10] found that, for the Celtic Sea Kinsale Field gas platform, mussels of *Mytilus spp* formed the dominant colonising organism between 6 and 20 m. Whilst, between -20 m and -30 m the soft coral, *Alcyonium digitatum*, and anemone, *Metridium senile*, dominate. At depths below -30 m *Serpulid* worms are the dominant organisms. In the case of the Montrose Alpha North Sea oil platform mussels were absent and down to -10 m epibenthic communities were dominated by macro algae, with arborescent bryozoa and hydroids [11]. However below -10 m macro algae gave way to arborescent bryozoa and hydroids and below -30 m hydroids, calcareous and encrusting bryozoa dominated [11].

The effects of wave action on growth rates and post settlement mortality or dislodgement of epibenthic organisms has received less attention in relation to offshore structures than on rocky shores. However, it is likely that areas of structures exposed to wave action would also show variation in MG over time and between seasons, as winter storms would increase wave action. It is also likely that variation in growth would be seen between sheltered and exposed areas of structures.

MG can increase surface complexity and roughness on marine substructures, which provides new habitat and secondary substrate for colonisation. For example, mussels have been found to provide secondary hard substrate and shelter for other epibenthic species on oil and gas platforms as well as wind turbine monopiles [8, 5].

Surface complexity, orientation and roughness are known to be important for settlement of invertebrates [9, 12]. On spatial scales of µm to cm, substratum topography or quality can affect survival after settlement of barnacles, hydrozoans and bryozoans [15]. Rough surfaces may increase survival rates as pits and crevices provide refuge from predators and physical disturbance. This was noted by Walters and Whethey [15] who found that in species with limited attachment ability post settlement survival was greatly increase on plates with rough surfaces.

Although MG is an important consideration in the design and operation of offshore structures, the dynamic response of epibenthic communities has not been fully realized by engineers. Indeed, it has been stated in recommended standards that MG 'tapers off after a few years' [16]. Whilst there is evidence supporting the idea of succession following a predictable pattern [17] it is expected that even an ecosystem with a mature community will experience cyclical change. Thick layers of growth can become dislodged, particularly by storms in the winter period, creating patches of new substrate for colonisation [4]. Furthermore, artificial structures present habitat for invasive species. In the North Sea and Baltic Sea invasive species have been recorded on offshore wind turbine substructures in [18]. It is possible that competition between introduced and indigenous species could result in changes to the surface profile of structures.

3 PARAMETRIC FEA MODELLING OF OWT SUPPORT STRUCTURES

This section summarises the parametric FEA model of an OWT support structure taken from [1], which is employed in this assessment.

3.1 *Geometry*

The reference site is located off the coast of North Wales. The reference turbine used for this analysis consists of a 3.6MW Siemens turbine, connected to an 80m tower, a transition piece (TP) and is sustained by a monopile (MP) foundation. The MP is 31m long and is embedded 18m into the soil and submerged 11m into the ocean. The TP is 24m in length and joins together the MP and the tower. Six stoppers located in the internal surface of the TP, would allow it to rest on top of the MP. The Grouted Connection (GC), located between the TP and the MP, is used for the appropriate transmission of loads and stresses. The OWT support structure was modelled using Abaqus 6.14, which is a widely used FEA software.

3.2 *Materials*

MP, TP, and tower are made of steel S355 with a density of 7850 kg/m^3, a Young's modulus of 210 GPa, a Poisson's ratio of 0.3 and a nominal yield strength of 355 MPa. GC's material properties are characterised by a density of 2740 kg/m^3, a Young's modulus of 88 GPa, a Poisson's ratio of 0.19 and friction coefficient of 0.6 [19].

An important part of the detailed parametric model is composed by the soil-structure interaction. The soil profile considered in this analysis consists of one layer of sand and 3 layers of clay. Due to space restrictions further description of the soil model and the variation of material properties across the depth can be found in [1].

Composition of soil profiles strongly depends on the geographical emplacement; the soil profile utilised in this analysis corresponds to the North of the UK. Winkler's approach was used to represent the soil profile. This method is widely used to model the soil-structure interaction by replacing the elastic soil medium by closely spaced and independent elastic springs [20,21]. Furthermore, it is the recommended by DNV-GL [22], where the stiffness of the linear springs used in the Winkler's approach, is calculated from the p-y curves [23]. This method is used for the design of horizontal loaded piles by the American Petroleum Institute (API) code [24], and it calculates the lateral soil resistance (p) as a function of lateral soil displacement (y).

3.3 *Mesh*

A mesh sensitivity analysis was performed in order keep a balance between the computational time of the simulations and the accuracy of the results. After the analysis, a mesh size of 0.1m for the whole system was found to be adequately accurate as results had already converged. C3D8R elements are used (eight-node brick **element** with reduced integration).

3.4 *Validation*

The validation of the parametric model was carried out comparing the results of the modal analysis of both the structure and the tower, against data from the reference OWT and can be found in [1].

4 LOADING CONDITIONS

4.1 *Wind*

For representation of wind climate, a distinction is made between normal and extreme wind conditions. The former generally concern cyclic structural loading conditions, which are important for fatigue assessment, while the latter are wind conditions that can lead to extreme loads, which might lead to the collapse of the structure due to excessive loading [25]. Both normal and extreme wind conditions used in this analysis were calculated in accordance with IEC 61400-1 [26].

4.2 *Wave*

Wave loading is another environmental load that influences the structural integrity of OWT support structures. Wave forces are calculated using Morrison's Equation [27], which is characterised by the inertia and drag terms, composed by their coefficients (C_m and C_D respectively). Morrison's Equation can be expressed as:

$$dF_t = dF_M + dF_D = C_M \rho \pi \frac{D^2}{4} \ddot{x} dz + C_D \rho \frac{D^2}{2} |\dot{x}| \dot{x} dz$$

where $\dot{x}$ represents the undisturbed fluid velocity, $\ddot{x}$ the acceleration of the fluid (calculated for the baseline turbine in [1]), ρ the water's density and D the effective diameter (including MG). According to [16], most of the variation in C_D and C_M due to MG is produced by variations in: relative surface roughness (e = k/D), Reynolds number ($\mathrm{Re} = \rho \dot{x} D / \upsilon$), Keulegan-Carpenter number ($KC = \dot{x} T / D$), and the member orientation. Being υ the kinematic viscosity of water, T the period of oscillation and k is the absolute roughness height.

Mass and drag coefficients, C_M and C_D, are usually estimated according to the offshore standards [22] and [16] by firstly, deriving the drag coefficient for steady-state flow (C_{DS}) and the wake amplification factor ($\psi(K_c/C_{DS})$), which depends on KC and C_{DS}.

There is a high dependence of C_{DS} on relative surface roughness, as shown in [16]. Natural MG on platforms will generally have e > 10^{-3}. The MG used in these case studies is in the range from 0.015< e

>0.002. C_M and C_D coefficients were calculated from the tables present in [16], for each one of the different MG cases. These can be found in Table 4.

4.3 *Tidal and current induced loads*

Tidal currents and wind driven currents are two environmental loads in which MG can have an impact and vice versa. Even though they do not represent major hazards to the structure's integrity in shallow waters, they contribute to other major excitations such as those produced by the wind and waves. The tidal current profile can be represented as the current speed $(v\ (z))$ at distance z, from still water level (positive upwards), which is the exponential variation of the current at still water level v_0 through the distance to the top of the water column z.

4.4 *Hydrostatic Pressure*

Hydrostatic pressure is referred to the pressure of the water column applied to the submerged parts of the MP and TP. It can be calculated from a control volume analysis of an infinitesimally small cube of fluid and simplified as density and gravity are constant through depth as in [1].

4.5 *Nacelle's and Rotor's Weight*

Since the nacelle's and rotor's (composed of the hub and blades) detailed modelling is not part of the parametric model, they are included in the FEA as concentrated or distributed masses in order to be able to reproduce accurately the OWT's structural behaviour. According to [28], there is no need to model the blades due to the fact that, aside from the mass added to the tower top, parked and feathered blades have minimal impact on the natural frequency of OWTs. The nacelle's and rotor's weights are 125 and 95 tons respectively, which makes a total of 220 tons that are accounted as a cylinder three metres high and with the same diameter as the top of the tower. The density was increased accordingly in order to account for the total weight. The nacelle's and rotor's weights were found in the official Siemens SWT-107 3.6 MW brochure [29].

5 EFFECT OF MARINE GROWTH IN OFFSHORE WIND TURBINE SUPPORT STRUCTURES

5.1 *Limit States Formulation*

Structural integrity of the system is checked according to DNV-OS-J101 [22]. Four limit states are considered in the design: ULS, FLS, Accidental Limit State (ALS) and Serviceability Limit State (SLS). Modifications in the design are checked upon ULS and FLS. ALS was not considered as this limit state is used for the assessment of structural damage in the structure, caused by accidental loads or to reassess the ultimate resistance and structural integrity after damage. Similarly, SLS was not taken into account as it considers tolerance criteria applicable to normal use of the OWT support structures. Furthermore, the structural performance of the system was also checked upon buckling and natural frequencies.

5.1.1 *ULS:*

ULS analysis is carried out considering extreme environmental conditions the worst case scenario for a 50 year return period. This is when wind, wave, tides and wind driven currents are aligned in the principal direction of the wind. The load factor to be used when different loads are combined to form the design load is 1.35 [22].

Table 1 shows the Maximum Utilisation Rates (MUR) for the MP the baseline case, which will be use to assess the loss or gain of the structural integrity of the different design cases considered.

5.1.2 *FLS*

FLS refers to the cumulative damage in the structure due to cyclic loads. The fatigue design of OWT support structures is governed by dynamic responses from simultaneous aerodynamic and hydrodynamic loads [30]. The load factor in the FLS is 1.0 for all load categories [22]. Normal sea state conditions (significant wave height and peak spectral period) were used for the calculation of wave loading [31]. Wind loads were taken from [32], where the fatigue thrust load for the tower of a 3.6 MW offshore wind turbine with 100m hub height are 143 kN.

S–N curve approach is the recommended by the standards [22] and [31]. Furthermore, the equivalent stress range (ΔS) can be determined from the parametric FEA model subjected to the before mentioned fatigue loads. Having obtained the equivalent stress range, the number of loading cycles to crack initiation can then be determined from the S – N curve.

The selection of the S – N curve plays a massive role in the results obtained. Offshore structures are prone to corrosion development due to the harsh marine environment, which leads to significant levels of damage to the structures and hence a reduction in service life [33]. For that reason, curve D in seawater with adequate cathodic protection is used in service life calculations [34]. Table 1 shows the stress range ΔS and the expected service life in the baseline turbine.

5.1.3 *Buckling*

Buckling is characterised by the sudden failure of a structural member subjected to high compressive stress, when this is, at the point of failure, less than the ultimate compressive stress of the material. When the applied load is increased on a slender structure, such as a WT, there is the possibility that it becomes large enough to cause the structure to lose its stability and buckle.

Eigenvalue linear buckling analysis is generally used to estimate the critical buckling load of the analysed structure. The buckling loads are calculated relative to the base state of the structure. The buckling stability of shell structures is often checked according to DNV-RP-C202 [35] or Eurocode 3/ EN 1993-1-1 and Eurocode 3/ EN 1993-1-6. In this analysis Abaqus CAE is used to assess it. Table 1 shows the buckling frequency in the baseline turbine, being the buckling frequency for a particular load combination, the inverse of the utilization factor for the structure to buckle.

5.1.4 *Natural frequencies*

A classic aspect of good structural design lies in optimizing stiffness-to-mass ratio through material and shape choices. Natural frequencies' sensitivity analysis were carried out for the different case studies with the aim to detect patterns of change in the characteristic natural frequencies of the structure. Table 1 shows the first 5 eigenfrequencies of the baseline turbine.

Table 1. Structural properties of the baseline OWT

ULS	MUR (%)	
	MP	64.73
FLS	ΔS (MPa)	Fatigue life (yr)
	33.9	33.1
Buckling Frequency		
	1.5316 Hz	
Natural Frequency		
Mode 1	0.2909 Hz	
Mode 2	0.2962 Hz	
Mode 3	1.6776 Hz	
Mode 4	1.7211 Hz	
Mode 5	1.9516 Hz	

5.2 *Case Study 1: Effects of Zonation*

This section analyses the impact that two different MG profiles have in the structure's integrity and modal frequencies. As pointed out in previous sections, MG profiles can substantially vary depending on a number of factors. For this case study, two different profiles were developed based on existing data from the North Sea and Irish Sea [4,10]. The submerged part of the structure is 11m. Three different zones and the types of MG for each of the two profiles are presented in Figure 1. In these cases, the thickness on the exposed part of the structure were assumed to be smaller based on dislodgement through hydrodynamic pressure. However, this assumption may not always hold true in nature.

Table 2 shows the material properties for each of the zones of the two profiles. In order to introduce MG in the parametric FEA model, two half, hollow, circular cylinders are made for each zone, to surround the MP. One of these was positioned in the side of the MP exposed to currents and waves and its thickness is denoted as *Ex. Thickness* and the other half was positioned in the sheltered side and therefore is denoted as *Sh. Thickness*.

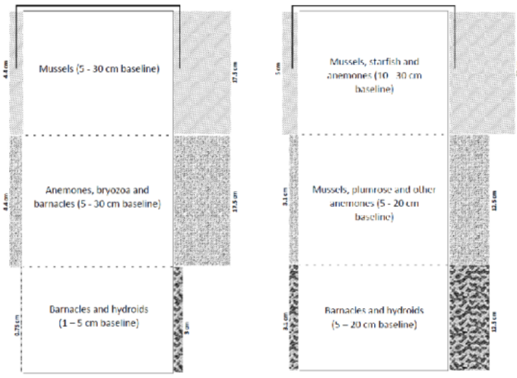

Figure 1 species zonation and variability in thickness under two case studies. Profile A (left) and Profile B (right).

Relevant material properties of the different species, like bulk density (ρ), thickness, Young's Modulus (E) and Poisson's ratio (υ), have been carefully taken from relevant literature [37, 38].

Table 2. Profile's material properties of the baseline OWT

Profile & Zone		ρ (g/cm³)	Thickness (cm) Sh.	Ex.	E (GPa)	υ -
A	I	3.1 [37]	17.5	4.4	0.85 [37]	0.5 [37]
	II	0.7* [38]	17.5	4.4	1.27* [38]	0.3 [36]
	III	0.6 † [38]	3.0	0.8	1.13† [38]	0.3 [36]
B	I	3.1 [37]	20.0	5.0	0.85 [37]	0.5 [37]
	II	3.1 [37]	12.5	3.1	0.85 [37]	0.5 [37]
	III	0.6† [38]	12.5	3.1	1.13† [38]	0.3 [36]

* Values correspond to the average value plus the standard deviation.
† Values correspond to the average value minus the standard deviation

5.3 *Case Study 2: Effects of Thickness*

In this section a sensitivity analysis of the MG thickness, both at the exposed and the sheltered parts of the MP, of the two profiles presented in the previous section, was developed. The mean value of the range of thicknesses at different depths presented at Figure 1, was the one used in the previous Case Study. Case Study 2 analyses the effect that these ranges of thickness have in the structural integrity of the unit. Table 3 presents the different cases that compose the sensitivity analysis.

Table 3. Thickness' Sensitivity analysis

Profile & Zone		Case 2 Sh.	Case 2 Ex.	Case 1 Sh.	Case 1 Ex.	Baseline Sh.	Baseline Ex.	Case 4 Sh.	Case 4 Ex.	Case 5 Sh.	Case 5 Ex.
A	I	5.0	1.3	11.3	2.8	17.5	4.4	23.8	5.9	30.0	7.5
	II	5.0	1.3	11.3	2.8	17.5	4.4	23.8	5.9	30.0	7.5
	III	1.0	0.3	2.0	0.5	3.0	0.8	4.0	1.0	5.0	1.3
B	I	10.0	2.5	15.0	3.8	20.0	5.0	25.0	6.3	30.0	7.5
	II	5.0	1.3	8.8	2.2	12.5	3.1	16.3	4.1	20.0	5.0
	III	5.0	1.3	8.8	2.2	12.5	3.1	16.3	4.1	20.0	5.0

Table 4. C_M and C_D coefficients for the different MG cases.

Profile		Case 2	Case 1	Baseline	Case 4	Case 5
A	C_D	0.78	0.84	0.852	0.852	0.86
	C_M	1.92	1.92	1.92	1.92	1.92
B	C_D	0.84	0.84	0.856	0.86	0.862
	C_M	1.92	1.92	1.92	1.92	1.92

6 RESULTS & DISCUSSION

6.1 *Case Study 1: Effects of Zonation*

Two different MG profiles typical from the North and Irish Sea were implemented in the parametric FEA model to analyse the impact that predominant species would have in the structural integrity and natural frequencies of the unit. This impact is mainly caused by the added mass of the MG and the how these species change the roughness of the structure and therefore its dynamic coefficients (C_M and C_D). Average values of MG for Profile A and B were used to compare the structural integrity and modal frequencies of the unit to the case where no MG exists (Table 5).

Table 5. Effect of zonation results: structural properties.

Profile & Zone	Profile A	No Marine Growth	Profile B
ULS			
MUR (%)	68.3	68.3	68.3
FLS			
ΔS (MPa)	40.4	33.9	40.5
F. Life (yr)	13.7	33.1	13.5
Buckling Freq. (Hz)	1.532	1.532	1.532
Natural Freq. (Hz)			
Md. 1	0.2913	0.2909	0.2911
Md. 2	0.2961	0.2962	0.2959
Md. 3	1.6647	1.6776	1.6587
Md. 4	1.7051	1.7211	1.6994
Md. 5	1.9547	1.9516	1.9547

Table 5 shows no significant variation either in MUR % or buckling frequencies, for both MG profiles in comparison to no MG development. The reason why these two structural checks show no variation due to MG might be due to the fact that extreme wave loading is not affected by MG. This is because extreme waves hit the turbine's support structure in a region well above the mean water level and splash zone, where MG does not develop. Therefore, dynamic coefficients are not affected and loading conditions are maintained. Hence the lack of variation.

Although the added mass does not have an influence in buckling frequency, the fact that organisms are stuck to the support structure's surface, affects the modal frequencies and deflections of the turbine. As could be expected, the presence of these organisms in the surface of the support structure increases its rigidity, increasing natural frequencies. However, the rate of variation of the natural frequencies is not high enough for MG to be considered a threat to the structure's integrity. This is due to the low rate of change and also due to restrictions on the growth of epibenthic organisms. Whilst layers of epibenthic growth of up to 300 mm may occur, intense wave action can dislodge thick layers of MG. Furthermore, a special degree of variation is observed in Mode three and four, which could potentially be used for Structural Health Monitoring purposes.

Table 5 also shows the impact that MG has in the stress range of the unit, at mudline level. Even if this variation is low, the impact that it has in the estimated service life of the structure is great. This is due the logarithmic scale present in the S – N curves. Nevertheless, the level of damage that can be expected due to MG is never going to be constant, as it will always depend on the current level of MG development, which is highly variable. According to Table 5, Mussel dominated profiles may present a greater threat to the structure than barnacle dominated profiles, showing a variation in expected service life from 33.1 to 13.5 years for Mussel-dominated profiles and from 33.1 to 13.7 years for Barnacle dominated profiles.

6.2 *Case Study 2: Effects of Thickness*

A sensitivity analysis of the MG thickness, both at the exposed and the sheltered parts of the MP, of the two profiles was carried out. The mean value of the range of thicknesses at different depths presented at Figure 1 and used in the previous Case Study constitutes the baseline scenario in this Case Study. This Case Study analyses the effect that these ranges of thickness have in the structural integrity of the unit compared to the baseline scenario of each profile. Table 6 presents the results for each one of the different cases that compose the sensitivity analysis.

Similar to the previous Case Study, there is no variation in the MUR and buckling frequencies in any of the cases of both profiles. This lack of variation is consistent to the results of the previous Case Study. This is because it is unlikely that the added mass from the positive variation in thickness of Cases three and four would impact the structural behaviour, when the transition from the "no MG scenario" to the baseline MG did not.

In line with the natural frequency results from the Effect of Zonation study, the rate of variation of the first natural frequency is maintained with the thickness variation and it is still not high enough for MG to be considered a threat to the structure's integrity. Besides, Modes three and four stand as the ones where higher variation in the natural frequency is seen. This fact makes them potentially useful to detect excessive MG development with Structural Health Monitoring Systems. The detection of excessive MG would be beneficial to extend the fatigue life of the structure, as according to Table 6, that constitutes the biggest threat that MG presents to OWT support structures.

Table 6. Sensitivity Analysis' results: structural properties.

Profile	Case 2	Case 1	Baseline	Case 3	Case 4
		ULS	MP's MUR (%)		
A	68.3	68.3	68.3	68.3	68.3
B	68.3	68.3	68.3	68.3	68.3
		FLS	Fatigue life (yr)		
A	14.5	14.4	13.7	13.3	12.7
B	15.9	14.0	13.5	10.2	9.7
		Buckling Frequency (Hz)			
A	1.532	1.532	1.532	1.532	1.532
B	1.532	1.532	1.532	1.532	1.532
		Natural Frequency (Hz)			
A					
Md. 1	0.2912	0.2912	0.2913	0.2913	0.2914
Md. 2	0.2960	0.2960	0.2960	0.2960	0.2960
Md. 3	1.6754	1.6701	1.6647	1.6592	1.6536
Md. 4	1.7154	1.7103	1.7051	1.6998	1.6944
Md. 5	1.9547	1.9547	1.9547	1.9548	1.9549
B					
Md. 1	0.2912	0.2911	0.2911	0.2911	0.2911
Md. 2	0.2960	0.2959	0.2959	0.2959	0.2959
Md. 3	1.6698	1.6642	1.6587	1.6529	1.6472
Md. 4	1.7101	1.7047	1.6994	1.6938	1.6884
Md. 5	1.9547	1.9547	1.9547	1.9547	1.9548

Fatigue is the structural feature most affected by MG, according to these analyses. As it can be appreciated from Table 6, MG has a great impact in the fatigue life of the structure, as a reduction of 58.6-59.2% is presented in the baseline scenarios. This impact is reduced to the 52% for the minimum MG development case, although this variation is still very high.

7 CONCLUSSION

This paper used the parametric FEA model of an OWT support structure developed in [1] to analyze the criticality of MG in the structural integrity of OWT support structures. To that aim, two MG profiles typical from the North and Irish Sea were introduced in the parametric FEA model. Due to this MG, dynamic coefficients needed to be recalculated, which also affected the loading conditions. ULS, FLS, buckling and natural frequencies have been investigated against different growth rates and patterns of zonation.

Results show no effect in the maximum utilisation ratios (MURs) and buckling frequencies, which draws the conclusion that the added mass of the MG has little or no influence in the system. Furthermore, natural frequencies were also not very affected due to this phenomenon. However, as could be expected, the presence of these organisms in the surface of the support structure slightly increases its rigidity, increasing natural frequencies in both profiles but especially in Profile A (barnacle dominated).

Fatigue is the structural feature most affected by MG, according to these analyses. MG has a great impact in the fatigue life of the structure, as a reduction of 58.6-59.2% is presented in the baseline scenarios. This impact is reduced to the 52% for the minimum MG development case, although this variation is still very high. It should be noted that MG shows considerable variability, which is likely to mitigate the reduction in fatigue life. On average settlement of invertebrates begins 2-3 weeks following immersion [39]. However, growth rates and development differ between species and may be influenced by environmental characteristics [40]. Operators should be aware that cleaning at times of routine maintenance or inspections could maximise the fatigue life of the turbine.

References

[1] Martinez-Luengo M, Kolios A, Wang L. Parametric FEA modelling of Offshore Wind Turbine Support Structures: towards scaling-up and CAPEX reduction. Int J Mar Energy 2017.

[2] Kerckhof F, Rumes B, Jacques T, Degraer S, Noro A. Early development of the subtidal marine biofouling on a concrete offshore windmill foundation on the Thornton Bank (southern North Sea): first monitoring results. Int J Soc Underw Technol 2010;29:137–49. doi:10.3723/ut.29.137.

[3] Reiss H, Kröncke I. Seasonal variability of epibenthic communities in different areas of the southern North Sea. ICES J Mar Sci 2004;61:882–905. doi:10.1016/j.icesjms.2004.06.020.

[4] Bouma S. Benthic communities on hard substrates of the offshore wind farm. Rep by Bur Waardenbg Bv Noordzeewind 2012:84.

[5] Crothers JH, Cowell EB. Variation in Nucella lapillus (L.) Shell Shape in Populations from Fensfjorden, Norway - Applied Example. J Molluscan Stud 1979;45:108–14.

[6] Wernberg T, Connell SD. Physical disturbance and subtidal habitat structure on open rocky coasts: Effects of wave exposure, extent and intensity. J Sea Res 2008;59:237–48. doi:10.1016/j.seares.2008.02.005.

[7] Steffani CN, Branch GM. Growth rate, condition, and shell shape of Mytilus galloprovincialis: Responses to wave exposure. Mar Ecol Prog Ser 2003;246:197–209. doi:10.3354/Meps246197.

[8] Paine RT, Levin SA. Intertidal landscapes: disturbance and the dynamics of pattern. Deep Sea Res Part B Oceanogr Lit Rev 1981;28:885–6. doi:10.1016/0198-0254(81)91582-X.

[9] Denny MW. Lift as a mechamism of patch initiation in mussel beds. J Exp Mar Bio Ecol 1987;113:231–45.

[10] Southgate T, Myers AA. Mussel fouling on the Celtic Sea Kinsale Field gas platforms. Estuar Coast Shelf Sci 1985;20:651–9. doi:10.1016/0272-7714(85)90023-X.

[11] Forteath G, Picken G, Ralph R, Williams J. Marine Growth Studies on the North Sea Oil Platform Montrose Alpha . Mar Ecol Prog Ser 1982;8:61–8. doi:10.3354/meps008061.

[12] Wolfson a, Van Blaricom G, Davis N, Lewbel G. The Marine Life of an Offshore Oil Platform. Mar Ecol Prog Ser 1979;1:81–9. doi:10.3354/meps001081.

[13] Qiu J-W, Thiyagarajan V, Leung AW, Qian P-Y. Development of a marine subtidal epibiotic community in Hong Kong: implications for deployment of artificial reefs. Biofouling 2003;19:37–46. doi:10.1080/0892701021000060851.

[14] Perkol-Finkel S, Shashar N, Benayahu Y. Can artificial reefs mimic natural reef communities? The roles of structural features and age. Mar Environ Res 2006;61:121–35. doi:10.1016/j.marenvres.2005.08.001.

[15] Walters LJ, Wethey DS. Settlement and early post-settlement survival of sessile marine invertebrates on topographically complex surfaces: The importance of refuge dimensions and adult morphology. Mar Ecol Prog Ser 1996;137:161–71. doi:10.3354/meps137161.

[16] API. Recommended Practice for Planning , Designing and Constructing Fixed Offshore Platforms — Working Stress Design. Api Recomm Pract 2007;24–WSD:242. doi:10.1007/s13398-014-0173-7.2.

[17] Bram JB, Page HM, Dugan JE. Spatial and temporal variability in early successional patterns of an invertebrate assemblage at an offshore oil platform. J Exp Mar Bio Ecol 2005;317:223–37. doi:10.1016/j.jembe.2004.12.003.

[18] Langhamer O. Artificial Reef Effect in relation to Offshore Renewable Energy Conversion: State of the Art. Sci World J 2012;2012:e386713. doi:10.1100/2012/386713.

[19] Densit. Ultra High performance grout - Ducorit Data Sheet n.d.

[20] Winkler E. Die Lehre von Elastizitat und Festigkeit. Prag : Dominicius; 1867.

[21] Koukoura C, Natarajan A, Vesth A. Identification of support structure damping of a full scale offshore wind turbine in normal operation. Renew Energy 2015;81:882–95. doi:10.1016/j.renene.2015.03.079.

[22] DNV (Det Norske Veritas). DNV-OS-J101 Design of Offshore Wind Turbine Structures. 2014.

[23] Kezdi A. Handbook of soil mechanics. Elsevier. Amsterdam: 1974.

[24] API Recommended Practice 2GEO/ISO 19901-4, Geotechnical and Foundation Design Considerations. n.d.

[25] Palutikof J, Brabson B, Lister D, Adcock S. A review of methods to calculate extreme wind speeds. Meteorol Appl 1999;6:119–32. doi:10.1017/S1350482799001103.

[26] International Electrotechnical Commission. IEC 61400-1 International Satandard. Wind turbines - Part 1: Design Requirements. Geneva, Switzerland: 2005. doi:10.5594/J09750.

[27] Sarpkaya T. Wave Forces on Offshore Structures. Cambridge. Cambridge: 2010.

[28] Carswell W, Johansson J, Løvholt F, Arwade SR, Madshus C, Degroot DJ, et al. Foundation damping and the dynamics of offshore wind turbine monopiles. Renew Energy 2015;80:724–36. doi:10.1016/j.renene.2015.02.058.

[29] Siemens. SWT-3.6-107 Wind Turbine. 2010.

[30] Passon P. Damage equivalent wind e wave correlations on basis of damage contour lines for the fatigue design of offshore wind turbines. Renew Energy 2015;81:723–36. doi:10.1016/j.renene.2015.03.070.

[31] International Electrotechnical Commission. International Standard IEC 61400-3 Wind turbines - Part 3: Design requirements for offshore wind turbines. 2009.

[32] LaNier MW. LWST Phase I Project Conceptual Design Study: Evaluation of Design and Construction Approaches for Economical Hybrid Steel/Concrete Wind Turbine Towers. Denver, Colorado, USA: 2005.

[33] Adedipe O, Brennan F, Kolios AJ. Review of Corrosion Fatigue in Offshore Structures: Present Status and Challenges in the Offshore Wind Sector. Renew Sustain Energy Rev 2016;61:141–54.

[34] (DNV) Det Norske Veritas. Fatigue Design of Offshore Steel Structures. 2005.

[35] DET NORSKE VERITAS AS. DNV RP-C202 Buckling Strength of Shells. 2013.

[36] Hui C-Y, Long R, Wahl KJ, Everett RK. Barnacles resist removal by crack trapping. J R Soc Interface 2011;8:868–79. doi:10.1098/rsif.2010.0567.

[37] Pearce T, Labarbera M. A comparative study of the mechanical properties of Mytilid byssal threads. J Exp Biol 2009;212:1442–8. doi:10.1242/jeb.025544.

[38] Astachov L, Nevo Z, Brosh T, Vago R. The structural, compositional and mechanical features of the calcite shell of the barnacle Tetraclita rufotincta. J Struct Biol 2011;175:311–8. doi:10.1016/j.jsb.2011.04.014.

[39] Yebra DM, Rasmussen SN, Weinell C, Pedersen LT. Marine Fouling and Corrosion Protection for Off-Shore Ocean Energy Setups. 3rd Int Conf Ocean Energy, 6 October, Bilbao 2010:1–6.

[40] Mallat C, Corbett A, Harris G, Lefranc M. Marine growth on North Sea fixed steel platforms – Insights from the decommissioning industry. Proc ASME 2014 33rd Int Conf Ocean Offshore Arct Eng Am Soc Mech Eng 2014; June 8-1:1–10.

Appendix B The damage equivalent load calculation using rainflow counting

In Section 4.2.1 a 50Hz strain dataset was reduced to 10min damage equivalent loads dataset. This process is necessary to synchronise this dataset with the environmental conditions (i.e., 30,000 strain measurements per each 10-min measurement of environmental conditions).

The first stage is to transform strain recordings into stresses. Hooke's Law for continuous elastic materials is used to this purpose:

$$\sigma = E * \varepsilon$$

where:

- σ is the bending stress in MPa,
- E = 200GPa, being the Young's Modulus for the steel
- ϵ being the strain measurements in microstrains

After the stresses are obtained, a solution to this synchronisation issue consists in the calculating the Damage Equivalent Loads (DELs) for 10-min intervals [303–305]. DELs represent the single load that would cause the same damage than the cumulative effect of the loads for the established interval (10min in this case). The expression is calculated with the following formula [303–305]:

$$DEL = \left(\sum_{i-1} \frac{n_i \sigma_i^m}{N_{eq}} \right)^{\frac{1}{m}} \qquad \textbf{4-2}$$

Where:

- n_i is the current cycle,
- σ_i is the stress range,
- N_{eq} is a fixed number of cycles
- m is the slope of the S-N curve representing the conditions of the material undergoing the loading

Values for N_{eq} and m can be obtained from standards such as the volume dedicated to fatigue design of offshore steel structures from DNVGL-RP-C203 [306]. Values used were: $N_{\text{eq}} = 10^7$, and m = 5.

Equation 4-2 is based on the Rainflow-counting algorithm, which is used to translate the recorded strains into fatigue. Based on the linear Palmgren-Miner's rule, the rainflow-counting algorithm was developed by Tatsuo Endo and M. Matsuishi in 1968. While not being the only cycle-counting algorithm, it can be argued that is the most popular among the most widely used cycle-counting algorithms present at the ASTM E 1049-85 standard.

To apply Rainflow Counting algorithm, an open source coded version of it developed for MATLAB by Adam Nieslony was used. This code is a small MATLAB Toolbox that allows for fatigue life assessment based on ASTME 1049-85. standard. This code was integrated in the MATLAB codes developed for data synchronisation, cleansing and missing data imputation activities so it would automatically provide the stress amplitudes (σi) and the accumulated cycles (ni) for each of them.

DELs every 10min would therefore be calculated by applying Equation 4-2 for the stresses and cycles counted for those 10min using the Rainflow counting algorithm.

$$DEL = \left(\sum_{i-1} \frac{n_i \sigma_i^5}{10^7} \right)^{\frac{1}{5}}$$